

Phosphorylation of the herpes simplex virus type 1 UL13 protein kinase and  
a putative target protein encoded by gene UL49

by

Philip Robin Antrobus

A thesis presented for the degree of Doctor of Philosophy

in

The Faculty of Science at the University of Glasgow

MRC Virology Unit,  
Institute of Virology,  
Church Street,  
Glasgow.

September 2000

ProQuest Number: 13818788

All rights reserved

INFORMATION TO ALL USERS

The quality of this reproduction is dependent upon the quality of the copy submitted.

In the unlikely event that the author did not send a complete manuscript and there are missing pages, these will be noted. Also, if material had to be removed, a note will indicate the deletion.



ProQuest 13818788

Published by ProQuest LLC (2018). Copyright of the Dissertation is held by the Author.

All rights reserved.

This work is protected against unauthorized copying under Title 17, United States Code  
Microform Edition © ProQuest LLC.

ProQuest LLC.  
789 East Eisenhower Parkway  
P.O. Box 1346  
Ann Arbor, MI 48106 – 1346

GLASGOW  
UNIVERSITY  
LIBRARY

COPY 1

## ACKNOWLEDGEMENTS

I would like to thank the following people who have contributed to the completion of this thesis:

Firstly, Professor Duncan McGeoch for the provision of facilities at the Institute of Virology.

My supervisor, Dr Andrew Davison for his advice and support throughout this project, help with sequence alignments and especially for his thorough and constructive criticism of this manuscript.

The members of this institute who provided materials and advice. All members, past and present, of labs 309 and 204, especially Charles Cunningham whose advice and good humour have helped immeasurably

Dr Matthew Davison and his staff at Zeneca for their help with the mass spectrometry and protein sequencing.

The washroom and media staff for provision of glassware and general solutions.

All my friends in Glasgow, too numerous to mention here but I shall thank you all in person.

Most of all I would like to thank my Mum, Dad and my sister, Caroline. Without their unfaltering help and support I certainly would not be here.

The author was in receipt of a Medical Research Council studentship and unless otherwise stated, all results were obtained by the author's own efforts.

## ABSTRACT

Protein kinases (PKs) are ubiquitous enzymes which utilise phosphorylation, a reversible post-translational modification, to regulate protein activity. Protein phosphorylation is widespread, affecting nearly all aspects of growth and homeostasis in eukaryotic cells. However, over twenty years ago certain viral transforming genes were found to possess PK activity, bringing protein phosphorylation to the attention of virologists.

Sequence analysis of the herpes simplex virus type 1 (HSV-1) genome identified two genes, US3 and UL13, whose products exhibit PK-specific amino acid sequence motifs. The US3 PK has been purified, the enzyme activity characterised and a number of targets for phosphorylation identified. The UL13 PK has not yet been purified, but its enzymatic characteristics and potential target proteins have been investigated. It localises in the nuclei of infected cells, utilises ATP or GTP to phosphorylate acidic but not basic substrates, and is a minor component of the virion tegument. The UL13 PK activity is stimulated by high salt concentration and is insensitive to inhibition by heparin. Several proteins have been identified as targets for the UL13 PK, one being the abundant viral tegument protein encoded by HSV-1 gene UL49.

The aims of this project were to confirm that the UL13 PK targets the UL49 protein for phosphorylation, to characterise further the UL13 PK activity, and to map phosphorylated residues within the UL13 and UL49 proteins.

From an analysis of three independent UL13 mutants, each with a lesion in a different region of the UL13 gene, it was confirmed using an *in vitro* assay that phosphorylation of the UL49 protein was dramatically reduced in the absence of a functional UL13 protein. In radiolabelled nuclear extracts of *wt* HSV-1 infected cells or membrane-stripped *wt* virions, the UL13 protein was detected as a highly radiolabelled 57 kDa phosphoprotein. Phosphorylation of this protein was stimulated by increasing salt concentrations. Thus, HSV-1 UL13 PK differs significantly from the previously characterised HSV-2 UL13 PK in both its salt sensitivity and optimum pH.

Radiolabelling of the UL13 PK maybe attributed to autophosphorylation. However, at least two hyperphosphorylated forms of the UL13 protein were detected in radiolabelled nuclear extracts incubated with excess unlabelled ATP or GTP. The level of hyperphosphorylation differed between cell lines, and hyperphosphorylated UL13 protein was not detected in radiolabelled membrane-stripped virions. Hyperphosphorylation was insensitive to heparin, but was completely abolished in the presence of a potent inhibitor of cellular casein kinase II.

The most obvious target for the UL13 PK identified during this study was a 38 kDa virion protein, which was confirmed by mass spectrometry and by use of a mutant virus expressing a C-terminally truncated form of the UL49 protein to be encoded by HSV-1 gene UL49. The UL49 protein was still phosphorylated, albeit to a greatly reduced level, in nuclear extracts prepared from UL13 mutant-infected cells. The additional PK or PKs targeting the UL49 were inhibited by heparin and sensitive to increasing salt concentrations. This suggests that a cellular PK targets the UL49 protein. However, an inhibitor of casein kinase II had little effect on phosphorylation of the UL49 protein.

Initially, the UL49 protein was found to cycle phosphate, and did not appear to be hyperphosphorylated beyond a basal level. However, under altered buffer conditions, it was hyperphosphorylated and also possibly nucleotidylated, these modifications seeming to require sequences near the C-terminus of the UL49 protein.

Phosphopeptide mapping experiments performed on the UL49 protein phosphorylated at low salt concentrations led to detection of a 2 kDa tryptic phosphopeptide by SDS-PAGE, and mass spectrometric analysis identified a phosphorylated 1703.91 Da tryptic peptide which was phosphorylated at high salt concentrations. It is likely that these two peptides represent cellular and viral PK target sites. Mapping of the UL13 protein suggested that phosphopeptide fragments are located in the serine-rich, N-terminal 100 residues of the protein, a region which lies outside the established catalytic domain of the UL13 PK.

As well as providing data in support of UL13 encoding a PK which targets the UL49 protein for phosphorylation, the data presented in this thesis represents a further

characterisation of the UL13 PK activity and provides new insights into phosphorylation of the UL49 and UL13 proteins.

---

**CONTENTS**

	<b>Page</b>
<b>Abstract</b>	i
<b>Contents</b>	iv
<b>List of Figures and Tables</b>	x
<b>Abbreviations</b>	xvi
 <b>Chapter 1 - Introduction</b>	
1.1 Protein phosphorylation	1
1.1.1 Protein kinases	2
1.1.1.1 <i>Protein kinase catalytic domains</i>	2
1.1.1.2 <i>Protein kinase structure</i>	3
1.1.1.3 <i>cAPK structure</i>	4
1.1.1.4 <i>Conservation and function of cAPK residues</i>	6
1.1.2 Subdomain conformations	8
1.1.2.1 <i>N-terminal lobe</i>	8
<i>Glycine-rich loop</i>	8
<i>Invariant lysine residue</i>	9
1.1.2.2 <i>Linker region</i>	9
1.1.2.3 <i>C-terminal lobe</i>	10
<i>Catalytic loop</i>	10
1.1.3 Protein kinase function	11
1.1.3.1 <i>MnATP/MgATP binding</i>	11
1.1.3.2 <i>Purine binding</i>	12
1.1.3.3 <i>Ribose binding</i>	12
1.1.3.4 <i>Triphosphate binding</i>	12
1.1.4 Protein kinase-substrate interactions	13
1.1.4.1 <i>cAPK substrate consensus sequence</i>	13
1.1.4.2 <i>Substrate binding</i>	14
1.1.4.3 <i>Ion pairs</i>	14
1.1.4.4 <i>Hydrogen bonds and hydrophobic interactions</i>	14
1.1.5 Protein kinase substrate specificity	15

---

1.1.5.1	<i>Substrate specific sequence variations</i>	15
1.1.5.2	<i>Discrimination between Ser/Thr and Tyr protein kinases</i>	16
1.1.6	Protein kinase mechanism	17
1.1.6.1	<i>The phosphotransferase reaction</i>	18
1.1.6.2	<i>Autophosphorylation</i>	18
1.2	<b>The Herpesviruses</b>	23
1.2.1	General properties of herpesviruses	23
1.2.2	Human herpesviruses	23
1.2.2.1	<i>Biological properties</i>	23
1.2.3	HSV-1 viral architecture	24
1.2.4	Classification and evolution	25
1.2.5	Genetic properties of herpesviruses	26
1.2.5.1	<i>Genome features</i>	26
1.2.5.2	<i>HSV-1 genome</i>	26
1.2.6	The infectious cycle of HSV-1	27
1.2.7	Virus assembly and release	30
1.2.8	Latency	30
1.3	<b>Herpesviral protein kinases</b>	30
1.3.1	Ribonucleotide Reductase (UL39)	31
1.3.1.1	<i>Ribonucleotide reductase function</i>	31
1.3.1.2	<i>Ribonucleotide reductase protein kinase activity</i>	31
1.3.2	HSV-1 US3	33
1.3.2.1	<i>Identification of the US3 ORF</i>	33
1.3.2.2	<i>US3 protein kinase activity</i>	35
1.3.2.3	<i>Growth characteristics of US3 mutant virus</i>	36
1.3.2.4	<i>Characteristics of the US3 protein kinase</i>	36
1.3.2.5	<i>US3 protein kinase targets</i>	36
	<i>US9</i>	37
	<i>UL12</i>	37
	<i>UL34</i>	38
	<i>Anti-apoptotic activity</i>	39

---

---

1.3.3	HSV-1 UL13	40
1.3.3.1	<i>Sequence analysis</i>	40
1.3.3.2	<i>Gene position and orientation</i>	43
1.3.3.3	<i>UL13 protein kinase activity</i>	44
1.3.3.4	<i>Protein kinase activity in the virion</i>	45
1.3.3.5	<i>Purification of the UL13 protein</i>	46
1.3.3.6	<i>Heterologous expression of UL13</i>	46
1.3.3.7	<i>UL13 mutants</i>	47
1.3.3.8	<i>Effect of UL13 mutations on HSV-1 growth</i>	48
1.3.3.9	<i>UL13/US3 double mutants</i>	47
1.3.3.10	<i>UL13 phosphorylation assay</i>	48
1.3.4	UL13 Homologues	49
1.3.4.1	<i>HSV-2 UL13</i>	49
1.3.4.2	<i>VZV ORF47</i>	50
1.3.4.3	<i>PRV UL13</i>	50
1.3.4.4	<i>HCMV UL97</i>	51
1.3.4.5	<i>EBV BGLF4</i>	51
1.3.4.6	<i>HHV-8 ORF36</i>	53
1.3.5	UL13 protein kinase targets	53
1.3.5.1	<i>ICP22</i>	54
1.3.5.2	<i>ICP0</i>	55
1.3.5.3	<i>RNA polymerase II</i>	56
1.3.5.4	<i>Eukaryotic elongation factor 1<math>\delta</math></i>	57
1.3.5.5	<i>Glycoproteins E and I (US8 and US7)</i>	58
1.3.5.6	<i>vhs (UL41)</i>	59
1.3.5.7	<i>VP22 (UL49)</i>	60
1.4	Aims	61
 <b>Chapter 2 - Materials</b>		
2.1	Cells and viruses	62
2.2	Cell culture growth media	62
2.3	Radiochemicals	64

---

---

2.4	Enzymes	64
2.5	Chemicals	65
2.6	Protein gels	65
2.6.1	Tris-glycine polyacrylamide gels	65
2.6.2	Tris-Tricine polyacrylamide gels	66
2.7	Protein blotting for mass spectrometric analysis	66
2.8	<i>In vitro</i> phosphorylation assay	67
2.9	Immune precipitation	68
2.10	Endoproteinase reaction buffers	68
2.11	Other buffers	69
 <b>Chapter 3 - Methods</b>		
3.1	Growth of cells and virus stocks	70
3.1.1	Cell culture	70
3.1.2	Virus stocks	70
3.1.3	Titration of virus stocks	70
3.1.4	Purification of virions and L-particles	71
	(a) <i>Production of gradients</i>	71
	(b) <i>Purification</i>	71
3.2	Analysis of HSV-1 induced polypeptides	71
3.2.1	Sodium dodecyl sulphate-polyacrylamide gel electrophoresis (SDS-PAGE)	71
	(a) <i>Tris-glycine gels</i>	71
	(b) <i>Tris-Tricine</i>	72
3.2.2	Protein visualisation	73
	(a) <i>Coomassie Brilliant Blue</i>	73
	(b) <i>Autoradiography</i>	73
3.2.3	Protease digestion and extraction of peptides from gel slices	73
	(a) <i>For analysis by SDS-PAGE</i>	73
	(b) <i>For mass spectrometric analysis</i>	74
3.2.4	Blotting polyacrylamide gels for mass spectrometric analysis	74
	(a) <i>General blotting protocol</i>	74
	(b) <i>For the UL49-encoded protein</i>	74

---

---

	(c) <i>Coomassie staining of PVDF blotted samples</i>	75
3.2.5	Mass spectrometric analysis of proteins	75
3.2.6	Immune precipitation	75
3.3	<i>In vitro</i> phosphorylation reactions	76
3.3.1	Preparation of nuclear and cytoplasmic extracts from infected cells	76
3.3.2	Treatment of virions for <i>in vitro</i> phosphorylation reactions	76
3.3.3	<i>In vitro</i> phosphorylation of infected cell extracts and virions	77
3.3.4	Assay for phosphate cycling	77
3.4	Computational analysis	77
 <b>Chapter 4 - Results</b>		
4.1	<i>In vitro</i> phosphorylation of nuclear extracts from infected cells	78
4.2	Multiple phosphorylation of the 57 kDa protein	82
4.3	Post-translational modification of the UL49 protein	88
4.4	Dependence of phosphorylation of the UL13 protein on cell type	92
4.5	Mapping sites of phosphorylation	96
4.5.1	Phosphorylation of the UL49 protein	97
4.5.2	Phosphorylation of the UL13 protein	101
 <b>Chapter 5 - Discussion</b>		
5.1	UL13	103
5.1.1	UL13 sequence analysis	103
5.1.2	Phosphorylation of the UL13 protein	106
5.1.3	Hyperphosphorylation of the UL13 protein	107
5.1.4	Mapping sites of phosphorylation in the UL13 PK	108
5.2	Targets for phosphorylation	111
5.2.1	Phosphorylation of the UL49 protein	111
5.2.2	Hyperphosphorylation of the UL49 protein	112
5.2.3	Phosphorylation mapping of the UL49 protein	112

---

5.2.3	Critical appraisal of identified UL13 PK targets	114
5.3	Future work	115

**List of Figures and Tables**

		<b>Page<sup>a</sup></b>
Figure 1.1	A schematic representation of the cAPK C-subunit topology	5
Figure 1.2	A linear alignment of the structural subdomains in residues 43 to 290 of cAPK and corresponding conserved regions	5
Figure 1.3	3-D structure of the catalytic core of the C-subunit of cAPK complexed with PKI(5-24) and MnATP	fp8
Figure 1.4	Schematic diagram of the interactions between the MgATP substitute MnAMP-PNP and the cAPK catalytic subunit	11
Figure 1.5	Sequence of PKI (5-24), an inhibitor peptide of cAPK derived from the N-terminal region of a naturally occurring heat stable PK inhibitor protein	13
Figure 1.6	A schematic representation of ATP and some of the key residues at the catalytic site and activation segment of cAPK	20
Figure 1.7	Illustration of PKC with the six autophosphorylation sites located close to the catalytic site	22
Figure 1.8	Schematic representation of a herpesvirus particle	24
Figure 1.9	A phylogenetic tree for the herpesviruses	26
Figure 1.10	Schematic representation of the HSV-1 genome	27
Figure 1.11	Amino acid sequence alignment of 2R1 and 1R1 with cAPK	32
Figure 1.12	Genomic location and organisation of the US3 gene	34
Figure 1.13	Amino acid sequence alignment of HSV-1 US3 and VZV ORF66 with cAPK	35
Figure 1.14	Amino acid sequence alignment of the putative herpesviral PKs identified by Chee <i>et al.</i> (1989) with cAPK	41
Figure 1.15	A section of EBV BGLF4 sequence, showing the two sites identified at the APE consensus motif indicative of PK subdomain VIII	42
Figure 1.16	A section of HCMV gene UL97 sequence, showing the two identified sites of the invariant catalytic lysine	42
Figure 1.17	Genomic location and organisation of the UL13 gene	44
Figure 4.1.1	Autoradiograph showing <i>in vitro</i> phosphorylation profiles	ap78

	of <i>wt</i> and UL13 mutant infected cell CNEs	
Figure 4.1.2	Autoradiograph showing the effects of varying <i>in vitro</i> phosphorylation incubation times	ap79
Figure 4.1.3	Autoradiograph showing the <i>in vitro</i> phosphorylation profiles of <i>wt</i> and UL13- <i>lacZ</i> CNE under a variety of buffer conditions	Ap80
Figure 4.2.1	Autoradiograph showing an <i>in vitro</i> assay for phosphate cycling	ap82
Figure 4.2.2	Autoradiographs showing an <i>in vitro</i> assay for phosphate cycling	ap82
Figure 4.2.3	Autoradiograph showing an <i>in vitro</i> assay to determine the effect of varied incubation and chase times on phosphorylation profiles	ap83
Figure 4.2.4	Autoradiograph showing an <i>in vitro</i> assay to determine the effect of varied chase times on phosphorylation profiles	ap83
Figure 4.2.5	Autoradiograph showing immunoprecipitation of <i>in vitro</i> phosphorylated CNE by a UL13 antiserum	ap84
Figure 4.2.6	Autoradiograph showing immunoprecipitation of <i>in vitro</i> phosphorylated chased and unchased <i>wt</i> CNE by a UL13 antiserum	ap84
Figure 4.2.7	Autoradiograph showing an <i>in vitro</i> assay for nucleoside specificity of phosphorylation	ap84
Figure 4.2.8	Autoradiograph showing an <i>in vitro</i> assay for phosphate cycling with decreasing unlabelled ATP chase concentrations	ap85
Figure 4.2.9	Autoradiograph showing an <i>in vitro</i> assay for phosphate cycling with decreasing unlabelled GTP chase concentrations	ap85
Figure 4.2.10	Autoradiograph showing the relative migration of the 57, 59 and 62 kDa phosphoproteins	ap86
Figure 4.2.11	Autoradiograph showing an <i>in vitro</i> assay for phosphate cycling over a range of NaCl concentrations	ap86
Figure 4.3.1	Coomassie stained gel of <i>wt</i> virions phosphorylated <i>in vitro</i>	ap88

	at different buffer concentrations	
Figure 4.3.2	Coomassie stained gels of <i>wt</i> virions phosphorylated <i>in vitro</i> at a range of ATP concentrations	ap88
Figure 4.3.3	Coomassie stained gels of <i>wt</i> virions phosphorylated <i>in vitro</i> at different buffer and NaCl concentrations	ap89
Figure 4.3.4	Coomassie stained gel of showing the migration of the UL49 protein in <i>wt</i> and vUL49ep virions	ap89
Figure 4.3.5	Coomassie stained gel showing the effect of a variety of dNTPs on migration of the UL49 protein derived from <i>wt</i> virions	ap90
Figure 4.3.6	Autoradiograph showing the <i>in vitro</i> phosphorylation profile of the UL49 protein in 50 mM MgCl <sub>2</sub> and 50 mM Tris-HCl phosphorylation buffer	ap90
Figure 4.3.7	Coomassie stained gel showing the effect of λ-protein phosphatase and heparin on migration of the UL49 protein	ap90
Figure 4.4.1	Autoradiographs showing <i>in vitro</i> phosphorylation profiles of <i>wt</i> and UL13 mutant infected RSC CNE	ap92
Figure 4.4.2	Autoradiograph showing the effect of an unlabelled ATP chase on radiolabelled <i>wt</i> -infected RSC CNE at a variety of NaCl concentrations	ap93
Figure 4.4.3	Autoradiograph comparing the effects of an unlabelled ATP chase on radiolabelled <i>wt</i> -infected MeWo CNE, RSC CNE and <i>wt</i> virions	ap93
Figure 4.4.4	Autoradiograph showing the effect of various unlabelled ATP chase concentrations on radiolabelled <i>wt</i> -infected RSC CNE	ap93
Figure 4.4.5	Autoradiograph showing an <i>in vitro</i> assay for heparin sensitivity of phosphorylation of the UL13 and UL49 proteins	ap94
Figure 4.4.6	Autoradiograph showing an <i>in vitro</i> assay for heparin sensitivity of the unlabelled ATP chase	ap94
Figure 4.4.7	Autoradiograph showing an <i>in vitro</i> assay to determine the effect of 5, 6-dichloro-1-β-D-ribofuranosylbenzimidazole	ap94

	(DRB) on the phosphorylation profile of MeWo CNE	
Figure 4.5.1	Autoradiograph showing the phosphopeptide profiles of <i>in vitro</i> phosphorylated <i>wt</i> and UL13- <i>lacZ</i> CNE	ap96
Figure 4.5.2	Autoradiograph showing the phosphopeptide profiles of chased and unchased <i>wt</i> and UL13- <i>lacZ</i> CNE phosphorylated at a variety of NaCl concentrations	ap975
Figure 4.5.3	Autoradiograph showing phosphopeptide profiles of the UL49 protein digested with various concentrations of selected proteolytic enzymes	ap98
Figure 4.5.4	Autoradiograph showing the tryptic phosphopeptide profile of the UL49 protein from <i>in vitro</i> phosphorylated <i>wt</i> virions	ap98
Figure 4.5.5	Autoradiograph showing the phosphopeptide profiles of the UL49 protein from <i>in vitro</i> phosphorylated <i>wt</i> RSC CNE	ap99
Figure 4.5.6	Coomassie stained gel showing the phosphorylation induced alteration in migration of the UL49 protein	ap99
Figure 4.5.7	Mass spectrometric analysis of the UL49 protein from phosphatase treated <i>wt</i> virions	ap99
Figure 4.5.8	Mass spectrometric analysis of the UL49 protein from <i>wt</i> virions phosphorylated at 0 M NaCl	ap99
Figure 4.5.9	Mass spectrometric analysis of the UL49 protein from <i>wt</i> virions phosphorylated at 0 M NaCl	ap99
Figure 4.5.10	Mass spectrometric analysis of the UL49 protein from <i>wt</i> virions phosphorylated at 1.5 M NaCl	ap99
Figure 4.5.11	Mass spectrometric analysis of the UL49ep protein from phosphatase treated vUL49ep virions	ap99
Figure 4.5.12	Mass spectrometric analysis of the UL49ep protein from vUL49ep virions phosphorylated at 0 M NaCl	ap99
Figure 4.5.13	Mass spectrometric analysis of the UL49ep protein from vUL49ep virions phosphorylated at 1.5 M NaCl	ap99
Figure 4.5.14	A schematic representation of the 301 residue UL49 protein showing the position of the peptides detected in mass spectra generated from dephosphorylated UL49	100
Figure 4.5.15	Autoradiograph showing the phosphopeptide profile of the	ap101

	UL13 protein from <i>in vitro</i> phosphorylated <i>wt</i> RSC CNE	
Figure 4.5.16	Autoradiograph showing the phosphopeptide profiles of the UL13 protein from <i>in vitro</i> phosphorylated <i>wt</i> RSC CNE	ap101
	UL13 protein from <i>in vitro</i> phosphorylated <i>wt</i> RSC CNE	
Figure 4.5.17	Autoradiograph showing the phosphopeptide profile of the UL13 protein from <i>in vitro</i> phosphorylated <i>wt</i> virions and <i>wt</i> MeWo CNE	ap101
Figure 5.1	A multiple sequence alignment of 10 alphaherpesvirus UL13 homologues	ap103
Figure 5.2	Amino acid sequence alignment of the catalytic cores of cAPK and the HSV-1 PKs encoded by US3 and UL13	105
Figure 5.3	Schematic representation of the positions of the lesions within the three UL13 mutants employed in this study	106
Figure 5.4	Amino acid sequences of the predicted Lys-C and Glu-C peptides containing UL13 PK motif VIII	109
Figure 5.5	Sequences of the Lys-C and Glu-C peptides derived from the N-terminal 100 amino acid residues of the UL13 PK	110
Figure 5.6	The sequence of the 1703.91 Da tryptic peptide representing residues 228 to 242 of the UL49 protein	113
Table 1.1	Conserved sequences indicative of the subdomains found within the catalytic core of PKs	2
Table 1.2	Designation of residue conservation groups in the catalytic domain of PKs	6
Table 1.3	Sequence and the functional properties of regions of cAPK subdomains	7
Table 1.4	Comparison of the Ser/Thr and Tyr PK sequences in two PK subdomains	15
Table 1.5	The eight herpesviruses known to infect humans and their corresponding designations by the International Committee on Taxonomy of Viruses (ICTV)	23
Table 1.6	Summary of the clinical manifestations of the eight herpesviruses known to infect humans	24
Table 1.7	Enzymes encoded by HSV-1	29

Table 1.8	Homologues of the HSV-1 gene US3, showing the size of each encoded protein and the predicted Mr	34
Table 1.9	Proteins identified as targets for phosphorylation by the US3 PK	37
Table 1.10	Homologues of the HSV-1 gene UL13, showing the size of each encoded protein and the predicted Mr	40
Table 1.11	Comparison of the HSV-1-induced PK activities	45
Table 1.12	Genotypes of UL13 mutants	fp47
Table 1.13	Growth characteristics of HSV-1 UL13 mutants on a variety of cell lines	47
Table 1.14	Summary of the compositions of UL13 PK phosphorylation buffers	48
Table 1.15	Substrate specificity of HSV-2 UL13 PK in comparison with CKI and CKII	49
Table 1.16	Summary of the proteins identified to date as targets for the HSV-1 UL13 PK	53

<sup>a</sup> ap = after the page number shown; fp = facing the page number shown

## Abbreviations

A	adenine-containing moiety
Å	Angstrom
APS	ammonium persulphate
ATP	adenosine triphosphate
BPB	bromophenol blue
bp	base pairs
BSA	bovine serum albumin
C	cytosine-containing moiety
C-subunit	catalytic subunit
Calm-k II	calmodulin-dependent protein kinase II
cAMP	cyclic adenosine monophosphate
cAPK	cyclic AMP protein kinase
CAV	cell associated virus
CDK 2	cyclin dependent kinase 2
Ci	Curie
CK I	casein kinase I
CK II	casein kinase II
CNE	crude nuclear extract
ConS	conservation group
cpe	cytopathic effect
cpm	count per minute
CRV	cell released virus
Da	daltons
°C	degrees Celsius
dATP	2'-deoxyadenosine-5'-triphosphate
dCTP	2'-deoxycytidine-5'-triphosphate
dGTP	2'-deoxyguanosine-5'-triphosphate
dH <sub>2</sub> O	deionised water
DNA	deoxyribonucleic acid
dNTPs	deoxynucleotide triphosphates
DR	direct repeat
DRB	5, 6-dichloro-1-β-D-ribofuranosylbenzimidazole
DTT	dithiothreitol
dTTP	2'-deoxythymidine-5'-triphosphate
dUTP	2'-deoxyuridine-5'-triphosphate
EBNA	Epstein-Barr virus nuclear antigen
EDTA	ethylenediaminetetra-acetic acid
EF-1δ	eukaryotic elongation factor 1δ
EGF	epidermal growth factor
EGTA	ethylene glycol-bis (β-aminoethyl ether)-N, N, N', N'-tetraacetic acid
EtOH	ethanol
FCS	foetal calf serum
G	guanine-containing moiety
g	gram
g/l	gram/litre
gp	glycoprotein

---

GST	glutathione S-transferase
GTP	guanosine triphosphate
h	hour
HEPES	N-2-hydroxyethyl piperazine-N'-2-ethane sulphonic acid
HSV	herpes simplex virus
HveA	herpesvirus entry mediator A
HveC	herpesvirus entry mediator C
ICP	infected cell polypeptide
IE	immediate early
Ig	immunoglobulin
IRL	internal long repeat
IRS	internal short repeat
k	kilo ( $10^3$ )
kb	kilobases
kbp	kilobase pairs
kDa	kilodaltons
L-particle	light particle
LATs	latency-associated transcripts
l	litre
LD <sub>50</sub>	the dose at which 50% of the animals are dead
M	molar
MALDI-TOF MS	matrix-assisted laser desorption time-of-flight mass spectrometry
MAPK	mitogen activated protein kinase
mCi	millicurie
MeOH	methanol
mg	milligram
MI	mock infected
min	minute
ml	millilitre
mm	millimetre
mM	millimolar
MnAMP-PNP	Mn <sup>2+</sup> adenylyl imidodiphosphate
moi	multiplicity of infection
Mr	relative mobility
mRNA	messenger ribonucleic acid
Mw	molecular weight
μCi	microcurie
μg	microgram
μl	microlitre
μM	micromolar
NCS	newborn calf serum
nM	nanomolar
NP40	Nonidet P40
Nuc	nucleotide binding site
ORF	open reading frame
<sup>32</sup> P	phosphorus-32 radioisotope
PAA	phosphoamino acid analysis
PAGE	polyacrylamide gel electrophoresis

---

PBS	phosphate-buffered saline
PCR	polymerase chain reaction
pfu	plaque forming unit
pi	post infection
PK	protein kinase
PKA	protein kinase A
PKC	protein kinase C
PKI	protein kinase inhibitor
PMSF	phenylmethylsulphonylfluoride
PVDF	polyvinylidene difluoride
R-subunit	regulatory subunit
R1	large subunit of ribonucleotide reductase
R2	small subunit of ribonucleotide reductase
RE	restriction enzyme
RNA	ribonucleic acid
RNAP II	RNA polymerase II
rpm	revolutions per minute
RR	ribonucleotide reductase
RT	room temperature
<sup>35</sup> S	sulphur-35 radioisotope
SDS-PAGE	sodium dodecyl sulphate-polyacrylamide gel electrophoresis
Sub	substrate binding site
T	thymidine-containing moiety
TEMED	N, N, N', N'-tetramethylethylene diamine
<i>tk</i>	thymidine kinase
TLC	thin layer chromatography
Tris	Tris (hydroxymethyl) aminomethane
TRL	long terminal repeat
TRS	short terminal repeat
U	unique
UL	long unique
US	short unique
UV	ultraviolet
V	volts
<i>vhs</i>	virion host shutoff protein
Vmw	molecular weight in kDa of HSV-induced polypeptides
vol	volume
VP	virion protein
v/v	volume/volume
<i>wt</i>	wild-type
w/v	weight/volume
w/w	weight/weight

## Cell lines

BHK C13	baby hamster kidney cells clone 13
RSC	rabbit skin cell line
MeWo	human melanoma cell line
Vero	African green monkey kidney cell line
Hel	human embryonic lung fibroblast cell line
Hela	human epithelial cell line
HEp-2	human epithelial cell line
HFL	human foetal lung cell line
Neuro-2a	mouse neuroblastoma cell line

## Herpesviruses

Virus name	Common Abbreviation	ICTV designation
Herpes simplex virus type 1	HSV-1	HHV-1
Herpes simplex virus type 2	HSV-2	HHV-2
Varicella-zoster virus	VZV	HHV-3
Epstein-Barr virus	EBV	HHV-4
Human cytomegalovirus	HCMV	HHV-5
Human herpesvirus 6	HHV-6	HHV-6
Human herpesvirus 7	HHV-7	HHV-7
Kaposi's sarcoma-associated herpesvirus	KSHV	HHV-8
Equine herpesvirus 1	EHV-1	EHV-1
Equine herpesvirus 2	EHV-2	EHV-2
Herpesvirus saimiri	HVS	SaHV-2
Channel catfish virus	CCV	IcHV-1
Simian herpesvirus	B virus	CeHV-1
Bovine herpesvirus 2	BHV-2	BoHV-2
Pseudorabies virus	PRV	SuHV-1
Cottontail rabbit herpesvirus	LHV-1	LeHV-1
Marek's disease virus	MDV	GaHV-2
Murine cytomegalovirus	MCMV	MuHV-1 <sup>a</sup>
Herpesvirus ateles	HVA	AtHV-2
Herpesvirus of turkey	HVT	MeHV-1 <sup>b</sup>
Avian infectious laryngotracheitis virus	ILTV	GaHV-1

<sup>a</sup> Murine herpesvirus 1. <sup>b</sup> Meleagrid herpesvirus 1.

**One and three letter abbreviations for amino acid residues**

<b>Amino acid</b>	<b>Three letter code</b>	<b>One letter code</b>
Alanine	Ala	A
Arginine	Arg	R
Asparagine	Asn	N
Aspartic acid	Asp	D
Cysteine	Cys	C
Glutamine	Gln	Q
Glutamic acid	Glu	E
Glycine	Gly	G
Histidine	His	H
Isoleucine	Ile	I
Leucine	Leu	L
Lysine	Lys	K
Methionine	Met	M
Phenylalanine	Phe	F
Proline	Pro	P
Serine	Ser	S
Threonine	Thr	T
Tryptophan	Trp	W
Tyrosine	Tyr	Y
Valine	Val	V

## INTRODUCTION

This thesis examines phosphorylation of the HSV-1 UL13 protein kinase and its target proteins. The introduction will cover three main subjects: protein phosphorylation and protein kinase function, herpesviruses and herpesviral protein kinases. It begins with a general introduction to protein kinases using cyclic AMP-dependent protein kinase, one of the best studied protein kinases, as the basis for a description of protein kinase structure and function. This is followed by a brief introduction to herpesviruses leading to a summary of herpesviral protein kinases, and culminates in a review of the current status of research on the HSV-1 UL13 protein kinase, its homologues in other herpesviruses, and their target proteins.

### 1.1 Protein phosphorylation

Since the discovery of its role in enzyme control by Krebs & Fischer (1956), phosphorylation has been regarded as a ubiquitous mechanism for regulating biochemical pathways. Protein phosphorylation requires covalent modification of specific serine (Ser), threonine (Thr) or tyrosine (Tyr) residues by attachment of the  $\gamma$ -phosphate derived from a nucleoside triphosphate. The nucleoside triphosphate is generally ATP, although in a few cases both ATP and GTP can act as phosphate donors (Hathaway & Traugh, 1982). These modifications can be reversed by hydrolysis of the phosphate ester linkage.

Metabolic pathways, cell division, ion transport and hormone responses are among the processes controlled by protein phosphorylation. In each case, the function of key proteins participating in these processes is modulated by phosphorylation state. Phosphate moieties on proteins can dramatically affect the catalytic activity of an enzyme by allosteric means or by altering the ability of a protein to interact with ligands or other proteins.

The family of proteins responsible for intracellular phosphorylation is the protein kinases (PKs). These proteins can be divided into two main groups based upon their ability to phosphorylate either Ser/Thr or Tyr residues. PKs and protein phosphatases are often themselves targets for regulation by protein phosphorylation as part of the cascades involved in signal transduction pathways (Lin *et al.*, 1992). Protein kinases also play a

key role in signal transduction pathways in prokaryotic cells, as well as prokaryotic cell growth, division and differentiation (Wu *et al.*, 1999; Motley & Lory, 1999).

### 1.1.1 Protein kinases

#### 1.1.1.1 Protein kinase catalytic domains

Amino acid sequences are considered to represent PKs if they include certain key residues found by Hanks *et al.* (1988) to be highly conserved in the catalytic core of known PKs. To identify these residues, Hanks *et al.* (1988) aligned sequences of the catalytic domains of 65 members of the PK family. The analysis was subdivided into two main groups based upon ability to phosphorylate either Ser/Thr or Tyr residues, and included known and putative PKs. In total, 38 Ser/Thr and 27 Tyr PKs were analysed.

Subdomain	Residues	Consensus sequence
I	48-58	xnGxGxx(GAS)xVx
II	69-75	xAnKxnx
III	90-92	xEx
IV	102-104	xnx
V	125-128	x(GVS)(DES)x
VI Ser/Thr	152-173	x(GAT)xxanxxxxxx(HY)RDnK(PLS)cNnx
VI Tyr	152-173	x(GA)(MC)x(YF)nxxxxxxHRDL(RA)A(RA)N(IVC)x
VII	181-188	xnxDFGnx
VIII Ser/Thr	200-209	x(TS)xxax(APS)PEx
VIII Tyr	200-209	xPnx(KR)(TM)(APS)(PL)Ex
IX	219-227	xDxW(SA)xGnx
X	257-259	xn/sx
XI	268-281	xnxxxxxxxxxxRx

**Table 1.1 Conserved sequences indicative of the subdomains found within the catalytic core of PKs** (derived from Hanks *et al.*, 1988; Hanks & Quinn, 1991).

Key: x = any residue; R = amino acid sidechain, n = nonpolar chain R group (M, L, I or V); a = aromatic or ring-containing R group (F, Y, W or H); s = small R group with near neutral polarity (A, G, S, T or P); c = acidic or uncharged polar R group (D, E, N or Q); b = basic polar R group (K, R or H). Residues shown in red are invariant. Residues shown in blue were conserved in 62 or more of the 65 PK sequences analysed. Residues enclosed within brackets signify alternatives for that position. Residue numbers refers to the position within the cAMP-dependent protein kinase (cAPK) sequence.

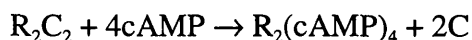
Hanks *et al.* (1988) found that the catalytic domain, which ranged in size from 250 to 300 residues, could be divided into 11 conserved subdomains (I-XI). However, the relative spacing of these subdomains varied from one PK to another. Consensus sequences were identified for each subdomain (see Table 1.1), with 9 invariant and 6 highly conserved residues scattered throughout the PK core. Residues outside the subdomains were also conserved, but to a lesser extent.

The conserved residues within the subdomains were considered to be important for catalytic function, either directly as components of the active site or indirectly by contributing to the formation of the active site through constraints imposed on secondary structure. Non-conserved regions are likely to occur in loop structures folded to allow the essential conserved regions to be positioned correctly. Conserved subdomains VI and VIII contain residues specifically conserved in either the Ser/Thr or the Tyr PKs. This substrate-specific sequence variation is likely to play a role in recognising the correct hydroxyamino acid.

Understanding PK function requires not only the identification of conserved regions but also a knowledge of how they are arranged spatially in the active enzyme. This was facilitated by determination of the crystal structure of a PK.

### 1.1.1.2 Protein kinase structure

This section will focus on one of the better-studied and simplest members of the PK family, the cAMP-dependent protein kinase (cAPK), also known as protein kinase A and formerly called phosphorylase kinase kinase (Walsh *et al.*, 1968). Like most non-oncogenic PKs, cAPK is maintained in an inactive state in the absence of the appropriate signal, in this case cAMP. The inactive tetrameric holoenzyme consists of two regulatory (R) and two catalytic (C) subunits. Binding of cAMP causes the complex to dissociate as follows:



The free catalytic C-subunits can then phosphorylate substrate proteins containing the relevant target sequence.

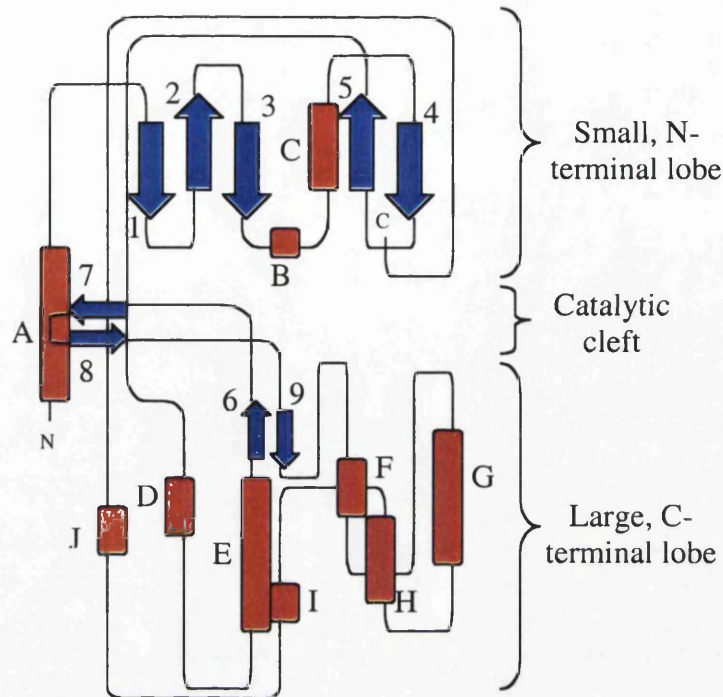
After phosphorylase kinase (Krebs *et al.*, 1959), cAPK was the second PK to be purified and the first PK for which the three-dimensional structure was solved (Knighton *et al.*, 1991a). The relative simplicity of cAPK aided elucidation of its 3-D structure. While in many PKs the regulatory and catalytic components are functional elements of one large protein, in cAPK they are separate, with activation involving subunit dissociation. This allowed the catalytic protein to be studied in the absence of its regulatory subunit. Nonetheless, cAPK has been shown to serve as a good general structural template for the entire PK family.

To date, three structures for cAPK have been reported. All were visualised complexed with a high-affinity 20-amino acid pseudosubstrate inhibitor peptide, PKI(5-24), derived from the N-terminal region of the heat stable PK inhibitor protein. Knighton *et al.* (1991a, b) analysed the binary complex, which comprised the recombinant mouse C-subunit bound to PKI (5-24) (Knighton *et al.*, 1991a). The ternary complex contains both MgATP and PKI(5-24) (Zheng *et al.*, 1993). Bossemeyer *et al.* (1993) solved the structure of the porcine heart C-subunit in a ternary complex with the MgATP analogue MnAMP-PNP.

### 1.1.1.3 cAPK structure

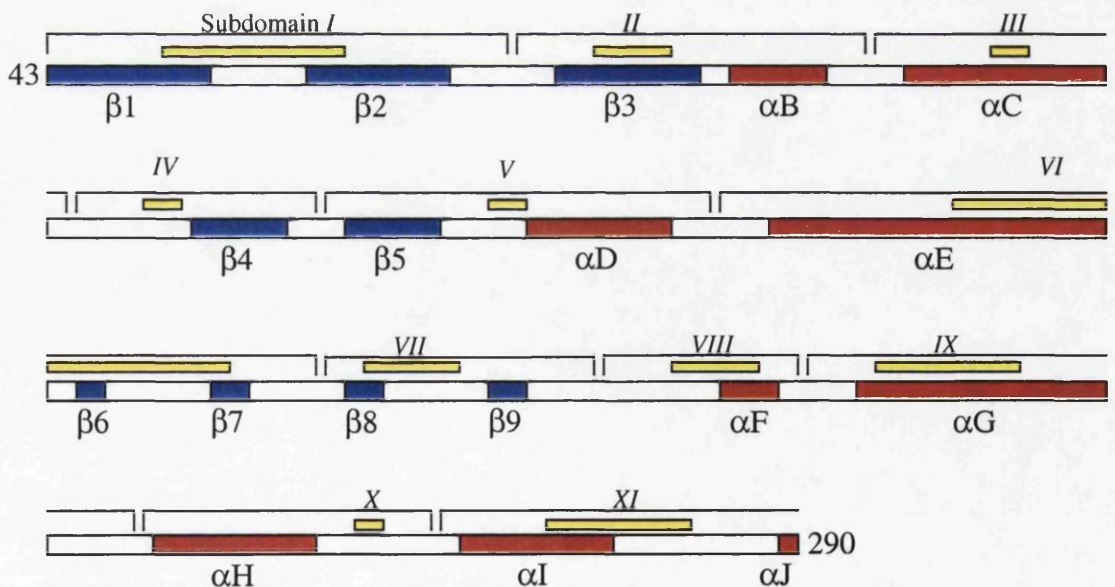
The C-subunit consists of two lobes, one somewhat larger than the other (Fig. 1.1). The smaller lobe is derived primarily from the N-terminal region, while the core of the larger lobe corresponds to the C-terminal region. A deep cleft is situated between the two lobes. In the binary complex the cleft is filled by a portion of the bound inhibitor, and in the ternary complex MgATP is located at the base of the cleft (Knighton *et al.*, 1991a).

Fig. 1.1 shows the general features of the C-subunit. The N-terminus begins with an amphipathic  $\alpha$ -helix that lies primarily along the surface of the large lobe. Within the small lobe the dominant secondary structure is an antiparallel  $\beta$ -sheet comprising five strands. Residues 120-126 link the two lobes and are important for anchoring the adenine moiety. The large lobe is dominated by helices, with a small  $\beta$ -sheet near the cleft that is essential for catalysis, and the 50 residues at the C-terminus wrap around the surface of both lobes (Knighton *et al.*, 1991a).



**Figure 1.1** A schematic representation of the cAPK C-subunit topology.

The blue arrows represent  $\beta$ -strands (size in residues shown in brackets);  $\beta$ 1(9),  $\beta$ 2(8),  $\beta$ 3(8),  $\beta$ 4(6),  $\beta$ 5(7),  $\beta$ 6(2),  $\beta$ 7(3),  $\beta$ 8(3) and  $\beta$ 9(2). The red boxes represent  $\alpha$ -helices,  $\alpha$ A,  $\alpha$ B(6),  $\alpha$ C(13),  $\alpha$ D(8),  $\alpha$ E(19),  $\alpha$ F(4),  $\alpha$ G(16),  $\alpha$ H(10),  $\alpha$ I(10) and  $\alpha$ J(2). Derived from Knighton *et al.* (1991a).



**Figure 1.2** A linear alignment of the structural subdomains in residues 43 to 290 of cAPK and corresponding conserved regions.

The yellow boxes represent the positions of the conserved sequences, the blue blocks represent  $\beta$ -strands, and red blocks represent  $\alpha$ -helices. Derived from Singh (1994) and Hanks *et al.* (1988)

Residues 40 to 280 constitute the conserved PK catalytic core. Fig. 1.2 shows a schematic representation in which the subdomains are aligned with the conserved sequences.

#### 1.1.1.4 Conservation and function of cAPK residues

Singh (1994) performed a multiple sequence alignment of 53 Ser/Thr and 33 Tyr PKs, mapping the results onto the 3-D structure of cAPK and calculating the degree of conservation of the residues within the catalytic core of cAPK. Each residue in the catalytic domain was grouped into one of five major (1 to 5) and three minor (6 to 8) groups (see Table 1.2), depending upon its conservation. A variety of other factors were also considered, such as whether residues were buried within the protein structure or exposed at the surface.

Group	Conserved within Ser/Thr PKs	Conserved within Tyr PKs	Conserved within Ser/Thr and Tyr PKs
1	Conserved	Conserved	Conserved
2	Conserved	Conserved	Varied
3	Conserved	Varied	Varied
4	Varied	Conserved	Varied
5	Varied	Varied	Varied
6	Conserved	Varied	Conserved
7	Varied	Conserved	Conserved
8	Varied	Varied	Conserved

**Table 1.2 Designation of residue conservation groups in the catalytic domain of PKs (derived from Singh (1994)).**

Group 5 has the greatest number of members. Residues in this group vary throughout the PK family and account for 101 (41%) of the 248 residues in the cAPK catalytic domain. The majority (69%) of these residues are located on the surface of the protein, suggesting that group 5 residues represent the exposed surface of the protein. In contrast, 86% of the residues in group 1 are buried within the protein. These represent the inner core of the enzyme, with the strict conservation of these hydrophobic residues underlining their importance. The majority of the residues in groups 2, 3 and 4 are also buried within the enzyme. However, unlike group 1 residues, they lie outside the enzyme's inner catalytic core. It is likely that group 3 and 4 residues include those involved in distinguishing

between Ser/Thr and Tyr substrates. The majority of the group 2 to 4 residues occur in the large C-terminal domain.

	← I →										← II →										
cAPK seq.	49	L	G	T	G	S	F	G	R	V	69	Y	A	M	K	I	L	82	L	K	Q
ConS.		1	1	5	1	3	1	1	5	1		2	1	1	1	5	1		5	5	5
Sub.			S	S	S	S	S												S	S	
Nuc.		N	R		R	P	P	C		N		N		P							
Access		B	B						B	B		B	B	B	B	B	B				B
	← III →					← IV →					← V →										
cAPK seq.	90	N	E	K	103	L	V	K	120	M	E	Y	V	127	E	M	F	S	H		
ConS.		5	1	4		1	7	5		3	1	1	4		3	1	5	5	4		
Sub.															S	S	S				
Nuc.						N				N	N	N			R						
Access		B	B	B		B	B			B	B	B			B				B		
	← VI →										← VII →										
cAPK seq.	132	L	R	136	G	165	R	D	L	K	P	E	N	L	L	182	V	T	D		
ConS.		1	4		5		1	1	1	2	4	2	1	2	I		1	4	1		
Sub.			S		S		S	S	S	S	S										
Nuc.							P	P		R	P		N					N	M		
Access		B					B	B	B	B			B	B	B		B	B			
	← VIII →					← IX →															
cAPK seq.	185	F	G	F	A	198	L	C	G	T	P	E	Y	L	A	P	E	220	D	W	
ConS.		1	1	1	1		4	5	2	2	4	4	1	4	1	1	1		1	4	
Sub.				S			S	S	S	S	S	S	S	S	S	S	S				
Nuc.																					
Access		B	B	B	B		B	B				B	B	B	B	B	B		B	B	
	← X →										← XI →										
cAPK seq.	222	W	A	L	G	V	L	I	230	E	M	A	A	G	Y	P	P	239	F	A	
ConS.		1	1	1	1	1	1	1		1	1	3	4	1	5	5	1		5	5	
Sub.										S		S	S	S	S			S	S		
Nuc.																					
Access		B	B	B	B	B	B	B		B	B	B	B			B	B				
	← XII →										← XIII →										
cAPK seq.	241	D	Q	P	I	Q	256	I	Y	E	K	I	V	S	269	L	R	N	L		
ConS.		3	5	5	5	5		3	3	5	5	6	5	5		1	5	5	2		
Sub.		S	S	S				S	S												
Nuc.																					
Access								B			B					B			B		
	← XIV →										← XV →										
cAPK seq.	273	L	Q	V	D	L	T	K	R												
ConS.		2	5	5	2	1	5	5	1												
Sub.																					
Nuc.																					
Access		B	B						B												

**Table 1.3 Sequence and the functional properties of regions of cAPK subdomains.**

Residue number refers to the position within cAPK. The conservation group is indicated by ConS. Substrate binding sites are shown as Sub and marked by an S, while nucleotide binding sites are shown as Nuc and are denoted by identifiers N, R, M, P and C depending upon whether the residue contacts the nucleotide, ribose, metal atoms, phosphate or a non-specific group. The buried residues of cAPK are shown in Access and are denoted by B. Derived from Singh (1994).

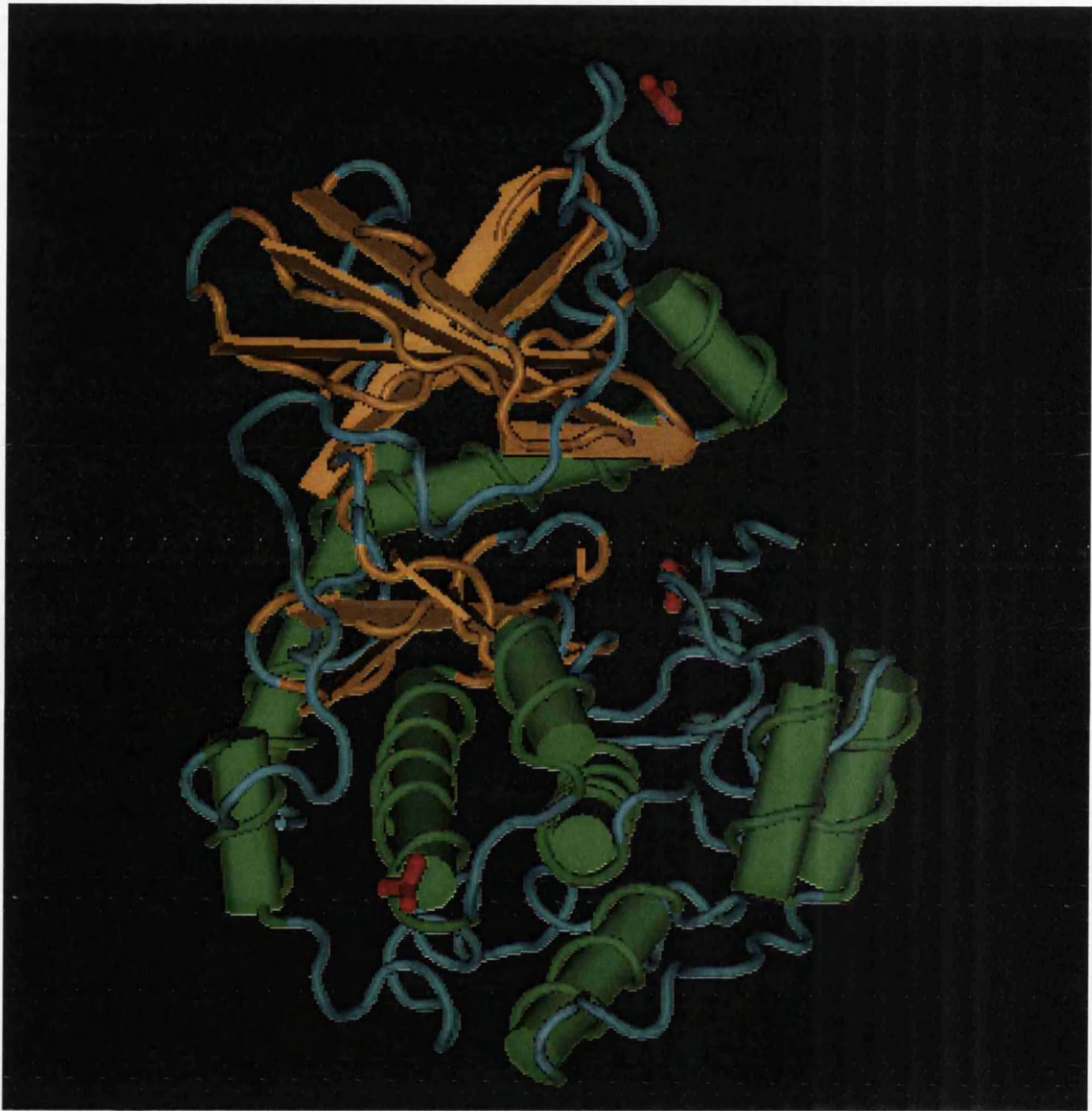


**Figure 1.3 3-D structure of the catalytic core of the C-subunit of cAPK complexed with PKI(5-24) and MnATP.**

This represents the ternary complex of cAPK solved by Zheng *et al.* (1993). The small lobe, corresponding to the nucleotide binding fold (residues 40 to 126) can be seen as dominantly  $\beta$ -strands, shown here as orange arrows. The large lobe (residues 127 to 280) can be seen as dominantly  $\alpha$ -helices, shown here as green barrels. The catalytic cleft can be seen between the two lobes.

Singh (1994) assigned functions to 50 residues in the cAPK catalytic domain. Nucleotide binding activity was attributed to 21 residues and substrate binding activity to 37 residues, and 8 residues were identified as interacting with both MgATP and substrate. These data are summarised in Table 1.3.

In most cases the regions implicated in nucleotide or substrate interactions correlate with the consensus sequences identified by Hanks *et al.* (1988). In some cases, the residues identified as interacting with substrate are distinct from the PK consensus sequences. For example, in subdomain VIII the APE consensus sequence is conserved, but it is the 8 residues immediately N-terminal which are implicated in substrate interaction. Some subdomains (e.g. subdomain XI) show conservation of buried residues but lack functional interactions. This implies that they are of conformational importance.

Table 1.3 shows that 13 of the 21 (62%) residues involved in nucleoside triphosphate binding are conserved in all PKs analysed, whereas only 8 of the 37 (22%) substrate binding residues are conserved. This may reflect the fact that PKs have maintained a narrow nucleoside specificity but have developed a broad substrate specificity.

### 1.1.2 Subdomain conformations

Fig. 1.3 shows the 3-D ternary structure of cAPK complexed with PKI(5-24) (Fig. 1.5) and MnATP. The N- and C-terminal lobes can be clearly seen, as can the catalytic cleft. This section will discuss the important features of each of the lobes, and the linker region connecting them together.

#### 1.1.2.1 N-terminal lobe

##### Glycine-rich loop

Non-PK mononucleotide triphosphate binding proteins share a characteristic consensus sequence Gly-X-X-Gly-X-Gly-Lys (Wierenga & Hol, 1983). This conserved nucleotide binding sequence forms part of a structure called the Rossmann fold, comprising a sheet of mostly parallel  $\beta$ -strands with helices above and below the plane of the sheet. The motif begins with a  $\beta$ -strand followed by a sharp turn and an  $\alpha$ -helix. The glycine-rich loop is typically located at this first turn, and is the only region within the Rossmann fold motif that shows sequence conservation.

While comparable to the Rossmann fold motif, the nucleotide binding motif within PK subdomain I does exhibit significant differences. The PK consensus sequence, Gly-X-Gly-X-X-Gly-X-Val, was shown by Bossemeyer *et al.* (1993) to form part of a  $\beta$ -strand, turn,  $\beta$ -strand structure. The  $\beta$ -strands are stabilised by backbone hydrogen bonds between Gly<sup>50</sup> and Val<sup>57</sup>, both invariant residues, and between the invariant Gly<sup>52</sup> and highly conserved Gly<sup>55</sup> (Hanks & Quinn, 1991). One of the most important motifs in the conserved catalytic core, the glycine-rich loop lies parallel to and embraces the entire nucleotide moiety. It is very mobile, demonstrating sufficient conformational flexibility to anchor the phosphoryl group and avoid steric clash with ATP (Bossemeyer *et al.*, 1993). It is also exquisitely sensitive to what occupies the active site cleft (Aimes *et al.*, 2000). Of the three conserved Gly residues, Gly<sup>52</sup> is the most important for catalysis because it allows the backbone amide of Ser<sup>53</sup> at the tip of the loop to hydrogen bond to the  $\gamma$ -phosphate of ATP (Grant *et al.*, 1998).

The glycine-rich loop in the small lobe is the first of two essential conserved loops, the second being the catalytic loop within subdomain VI (Fig. 1.6). Both loops lie on the surface that lines the cleft between the two lobes. Seven of the invariant residues are located either in the loops themselves or connected directly with loop residues, providing a finely tuned scaffold for communication at the active site (Knighton *et al.*, 1991a).

### **Invariant lysine residue**

The lysine residue in subdomain II (Table 1.3), Lys<sup>72</sup>, appears to be functionally irreplaceable (Chen *et al.*, 1987) and invariant in all PKs. Situated within  $\beta$ -strand 3 (Fig. 1.2), Lys<sup>72</sup> is thought to be directly involved in the phosphotransfer reaction (Kamps & Sefton, 1986). The position of Lys<sup>72</sup> is fixed by its ionic interaction with the invariant glutamic acid (Glu<sup>91</sup>) (Fig. 1.4) in subdomain III. Subdomain III is the final subdomain situated in the small lobe of the PK catalytic subunit.

#### **1.1.2.2 Linker region**

The two lobes of the PK are joined by an extended coil, composed of two strands (Fig. 1.1). One of these strands is derived from the N-terminal region and one from the C-terminal region. Residues 120-127, from subdomain V (Table 1.3), form one strand of

the linker region. The subdomains following subdomain V are considered to lie in the C-terminal lobe. A stretch of amino acids within the last 70 residues of the C-terminal lobe also lie in the linker region. These C-terminal residues lie outside the conserved catalytic core (Knighton *et al.*, 1991a).

### 1.1.2.3 C-terminal lobe

The central core of the catalytic domain consists of subdomains VI and VII (Fig. 1.2). These catalytically important, conserved sequence motifs (Table 1.3) lie in two loops that connect  $\beta$ -strands at the surface of the cleft. Their importance is underlined by their conservation in PKs of prokaryotes and eukaryotes.

#### Catalytic loop

A highly conserved loop extends from Arg<sup>165</sup> through Asn<sup>171</sup> and is termed the “catalytic loop” (Fig. 1.6). The loop, Arg<sup>165</sup>-Asp<sup>166</sup>-Leu<sup>167</sup>-Lys<sup>168</sup>-Pro<sup>169</sup>-Glu<sup>170</sup>-Asn<sup>171</sup>, contains two invariant residues (Asp<sup>166</sup> and Asn<sup>171</sup>) and two highly conserved residues (Arg<sup>165</sup> and Leu<sup>167</sup>), and is a hub for communicating with different parts of the molecule. Arg<sup>165</sup> precedes the loop and interacts with Thr<sup>197</sup>, the autophosphorylation site (Fig. 1.6). The loop is stabilised by Asn<sup>171</sup> hydrogen bonding with the backbone carbonyl of Asp<sup>166</sup> (Taylor *et al.*, 1993). In the ternary complex, Asp<sup>166</sup> is oriented towards the pseudo-phosphorylation site in PKI(5-24) (Fig. 1.5), leading to the suggestion that Asp<sup>166</sup> acts as the catalytic base, abstracting the proton from the attacking hydroxyl group (Bossemeyer *et al.*, 1993).

Subdomain VII contains the most conserved short stretch in the catalytic domain (Table 1.3). It is flanked for two positions on either side by hydrophobic or near-neutral residues. This motif forms a tight loop between  $\beta$ -strands 8 and 9 (Taylor *et al.*, 1993). Very large inserts, in excess of 60 residues, can occur between subdomains VII and VIII.

The remaining conserved sequence motifs appear to confer structural stability and do not interact directly with substrates at the active site. The Glu in subdomain VIII (Glu<sup>203</sup>) and the arginine in subdomain XI (Arg<sup>280</sup>) form an ionic pair, while the highly conserved aspartic acid in subdomain IX (Asp<sup>223</sup>) hydrogen bonds with the two backbone amides that precede the catalytic loop.

### 1.1.3 Protein kinase function

PK function will be explained through the interactions occurring between the PK, MnATP/MgATP and substrate. This is a highly complex situation, with many interactions involving residues from different subdomains meeting in the active conformation of the enzyme.

#### 1.1.3.1 MnATP/MgATP binding

Binding of MgATP can be divided into four parts: the purine base, the ribose, the triphosphate group and the metal ions. The interactions can be illustrated as shown in Fig. 1.4, where MgATP has been substituted by the analogue MnAMP-PNP (Bossemeyer *et al.*, 1993)

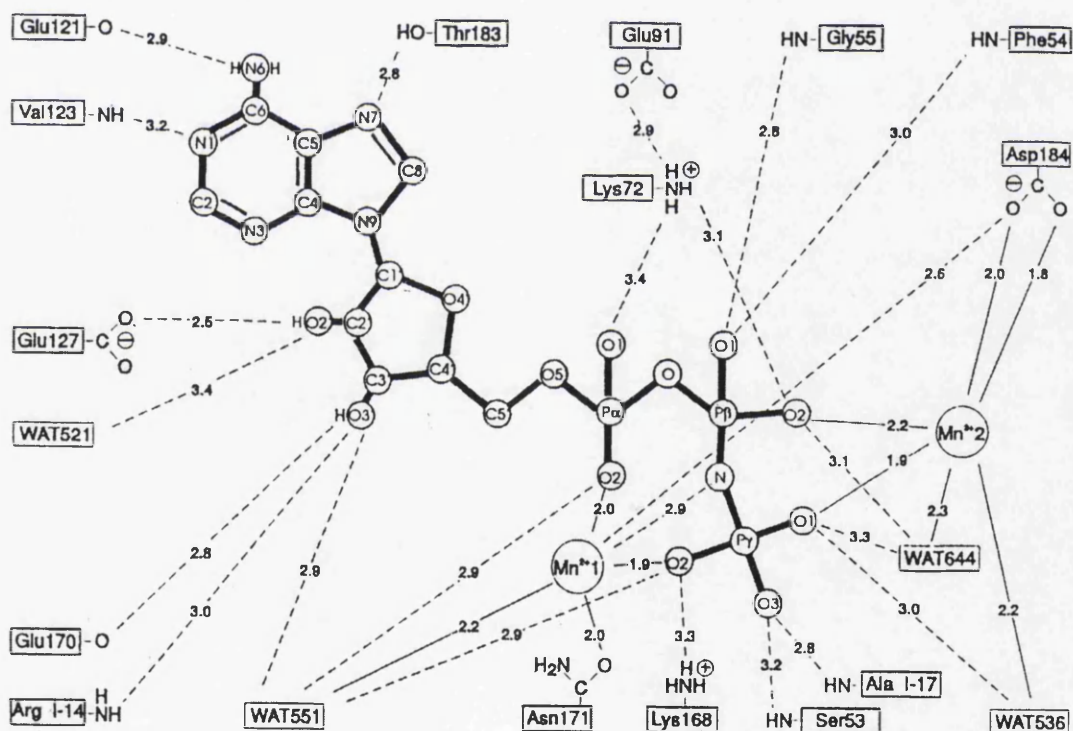


**Figure 1.4 Schematic diagram of the interactions between the MgATP substitute MnAMP-PNP and the cAPK catalytic subunit.**

Dashed lines correspond to hydrogen bonds ( $<3.5 \text{ \AA}$ ) and thin solid lines indicate metal-ligand bonds (reproduced from Bossemeyer *et al.*, 1993).

### 1.1.3.2 Purine binding

Fig. 1.4 shows the hydrogen bonds between the adenine base and three residues in the enzyme. Two hydrogen bonds exist between N6 and the backbone carbonyl of Glu<sup>121</sup>, and N1 and backbone amide of Val<sup>123</sup>. Both Glu<sup>121</sup> and Val<sup>123</sup> lie within PK subdomain V (Table 1.3). The third hydrogen bond is between N7 and the hydroxyl group of Thr<sup>183</sup> in subdomain VII (Bossemeyer *et al.*, 1993). Singh (1994) identified Val<sup>123</sup> and Thr<sup>183</sup>, but not Glu<sup>121</sup>, as nucleotide binding residues (Table 1.3), and whereas Glu<sup>121</sup> is conserved across the PK family, Val<sup>123</sup> and Thr<sup>183</sup> are conserved only in Tyr PKs. Although not shown in Fig. 1.4, non-polar interactions with one side of the purine ring occur with the highly conserved Leu<sup>49</sup> and invariant Val<sup>57</sup>, while further non-polar interactions from the opposite direction come from Leu<sup>173</sup> in subdomain VI.

### 1.1.3.3 Ribose binding

The sidechain of Glu<sup>127</sup> and the carbonyl group of Glu<sup>170</sup> are hydrogen bonded to the ribose hydroxyl groups (Fig. 1.4). A third hydrogen bond occurs between the 3'OH and the sidechain of the inhibitor peptide substrate residue Arg I-14 (Fig. 1.5).

### 1.1.3.4 Triphosphate binding

Binding of the triphosphate group is complex, involving a large number of hydrogen bonds. Fig. 1.4 shows the stabilising hydrogen bonds formed to the phosphate oxygen atoms by the mainchain amides of Ser<sup>53</sup>, Phe<sup>54</sup> and Gly<sup>55</sup> (subdomain I), the sidechains of Lys<sup>72</sup> (subdomain II) and Lys<sup>168</sup> (subdomain VII) and the backbone amide of Ala I-17 (Fig. 1.5). The invariant residues within the highly conserved phosphate-binding flap (Gly<sup>50</sup>, Gly<sup>52</sup> and Val<sup>57</sup>) lie parallel to the nucleotide but do not interact directly with any of the phosphoryl groups (Bossemeyer *et al.*, 1993).

Both Lys<sup>72</sup> (subdomain II) and Asp<sup>184</sup> (subdomain VII) are invariant (Table 1.3) and are considered to be essential residues, since mutating either residue completely abolishes PK activity (Taylor *et al.*, 1993; Gibbs *et al.*, 1992). Buechler & Taylor (1989) demonstrated the close proximity of these two residues by crosslinking experiments. Bossemeyer *et al.* (1993) showed that Lys<sup>72</sup> ion-pairs with the non-transferable  $\alpha$ - and  $\beta$ -phosphates of MgATP (Fig. 1.4) and forms a salt bridge to the carboxyl group of the invariant Glu<sup>91</sup>. However, Lys<sup>72</sup> is too far away from the catalytic site to participate in the

immediate catalytic act. Asp<sup>184</sup> chelates the activating metal ion, shown in Fig. 1.4 as Mn<sup>2+</sup>, which in turn binds the  $\beta$  and  $\gamma$ -phosphate group oxygens. When  $\beta$ - and  $\gamma$ -phosphates are present, divalent metals are required for positioning of these phosphates. Heberg *et al.* (1999) showed that complexes containing two metal ions are the most stable.

Invariant residue Asn<sup>171</sup> interacts indirectly with phosphoryl oxygens via Mn<sup>2+</sup> (Fig. 1.4). In addition, Asn<sup>171</sup> forms a hydrogen bond with the backbone carbonyl of Asp<sup>166</sup>, stabilising the catalytic loop. The hydroxyl of the substrate phosphotransfer site, or P-site, serine is 2.7 Å from the carbonyl oxygen of Asp<sup>166</sup>, an ideal position for a concerted phosphotransferase reaction.

### 1.1.4 Protein kinase-substrate interactions

The crystal structure of cAPK revealed at least three factors which are important for substrate recognition. Firstly, recognition of the substrate to be phosphorylated. Secondly, recognition of positively charged residues N-terminal to the residue to be phosphorylated. Finally, the presence of a hydrophobic pocket responsible for substrate-specific variations.

#### 1.1.4.1 cAPK substrate consensus sequence

The position of the peptide consensus sequence is firmly fixed and precisely oriented in relation to the enzyme by a combination of ion pairs, hydrogen bonds and hydrophobic interactions. Fig. 1.5 shows the cAPK substrate recognition sequence as described by Knighton *et al.* (1991b). It represents the 20-amino acid peptide inhibitor, PKI (5-24), used in derivation of the crystal structure of cAPK.

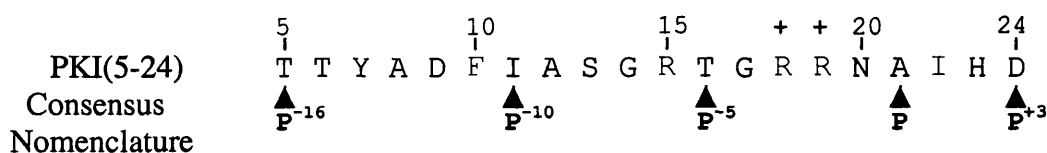


**Figure 1.5** Sequence of PKI (5-24), an inhibitor peptide of cAPK derived from the N-terminal region of a naturally occurring heat stable PK inhibitor protein.

Residues important for peptide recognition are shown in blue; +, indicates the positions of the basic residues integral to the consensus sequence (derived from Knighton *et al.*, 1991b).

The substrate recognition sequence of cAPK is characterised by two basic residues, usually arginines, followed by one intervening small residue preceding the site of phosphotransfer. The phosphate acceptor site, either Ser or Thr, is followed immediately by a large hydrophobic residue. In the case of PKI(5-24) the Ser has been replaced with an Ala to create an inhibitor peptide with poorer affinity (Knighton *et al.*, 1991b).

#### 1.1.4.2 Substrate binding

The substrate-binding residues are widely dispersed both in the linear sequence and on the surface of the enzyme. The portion of the substrate which contains the consensus recognition sequence lies within the large lobe, along the surface of the cleft.

#### 1.1.4.3 Ion pairs

The cAPK residues Glu<sup>127</sup>, Glu<sup>170</sup> and Glu<sup>230</sup> are important in substrate binding. Singh (1994) showed that Glu<sup>127</sup> is conserved in Ser/Thr PKs, residue Glu<sup>170</sup> is conserved as an acidic and uncharged polar residue (Asp, Glu, Asn or Gln) in Ser/Thr PKs or as Ala or Arg in Tyr PKs, and Glu<sup>230</sup> is conserved in all PKs. Both Glu<sup>170</sup> and Glu<sup>230</sup> are situated in the large lobe of the PK, and Glu<sup>127</sup> is situated in the coil connecting the two lobes. These residues characteristically recognise basic substrate residues. In the structure of the binary (Knighton *et al.*, 1991a) and the ternary complexes (Bossemeyer *et al.*, 1993), substrate residue ArgI-15 makes ion pairs with Glu<sup>230</sup> and Glu<sup>170</sup>. A second substrate residue, ArgI-14, forms ion pairs with Glu<sup>127</sup>. Knighton *et al.* (1991a) identified a further ion pair of ArgI-14-Glu<sup>331</sup>, but neither Bossemeyer *et al.* (1993) nor Singh (1994) registered this interaction.

#### 1.1.4.4 Hydrogen bonds and hydrophobic interactions

As well as the interactions seen in the binary complex, the ternary complex shows that the sidechain of ArgI-14 forms a hydrogen bond to the 3'-hydroxyl group of the ribose and also to Thr<sup>51</sup> in the glycine-rich flap. The substrate analogue therefore interacts directly with the small lobe of the PK as well as with the large lobe and connecting coil structure. In addition to these interactions, the sidechain of IleI-18 lies in a hydrophobic pocket provided by Pro<sup>202</sup>, Leu<sup>205</sup> and Leu<sup>198</sup>, and the backbone amide of IleI-18 forms a hydrogen bond with the backbone carbonyl of Gly<sup>200</sup>. The helical segment of the peptide

is amphipathic, with its hydrophobic face lying in a hydrophobic pocket on the surface of the large lobe (Knighton *et al.*, 1991a).

### 1.1.5 Protein kinase substrate specificity

The discovery of the Tyr PKs (Eckhart *et al.*, 1979) raised the issue of how amino acid substrate specificity is achieved. Despite a few dual-specificity protein kinases, such as the MAP kinase kinase that can phosphorylate both Ser/Thr and Tyr substrates, most PKs thus far characterised are either Ser/Thr- or Tyr-specific. Although both Ser/Thr and Tyr PKs have very similar catalytic domain structures, a number of residues within the catalytic domain are highly conserved within each type of PK, creating Ser/Thr or Tyr PK specific signature motifs (Hanks *et al.*, 1988).

#### 1.1.5.1 Substrate specific sequence variations

Hanks *et al.* (1988) identified subdomains VI and VIII as containing residues specifically conserved in either the Ser/Thr or Tyr PKs. The sequences are shown in Table 1.4.

		Subdomain VI					
Ser/Thr PK		D	L	K	P	E	N
Tyr PK (for vertebrate members of the Src family)		D	L	R	A	A	N
Tyr PK (for all others)		D	L	A	A	R	N

		Subdomain VIII								
Ser/Thr PK		G	T/S	X	X	Y/F	X	A	P	E
Tyr PK		X	P	I/V	K/R	W	T/M	A	P	E

**Table 1.4 Comparison of the Ser/Thr and Tyr PK sequences in two PK subdomains.** Subdomain sequences as defined by Hanks *et al.* (1988). Variable residues are shown in blue.

The most striking indicator of amino acid specificity is found in subdomain VI. In cAPK this lies between Asp<sup>166</sup> and Asn<sup>171</sup>, both residues that are implicated in ATP binding. The second region in subdomain VIII lies immediately on the N-terminal side of the APE consensus. This region is highly conserved among Tyr PKs, with less conservation among Ser/Thr PKs (Hanks *et al.*, 1988). Singh (1994) also showed that cAPK residues 168 and 204 demonstrate substrate specific variation, and attributed substrate binding functions to Tyr<sup>204</sup> and phosphate binding functions to Lys<sup>168</sup>.

The majority of differences between Ser/Thr PK and Tyr PK sequences occurred in the large C-terminal lobe, with less than a quarter of them occurring in the N-terminal lobe (Singh, 1994). This seems reasonable, since the N-terminal lobe is primarily involved in nucleotide binding. However, there are substrate-specific residue variations in the N-terminal lobe and linker region. For example,  $\beta 4$  and part of  $\alpha C$ , corresponding to subdomains III and IV, are tightly conserved in Tyr PKs but not in Ser/Thr PKs.

Attempts to alter the substrate specificity of the PK by switching the motifs from a Ser/Thr to a Tyr PK simply inactivated the enzyme (Hanks *et al.*, 1988). Purified Tyr PKs show an exquisite selectivity for tyrosine and do not phosphorylate serine or threonine even when they are substituted for tyrosine in a known acceptor sequence (Weinmaster & Pawson, 1986). Conversely, most Ser/Thr PKs do not phosphorylate tyrosine.

#### 1.1.5.2 Discrimination between Ser/Thr and Tyr protein kinases

The structure of the catalytic subunit of cAPK bound to ATP and an inhibitor peptide gave an idea of the structural restrictions imposed upon substrate binding. The substrate:ADP complex of cAPK showed that the hydroxyl of the Ser at the phosphotransfer site (P-site) is 2.7 Å from the carboxyl oxygen of the proposed catalytic base (Asp<sup>166</sup>). This is an ideal position to undergo a concerted phosphotransferase reaction. Because the serine and threonine hydroxyls are both linked to the  $\beta$ -carbon atom, they are equivalent in terms of catalysis. The only difference is that the extra methyl group has to be accommodated in the active site without interfering with phosphate transfer if threonine is to be phosphorylated. From the structure it became clear that if the substrate peptide backbone was maintained in the same position, the tyrosine side chain would not fit correctly into the active site so that the O<sup>4</sup>-hydroxyl group could be positioned to receive the phosphate group.

When the structure of the epidermal growth factor (EGF) receptor protein-tyrosine kinase was modelled on the known cAPK structure (Knighton *et al.*, 1993) the predicted general folding of the EGF receptor catalytic domain was similar to that of cAPK. However, the backbone of the substrate peptide must be positioned differently at the active site in order

to accommodate the tyrosine and prevent its hydroxyl group from protruding into the ATP-binding site. Conversely, if the catalytic cleft of the protein-tyrosine kinase is configured to allow the hydroxyl group of tyrosine to accept phosphate this will preclude phosphorylation of serine and threonine, since their hydroxyls would not penetrate deep enough to act as acceptors. This raises interesting questions concerning the dual-specificity PKs, such as MAP kinase kinase.

The 3-D structure of the unphosphorylated, inactive insulin receptor protein-tyrosine kinase catalytic domain helped reveal why this enzyme is specific for Tyr (Hubbard *et al.*, 1994). As predicted from sequence similarities (Hanks *et al.*, 1988) the overall folding of the polypeptide chain is the same. With the exception of inserts, such as a large one between  $\alpha 4$  and  $\alpha 5$ , the general secondary structure is conserved. With one exception, invariant residues in the catalytic core are located in the same position in all known PK structures. However, as expected, there are some differences in the small lobe and in the orientation of the two lobes relative to each other. The major differences between the enzymes are in the activation loop in the large lobe near the cleft interface.

### 1.1.6 Protein kinase mechanism

As mentioned above, non-PK nucleotide binding proteins possess a conserved Lys in their glycine-rich loop structure. This is almost analogous to the invariant Lys<sup>72</sup> in PK subdomain III, but does demonstrate some functional differences. In adenylate kinase the Lys residue forms hydrogen bonds with both the  $\beta$ - and  $\gamma$ -phosphoryl groups, and is proposed to follow the  $\gamma$ -phosphoryl group during transfer (Schulz *et al.*, 1992). However, as shown in Fig. 1.4, in PKs the conserved active site lysine (Lys<sup>72</sup>) is bonded to  $\alpha$  and  $\beta$ -phosphoryl oxygens (Bossemeyer *et al.*, 1993). Lys<sup>72</sup> is situated in the third anti-parallel  $\beta$ -strand (Fig. 1.2), and contacting the  $\gamma$ -phosphoryl group would require large structural movements of the  $\beta$ -strand. Bossemeyer *et al.* (1993) suggested that a better candidate for stabilising the transition state of the  $\gamma$ -phosphoryl is Lys<sup>168</sup>. Although this residue is conserved in Ser/Thr PKs but is present as an Arg in Tyr PKs, both are capable of neutralising the negative charge of the  $\gamma$ -phosphoryl group during transfer, thus lowering the free energy of the transition state.

A catalytic base is absolutely required to abstract a proton from the attacking hydroxyl group during PK catalysis (Yoon & Cook, 1987). It has been suggested that Asp<sup>166</sup> exerts this function (Fig. 1.6). Asp<sup>166</sup> is an invariant amino acid found not only in all PKs but also in phosphotransferases, and is well positioned to hydrogen bond to the hydroxyl group of a Ser modelled into the position of Ala I-17 (Fig. 1.5).

### 1.1.6.1 The phosphotransferase reaction

The transfer of the  $\gamma$ -phosphoryl group to the hydroxyl group of an amino acid on a substrate has been the subject of a great deal of research. The structure of the cAPK ternary complex (Knighton *et al.*, 1991a) set the stage for understanding the catalytic reaction. There is a short distance between the  $\gamma$ -phosphate and AlaI-17 (3.7Å), indicating that this could be the position of the substrate residue to be phosphorylated. Substituting the AlaI-17 with a serine gives an effective model of the situation within the active site, and essentially changes the PK-inhibitor structure obtained by Knighton *et al.* (1991b) to an effective model of PK-substrate interaction (Bossemeyer *et al.*, 1993). This gives a distance between the oxygen of the seryl group (seryl O $\gamma$ ) and the  $\gamma$ -phosphorus atom as 2.7Å. As stated above, a catalytic base is required for proton abstraction from SerI-17 O $\gamma$ . It was initially thought that this may be the carboxylate group of Asp<sup>166</sup> at a distance of 2.8Å, as this structure is clearly poised towards a P $\gamma$  transition state (Bossemeyer *et al.*, 1993). However, more recent research found that Asp<sup>166</sup> does not accept a proton at any of the reaction steps. Asp<sup>166</sup> is less important in the phosphoryl transfer than it is in maintaining the configuration of the active site. In fact the side chain of Lys<sup>168</sup> is necessary to stabilise the intermediate reaction states (Hutter & Helms, 1999).

### 1.1.6.2 Autophosphorylation

If cellular life is to function in an orderly manner, the switching on and off of PKs and phosphatases is as crucial for their function as their catalytic activity. Multiple sequence alignments indicate that all PKs are likely to have similar structures, with conserved features identified in the subdomains of all PKs (Hanks *et al.*, 1988). However, there is a wide degree of variability in other parts of the PK domain, and different PKs may contain additional domains or subunits. As a result, several different mechanisms for PK control are evident.

A variety of control mechanisms have been identified. These can involve regulation by additional, non-catalytic subunits or domains, or control by phosphorylation and dephosphorylation of the PK itself, a process referred to as autophosphorylation. Autophosphorylation is a feature common to many PKs, but its physiological significance was questioned since it was considered that regulation of an autocatalytic event would be excessively complex (Hallenbeck & Walsh, 1983). Indeed, there are multisubunit PKs which undergo interpeptide autophosphorylation. However, it has been shown that a number of PKs, for example protein kinase C (PKC), are capable of intrapeptide autophosphorylation, in which a single polypeptide chain phosphorylates itself.

A key aspect of regulation demonstrated by many, but not all PKs, is activation by phosphorylation of residues within a segment located between subdomains VII and VIII of the catalytic domain. Two areas have been identified, both lying in the same region. The activation segment, which spans the conserved DFG (subdomain VII) and APE (subdomain VIII) sequences, corresponding to residues 184-208 in cAPK. The activation loop (Johnson *et al.*, 1996) is located between 5 and 10 residues N-terminal to the conserved APE motif, corresponding to residues 196-201 in cAPK (Romano *et al.*, 1998). The conformation of the activation segment, controlled by phosphorylation, plays a key role in the transformation of an inactive to an active PK. Conformational changes in the protein are stimulated, leading to the correct disposition of substrate binding and catalytic groups and relief of steric blocking to allow access of substrates to the catalytic site.

Steinburg *et al.* (1993) showed definitively that phosphorylation in cAPK is promoted by an autocatalytic event which is crucial for activation. Previously, Knighton *et al.* (1991a) demonstrated the structural importance of Thr<sup>197</sup>, which forms hydrogen bonds with the charged sidechains of Arg<sup>165</sup> and Lys<sup>189</sup>, and the possible roles of phosphorylation in promotion of activation. Bossemeyer *et al.* (1993) showed that the ternary complex of porcine cAPK was phosphorylated on one residue, Thr<sup>197</sup>. The activation segment of cAPK was shown to contain the sequence RTWT\*L, with T\* the phosphorylated Thr<sup>197</sup>. This sequence is consistent with the consensus recognition sequence for cAPK, RXXT\*/S\*Hy, where X denotes any residue and Hy denotes a hydrophobic residue

(Hardie & Hanks, 1995). However, this is not the case with all PKs. For example, neither CDK2 nor MAPK exhibit conservation between activation segment and recognition sequences, indicating that phosphorylation by other PKs is required for activation of these enzymes (Taylor *et al.*, 1995).

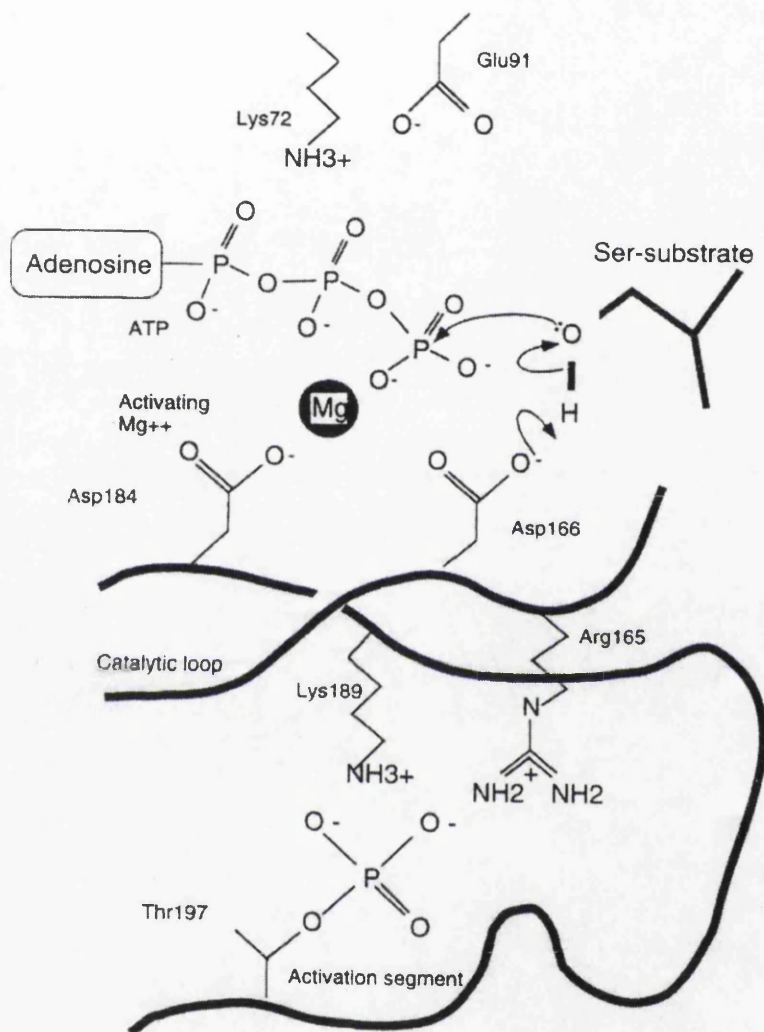


**Figure 1.6** A schematic representation of ATP and some of the key residues at the catalytic site and activation segment of cAPK. Reproduced from Johnson *et al.* (1996).

The structure and functional interactions of cAPK have been described above. However, since PK activation by autophosphorylation is intrinsically linked to PK function, the relevant interactions are summarised in Fig 1.6. In addition, the relative position of the activation segment is shown. As detailed earlier, the adenine is positioned in a hydrophobic pocket and the ribose is stabilised by hydrogen bonds. The phosphates are aligned for catalysis by interactions with the main chain nitrogens of the glycine-rich loop, Lys<sup>72</sup> and interactions with Mg<sup>2+</sup> ions, notably the activatory Mg<sup>2+</sup>, which binds to

the  $\beta$ - and  $\gamma$ -phosphate groups of ATP and to Asp<sup>184</sup>. The catalytic aspartate (Asp<sup>166</sup>), located within the catalytic loop, is presumed to act as a base to remove a proton from the protein substrate hydroxyl group, and the resulting ion is then positioned to attack the  $\gamma$ -phosphate of ATP. The activation segment, beginning with Asp<sup>184</sup>, consists of a  $\beta$ -strand ( $\beta$ 9), followed by a loop containing the autophosphorylation site, Thr<sup>197</sup>. The final residue of the activation segment is Glu<sup>208</sup>, a highly conserved residue of the APE motif, and is hydrogen bonded to Arg<sup>280</sup>. The position of the activation segment appears to be important in aligning the catalytic residues.

It is known that the phosphothreonine (Thr<sup>197</sup>-P) contacts His<sup>87</sup>, Arg<sup>165</sup>, Lys<sup>189</sup> and Thr<sup>195</sup>, the phosphate compensating for the cluster of positively charged residues (Taylor & Radzio-Andzelm, 1994). The contact of the phosphothreonine of the activation segment to Arg<sup>165</sup>, adjacent to the catalytic base (Asp<sup>166</sup>), appears especially important, providing a direct link between the phosphorylated, charged residue and the catalytic site. Adams *et al.* (1995) showed that mutating Thr<sup>197</sup> in cAPK resulted in reduced catalytic efficiency. The reduced activity was specifically due to lower ATP affinity and reduced rates of phosphoryl transfer, not to peptide substrate binding affinity.

The importance of Thr<sup>197</sup>-P in PK activation is apparent, but its role remains ambiguous. It is clear that Thr<sup>197</sup>-P stabilises the positively charged cluster Arg<sup>165</sup>, Lys<sup>189</sup> and His<sup>87</sup>. The interaction with Arg<sup>165</sup> may facilitate the orientation of Asp<sup>166</sup>, the catalytic base, while interactions between Thr<sup>197</sup>-P and Lys<sup>189</sup> may help orientate Asp<sup>184</sup>, which contacts the activatory Mg<sup>2+</sup>. Contact between Thr<sup>197</sup>-P and His<sup>87</sup>, which is situated in the N-terminal domain, may promote correct domain-domain interactions, critical for ATP binding.

In addition to autophosphorylation within the activation loop, multiple autophosphorylation can occur on specific residues located in the N- or C-terminal portions of the polypeptide chain, as in PKC (Fig. 1.7). However, an individual molecule of PKC does not have every site modified.

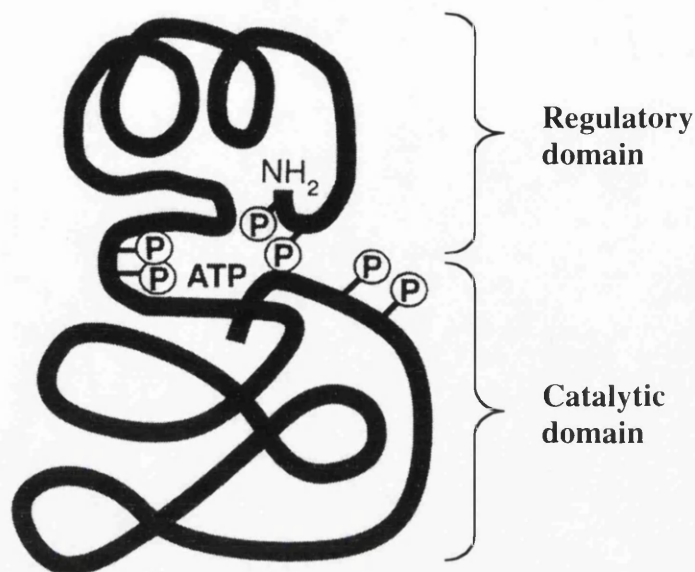


**Figure 1.7 Illustration of PKC with the six autophosphorylation sites located close to the catalytic site.**

Individual phosphorylation sites are marked. Reproduced from Flint *et al.*, 1990.

As already outlined, intramolecular autophosphorylation, especially at multiple sites of a single polypeptide chain, would require significant protein flexibility. Alternatively, phosphorylation could be intermolecular. The first step in the activation of the dimeric insulin receptor upon insulin binding is an intermolecular autophosphorylation event that occurs between two catalytic domains. As many as seven tyrosines can be autophosphorylated, but kinetically the first three to be phosphorylated lie within the activation loop.

An autophosphorylation event may produce a variety of effects. Bronstein *et al.* (1986) showed that autophosphorylation of purified calmodulin kinase II (Calm-k II) dramatically inhibited PK activity and enhanced substrate selectivity. It was hypothesised that autophosphorylation of Calm-k II may be a mechanism for limiting phosphorylation to physiological substrates. For example, when incubated with several substrates, Calm-k II phosphorylated glycogen synthase, then itself, in the process dramatically reducing its ability to phosphorylate histones. This type of mechanism could enhance substrate specificity *in vivo* and limit phosphorylation to selected proteins.

## 1.2 The Herpesviruses

### 1.2.1 General properties of herpesviruses

The *Herpesviridae* are a large family of eukaryotic viruses comprising at least 112 members, divided into three sub-families, the *Alpha-*, *Beta-* and *Gammaherpesvirinae*. They infect a wide range of vertebrates, including fish, amphibians, reptiles, birds, marsupials and mammals, including humans (Roizman & Sears, 1993) and at least one invertebrate, the oyster (Comps & Cochenec, 1993). Herpesviruses exhibit a high degree of host specificity, usually being limited to a single species in natural infections. However, single animal species can be host to several herpesviruses. The eight herpesviruses associated with humans form the focus of the following introduction to herpesviruses.

### 1.2.2 Human herpesviruses

#### 1.2.2.1 Biological properties

The eight herpesviruses known to infect humans are shown in Table 1.5. Most are widespread in both the developed and the underdeveloped world (Whitely & Schlitt, 1991), and humans remain the sole known reservoir for transmission, which occurs via person to person contact. Symptoms, which are summarised in Table 1.6, cover a broad spectrum of clinical manifestations, from minor lesions to severe and life-threatening encephalopathies.

Virus	ICTV designation	Subfamily	Genus	Review
HSV-1	HHV-1	<i>Alphaherpesvirinae</i>	Simplexvirus	Subak-Sharpe & Dargan (1998)
HSV-2	HHV-2	<i>Alphaherpesvirinae</i>	Simplexvirus	Levine (1992)
VZV	HHV-3	<i>Alphaherpesvirinae</i>	Varicellovirus	Gelb (1990)
EBV	HHV-4	<i>Gammaherpesvirinae</i>	Lymphocryptovirus	Miller (1990)
HCMV	HHV-5	<i>Betaherpesvirinae</i>	Cytomegalovirus	Britt (1996)
HHV-6	HHV-6	<i>Betaherpesvirinae</i>	Roseolovirus	Levy (1997)
HHV-7	HHV-7	<i>Betaherpesvirinae</i>	Roseolovirus	Levy (1997)
KSHV	HHV-8	<i>Gammaherpesvirinae</i>	Rhadinovirus	Levy (1997)

**Table 1.5** The eight herpesviruses known to infect humans and their corresponding designations by the International Committee on Taxonomy of Viruses (ICTV).

Virus	Associated illness
HSV-1	80-95% of oral lesions, or "cold sores," and 30-50% of genital lesions are caused by HSV-1. Primary infection and reactivation give similar symptoms. In rare cases it causes conjunctivitis, herpetic whitlow, keratitis and encephalitis. Neonatal infections are often life threatening.
HSV-2	5-20% of oral lesions and 50-70% of genital lesions are caused by HSV-2. Primary infection and reactivation give similar symptoms. In rare cases it causes conjunctivitis, herpetic whitlow, keratitis and encephalitis. Neonatal infections are often life threatening.
VZV	Primary infection: chicken pox- a rash which appears 14-15 days post-infection, accompanied by a fever. Reactivated infection, "shingles," appears at the relevant dermatome often accompanied by extreme pain.
HCMV	Primary infection: enlargement and fusion of macrophages often occurs, Usually asymptomatic but can be fatal. Reactivation can occur. Infection is problematic in immunocompromised individuals. Symptoms include gastro-enteritis and retinitis.
HHV-6	Infant rash exanthem subitum
HHV-7	Febrile illness
EBV	Primary infection is often asymptomatic in young children, but occurs as infectious mononucleosis in older children and adults. Associated with Burkitt's lymphoma and nasopharyngeal carcinoma.
KSHV	Associated with Kaposi's sarcoma, a vasculated nodular skin lesion

**Table 1.6 Summary of the clinical manifestations of the eight herpesviruses known to infect humans.**

### 1.2.3 HSV-1 viral architecture

The HSV virion is composed of four morphologically distinct structures (Fig. 1.8), the DNA core, the icosahedral nucleocapsid, the amorphous tegument and the outer lipid envelope from which the glycoprotein spikes protrude (Dargan, 1986; Beers *et al.*, 1994).

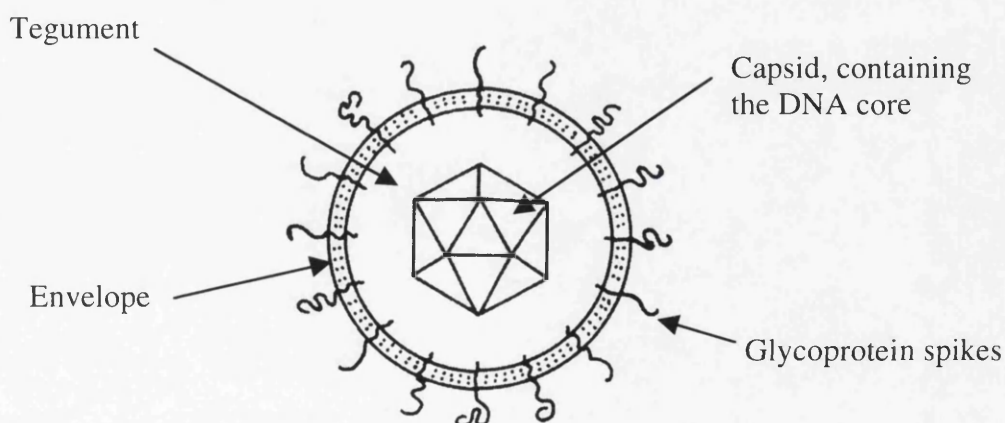


**Figure 1.8 Schematic representation of a herpesvirus particle.**

The core contains the viral genome in a tightly packed structure (Booy *et al.*, 1991). The capsid is approximately 125 nm in diameter, and is composed of 162 capsomeres, of which 150 are hexameric (hexons) and 12 pentameric (pentons), and 320 triplexes that

provide intercapsomeric connections (Wildy *et al.*, 1960; Schrag *et al.*, 1989; Zhou *et al.*, 1994). The hexons and pentons are composed of VP5 (coded by gene UL19) with VP26 (UL35) located at the tips of the hexons, while the intercapsomeric triplex is composed of one copy of VP19C (UL38) and two copies of VP23 (UL18). VP24 (UL26, 5' portion) is a protease involved in capsid formation, and VP21 (UL26, 3' portion) and VP22a (UL26.5) are the major and minor scaffolding proteins, respectively.

The tegument is an amorphous proteinaceous layer (Zhou *et al.*, 1999) which lies between the nucleocapsid and envelope (Wildy *et al.*, 1960). It consists of at least 18 proteins, the functions of many of which have not been fully elucidated. Certain functions related to morphogenesis, uncoating and regulation of gene expression have been assigned to its component proteins.

The virion is enclosed by a lipid envelope (Wildy *et al.*, 1960) containing protruding glycoprotein spikes (Wildy *et al.*, 1960; Stannard *et al.*, 1987) which vary in size from 8-24 nm (Stannard *et al.*, 1987). Thus far eleven glycoproteins have been identified (reviewed by Spear, 1993; Haarr & Skulstad, 1994) gB, gC, gD, gE, gG, gH, gI, gJ, gK, gL and gM encoded by the genes UL27, UL44, US6, US8, US4, UL22, US7, US5, UL53, UL1 and UL10, respectively. Of these, gB, gD, gH and gL are essential for infectivity in cell culture (Cai *et al.*, 1988; Ligas & Johnson, 1988; Desai *et al.*, 1988; Hutchinson *et al.*, 1992).

A species of membrane-enclosed particles termed Light particles (L particles) were identified by Szilágyi & Cunningham (1991). The L particles resembled HSV virions in appearance, but lacked the viral nucleocapsid and were not infectious. However, differences in the phosphoprotein content suggested that L particles were genuine products of the HSV-1 infectious process and not merely virions which formed without the inclusion of a nucleocapsid or lose their nucleocapsid during preparative handling.

#### 1.2.4 Classification and evolution

Historically, herpesviruses were subdivided into three subfamilies, *Alpha-*, *Beta-* and *Gammaherpesvirinae*, according to biological properties (Roizman *et al.*, 1981). Genetic content is now the chief tool for classifying herpesviruses.

While herpesviruses are highly divergent, conservation of a subset of core genes across the three subfamilies suggests a common evolutionary origin. It is believed that herpesviruses evolved with their hosts, allowing McGeoch & Cook (1994) and McGeoch *et al.* (1995) to propose an evolutionary timescale (Fig. 1.9). Herpesvirus evolution is thought to have proceeded through mutational and recombinational processes, including large scale genomic rearrangements, gene capture and gene duplications (McGeoch, 1989; McGeoch & Cook, 1994).

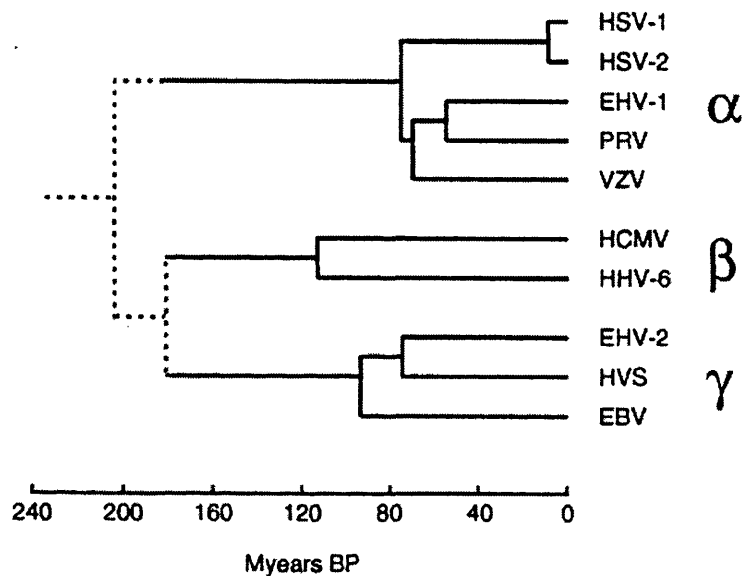


**Figure 1.9 A phylogenetic tree for the herpesviruses.**

Derived from herpesvirus sequence comparisons, the time scale (millions of years before present) is based on the hypothesis that the viruses have co-specified with their hosts. Broken lines indicate regions of lower confidence. Reproduced from McGeoch *et al.* (1995).

## 1.2.5 Genetic properties of herpesviruses

### 1.2.5.1 Genome features

Herpesvirus genomes vary in size from 125 to 250 kbp and contain from 70 to 200 genes (Roizman & Sears, 1990, 1993). All genomes investigated contain direct or inverted repeat sequences located internally or at the genome termini.

### 1.2.5.2 HSV-1 genome

The genome of HSV-1 (Fig. 1.10) is a 152 kbp linear molecule of double-stranded DNA (McGeoch *et al.*, 1985, 1986, 1988), consisting of two covalently linked regions, L and

S. Each region comprises a unique region (UL, 107.9 kbp and US, 13 kbp) flanked by inverted repeats, RL (9 kbp) and RS (6.5 kbp) (McGeoch *et al.*, 1988). The sequences of RL and RS are unrelated, with the exception of a direct repeat (the *a* sequence) of approximately 400 bp located at the genome termini. One copy of the *a* sequence is present at the S terminus, but the L terminus sometimes contains more. The *a* sequence is also present at the L-S joint as an inverted copy (Wagner & Summers, 1978).

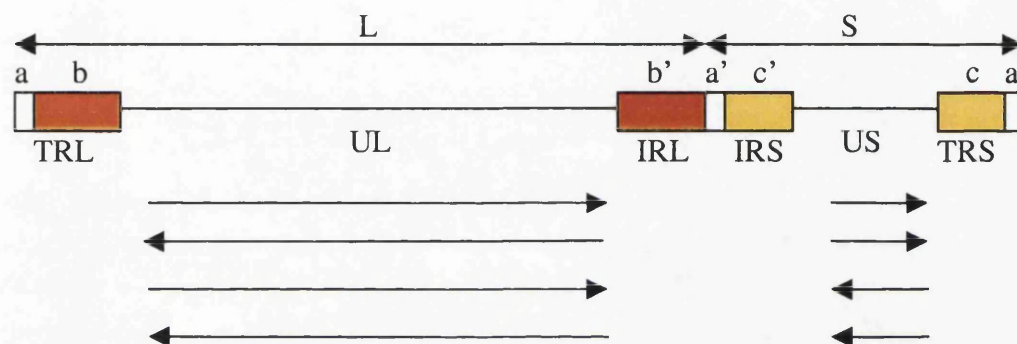


**Figure 1.10 Schematic representation of the HSV-1 genome.**

Showing the 2 covalently linked components, L and S (double headed arrows) which contain unique elements UL and US (solid lines) flanked by inverted repeats (red and yellow rectangles). The *a* sequence is represented by the unshaded box and is present at each end of the genome and in an inverted orientation at the L-S junction. The L and S region can invert relative to each other to produce four isomers (single headed arrows).

Recombination between the repeat sequences results in inversion of UL and US (Sheldrick & Berthelot, 1974). Four equimolar populations, differing with respect to the relative orientations of the two unique regions, exist in virion DNA (Hayward *et al.*, 1975).

The complete sequence of the HSV-1 strain 17<sup>+</sup> contains 152,260 residues and encodes at least 77 genes. The UL region encodes 59 genes, and the US region encodes 13. The inverted repeats encode four genes in duplicate. The genome contains three origins of DNA replication, one in UL (*ori<sub>L</sub>*) and one in RS (*ori<sub>S</sub>*; two copies).

### 1.2.6 The infectious cycle of HSV-1

Infection begins with binding of viral glycoproteins to the cell surface, followed by fusion with the plasma membrane and release of the tegument and capsid into the cytoplasm. A variety of targets appear to be employed in viral attachment. gC binds to heparin sulphate proteoglycan, and gD interacts with a human TNF receptor-like

molecule designated herpesvirus entry mediator (HveA) (Montgomery *et al.*, 1996). HSV-1 was also found to interact with a poliovirus receptor-related protein, designated HveC (Geraghty *et al.*, 1998) whose cellular distribution suggests it may be a prime mediator for HSV-1 infection of mucosal surfaces and spread to the nervous system.

It is thought that capsids then use the microtubule network to traverse the cytoplasm to the nuclear pores (Penfold *et al.*, 1994). Sodeik *et al.* (1997) showed that the capsid, having shed the tegument proteins, binds dynein, a cytoplasmic component responsible for direction of chromosomes and membrane organelles along microtubules (Mitchison, 1988). Once at the nucleus, the capsid probably releases its viral DNA through the nuclear pores by an unknown mechanism.

Certain tegument proteins also migrate to the nucleus. These include the UL41 and UL48 proteins. The UL41 protein possesses host shut-off activity, and is thus designated virion host shut-off protein (*vhs*) (Kwong *et al.*, 1988). *Vhs*, which displays limited amino acid sequence homology to the fen-1 nuclease family, accelerates mRNA degradation during the early stages of HSV infection through endoribonucleolytic cleavage (Elgadi & Smiley, 1999). VP16, encoded by UL48, serves multiple functions, including transcriptional activation of viral IE genes, a role in virus assembly and maturation and downregulation of *vhs*.

All HSV-1 genes are transcribed in the nucleus (Wagner & Roizman, 1969) by the cellular RNA polymerase II (Costanzo *et al.*, 1977). They are expressed in an ordered cascade. The first genes transcribed are the immediate early (IE) or  $\alpha$  genes, followed by the early (E) or  $\beta$  genes and finally the late (L) or  $\gamma$  genes (Swanstrom & Wagner, 1974; Honess & Roizman, 1974).

Transcription of the IE genes is stimulated by VP16 (Batterson & Roizman, 1983; Campbell *et al.*, 1984). Four of the five IE proteins ICP27, ICP22 and in particular ICP0 (Everett, 1984) and ICP4 (Preston, 1979), have a regulatory role in initiating E gene expression (reviewed by Hayward, 1993; Subak-Sharpe & Dargan, 1998). The fifth IE protein, ICP47, plays a role in inhibiting antigen presentation by infected cells (Jugovic *et al.*, 1998). E gene transcription is not stimulated in the absence of IE proteins.

Expression of E genes signals the onset of viral DNA synthesis and expression of L genes. These encode mainly the viral structural proteins. Their transcription levels are enhanced during DNA replication and peak 8-10 h pi, persisting for the remainder of the lytic cycle (Hones & Roizman, 1974; Harris-Hamilton & Bachenheimer, 1985).

Gene	Status	Protein function
UL2	NE	Uracil-DNA glycosylase
UL5	E	Component of DNA helicase-primase complex; possesses helicase motifs
UL12	NE	Deoxyribonuclease; role in maturation/packaging of DNA
UL13	NE	Protein kinase
UL23	NE	Thymidine kinase
UL26	E	Protease; acts in virion maturation
UL30	E	Catalytic subunit of replicative DNA polymerase
UL39	NE	Ribonucleotide reductase large subunit (ICP6, Vmw136, R1)
UL40	NE	Ribonucleotide reductase small subunit (Vmw38, R2)
UL50	NE	Deoxyuridine triphosphatase
US3	NE	Protein kinase

**Table 1.7 Enzymes encoded by HSV-1**

Enzymes shown in blue are directly involved in DNA replication, those shown in red are indirectly involved in DNA replication. E indicates that the function is absolutely required for viral growth in cell culture, and NE that it is not.

HSV-1 encodes a number of enzymes (Table 1.7), the majority of which are involved, directly or indirectly, in viral DNA replication. DNA replication (reviewed by Challberg, 1991; Boehmer & Lehman, 1997) appears to initiate at distinct virus specific structures in the nucleus, designated replication compartments (Quinlan *et al.*, 1984), with the entire nucleus becoming involved as infection proceeds (Roizman & Sears, 1996). It is proposed that the DNA circularises in the nucleus (Jacob & Roizman, 1977) by ligation of the terminal *a* sequences (Davison & Wilkie, 1983), and is replicated by a rolling circle mechanism (Roizman, 1979).

Seven HSV-1 genes are essential for viral DNA replication, two of which are shown in Table 1.7. UL5, UL8 and UL52 primarily form the helicase/primase complex. UL30 and

UL42 represent the catalytic and accessory subunit of a heterodimeric DNA polymerase. UL29 encodes a single stranded DNA-binding protein, and the UL9 protein acts as an origin-binding protein with helicase activity.

DNA replication produces “endless” molecules which must be cleaved for packaging into preformed capsids. The signal for cleavage has been determined as the *a* sequence.

### 1.2.7 Virus assembly and release

The mechanism by which tegument proteins assemble around the capsid is unknown, and may occur in the nucleus or cytoplasm. The envelope consists of altered host cell membranes containing viral glycoproteins, probably derived from a Golgi component. The virion is released from the cell by exocytosis (Rixon, 1993).

### 1.2.8 Latency

Following primary infection and replication, HSV-1 can be transported to the trigeminal ganglia by retrograde transport through the axons (Cook & Steven, 1973; Kristensson *et al.*, 1986), where it establishes latency. The genome is not integrated into the host genome (Mellerick & Fraser, 1987), and the number of viral genome copies within individual latently infected neurons is extremely variable (Sawtell *et al.*, 1998).

The only expression known to occur during HSV latency occurs from a 10.4 kb fragment within RL/RS (Stevens *et al.*, 1987; Deatly *et al.*, 1987; Stevens *et al.*, 1988). The latency-associated transcripts (LATs) accumulate during latent infection (Spivack & Fraser, 1988). LAT-negative mutants retain their ability to become latent, but their ability to reactivate is hindered (Javier *et al.*, 1988; Ho & Mocarski, 1989; Hill *et al.*, 1990; Trousdale *et al.*, 1991). Despite much research, the molecular mechanisms of latency remain elusive (reviewed by Preston, 2000; Millhouse & Wigdahl, 2000).

## 1.3 Herpesviral protein kinases

Phosphorylation of viral and cellular proteins occurs during the lytic infection of cells by herpesviruses (Pereira *et al.*, 1977; Marsden *et al.*, 1978; Wilcox *et al.*, 1980; Kennedy *et al.*, 1981). It is possible that some of these proteins are phosphorylated by virally encoded PKs. It is difficult to distinguish virally encoded PK activities from those of the

host cell on a biochemical basis (Stevely *et al.*, 1985). Therefore, the number, origin and substrate specificity of herpesviral PKs was elucidated when DNA sequence data became available.

Searches for amino acid sequence motifs diagnostic of conserved regions within PK catalytic domains identified three potential PKs in herpesviruses: the HSV-1 US3 and UL13 gene products (Table 1.7) and the large subunit of ribonucleotide reductase (RR; encoded by gene UL39).

### **1.3.1 Ribonucleotide Reductase (UL39)**

#### **1.3.1.1 Ribonucleotide reductase function**

Ribonucleotide reductase (RR) catalyses the conversion of ribonucleotides to the corresponding deoxyribonucleotides, essential for *de novo* synthesis of DNA (Reichard, 1993). Many herpesviruses encode an active RR, the active enzyme consisting of homodimeric large (R1) and small (R2) subunits in an  $\alpha_2\beta_2$  configuration (Conner *et al.*, 1994).

The HSV-1 R1 (1R1) and HSV-2 R1 (2R1) subunits are 1137 and 1142 amino acid residues in size respectively, and possess an additional N-terminal domain in comparison to eukaryotic, prokaryotic and other viral counterparts (Nikas *et al.*, 1986). Proteolytic degradation studies located RR activity to the C-terminal two-thirds of 1R1, leading to the suggestion that the unique N-terminal domain of the HSV protein may be functionally distinct (Clements *et al.*, 1977). Potential bifunctionality of R1 was reinforced when it was found that R1 mRNA demonstrated IE kinetics, whereas R2 mRNA was not expressed until early times postinfection (Clements *et al.*, 1977).

#### **1.3.1.2 Ribonucleotide reductase protein kinase activity**

Sequence analysis of 2R1 identified regions corresponding to eight of the eleven PK domains clustered within the N-terminal 411 residues. Eight of the nine conserved residues indicative of these PK subdomains were present in 2R1. Sequence analysis of 1R1 also identified PK subdomains, but only six of the nine conserved residues were present (Chung *et al.*, 1989; Ali *et al.*, 1992). Fig. 1.11 shows the relevant sequence details.



groups found 1R1 capable of transphosphorylating histone and calmodulin, attributing the inability of other groups to reproduce these results as due to HSV-1 strain variations. Ali (1995) performed a study of R1 PK activity across a broad variety of HSV-1 and HSV-2 strains, finding that the R1 subunit was consistently capable of autophosphorylation but not transphosphorylation.

It was perhaps no surprise when 1R1 was eventually found to be a target for phosphorylation by cellular casein kinase II (CKII), with multiple phosphorylation sites mapping to the N-terminal domain (Langelier *et al.*, 1998; Conner, 1999). Residual amounts of CKII were shown to contaminate immunoprecipitated 1R1, explaining the apparent autophosphorylation-positive but transphosphorylation-negative nature of the R1 PK. In proving that the N-terminal domain of 1R1 does not possess intrinsic PK activity, these data strongly suggest that all previous results were due to contaminating cellular PKs, principally CKII (Conner, 1999). In this respect, this train of events provides a signal lesson in the pitfall of research in protein kinases.

### 1.3.2 HSV-1 US3

#### 1.3.2.1 Identification of the US3 ORF

McGeoch *et al.* (1985) identified the US3 gene within the HSV-1 genome (Fig. 1.12). Mapping experiments detected the 5'-termini of two mRNA species in this region, both specifying a 481 residue protein with an Mw of 52,831 (McGeoch *et al.*, 1985).

McGeoch & Davison (1986) compared the sequences of the predicted products of HSV-1 US3 and its homologue VZV ORF66 with available PK sequences. Both proteins demonstrated strongest homology to CDC28, a PK involved in yeast cell division. The best conserved region resides in an 80 amino acid region of US3 (residues 295-376) and contains PK subdomains VI to IX which include the DFG and APE consensus sequences. A careful search of EBV ORFs failed to identify a US3 homologue (McGeoch & Davison, 1986). HSV-1 US3 is now known to have homologues only among the *Alphaherpesvirinae* (Table 1.8).

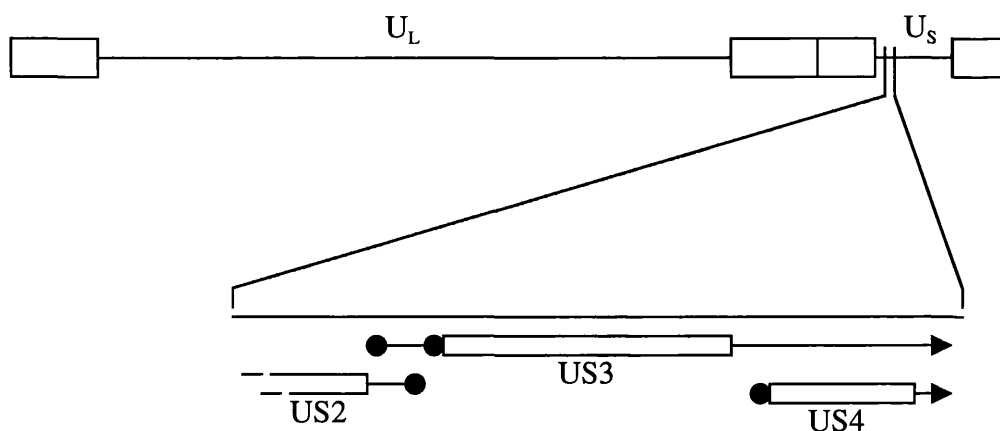


**Figure 1.12 Genomic location and organisation of the US3 gene.**

The upper part of the figure shows a schematic representation of the HSV-1 genome, with unique regions shown as lines and major repeat elements as open boxes. The lower part of the figure shows a 3 kb section of the short unique ( $U_S$ ) region containing the US3 gene. The positions and orientations of mRNAs for genes US2, US3 and US4 are shown by arrows. Filled circles indicate 5' termini of mRNAs (two for gene US3) and open boxes the locations of predicted protein coding regions (adapted from Rixon & McGeoch, 1984; McGeoch & Davison, 1986).

Virus	Gene	Size of protein (amino acid residues)	Mw of protein
HSV-1	US3	481	52 831
HSV-2	US3	481	52 674
VZV	ORF66	393	43 677
PRV	US3	334	36 879
EHV-1	ORF69	382	42 541
HVT	US3	358	41 200
MDV	US3	402	44 700
ILTV	ORF2	471	53 800

**Table 1.8 Homologues of the HSV-1 gene US3, showing the size of each encoded protein and the predicted Mr.**

Derived from McGeoch *et al.* (1985); McGeoch *et al.* (1987); Daikoku *et al.* (1993); Davison, (1982); Davison & Scott (1986); Zhang *et al.* (1990); Katan *et al.* (1985); Telford *et al.* (1992); Zelnik *et al.* (1993); Brunovskis & Velicer (1995) and Kongsuwan *et al.* (1995).

A fuller analysis of the HSV-1 US3 protein was performed by Hanks *et al.* (1988). The predicted catalytic domain was aligned with 64 known or putative PKs. Conserved PK subdomains and consensus sequences were identified as shown in Fig. 1.13.

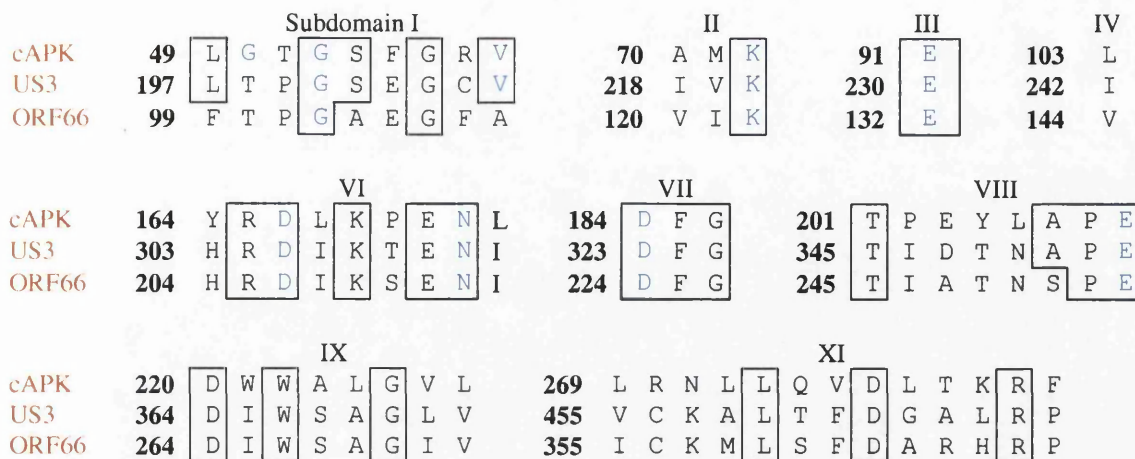


**Figure 1.13** Amino acid sequence alignment of HSV-1 US3 and VZV ORF66 with cAPK.

Subdomain numbering is in line with Hanks *et al.* (1988). Boxed residues are conserved between cAPK and the putative PKs. Blue residues are highly conserved or invariant in known PKs. Numbers refer to the first residue in the relevant sequence.

Both HSV US3 and VZV ORF66 deviate from the classic PK consensus sequence in the nucleotide binding domain. The established PK consensus sequences of subdomains I and II are GxGxxGxV followed 11 to 28 residues later by AxL. In the predicted US3 gene product the corresponding sequences are TxGxxGxV followed 13 residues later by IxL. Sequence alignment of 65 PKs showed the HSV US3 PK was the only to vary at Glu<sup>50</sup> and only two others vary at Ala<sup>70</sup> (Hanks *et al.*, 1988).

### 1.3.2.2 US3 protein kinase activity

Blue & Stobbs (1981) and Purves *et al.* (1986) detected a novel PK activity in the cytoplasm of HSV-1- and PRV-infected cells. The enzyme was expressed with E kinetics. Induction of the enzyme did not occur in cells treated with cycloheximide or cells infected with UV-inactivated virus, and was dependent on IE gene expression. These data indicated that expression of the viral genome was required for induction of the novel PK, and further suggested that the PK may be virally encoded.

In a later study, the novel PK activity was not detected in the cytoplasm of cells infected with HSV-1 US3 mutants (Purves *et al.*, 1987). Immunoblotting with an antibody raised against the C-terminal eight amino acid residues of the US3 protein specifically

recognised a polypeptide with a Mr of 68,000, and a 68 kDa protein was detected when immunoblots were performed on extensively purified preparations of the novel PK. Incubating the purified PK *in vitro* with [ $\gamma$ - $^{32}$ P]ATP stimulated phosphorylation of a 68 kDa protein. All these data are consistent with the US3 protein encoding a 68 kDa PK located in the cytoplasm of HSV-1-infected cells.

### 1.3.2.3 Growth characteristics of US3 mutant virus

Nishiyama *et al.* (1992) characterised the *in vitro* and *in vivo* phenotype of an HSV-2 US3-*lacZ* mutant. As with HSV-1, the HSV-2 US3 gene was shown to be non-essential for virus replication *in vitro*, but the US3-*lacZ* mutant demonstrated a route-dependent reduction of virulence *in vivo*. Footpad or intraperitoneal inoculation exhibited a 10,000-fold decrease in virulence, while corneal or intracerebral inoculation resulted in only a 10-fold decrease. Mutant virus replication was restricted in the liver and spleen of adult mice, but in new-born mice the mutant grew as well as *wt* virus.

### 1.3.2.4 Characteristics of the US3 protein kinase

Purified HSV-1 US3 PK was shown to utilise ATP but not GTP as a phosphate donor to phosphorylate Ser or Thr residues of basic but not acidic peptides (Katan *et al.*, 1985). Using synthetic oligopeptides, it was shown that the major feature of the US3 PK phosphorylation site is a string of Arg residues on the N-terminal side of the target Ser or Thr, giving a consensus sequence of (R)<sub>n</sub>X(S/T)YY, where  $n \geq 3$ , with X preferentially being Arg, Ala, Val, Pro or Ser and Y preferentially being Arg, Ala, Val, or Ser with Ser/Thr as the target residue (Frame *et al.*, 1987; Leader *et al.*, 1991). In addition, the US3 PK was found to be active at 1 M KCl, which clearly distinguishes it from the considerably more salt sensitive cellular PKs (Frame *et al.*, 1987).

### 1.3.2.5 US3 protein kinase targets

A variety of proteins have been identified as targets for phosphorylation by the US3 PK. The targets and their proposed physiological significance are summarised in Table 1.9, and the evidence is described below.

Target	Function	Reference
US9	tegument protein.	Daikoku <i>et al.</i> (1994)
UL12	deoxyribonuclease	Daikoku <i>et al.</i> (1995)
UL34	Nonglycosylated membrane protein	Purves <i>et al.</i> (1991)
US1 (ICP22)	IE protein	Purves & Roizman (1992)

**Table 1.9 Proteins identified as targets for phosphorylation by the US3 PK.**

### US9

To determine the targets of the US3 PK, Daikoku *et al.* (1994) performed a series of *in vitro* phosphorylation experiments with an HSV-2 US3 *lacZ* insertion mutant (L1BR1). Compared to cytoplasmic extracts from *wt* HSV-2 infected cells, L1BR1 extracts showed reduced phosphorylation of a number of proteins ranging from 14 to 22 kDa. The PK activity was detected at NaCl concentrations above 500 mM and phosphorylation of the 14 to 22 kDa proteins was inhibited by 50 mM quercetin, a potent inhibitor of HSV-2 US3 PK (Daikoku *et al.*, 1993). These data indicated that US3 is involved, directly or indirectly, in the phosphorylation of these proteins.

While the identity of the 14 to 22 kDa proteins was unknown, HSV-1 gene US9 was known to encode a tegument protein migrating on SDS-PAGE as 12 distinct phosphoproteins ranging from 12 to 20 kDa (Frame *et al.*, 1986). Because no HSV-2 US9 mutants existed, Daikoku *et al.* (1994) performed *in vitro* phosphorylation reactions on extracts of cells infected with *wt* HSV-1, an HSV-1 US9 mutant or L1BR1. A range of phosphorylated proteins from 14 to 22 kDa was detected in the cytoplasm from *wt* HSV-1 infected cells but not the US9 mutant.

Daikoku *et al.* (1994) repeated these experiments with membrane-stripped virions, obtaining similar results. This reinforced the conclusion that the 14 to 22 kDa proteins represent various phosphorylated species of the US9 protein which are targeted by the US3 PK.

### UL12

Daikoku *et al.* (1994) also observed increased phosphorylation of a 76 kDa protein in the cytoplasm of L1BR1 infected cells. Further studies identified a series of strongly

phosphorylated proteins between 75 and 80 kDa in *wt* HSV-2 infected cell cytoplasm that were absent in L1BR1 infected cells (Daikoku *et al.*, 1995).

The 80 kDa protein was shown to be of viral origin, and its size, cellular distribution and kinetics of expression suggested that it was the viral alkaline nuclease encoded by gene UL12. Immunoprecipitations performed on *in vitro* phosphorylated *wt* and L1BR1 infected cell extracts using an anti-alkaline nuclease monoclonal antibody precipitated an 80 kDa phosphoprotein from *wt* but not L1BR1 infected cells, suggesting the UL12 protein may be targeted for phosphorylation by the US3 PK.

Since the 76 kDa UL12 protein was phosphorylated in L1BR1 extracts, albeit to a lower level, it was concluded that UL12 is also targeted by PKs other than US3. Indeed, no significant difference was detected between the *in vivo* phosphorylation profile of the UL12 protein in *wt* and L1BR1 infected cells, thus calling into question the physiological relevance of the US3 PK in functions of the UL12 protein. Since PKC and CKII phosphorylation sites are present in the UL12 protein, it was concluded that it is phosphorylated by viral and cellular PKs.

### UL34

Cells infected with *wt* or an HSV-1 US3 mutant (R7041) and radiolabelled *in vivo* demonstrated different phosphorylation profiles (Purves *et al.*, 1991). A 30 kDa phosphoprotein in *wt*-infected cells was absent from R7041-infected cells, in which a novel 33 kDa phosphoprotein was detected. Analysis of HSV-1/HSV-2 intertypic recombinants identified the gene encoding the 30 kDa protein as UL34. The predicted UL34 gene product possessed a recognisable US3 PK target site, in this case RRRRIRRSRE, with both the Ser and Thr potential targets.

A UL34 mutant (R7314) was constructed with the native UL34 gene replaced by UL34 tagged at its N-terminus with a 17-residue epitope. Extracts of cells infected with R7314 demonstrated a novel phosphoprotein migrating more slowly than either the 30 or the 33 kDa proteins. A monoclonal antibody, raised against the epitope tag, identified the novel phosphoprotein as the modified UL34 protein. When the Ser and Thr residues in the potential phosphorylation site within UL34 were separately mutated to Ala, both mutants

produced a phosphoprotein indistinguishable from the 33 kDa phosphoprotein. Since these UL34 mutants possessed phenotypes similar to the US3<sup>-</sup> mutant, it was concluded that the US3 PK is necessary for post-translational processing of the UL34 protein. However, the 33 kDa protein was still phosphorylated in US3<sup>-</sup>-infected cells, and it remained unclear why UL34 appeared to migrate more slowly in its unphosphorylated form. Purves *et al.* (1991) attributed the phosphorylation-induced reduction in Mr to a change in charge, shape or proteolytic cleavage of the phosphoprotein.

This complex situation was resolved by Purves *et al.* (1992), who showed that a polyclonal antiserum raised against UL34 sequences did not react with the 33 kDa phosphoprotein, indicating it was not a product of the UL34 gene. The protein detected by the antiserum was actually shown not to be phosphorylated in US3 mutant-infected cell extracts. The unphosphorylated UL34 protein migrated faster than phosphorylated UL34 protein, as would be expected.

A range of at least four proteins was also found in US3<sup>-</sup>-infected cells (25-35 kDa) which were phosphorylated with varying degrees of efficiency and were genetically unrelated to UL34. The identity and functions of the 25 to 35 kDa proteins remain unclear, but they were detected only in lysates of cells infected with viruses incapable of phosphorylating UL34. They were shown to co-immunoprecipitate with UL34, suggesting they may be functionally related.

### **Anti-apoptotic activity**

Viruses have developed a variety of anti-apoptotic mechanisms to maximise production of virus from infected cells. HSV-1 mutants lacking the major regulatory RS1 gene (encoding ICP4) were shown to induce apoptosis, whereas *wt* virus did not. In fact *wt* virus protected cells from apoptosis induced by thermal shock (Leopardi & Roizman, 1996). However, when rescuants produced from the RS1<sup>-</sup> mutant failed to protect cells from apoptosis it became apparent that a second mutation had been introduced into US3 (Leopardi *et al.*, 1997a). ICP4 lacks a candidate phosphorylation site for the US3 PK, and Leopardi *et al.* (1997a) found no evidence to suggest that the US3 PK phosphorylates ICP4. These findings raised the possibility that US3 itself may be the principal viral protein required to block apoptosis. In a further development, Jerome *et al.*

(1999) showed that US3 co-operates with US5 to inhibit apoptosis. With deletion of US3 reducing inhibition of UV-induced apoptosis and deletion of US5 reducing protection from Fas-mediated apoptosis.

### 1.3.3 HSV-1 UL13

In work subsequent to detection of PK motifs in HSV-1 US3 and its homologues, Chee *et al.* (1989) and Smith & Smith (1989) identified a second herpesviral gene predicted to encode PK sequence motifs. Unlike HSV-1 US3, which has homologues only in the *Alpha*herpesvirinae, Chee *et al.* (1989) found PK motifs in related genes from HSV-1, VZV, EBV, HHV-6 and HCMV. Table 1.10 lists several of the known homologues to HSV-1 UL13, illustrating conservation across the *Alpha*-, *Beta*- and *Gamma*herpesvirinae.

Subfamily	Virus	Gene	Size of protein (amino acid residues)	Mw of protein
<i>Alpha</i> herpesvirinae	HSV-1	UL13	518	57 197
<i>Alpha</i> herpesvirinae	HSV-2	UL13	518	57 045
<i>Alpha</i> herpesvirinae	VZV	ORF47	510	57 351
<i>Alpha</i> herpesvirinae	EHV-1	ORF49	594	65 244
<i>Alpha</i> herpesvirinae	PRV	UL13	398	41 500
<i>Beta</i> herpesvirinae	HCMV	UL97	707	78 233
<i>Beta</i> herpesvirinae	HHV-6	15R	562	63 718
<i>Gamma</i> herpesvirinae	EBV	BGLF4	429	48 352
<i>Gamma</i> herpesvirinae	HHV-8	ORF36	444	50 334
<i>Gamma</i> herpesvirinae	HVS	ORF36	431	48 900

**Table 1.10 Homologues of the HSV-1 gene UL13, showing the size of each encoded protein and the predicted Mr.**

Derived from McGeoch *et al.* (1986, 1988); Chee *et al.* (1989); Davison & Scott, (1986); Telford *et al.* (1992); de Wind *et al.* (1992); He *et al.* (1997); Chee *et al.* (1989); Russo *et al.* (1996); Albrecht *et al.* (1992); Lawrence *et al.* (1990) and Baer *et al.* (1984).

#### 1.3.3.1 Sequence analysis

The sequence alignments of HSV-1 UL13 and its homologues with cAPK in Fig. 1.14 show that the herpesvirus sequences depart from the consensus sequences at certain positions thought to be highly conserved. The herpesvirus homologues exhibit little conservation of sequences outside the PK domain, and vary extensively in the length of their N-terminal domains.

Smith & Smith (1989) performed a similar sequence analysis on HSV-1 UL13 and its counterparts in VZV and EBV, confirming six conserved motifs corresponding to subdomains I, II, VI, VII, VIII and IX. In addition, Smith & Smith (1989) identified a Ser/Thr PK-specific pattern in the three putative herpesvirus PKs. Despite the autophosphorylation domain between motifs VII and IX being poorly conserved in UL13 and its counterparts and being about 40 residues longer than in classic PKs, a Ser/Thr PK pattern is well conserved in the herpesviral sequences around motif VII.

		I						II					III			IV										
cAPK	49	L	G	T	G	S	F	G	R	V	70	A	M	K	I	91	E	119	V							
UL13	157	G	G	S	G	G	Y	G	D	V	178	A	V	K	T	91	E	148	V							
VZV47	138	A	G	R	G	T	Y	G	R	V	155	A	V	K	T	167	E	178	S							
BGLF4	84	L	G	R	G	S	Y	G	A	V	100	T	V	K	L	113	E	122	I							
15R	201	L	G	V	G	A	Y	G	K	V	216	A	I	K	T	242	D	249	V							
UL97	337	L	G	Q	G	S	F	G	E	V	353	V	V	K	V	380	E	392	V							
		VI													VII											
cAPK	153	T	F	E	Y	L	H	S	L	-	D	L	I	Y	R	D	I	K	P	E	N	L	184	D	F	G
UL13	264	A	V	V	F	L	N	T	T	C	G	I	S	H	L	D	I	K	C	A	N	I	301	D	F	S
VZV47	243	A	L	T	F	L	N	R	T	C	G	L	T	H	L	D	V	K	C	G	N	I	282	D	Y	S
BGLF4	181	A	V	Y	F	L	N	R	H	C	G	L	F	H	S	D	L	S	P	S	N	I	219	D	Y	G
15R	299	A	V	R	F	L	N	L	K	C	R	I	N	H	F	D	I	S	P	M	N	I	335	D	Y	S
UL97	442	A	I	K	F	L	N	H	Q	C	R	V	C	H	F	D	I	T	P	M	N	V	481	D	Y	S
		VIII						IX																		
cAPK	206	A	P	E	220	D	W	W	A	L	G															
UL13	353	P	P	E	382	D	L	Y	A	L	G															
VZV47	333	P	P	E	362	D	L	Y	A	L	G															
BGLF4	279	I	P	D	297	D	L	C	S	L	G															
15R	386	L	V	N	428	R	E	A	Q	L	Y															
UL97	533	I	C	D	573	D	E	V	R	M	G															

**Figure 1.14** Amino acid sequence alignment of the putative herpesviral PKs identified by Chee *et al.* (1989) with cAPK.

The alignment shows the subdomains identified as homologous to known PK catalytic domains. Residues shown in blue were identified by Hanks *et al.* (1988) as highly conserved in the catalytic domain. The numbers refer to the position of the first residue in each indicated subdomain in the relevant sequence.

There is confusion in the literature over the location of some of the PK consensus sequences. Chee *et al.* (1989) and Smith & Smith (1989) disagree over the position of the APE consensus sequence in subdomain VIII of EBV BGLF4. Also, Chee *et al.* (1989)

and Cannon *et al.* (1999) identified different residues as the catalytic lysine in HCMV UL97. Figs. 1.15 and 1.16 show the consensus sequences identified.

While the APE motifs identified by Smith & Smith (1989) and Chee *et al.* (1989) lie within subdomain VIII, one lies 16 residues downstream of the other (Fig. 1.15). However, the sequence identified by Smith & Smith (1989) is closer to the recognised sequence of the classic APE consensus motif. Referring to Fig. 1.16, the sequence identified by Cannon *et al.* (1999) is in closer agreement with the subdomain II consensus sequence (AxK) determined by Hanks *et al.* (1988). While these examples represent minor differences in interpretation, they serve to highlight the problems encountered when trying to identify sequence motifs in PKs.

261 YK PLCLLSKCYILRGAGHIPDPSA 284

**Figure 1.15 A section of EBV BGLF4 sequence, showing the two sites identified at the APE consensus motif indicative of PK subdomain VIII.**

Residues shown in blue represent the motif identified in Smith & Smith (1988) and residues in red represent the motif identified by Chee *et al.* (1988). Residue numbers refer to the predicted EBV BGLF4 amino acid sequence.

352 R V V K V A R K H 360

**Figure 1.16 A section of HCMV gene UL97 sequence, showing the two identified sites of the invariant catalytic lysine.**

Residues shown in blue represent the motif identified by Chee *et al.* (1989) and residues in red represent the motif identified by Cannon *et al.* (1999). In each case the predicted catalytic lysine is boxed. Residue numbers refer to the predicted HCMV UL97 amino acid sequence.

Several differences exist between the classic PKs and the UL13-related PKs. There are minor differences, for example the hydrophobic residue at position -7 in subdomain I does not appear to be conserved in UL13 and ORF47, as well as major differences. In all putative herpesviral PKs analysed by Chee *et al.* (1989), the C-terminal part of subdomain I and the loop between subdomains I and II are absent. Although not well conserved in classic PKs, these residues form part of the hydrophobic core in the small

lobe of the catalytic subunit (Singh, 1994). In cAPK, these residues lie towards the C-terminus of  $\beta 2$ , and are involved in holding the adenine ring (Taylor *et al.*, 1993).

Residues 79 to 88 in cAPK, which comprise the C-terminal portion of  $\alpha B$  and the N-terminal portion of  $\alpha C$ , are absent from most herpesviral PK sequences, including UL13. Most residues in this region are poorly conserved and excluded from the enzymatic core, but some have been implicated in substrate binding (Singh, 1994). Although the catalytic Lys is conserved throughout, in herpesviruses the spacing between it and the nucleotide binding site is between one and three amino acids, considerably smaller than the minimum of 14 amino acid residues found in classic PKs.

Although subdomain VI is the region with greatest frequency of highly conserved residues in both herpesvirus and cellular PKs, most divergence between the herpesviral and the classic enzymes resides in the region from subdomain V to XI. Some herpesviral PK sequences contain inserts between  $\alpha D$  (subdomain V) and  $\alpha E$  (VI), and all contain extensive inserts between  $\beta 9$  (subdomain VII) and  $\alpha F$  (VIII). Inserts at these sites would not be expected to interfere with PK activity, and probably forms loops between the regions of secondary structure in cAPK.

The herpesviral UL13 PK sequences show dramatic differences from the established consensus in subdomain VIII, in which the conserved triplet Ala-Pro-Glu (see Fig. 1.14) is considered an important PK catalytic domain indicator. Glu<sup>208</sup> is invariant in all 65 Ser/Thr PKs aligned by Hanks *et al.* (1988), but is conserved in only two of the five UL13-related PKs. The region immediately N-terminal to the APE consensus in cAPK contains the highly conserved Thr<sup>201</sup> which, while acting as an indicator of Ser/Thr specificity, diverges in most of the herpesviral PK sequences.

### 1.3.3.2 Gene position and orientation

In HSV-1 the UL13 gene is orientated leftwards in the prototype representation of the HSV-1 genome, with its ORF located between nucleotides 28502 and 26946. The gene partly overlaps its neighbours: the promoter, transcript start site and first 82 codons of UL13 lie within the coding region of UL14, while the transcribed 5' non-coding region

of UL12 overlaps the final 34 codons of the UL13 reading frame. Fig. 1.17, lines 1 and 2 illustrate the position and orientation of the UL13 gene.

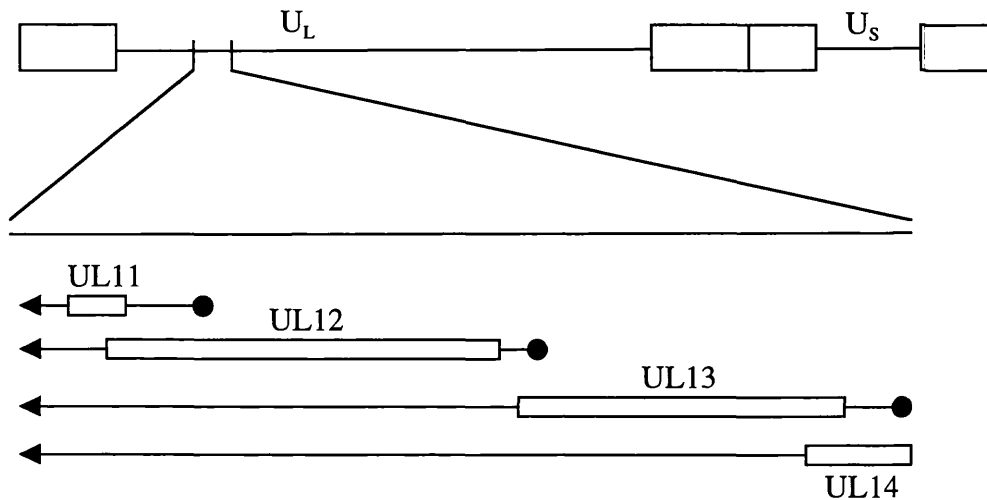


**Figure 1.17 Genomic location and organisation of the UL13 gene.**

The upper line of the figure shows a schematic representation of the HSV-1 genome, with unique regions shown in lines and major repeat elements as open boxes. The position of the UL11-UL14 gene cluster is indicated. The lower part expands this region, showing the relative positions of UL11 to UL14. Filled circles represent the 5' termini of the transcripts while arrowheads represent the transcript stop sites. The open boxes represent the predicted protein coding regions. Reproduced from Coulter (1993).

### 1.3.3.3 UL13 protein kinase activity

Cunningham *et al.* (1992) found that HSV-1 infected cells possess a novel nuclear PK activity. Nuclear PK activity increased until 5 h post infection, and remained approximately constant thereafter. The nuclear PK activity was stimulated by high salt concentrations, similar to the previously characterised US3 PK activity. However, the US3 PK was specifically localised in the cytoplasm of infected cells, suggesting the nuclear PK is a distinct enzyme. The major substrate of the nuclear PK was a 57 kDa protein, and initial findings suggested that the 57 kDa phosphoprotein is a phosphorylated form of the nuclear PK.

Nuclear extracts from HSV-2 infected cells phosphorylated *in vitro* demonstrated a 59 kDa phosphoprotein, slightly larger than the 57 kDa phosphoprotein in HSV-1 infected cells. The use of intertypic recombinants between HSV-1 and HSV-2 located the gene encoding the 57 kDa HSV-1 phosphoprotein to a region containing UL9 to UL15, with UL13 predicted to encode a protein with Mr nearest 57 kDa. To test whether the 57 kDa

protein was the UL13 gene product, antibodies were raised to a fusion protein of  $\beta$ -galactosidase linked to amino acid residues 149 to 207 of the predicted UL13 protein. The antiserum specifically immunoprecipitated a 57 kDa phosphoprotein, confirming that the 57 kDa phosphoprotein is encoded by UL13. In addition, the 57 kDa phosphoprotein was immunoprecipitated from phosphorylated purified virions, indicating that the 57 kDa protein is a virion component.

Although the US3 and putative UL13 PKs demonstrate similar salt sensitivities, Cunningham *et al.* (1992) noted that the cellular distributions of the two PKs are different. Further characterisation of the nuclear PK established additional differences, as summarised in Table 1.11. The UL13 PK was found to utilise GTP but the US3 PK did not. In addition, the two PKs demonstrated different substrate specificities, with the US3 PK targeting basic but not acidic substrates, and the UL13 PK targeting acidic but not basic substrates. The nuclear PK was also significantly less sensitive to inhibition by heparin. Cunningham *et al.* (1992) concluded that the UL13 PK in HSV-1 infected cells is distinct from both the US3 PK or previously characterised nuclear PK activities.

PK	Cellular location	Substrate	Phosphate donor	NaCl sensitivity
US3	Cytoplasm	Basic	ATP	Stimulated by high salt (1.5 M)
UL13	Nucleus	Acidic	ATP & GTP	Stimulated by high salt (1.5 M)

**Table 1.11 Comparison of the HSV-1-induced PK activities.** Derived from Cunningham *et al.* (1992).

#### 1.3.3.4 Protein kinase activity in the virion

Early work showed that purified membrane-stripped HSV-1 virions incubated with [ $\gamma$ - $^{32}$ P]ATP demonstrated radiolabelling of a number of viral proteins, indicating that virions contain a PK (Rubenstein *et al.*, 1972; Lemaster & Roizman, 1980). However, it was unclear whether the enzymatic activity was associated with a virus or host cell encoded PK.

Subsequently, Overton *et al.* (1992) phosphorylated a purified preparation of membrane-stripped HSV-1 virions *in vitro* and subjected the products to western blot analysis using a UL13 antiserum prepared against a GST fusion protein (Overton *et al.*, 1992). The

antiserum recognised a 55 kDa protein which comigrated with a phosphorylated virion component. Immunoprecipitations were also performed on radiolabelled virions using the antiserum. A single species, corresponding in size to the predicted UL13 gene product, was immunoprecipitated from the virion lysate. Similar results were found with HSV-2, confirming that the UL13 protein is a component of the virion.

In addition, mass spectrometric analysis identified the UL13 protein in minor amounts in membrane-stripped HSV-1 virions and L-particles (A. Davison, unpublished data), suggesting that the UL13 protein is present in the HSV-1 tegument.

### 1.3.3.5 Purification of the UL13 protein

Attempts were made by Cunningham *et al.* (1992) to purify the HSV-1 UL13 PK, but activity was lost after initial chromatographic steps. However, the HSV-2 UL13 protein was purified by Daikoku *et al.* (1997). Nuclear extracts were prepared from Vero cells infected for 20 h with HSV-2, and subjected to phosphocellulose column chromatography, assaying PK activity in the eluted fractions by using casein as substrate. The fraction with greatest PK activity was shown by western blotting with an anti-UL13 antibody to contain a 56 kDa protein. This fraction was subjected to sequential column chromatography on DEAE-cellulose and hydroxyapatite. The fraction demonstrating peak PK activity correlated in each case with antibody detection of a 56 kDa protein. The final preparation of the purified protein, visualised by silver staining, consisted predominantly of a protein of 56 kDa which reacted with anti-UL13 antiserum. Purification of the HSV-2 UL13 protein allowed detailed characterisation of the putative UL13 PK.

### 1.3.3.6 Heterologous expression of UL13

Native HSV-1 UL13 has not yet been expressed successfully to high levels in heterologous systems. Expression of the HSV-1 UL13 protein in a heterologous system was attempted using *E. coli* and recombinant baculovirus expression systems (Overton *et al.*, 1992). A GST-UL13 fusion protein expressed to a high level in *E. coli* was highly insoluble, but was used to prepare UL13 specific antiserum. The antiserum recognised a 55 kDa protein in insect cells infected with a UL13-expressing baculovirus, but not in *wt*

Name	Mutation			References
	UL23 ( <i>tk</i> )	US3	UL13	
R7350	500 bp deletion	Codon 135424-136291 deleted	$\alpha$ 27-tk insertion at 27269	Purves <i>et al.</i> (1992)
R7351	500 bp deletion	Codon 135424-136291 deleted	Codon 28043-27267 deleted	Purves <i>et al.</i> (1992)
R7352	500 bp deletion	Codon 135424-136291 deleted	Rescue of codon 28043-27267 deletion	Purves <i>et al.</i> (1992)
R7354	500 bp deletion	-	$\alpha$ 27-tk insertion at 27269	Purves <i>et al.</i> (1992)
R7355	500 bp deletion	-	Codon 28043-27267 deleted	Purves <i>et al.</i> (1992)
R7356	-	-	Codon 28043-27267 deleted	Purves <i>et al.</i> (1993)
R7357	500 bp deletion	Codon 135424-136291 deleted	-	Purves <i>et al.</i> (1992)
R7358	500 bp deletion	-	$\alpha$ 27-tk insertion mutant rescued	Purves <i>et al.</i> (1992)
R4969	-	-	$\alpha$ 27-tk mutant restored with HCMV UL97 gene	Ng <i>et al.</i> (1996)
R4970	500 bp deletion	-	$\alpha$ 27-tk mutant restored with HCMV UL97 gene	Ng <i>et al.</i> (1996)
UL13- <i>lacZ</i>	-	-	<i>E. coli lacZ</i> gene inserted at residue 28058	Coulter <i>et al.</i> (1993)
UL13' (1) & (5)	-	-	Multiple stop codons inserted at codons 28043	Overton <i>et al.</i> (1994)
UL13D-4bp	-	-	4 base pair deletion at residue 27587	C. Cunningham, (unpublished)
UL13I-16bp	-	-	16 base pair insertion at residue 28177	C. Cunningham, (unpublished)

**Table 1.12 Genotypes of UL13 mutants**

baculovirus. Degradation appeared to be minimal but low expression levels were indicated by the inability to detect the protein in Coomassie-stained gels.

Attempts to isolate a recombinant vaccinia virus expressing the UL13 protein by transcription from a powerful late promoter proved unsuccessful (Cunningham *et al.*, 1992). It was suggested that high levels of the UL13 protein may be lethal to growth of vaccinia virus.

### 1.3.3.7 UL13 mutants

Several studies have been performed using HSV-1 mutants with insertions or deletions in the UL13 gene. Table 1.12 summarises the properties of these mutants.

### 1.3.3.8 Effect of UL13 mutations on HSV-1 growth

Using a panel of UL13 mutants (Table 1.12), Purves & Roizman (1992), Coulter *et al.* (1993), Purves *et al.* (1993) and Overton *et al.* (1994) showed that the UL13 protein, like the US3 PK, is not essential for HSV-1 replication in cell culture. The growth properties of UL13 mutants are summarised in Table 1.13.

Virus	Cell type tested	m.o.i.	Growth characteristics
UL13- <i>lacZ</i>	BHK-21, HFL, Vero	0.001	In BHK-21 cells UL13- <i>lacZ</i> plaques were about half the diameter of <i>wt</i> . UL13- <i>lacZ</i> yields were approximately 3.5 times less than <i>wt</i> after 72 h on BHK cells.
UL13- <i>lacZ</i>	BHK-21	10	UL13- <i>lacZ</i> yields were approximately 4 times less than <i>wt</i> after 30 h on BHK cells.
R7350, 7351, 7354, 7355	143TK <sup>-</sup> , HEp-2, Vero, BHK, RSC	-	Yielded fewer and smaller plaques than <i>wt</i> virus.
UL13 <sup>-</sup> (1) & (5)	BHK-21, Hel, Neuro 2a	10	Yield of virus 24 h post-infection was 10-fold less than <i>wt</i> virus. Mutant plaques consistently smaller than <i>wt</i> .
UL13 <sup>-</sup> (1) & (5)	Vero	10	Yield of virus 24 h post-infection was 2- to 5-fold less than <i>wt</i> virus. Mutant plaques smaller than <i>wt</i> .

**Table 1.13 Growth characteristics of HSV-1 UL13 mutants on a variety of cell lines.** Derived from Coulter *et al.* (1993); Purves & Roizman (1992); Overton *et al.* (1994) and Purves *et al.* (1993). See Table 1.12 for genotypes.

### 1.3.3.9 UL13/US3 double mutants

De Wind *et al.* (1992) constructed a PRV mutant with oligonucleotide inserts in both the UL13 and US3 ORFs. Individually, mutations in these ORFs have modest effects on virus growth *in vitro*, but the double mutant yielded a greatly reduced end titre compared with *wt*. In addition, the plaque size of the double mutant was very small. An HSV-1 UL13-US3 double mutant formed plaques approximately 20-30% the diameter of *wt* plaques (Coulter, 1993). Yields of the HSV-1 UL13-US3 double mutant were shown to be 800-fold less than that of *wt* HSV-1.

Coulter (1993) suggested that the two PKs may have common substrates, and can therefore partially substitute for each other. This is unlikely, however, since both have very different substrate specificities (Purves *et al.*, 1986; Cunningham *et al.*, 1992). Alternatively the two PKs could play overlapping roles in the viral life cycle, while targeting different substrates.

### 1.3.3.10 UL13 phosphorylation assay

Buffer concentration						Reference
mM					%	
Tris-HCl (pH)	MgCl <sub>2</sub>	MgAc	DTT	NaCl	NP40	
50 (8)	-	50	1	1000 or 1500	0.1	Cunningham <i>et al.</i> (1992)
50 (7.5)	10	-	1	0 to 1500	-	Coulter <i>et al.</i> (1993)
50 (8)	25	-	0.5	1000	0.1	Overton <i>et al.</i> (1994)
50 (8)	50	-	1	1500	0.1	Prod'hon <i>et al.</i> (1996)
20 (8)	50	-	1	-	0.1	Ogle <i>et al.</i> (1997)
50 (8)	10	-	1	-	-	Daikoku <i>et al.</i> (1997)
10 (8)	50	-	1	200	0.1	Ng <i>et al.</i> (1998)
50 (8)	50	-	1	200	0.1	Kawaguchi <i>et al.</i> (1998)

**Table 1.14 Summary of the compositions of UL13 PK phosphorylation buffers.**

A variety of buffers have been used to detect activity of the putative UL13 PK *in vitro*. These are summarised in Table 1.14. Extensive purification allowed the optimal buffer conditions of HSV-2 UL13 PK to be identified. In contrast to Cunningham *et al.* (1992) and Coulter *et al.* (1993), who found the HSV-1 UL13 PK to be stimulated by increasing

salt concentrations, the purified HSV-2 UL13 PK was most active at 0 M NaCl, with activity decreasing as NaCl concentration increased (Daikoku *et al.*, 1997).

### 1.3.4 UL13 homologues

#### 1.3.4.1 HSV-2 UL13

There is 85.9% amino acid sequence homology between the HSV-1 and HSV-2 UL13 PKs. Daikoku *et al.* (1997) characterised the activity of purified preparations of HSV-2 UL13 PK. It demonstrated optimal activity in the absence of salt, with activity inhibited by about 70% at 500 mM NaCl. Both CKI and CKII were stimulated by salt concentrations up to 200 mM, but at 500 mM NaCl CKI activity was inhibited by 70% and CKII activity was undetectable. All three PKs were active over a broad pH range, with the optimal pHs of the UL13 PK, CKI and CKII being 9.0, 6.8 and 8.4, respectively. As expected, the UL13 PK demonstrated an absolute requirement for divalent cations, with an optimal  $Mg^{2+}$  concentration of 10-20 mM.

	Percentage of activity		
	UL13	CKI	CKII
<b>Casein</b>	100	100	100
<b><math>\alpha</math>-Casein</b>	52	43	<3
<b><math>\beta</math>-Casein</b>	118	129	68
<b><math>\kappa</math>-Casein</b>	79	167	37
<b>Histone</b>	86	85	16
<b>Protamine</b>	<3	<3	<3
<b>Phosvitin</b>	63	94	30

**Table 1.15 Substrate specificity of HSV-2 UL13 PK in comparison with CKI and CKII.** Derived from Daikoku *et al.* (1997).

Under optimal conditions, casein was shown to be phosphorylated mainly at serine residues by the UL13 PK, with a minor degree of phosphorylation at threonine residues. The substrate specificity of the purified UL13 PK was tested (Table 1.15). The UL13 PK efficiently phosphorylated all acidic proteins assayed. It did not detectably phosphorylate one basic protein, protamine, but did phosphorylate a second, histone. The substrate specificities of CKI and CKII were similar to that of UL13 PK. Unlike CKI and CKII, the UL13 PK was resistant to inhibition by heparin. The HSV-2 UL13 PK was unable to utilise GTP as a phosphate donor, unlike CKI and CKII.

#### 1.3.4.2 VZV ORF47

Ng *et al.* (1994) attempted to identify substrates for the ORF47 PK by analysing modification of individual viral phosphoproteins. Coimmunoprecipitation coupled with *in vitro* phosphorylation of the immune complex identified the ORF62 protein (the homologue of HSV-1 ICP4) as a potential target. However, the ORF62 protein was also shown to be phosphorylated by CKII. Both ORF47 and CKII were shown to utilise ATP and GTP as phosphate donors, although ATP was the preferred donor in both cases. Both the ORF62 and ORF47 proteins were phosphorylated *in vitro* in the presence of heparin concentrations ten times higher than the CKII inhibitory level, thus indicating that ORF62 was phosphorylated by the ORF47 PK. In addition, the ORF62 protein was phosphorylated mainly on Ser residues with minor phosphorylation on Thr residues.

#### 1.3.4.3 PRV UL13

De Wind *et al.* (1992) produced two mutants in PRV gene UL13 by inserting oligonucleotides containing stop codons. The mutant showed a very small reduction in titre and plaque size compared to *wt* virus. Immunoprecipitation of transiently expressed C-terminally tagged PRV UL13 allowed *in vitro* kinase assays to be performed. These demonstrated that the protein had intrinsic  $Mn^{2+}$ -dependent PK activity, and was able to autophosphorylate and transphosphorylate acidic and basic substrates.

To ensure that phosphorylation of the UL13 protein was due to autophosphorylation and not transphosphorylation by a contaminating PK, a full length inactivated UL13 mutant was produced. In this mutant, the invariant lysine residue (Lys<sup>103</sup>) was changed to Met, a substitution which has been shown to abolish the activity of other PKs (Chen *et al.*, 1987; Saris *et al.*, 1991). When *in vitro* phosphorylation reactions were performed on immunoprecipitated samples, the mutant protein was not phosphorylated, leading De Wind *et al.* (1992) to conclude that the PRV UL13 protein was capable of autophosphorylation. Phosphoamino acid analysis of autophosphorylated UL13 protein and histone phosphorylated by the UL13 PK revealed the presence of phosphoserine and phosphothreonine residues.

#### 1.3.4.4 HCMV UL97

Research on the HCMV-encoded PK activity was prompted by the need to identify the enzyme responsible for phosphorylating ganciclovir in HCMV-infected cells (Littler *et al.*, 1992). To function as an antiviral agent, the nucleoside analogue 9-(1,3-dihydroxy-2-propoxymethyl)-guanine, or ganciclovir, must be phosphorylated to the triphosphate. In HSV-1, initial phosphorylation of ganciclovir is carried out by thymidine kinase (*tk*) and is completed by cellular enzymes. However, HCMV does not encode a *tk*. By analogy with phosphorylation of aminoglycoside antibiotics by bacterial kinases, HCMV UL97 was suggested as the kinase which phosphorylates ganciclovir. In confirmation, Littler *et al.* (1992) showed that ganciclovir could be phosphorylated by the catalytic domain of UL97 cloned into a prokaryotic expression vector.

Using a recombinant baculovirus expressing full-length UL97, He *et al.* (1997) demonstrated that UL97 was phosphorylated on Ser and Thr residues when incubated with [ $\gamma$ - $^{32}$ P]ATP. Phosphorylation was optimal at high NaCl concentration and high pH. PK activity required either  $Mg^{2+}$  or  $Mn^{2+}$ , with a preference for  $Mn^{2+}$ , and utilised either ATP or GTP as a phosphate donor.

To determine whether HCMV UL97 can substitute for HSV-1 UL13, Ng *et al.* (1996) constructed a HSV-1 recombinant in which UL13 was replaced by UL97 and the *tk* gene deleted. In BHK cells, which restrict the growth of UL13 mutant virus, the recombinant grew as well as *wt* virus. The UL97 protein partially restored phosphorylation of ICP22, supposedly targeted by the UL13 protein, and the recombinant virus was sensitive to ganciclovir in all but *tk* negative cell lines.

#### 1.3.4.5 EBV BGLF4

BGLF4 is the only EBV gene encoding a PK. To evaluate the potential PK activity of BGLF4, Chen *et al.* (2000) expressed the protein in a range of prokaryotic and eukaryotic systems. BGLF4 expressed by a recombinant vaccinia virus and partially purified by immunoprecipitation was found to be phosphorylated. Despite carrying out only partial purification, Chen *et al.* (2000) suggested this could be due to autophosphorylation.

An antiserum against BGLF4 was required, but to avoid cross reactivity with cellular PKs a fusion protein comprising EBNA-1 residues 408-446 and BGLF4 was manufactured. The fusion protein, E1/BGLF4, could be specifically immunoprecipitated using monoclonal antibodies against the cognate EBNA-1 epitope. Transfected E1/BGLF4 was principally detected in the cytoplasm, and the immunoprecipitated fusion protein was shown to possess autophosphorylation activity similar to native BGLF4. Prior to phosphorylating the anti-EBNA-1-E1/BGLF4 immunocomplexes, Chen *et al.* (2000) performed washes with high salt buffers in an attempt to eliminate contaminating cellular PK activity. These experiments, in conjunction with the observed resistance of BGLF4 phosphorylation to heparin or okadaic acid, potent inhibitors of CKII, supported autophosphorylation of BGLF4.

PK activities of the authentic BGLF4 protein and E1/BGLF4 fusion protein were characterised. PK activity peaked between pH 6.5 and 8.0, required ATP or GTP as phosphate donor for autophosphorylation and showed a preference for magnesium, rather than manganese ions. Monovalent cations further increased PK activity, with 300 mM KCl or NaCl proving optimal.

Membrane-bound phosphorylated BGLF4 immunoprecipitates were probed with antibodies specific for three phosphoamino acids. Only phosphoserine and phosphothreonine were detected, in line with the prediction that BGLF4 encodes a Ser/Thr PK. BGLF4 was found to phosphorylate casein and histone, and also the EBV protein EA-D (Chen *et al.*, 2000; Li *et al.*, 1987).

Chen *et al.* (2000) introduced a number of site specific mutations into BGLF4. The residue predicted to be the catalytic lysine was changed to Met, two mutants with invariant residues in subdomains VI and VII changed to Ala were produced, and a fourth mutant was made with a residue in a nonconserved region changed to Ala. When phosphorylated *in vitro* all four mutants showed autophosphorylation activity very similar to that of *wt* BGLF4. A series of mutants with deletions around the ATP-binding site and the basic amino acids from residues 367-403 or at the N-terminus were produced. Deletion of residues 35 to 65, a thirty residue region just N-terminal to

subdomain I, stimulated autophosphorylation approximately two-fold. However, residues 1 to 26 were identified as essential for the autophosphorylation of the BGLF4 protein.

#### 1.3.4.6 HHV-8 ORF36

To determine whether ORF36 possesses PK activity, Park *et al.* (2000) expressed the full-length protein as a GST fusion protein in mammalian cells, purified the protein and subjected it to *in vitro* phosphorylation conditions. The purified protein was found to autophosphorylate on serine residues alone. In addition, Park *et al.* (2000) found that ORF36 is a late gene, and that the protein localised in the nucleus of transiently transfected cells.

Park *et al.* (2000) generated a ORF36 mutant in which the invariant Lys residue was replaced by Gln. This resulted in dramatically reduced phosphorylation of the mutant ORF36, and thus supported the view that the ORF36 protein possesses intrinsic PK activity and is capable of autophosphorylation. The *wt* and mutant proteins were phosphorylated on serine residues, the latter to a much lower level.

#### 1.3.5 UL13 protein kinase targets

Several proteins have been identified as potential targets for the HSV-1 UL13 PK (Table 1.16). This section will concern itself with summarising the published data without commenting on their significance. A brief appraisal of their significance is given in the Discussion.

Target	Function	References
ICP22 (US1)	Viral gene trans-activation	Purves & Roizman (1992)
RNA polymerase II	mRNA transcription	Long <i>et al.</i> (1999)
EF-1 $\delta$	Cellular translation regulatory protein	Kawaguchi <i>et al.</i> (1998)
VP22 (UL49)	Major tegument protein	Coulter <i>et al.</i> (1993), Morrison <i>et al.</i> (1998)
gE and gI (US8 & US7)	Fc receptor	Ng <i>et al.</i> (1998)
ICP0 (RL1)	Transactivator	Ogle <i>et al.</i> (1997)
<i>vhs</i> (UL41)	Viral host shutoff	Overton <i>et al.</i> (1994)

**Table 1.16 Summary of the proteins identified to date as targets for the HSV-1 UL13 PK.**

### 1.3.5.1 ICP22

Purves & Roizman (1992) used the HSV-1 UL13 mutants shown in Table 1.12 to distinguish the activities of the US3 and UL13 PKs. *In vitro* phosphorylated extracts from *wt*-infected cells showed a series of five phosphoproteins from 70 to 82 kDa, shown to be the products of the gene US1 (ICP22), while UL13 mutant-infected cell extracts demonstrated increased radiolabelling of the 70 kDa phosphoprotein and reduced radiolabelling of the four others. These differences in phosphorylation profile depended on the cell type used. Purves & Roizman (1992) concluded that the UL13 protein mediates cell type-specific posttranslational processing of ICP22. These observations were made using mutants containing a functional US3 gene, and the situation was later made more complex when it was found that the US3 PK phosphorylates ICP22 at different sites from UL13 PK (Purves *et al.*, 1993).

ICP22 is among the first viral proteins made after infection, and Purves & Roizman (1992) suggested that the UL13 protein modifies ICP22 late in infection, thereby altering its function. Because ICP22 was implicated in transactivation of late viral proteins (Sears *et al.*, 1985), Purves *et al.* (1993) investigated whether phosphorylation of ICP22 affects synthesis of late viral proteins. Purves *et al.* (1993) detected reduced accumulation of ICP0 (RL2), ICP22 (US1), ICP35 (UL26) and the US11 proteins and mRNAs in UL13 mutant-infected cell extracts.

UL13 is expressed late in infection and it is a component of the virion (Cunningham *et al.*, 1992; Overton *et al.*, 1992). Consequently Purves *et al.* (1993) examined whether UL13 in the virion mediates posttranslational processing of newly synthesised ICP22. *Wt* infected cells were incubated for 6 h in the presence of cycloheximide followed by actinomycin D to block further RNA synthesis and permit translation of IE mRNA. The newly synthesised ICP22 was not modified, and thus not phosphorylated by UL13 packaged within the infecting virus particle. When *in vitro* transcribed and translated UL13 (pUL13) and  $\alpha$ 22 (p22) were incubated in phosphorylating conditions several phosphoproteins between 68 and 82 kDa were detected (Prod'hon *et al.*, 1996). These corresponded to the phosphoproteins identified by Purves & Roizman (1992) as ICP22, suggesting that UL13 directly phosphorylates ICP22.

These data suggest that UL13 encodes a PK expressed late in infection which directly phosphorylates ICP22, and that this modification is required for accumulation of a subset of late viral mRNAs and proteins. While it seems unlikely that a PK expressed late in infection would affect the kinetics of gene expression of other late genes, certain late genes can be expressed at low levels early in infection, UL13 might be one of these.

Leopardi *et al.* (1997b) showed that ICP22 co-localises with ICP4, EBER-associated protein (EAP) and RNA polymerase II as transcriptional complexes with viral DNA in defined nuclear structures. A truncated, non-phosphorylated form of ICP22 still associated with EAP, showing that phosphorylation is not required for ICP22 to interact with EAP. However, because ICP22 did not associate with these nuclear structures in UL13 mutants it was proposed that UL13 may be required for the localisation of ICP22 to the nuclear bodies.

These complex studies support the view that ICP22 may have a role in transcription of viral genes, apparently enhancing the expression of at least one IE gene (RL2 encoding ICP0) and a subset of late genes at both mRNA and protein levels. ICP22 is extensively posttranslationally modified, with both the UL13 and US3 PKs contributing. Mutational studies suggested that ICP22 may express functions both early and late in infection, consistent with the kinetics of expression of UL13 and US3. Finally, modification of ICP22 by one or both PKs is required for colocalisation with viral DNA, ICP4, EAP and RNA polymerase II in a nuclear compartment at the time of transcription of late genes.

### 1.3.5.2 ICP0

The HSV-1 gene transactivator ICP0, encoded by RL2, is posttranslationally modified by nucleotidylation and phosphorylation (Ackerman *et al.*, 1984; Blaho *et al.*, 1993, 1994; Mitchell *et al.*, 1994). To determine whether the UL13 PK targeted ICP0, Ogle *et al.* (1997) examined the phosphorylation profiles of *wt* and UL13 mutant cell extracts. In *wt*-infected RSC cells, three closely migrating bands representing ICP0, were detected. They were designated *a* to *c* in order of decreasing Mr. Only the *a* form was detected in *wt*-infected Vero cells. In extracts of UL13 mutant-infected cells, ICP0 was identified predominantly in the *c* form in RSC and in the *b* form in Vero cells. These data indicated both a UL13 and a cell-type dependent modification of ICP0, leading Ogle *et al.* (1997)

to suggest that posttranslational processing of ICP0 was a dynamic process, perhaps reflecting the availability of cellular factors and the requirements for ICP0 during the course of the HSV-1 replication cycle.

The UL13 PK was shown to phosphorylate ICP0 directly when immune-complexes of UL13 and ICP0 were mixed under *in vitro* phosphorylation conditions. But when UL13 mutant-infected cells were labelled *in vivo*, ICP0 was phosphorylated, albeit to a lower level than in *wt*-infected cells. This indicates that ICP0 is not phosphorylated exclusively by the UL13 PK.

The relationships between UL13, ICP0 and ICP22 appear complex, with their expression being interactive and independent. ICP22 is modified by UL13 (Purves & Roizman, 1992; Purves *et al.*, 1993), and ICP22 regulates the utilisation of splice acceptor sites and longevity of ICP0 mRNA (Carter & Roizman, 1996). Ogle *et al.* (1997) showed that UL13 is involved in posttranslational modification of ICP0, that it controls the abundance of ICP22 and that the posttranslational modification of ICP0 does not require ICP22. Both ICP0 and ICP22 are proposed targets for the UL13 PK and by other cellular or viral PKs.

### 1.3.5.3 RNA polymerase II

RNA polymerase II (RNAP II) is a multi-subunit enzyme responsible for mediating mRNA transcription. The largest subunit, which possesses catalytic activity, is highly phosphorylated in its C-terminal domain. As a result, RNAP II exists in two forms, one hypophosphorylated and the other heavily phosphorylated. Each form is associated with distinct aspects of transcription, the hypophosphorylated form with transcription initiation and the highly phosphorylated form with transcription elongation (Payne *et al.*, 1989). As a result, phosphorylation of RNAP II is required *in vivo* for efficient transcription elongation.

HSV-1 infection has been shown to alter the phosphorylation state of the large subunit of RNAP II (Rice *et al.*, 1994), stimulating production of a new species of RNAP II which demonstrates intermediate electrophoretic mobility. This mobility change can be attributed to phosphorylation, as phosphatase treatment of the intermediate species

converts it to the hypophosphorylated form. Rice *et al.* (1995) showed that in cells infected with an ICP22 mutant the hypophosphorylated form of RNAP II was slightly depleted and that very low levels of the intermediate form were detected. This minor variation from the *wt* profile suggested that an additional viral gene product may be involved in processing RNAP II. Rice *et al.* (1995) suggested that two viral gene products, UL13 and *vhs*, may be responsible.

Long *et al.* (1999) used a UL13 mutant and a *vhs* mutant to test which gene was involved in processing RNAP II. The UL13 mutant failed to stimulate production of the intermediate form of RNAP II or to deplete the hypophosphorylated form, while the *vhs* mutant was indistinguishable from *wt* HSV-1. Long *et al.* (1999) then showed that infection with either UL13 or ICP22 mutants led to significantly reduced amounts of viral genome transcription at late times post-infection, suggesting both ICP22 and UL13 are involved in a common pathway that alters RNAP II phosphorylation and consequently promotes viral late transcription.

#### 1.3.5.4 Eukaryotic elongation factor 1 $\delta$

Translation elongation factor (EF-1) is a complex of proteins which mediates the elongation of polypeptide chains during translation of mRNA. The complex consists of EF-1 $\alpha$ , which transports aminoacyl tRNA for binding to ribosomes concurrent with hydrolysis of GTP, and the EF-1 $\beta\gamma\delta$  complex, which is responsible for the GDP-GTP exchange on EF-1 $\alpha$ . EF-1 $\delta$ , a component of the EF-1 $\beta\gamma\delta$  complex, is phosphorylated by several cellular PKs, including CKII (Palen *et al.*, 1994), *cdc2* kinase (Mulner-Lorillon *et al.*, 1994) and PKC (Venema *et al.*, 1991a,b). Studies suggest that hyperphosphorylation of EF-1 $\delta$  alters translational efficiency (Minella *et al.*, 1994; Mulner-Lorillon *et al.*, 1994; Richter *et al.*, 1982; Venema *et al.*, 1991a,b; Wasserman *et al.*, 1982).

Kawaguchi *et al.* (1998) showed that HSV-1 infection stimulates phosphorylation of EF-1 $\delta$  and that hyperphosphorylation of EF-1 $\delta$  occurs in cells infected with *wt* virus or a UL13 revertant (R7358), but not in mock-infected or cells infected with a UL13 mutant (R7355 or R7356). Mutating the US3 ORF had no effect on phosphorylation of EF-1 $\delta$ . These results indicate that a functional UL13 protein is required for hyperphosphorylation of EF-1 $\delta$ . Because ICP0 associates with EF-1 $\delta$  (Kawaguchi *et al.*,

1997), it was necessary to test whether ICP0 is a cofactor in the modification of EF-1 $\delta$ . It was found that EF-1 $\delta$  was hyperphosphorylated in ICP0 mutant infected cell extracts, thus indicating that ICP0 was not involved in modification of EF-1 $\delta$ .

Incubating immunoprecipitated UL13 protein and EF-1 $\delta$  together under phosphorylating conditions stimulated hyperphosphorylation of EF-1 $\delta$ , whereas phosphorylation was not detected when immune precipitates from MI and UL13 mutant-infected cells were used. These data showed that either UL13 or a protein complexed with UL13 directly phosphorylates EF-1 $\delta$ .

Further work by Kawaguchi *et al.* (1999) showed that EF-1 $\delta$  is hyperphosphorylated in cells infected with representative members of the *Alpha*-, *Beta*- and *Gammaherpesviruses*. Indeed, UL13 homologues can partially compensate for each other, with HSV-1 UL13 mutants expressing HCMV UL97 (Table 1.12) phosphorylating EF-1 $\delta$  to almost *wt* levels.

### 1.3.5.5 Glycoproteins E and I (US8 and US7)

Phosphorylation of viral glycoproteins is a rare post-translational modification occurring during virus infections (Grose, 1990). Glycoprotein E (gE), which acts as an Fc receptor by itself and more strongly in association with glycoprotein I (gI), was found to be phosphorylated and glycosylated in HSV-1, HSV-2, VZV and PRV (Edson, 1993; Edson *et al.*, 1987; Montalvo & Grose, 1986; Olson *et al.*, 1997). The VZV homologue of HSV-1 gI is also phosphorylated.

Ng *et al.* (1998) found that antibodies to HSV-1 UL13 formed immune complexes of UL13, gE and gI. Incubating these immune-complexes in phosphorylation conditions stimulated phosphorylation of all three proteins. Immune-complexes formed by monoclonal antibodies to gE but not to gI contained the UL13 protein, indicating that UL13 and gE interact (Ng *et al.*, 1998).

Both gE and gI showed reduced phosphorylation in UL13 mutant-infected cells. However, UL13 does not account for all the phosphorylation of gE and gI. An acidic region in the cytoplasmic domain of gE contains CKII recognition sequences (Litwin *et*

*al.*, 1992). Moreover, VZV gE is phosphorylated, *in vitro*, at its cytoplasmic tail by host cell PKs, including CKI and II (Grose *et al.*, 1989; Yao *et al.*, 1993). Ng *et al.* (1998) showed that purified CKII phosphorylated gE in immune complexes where the endogenous PK activity has been heat-inactivated, and Miriagou *et al.* (2000) showed that CKII phosphorylates the C-terminus of gE on serines 476 and 477. It is unclear whether there is any physiological relevance to multiple PKs targeting gE and gI. Ng *et al.* (1998) suggested that gE and possibly gI perform several functions and that PKs direct the functions of the glycoproteins by modifying them at different sites. This has yet to be borne out.

While the biological significance of the phosphorylation of gE in HSV-1 infections remains elusive it has been suggested that phosphorylated gE could act as an anchor for packaging UL13 in the tegument. Whatever the reason, because phosphorylation of gE is conserved in HSV-2, VZV and PRV, it is likely to play an important role.

#### 1.3.5.6. *vhs* (UL41)

As outlined in section 1.2.6, HSV-1 encodes *vhs*, a virion protein which shuts off host cell protein synthesis. Host shutoff can be visualised as reduced actin synthesis in [<sup>35</sup>S]-labelled profiles of *wt* HSV-1 infected cells when compared to mock-infected cells. Using a UL13 mutant (Table 1.12), Overton *et al.* (1994) found actin levels were similar between MI and UL13 mutant-infected cells. Repeating this experiment in the presence of actinomycin D, which inhibits viral gene expression and thus allows the effects on host protein synthesis to be seen more clearly, showed *wt* HSV-1 inhibited the synthesis of host cell proteins whereas the UL13 mutant did not (Overton *et al.*, 1994).

The product of HSV-1 gene UL41 has been assigned the virion-associated host shut-off function (*vhs*) (Kwong *et al.*, 1988; Fenwick & Everett, 1990). Overton *et al.* (1994) showed that *vhs* levels were drastically reduced in UL13 mutant-infected cells compared to *wt*-infected cells. Interestingly, while the level of *vhs* was reduced in UL13 mutant extracts, the kinetics of synthesis were the same as in *wt*-extracts. Overton *et al.* (1994) attributed the reduced *vhs* levels to the reduced virus yield in UL13 mutant infections.

Overton *et al.* (1994) suggested a variety of interactions between UL13 and *vhs*. UL13 might up-regulate expression of *vhs*, target *vhs* to the virion tegument or activate *vhs* by phosphorylation. Indeed, Read *et al.* (1993) detected a hyperphosphorylated form of *vhs* which was preferentially packaged into virions.

### 1.3.5.7 VP22 (UL49)

Coulter *et al.* (1993) manufactured an HSV-1 UL13 mutant in which the UL13 ORF was disrupted by insertion of the *E. coli lacZ* gene (Table 1.12), and performed *in vitro* phosphorylation reactions on UL13-*lacZ* infected CNE or membrane-stripped virions. The *in vitro* phosphophorylation assays, performed over a range of NaCl concentrations, revealed two highly radiolabelled proteins of 38 and 57 kDa. The 57 kDa protein was highly radiolabelled at all NaCl concentrations, while radiolabelling of the 38 kDa protein increased with increasing NaCl concentration. The phosphorylated 57 kDa protein was completely absent from UL13-*lacZ* CNE, and phosphorylation of a variety of other proteins, including the 38 kDa protein, was reduced. In UL13-*lacZ* CNE the 38 kDa protein was most highly phosphorylated at low NaCl concentrations.

Cunningham *et al.* (1992) detected a 57 kDa phosphoprotein which possessed PK activity and localised in the nucleus of infected cells. It was thought that the 57 kDa phosphoprotein was encoded by the HSV-1 gene UL13. The absence of the highly phosphorylated 57 kDa protein from UL13-*lacZ* CNE confirmed this (Coulter *et al.*, 1993), and reduced phosphorylation of proteins in UL13-*lacZ* CNE was consistent with the UL13 gene encoding a PK. The data from Coulter *et al.* (1993) indicates the 38 kDa protein, shown to be encoded by the gene UL49, is a target for phosphorylation by the UL13 PK. But, since the 38 kDa protein was phosphorylated in UL13-*lacZ* CNE it must be targeted by at least one other PK.

Coulter *et al.* (1993) suggested that the UL49 protein was phosphorylated at high NaCl concentrations by the UL13 PK, and at low NaCl concentrations by an unknown cellular PK. However, Coulter *et al.* (1993) manufactured and used only a single UL13 mutant and did not produce a rescuant, and hence the results require confirmation. In addition, Daikoku *et al.* (1997) showed that the purified HSV-2 UL13 PK was inhibited at NaCl

concentrations above 0 M, in contrast to the HSV-1 UL13 PK. This discrepancy has yet to be fully addressed.

It is unclear whether VP22 is phosphorylated in the virions. Szilágyi & Cunningham (1991) identified an abundant radiolabelled 40 kDa phosphoprotein in virions labelled with [<sup>32</sup>P]orthophosphate. This phosphoprotein correlated in size with VP22. However, Elliot *et al.* (1996) identified two species of VP22, which were shown to represent phosphorylated and unphosphorylated forms of the protein. Both forms were present in infected cells, the phosphorylated form alone was present in transfected cells and the unphosphorylated form alone found in virions.

While investigating tegument dissociation, Morrison *et al.* (1998) found that major structural components of the HSV-1 tegument were phosphorylated upon cell entry. *In vitro* assays showed that phosphorylation mediated dissociation of VP13/14 and VP22 from the virion, with CKII specifically promoting VP22 release. However, Morrison *et al.* (1998) maintained that by virtue of its proximity and higher local concentration, UL13 PK is the major contributor to VP22 dissociation *in vivo*. This was supported when it was found that UL13 mutant demonstrated severely impaired VP22 release. However, addition of CKII compensated for the loss of the UL13 PK.

## 1.4 Aims

The aims of this thesis were firstly to confirm and extend the work of Coulter *et al.* (1993) in regard to the possible role of VP22 as a target of the HSV-1 UL13 PK. The PK activity was then characterised further, and attempts made to map the phosphorylated residues within VP22 and the UL13 PK.

## 2 MATERIALS

### 2.1 Cells and viruses

Wild-type HSV-1 strain 17<sup>+</sup> (Brown *et al.*, 1973) and mutants derived therefrom were grown in baby hamster kidney clone C13 (BHK C13) cells (MacPherson & Stoker, 1962), MeWo cells (Bean *et al.*, 1975) or rabbit skin cells (RSC).

The HSV-1 mutant with the UL13 gene disrupted by insertion of the *Escherichia coli lacZ* gene was produced by Lesley Coulter (Coulter, 1993; Coulter *et al.*, 1993) and was obtained from Mary Murphy. The two further HSV-1 UL13 mutants, UL13D-4bp and UL13I-16bp (Table 1.12), were produced by and obtained from Charles Cunningham. The HSV-1 UL49 truncation mutant, vUL49del268-301 (Leslie, 1996), was obtained from Dr. J. McLauchlan.

### 2.2 Cell culture growth media

Eagles A:	0.23 g/l CaCl <sub>2</sub> ·2H <sub>2</sub> O
	0.23 g/l MgSO <sub>4</sub> ·7H <sub>2</sub> O
	0.1 ml/l conc. HCl
Eagles B:	50% (v/v) salts/plus
	40% (v/v) amino acids/plus
	3.2% (v/v) vitamins
salts/plus:	10.24 g/l NaCl
	0.64 g/l KCl
	0.24 g/l NaH <sub>2</sub> PO <sub>4</sub> ·2H <sub>2</sub> O
	7.2 g/l glucose
	0.00016% (v/v) Fe <sub>2</sub> (NO <sub>3</sub> ) <sub>3</sub>
	0.468 g/l L-glutamine
	0.016% (v/v) penicillin
	0.016 g/l streptomycin
	0.00032% (v/v) amphotericin B

amino acids/plus:	0.84 g/l arginine mono-HCl
	0.48 g/l cystine
	0.384 g/l histidine mono-HCl
	1.048 g/l isoleucine
	1.048 g/l leucine
	1.462 g/l lysine mono-HCl
	0.66 g/l phenylalanine
	0.952 g/l threonine
	0.16 g/l tryptophan
	0.724 g/l tyrosine
	0.936 g/l valine
	0.3 g/l methionine
	0.07% inositol
	0.03% (v/v) phenol red
	55 g/l NaHCO <sub>3</sub>
vitamins:	0.05 g/l choline chloride
	0.05 g/l folic acid
	0.05 g/l nicotinamide
	0.05 g/l pantothenic acid, Ca salt
	0.05 g/l pyridoxal-HCl
	0.05 g/l thiamine-HCl
	0.005 g/l riboflavine
ETC10:	70% (v/v) Eagles A
	10% (v/v) Eagles B
	10% (v/v) tryptose phosphate
	10% (v/v) newborn calf serum (NCS)
ETF10:	As above with NCS replaced by foetal calf serum (FCS).
EC2:	85.75% (v/v) Eagles A

	12.25% (v/v) Eagles B
	2% (v/v) NCS
EF2:	As above with NCS replaced by FCS
Methylcellulose overlay:	39% (v/v) carboxymethylcellulose
	1.56% (v/v) tryptose phosphate
	3.9% (v/v) NCS
	24.3% (v/v) NaCO <sub>3</sub> (7.5%)
	1.56% (v/v) penicillin/streptomycin (10000 IU/ml)
	0.8% (v/v) L-glutamine (200 mM)
	0.08% (v/v) amphotericin B
	7% (v/v) 10 x Glasgow's modified medium
Dulbecco's medium:	500 ml Dulbecco's modified Eagles medium
	9% (v/v) FCS
	1% (v/v) penicillin/streptomycin
	1% (v/v) L-glutamine
	1% (v/v) non-essential amino acids
BHK growth medium:	500 ml BHK-21 medium (Glasgow MEM)
	9.8% (v/v) tryptose phosphate
	8.2% (v/v) NCS

### 2.3 Radiochemicals

Radiochemicals were supplied by Amersham International plc:

[ $\gamma$ -<sup>32</sup>P]ATP, 10mCi/ml; 370 MBq/ml

### 2.4 Enzymes

Sequencing grade clostripain (endoproteinase Arg-C), *S. aureus* V8 protease (endoproteinase Glu-C), endoproteinase Lys-C and modified trypsin with storage buffers were obtained from Sigma Chemical Co. or Promega.

Lambda protein phosphatase ( $\lambda$ -PPase) was obtained from New England Biolabs Inc.

## 2.5 Chemicals

All chemicals used were of analytical grade and were supplied by BDH and Sigma Chemical Co.

The exceptions were:

Ammonium persulphate (APS) and Coomassie Brilliant Blue R250: Bio-Rad Laboratories Ltd.

Sulforhodamine B: Kodak

Ultrapure NTPs: Pharmacia Biotech

### Miscellaneous materials and suppliers

Rainbow<sup>TM</sup> protein molecular weight marker supplied by Amersham International plc.

X-Omat-S-film supplied by Kodak Ltd.

## 2.6 Protein gels

### 2.6.1 Tris-glycine polyacrylamide gels

8 x Stacking gel buffer:	0.5 M Tris-HCl pH 6.8
4 x Resolving gel buffer:	1.5 M Tris-HCl pH 8.8
Electrophoresis buffer:	50 mM Trizma base 380 mM glycine 0.2% (w/v) SDS
Fixing solution:	40% (v/v) methanol 10% (v/v) acetic acid
Coomassie staining solution:	Fixing solution containing 0.1% (w/v) Coomassie brilliant blue R250
Destaining solution:	5% (v/v) methanol 10% (v/v) acetic acid

Boiling buffer: 30% (v/v) stacking buffer  
24% (v/v) 25% SDS  
30% (v/v) glycerol  
15% (v/v) 14.3 M 2-mercaptoethanol  
1% (w/v) bromophenol blue

### 2.6.2 Tris-Tricine polyacrylamide gels

Acrylamide solution: 37.5 g acrylamide  
1 g NN' methylenebisacrylamide  
to 100 ml in dH<sub>2</sub>O

Gel buffer 3.0 M Tris-HCl pH 8.45  
0.3% (w/v) SDS

Electrophoresis buffer (anodic) 0.2 M Tris-HCl pH 8.9

Electrophoresis buffer (cathodic) 0.1 M Trizma base  
0.1 M Tricine  
0.1% (w/v) SDS  
(approximate pH 8.25)

Boiling buffer: 0.05 M Trizma  
4% (w/v) SDS  
12% (v/v) glycerol  
2% (v/v) mercaptoethanol  
1% (w/v) bromophenol blue

### 2.7 Protein blotting for mass spectrometric analysis

10 x PVDF buffer: 0.5 M Trizma base  
0.5 M glycine

Transfer buffer: 1 x PVDF buffer

	20% (v/v) methanol
	0.01% (w/v) SDS
Matrix:	10 mg/ml $\alpha$ -cyano-4-hydroxycinnamic acid in 50% (v/v) acetonitrile plus 0.1% (v/v) trifluoroacetic acid
Sulforhodamine stain:	50 mg/l sulforhodamine 30% (v/v) methanol 0.2% (v/v) acetic acid
PVDF Coomassie stain:	0.1% (w/v) Coomassie Brilliant Blue R250 1% (v/v) acetic acid 40% (v/v) methanol 59% (v/v) dH <sub>2</sub> O
PVDF membrane destain:	50% (v/v) methanol 50% (v/v) dH <sub>2</sub> O
Formic acid/ethanol:	1:1 (v/v) formic acid:ethanol

## 2.8 *In vitro* phosphorylation assay

Buffer A:	10 mM Hepes pH 8.0 50 mM NaCl 0.5 M sucrose 1 mM EDTA 0.5% (v/v) Triton X-100 1 mM PMSF 7 mM 2-mercaptoethanol
Phosphorylation buffer:	50 mM Tris-HCl pH 7.5 10 mM MgCl <sub>2</sub> 1 mM DTT

## 2.9 Immune precipitation

Buffer E:	100 mM Tris-HCl pH 8 100 mM NaCl 2 mM EDTA 2 mM EGTA 1% (v/v) NP40 0.5% (w/v) sodium deoxycholate 0.5 mM PMSF
Buffer EN:	100 mM Tris-HCl pH 8 500 mM NaCl 2 mM EDTA 2 mM EGTA 1% (v/v) NP40 0.5% (w/v) sodium deoxycholate 0.5 mM PMSF
Buffer EB:	Buffer E containing 2 mg/ml BSA

## 2.10 Endoproteinase reaction buffers

Clostripain (endoproteinase Arg-C):	50 mM Tris-HCl pH 7.5 20 mM DTT 1 mM CaCl <sub>2</sub>
V8 protease (endoproteinase Glu-C):	
For cleavage at Glu	50 mM NH <sub>4</sub> HCO <sub>3</sub> pH 7.8
For cleavage at Glu and Asp	50 mM NaH <sub>2</sub> PO <sub>4</sub> pH 7.8
Endoproteinase Lys-C	25 mM Tris-HCl pH 7.7 1 mM EDTA

Trypsin 50 mM  $\text{NH}_4\text{HCO}_3$  pH 7.8

## 2.11 Other buffers

Ficoll gradient solution:  
(Eagles AB) 5% (w/v) Ficoll 400 in Eagles A plus  
Eagles B without phenol red  
15% (w/v) Ficoll 400 in Eagles A plus Eagles  
B without phenol red

Versene: 0.6 mM EDTA  
0.0002% (w/v) phenol red  
in PBS A

Trypsin: 0.25% (w/v) trypsin dissolved in Tris-saline

Tris-saline: 140 mM NaCl  
30 mM KCl  
280 mM  $\text{Na}_2\text{HPO}_4$   
25 mM Tris-HCl pH 8  
1 mg/ml glucose  
0.1 mg/ml streptomycin  
100 units/ml penicillin  
0.0015% (w/v) phenol red

Trypsin/versene: 1:1 (v/v) trypsin:versene

## 3 METHODS

### 3.1 Growth of cells and virus stocks

#### 3.1.1 Cell culture

RSC and MeWo cells were grown in Dulbecco's medium supplemented with 9% (v/v) FCS, and BHK C13 cells were grown in GMEM supplemented with 8% (v/v) NCS. All cells were grown at 37°C in a humidified atmosphere comprising 95% (v/v) air and 5% (v/v) CO<sub>2</sub>. The cells were harvested from plastic roller bottles by pouring off the medium and washing the monolayer with 20 ml versene. They were then washed with 20 ml trypsin/versene to remove the monolayer and resuspended in fresh medium at a concentration of approximately 10<sup>7</sup> cells/ml. Aliquots of 10<sup>7</sup> cells were seeded into roller bottles containing 100 ml of the relevant medium.

#### 3.1.2 Virus stocks

Cells were grown in roller bottles containing 100 ml Dulbecco's medium until 90% confluent. The medium was replaced with 40 ml Dulbecco's medium supplemented with 2% (v/v) FCS. The appropriate amount of virus (usually 0.01 pfu/cell) was added in 500 µl Dulbecco's medium and the roller bottles returned to 37°C. The infected cells were incubated until maximal cpe was observed (usually 2-4 days pi). The medium was poured off and infected cells pelleted by centrifugation for 15 min at 2500 rpm and 4°C using a Sorvall RC-5B refrigerated Superspeed centrifuge. The supernatant was decanted and centrifuged at 12,000 rpm for 2 h in a Sorvall RC-5B refrigerated Superspeed centrifuge. The pellet was resuspended in approximately 1 ml of Dulbecco's medium to give the cell-released virus stock. Stocks were disrupted in a bath ultrasonicator at 4°C, frozen on dry ice and stored at -70°C. Virus stocks were titrated before use.

#### 3.1.3 Titration of virus stocks

Virus stocks were titrated at 37°C on 90% confluent monolayers of RSC, MeWo or BHK C13 cells (depending on the cell type used to grow the stock) on 35 mm 6-well trays in Dulbecco's medium. Serial dilutions of the virus (usually from 10<sup>-3</sup> to 10<sup>-8</sup>) were made and 1 ml of each dilution added to drained monolayers. The plates were returned to the incubator for 90 min, after which the inoculum was removed and the plates overlaid with 4 ml methyl cellulose. After 2-4 days the overlay was removed and the plates were

stained with Giemsa stain for 30 min at RT and washed. The plaques were counted under a dissecting microscope and the virus titre calculated.

### **3.1.4 Purification of virions and L-particles**

Virions and L-particles were purified as described by Szilagyi & Cunningham (1991).

#### **(a) Production of gradients**

Virions and L-particles were purified using 5-15% Ficoll 400 gradients prepared as follows in 35 ml cellulose nitrate centrifuge tubes using a Biocomp Gradient Master. Five percent (w/v) and 15% (w/v) solutions of Ficoll were made in E<sub>AB</sub>. The required volume of 5% Ficoll was poured into a fresh centrifuge tube, and underlayered with the required volume of 15% Ficoll. The tube was sealed with a rubber cap, ensuring that air bubbles were excluded. The platform on the gradient maker was levelled and the tubes placed in the magnetic holder. Two settings were used to mix the gradient: 5 min at an angle of 50° and a speed of 25, followed by 40 sec at 80° and a speed of 25.

#### **(b) Purification**

A virus stock was prepared and pelleted as described in section 3.1.2 and 5%-15% Ficoll 400 gradients were prepared as described in section 3.1.4(a). The virus pellet was resuspended in a minimal volume of Dulbecco's medium, layered onto the gradient and centrifuged for 2 h at 12,000 rpm in a Sorvall AH629 rotor. The virions, which formed a well defined lower band, and the L-particles, which formed a more diffuse upper band, were withdrawn separately from the gradient using a wide bore needle. Both virions and L-particles were diluted to 34 ml in complete PBS and pelleted by centrifugation at 20,000 rpm for 1 h in a Sorvall AH629 rotor. The pellets were resuspended in a minimum volume of complete PBS, frozen on dry ice and stored at -70°C.

## **3.2 Analysis of HSV-1 induced polypeptides**

### **3.2.1 Sodium dodecyl sulphate-polyacrylamide gel electrophoresis (SDS-PAGE)**

#### **(a) Tris-glycine gels**

SDS-PAGE was carried out using slab gels cast vertically in a sandwich consisting of two glass plates separated by perspex spacers. Two types of gels were used; "mini-gels" were run on a Bio-Rad Mini Protean II<sup>TM</sup> apparatus, large gels were run on a Life Technologies, Inc BRL V 15.17 apparatus. A 45 ml gel mix was prepared for the large

gels and a 5 ml gel mix prepared for “mini-gels” using commercial polyacrylamide (40% acrylamide/Bis-acrylamide 37.5:1, Sigma) and a resolving gel buffer containing 375 mM Tris-HCl pH 8.8 and 0.1% (w/v) SDS. Polymerisation was initiated by addition of 0.006% (w/v) ammonium persulphate (APS) and 0.004% (v/v) N,N,N',N', tetramethylenediamine (TEMED) just prior to pouring. The resolving gel was left to polymerise under a thin layer of butan-2-ol. Before the stacking gel was poured the butan-2-ol was removed and the surface of the resolving gel rinsed with dH<sub>2</sub>O.

The stacking gel was composed of 5% acrylamide in stacking gel buffer composed of 125 mM Tris-HCl (pH 6.8) and 0.1% (w/v) SDS. Just before pouring, 0.006% (w/v) APS and 0.004% (v/v) TEMED were added to initiate polymerisation. A comb was used to form wells. Before electrophoresis protein samples were boiled for 5 min in protein boiling mix to denature them and then applied to the gel. Electrophoresis was carried out in electrophoretic buffer at 10-15 mA at RT.

#### **(b) Tris-Tricine**

Tris-Tricine gel electrophoresis for resolution of smaller proteins and peptides was performed as detailed by Schagger & Von Jagow (1987). Acrylamide stock solutions of the ratios 48:1.5 and 46.5:3 acrylamide/NN'-methylenebisacrylamide were prepared and deionised using Amberlite beads. The resolving gel solution with the desired acrylamide concentration, usually 16.5%, and final concentrations of 1 M Tris-HCl pH 8.45 and 0.1% (w/v) SDS was poured as outlined in the protocol for Tris-glycine gels (section 3.2.1(a)). Polymerisation of resolving gel was initiated by addition of 0.05% (w/v) APS and 0.0005% (v/v) TEMED, and proceeded under a thin layer of butan-2-ol.

The stacking gel comprised 4% acrylamide with a final concentration of 1 M Tris-HCl pH 8.45 and 0.1% (w/v) SDS. Polymerisation was initiated by 0.08% (w/v) APS and 0.0008% (v/v) TEMED. The stacking gel was poured on top of the resolving gel and the well-forming comb inserted. Electrophoresis was carried out for 16 h at 105 V at RT.

### 3.2.2 Protein visualisation

#### (a) Coomassie Brilliant Blue

Following electrophoresis, proteins were fixed for 30 min in fixing solution and then stained using Coomassie staining solution, followed by destaining in destain solution for at least 1 h at 37°C or (usually) overnight at RT.

#### (b) Autoradiography

Gels were fixed, stained and destained as detailed in section 3.2.3.(a). They were dried under vacuum onto Whatman grade 182 filter paper and exposed to Kodak X-Omat XS-1 film at RT.

Preparative gels for in-gel protease digestion and Tris-Tricine gels were fixed, stained and destained as detailed in section 3.2.3(a). The wet gels were carefully sealed in plastic bags and exposed in the same manner as dried gels.

### 3.2.3 Protease digestion and extraction of peptides from gel slices

#### (a) For analysis by SDS-PAGE

In-gel protease digestions were performed as detailed by Rothmann *et al.* (1998). Coomassie Brilliant Blue-stained bands were excised from SDS-PAGE gels and cut into small cubes (approximately 2 mm by 2 mm). Gel pieces were destained four times with 100 µl of acetonitrile:water (1:1 v/v) and suspended in 50 µl of acetonitrile, resulting in shrinkage of the gel cubes. The supernatant was discarded, and 50 µl of 100 mM  $\text{NH}_4\text{HCO}_3$  was added. After 15 min of swelling, the gel pieces were again shrunk in 50 µl of acetonitrile and dried briefly in a Speed-Vac. The dried pieces were then submerged in 100 µl of protease digestion buffer containing 12.5 µg/ml of protease (see section 2.10). After incubation for 30 min on ice, surplus digestion buffer was replaced by buffer without protease so that the gel pieces were just covered, and the samples were incubated overnight at the required temperature. Peptides were extracted from the gel pieces by washing twice with 50 µl of 25 mM  $\text{NH}_4\text{HCO}_3$ , and then three times with 50 µl of 5% formic acid (or twice with 70% aqueous trifluoroacetic acid and twice with trifluoroacetic acid-acetonitrile [1:1 (v/v)]), the gel slices were shrunk by a 50 µl acetonitrile wash after every step. All extraction steps were carried out with gentle shaking at 30-37°C, and volumes were kept as low as possible to reduce the final volume containing the eluted

peptides. All washes, including the acetonitrile from shrinkage steps, were pooled and dried down in a Speed-Vac. For analysis by SDS-PAGE, the peptides were resuspended in protein boiling mix and separated on a 16.5% Tris-Tricine gel.

**(b) For mass spectrometric analysis**

Peptide bands (approximately 8 mm by 2 mm) were excised, cut into very small cubes (1 mm by 1 mm), washed for 15 min with 40  $\mu$ l of 50% aqueous methanol-10% acetic acid and then for 10 min in 40  $\mu$ l of 10% aqueous methanol-7.5% acetic acid, and shrunk with 20  $\mu$ l of acetonitrile. Washes were discarded, and peptides were extracted by incubating the gel pieces for 1 h each in 30  $\mu$ l of 100 mM  $\text{NH}_4\text{HCO}_3$ , 30  $\mu$ l of 25 mM  $\text{NH}_4\text{HCO}_3$  and 30  $\mu$ l of 25 mM  $\text{NH}_4\text{HCO}_3$ -acetonitrile (1:1 v/v), shrinking with 20  $\mu$ l of acetonitrile after every step. Extractions were carried out with gentle shaking at 37°C in 500  $\mu$ l tubes with a tiny hole in the bottom so that liquid could be removed into a collection tube by brief centrifugation. Pooled extracts were concentrated to 2-5  $\mu$ l in a Speed-Vac and directly analysed by mass spectrometry.

### 3.2.4 Blotting polyacrylamide gels for mass spectrometric analysis

**(a) General blotting protocol**

PVDF membrane was cut to size and soaked in methanol for approximately 5-10 seconds, followed by soaking in water and then PVDF transfer buffer for at least 5 min. The electrophoresed gel was cut to size and soaked in PVDF transfer buffer for at least 5 min. The membrane was applied to the gel, sandwiched between two filter papers and electroblotted at 100 V for 1 h at RT. The membrane was removed, washed extensively in  $\text{dH}_2\text{O}$  and dried *in vacuo* overnight. The membrane was stained with sulforhodamine solution until bands were clearly visible, usually after about 1 min, washed in water and air dried.

**(b) For the UL49-encoded protein**

Blotting was carried out as described in section 3.2.7.(a), except that the PVDF blotting buffer contained 0.1% SDS rather than 0.01% SDS.

### (c) Coomassie staining of PVDF blotted samples

The membrane was removed from the blotting assembly and wet for a few seconds with methanol. PVDF Coomassie stain was added and gently agitated for 1 min. The stain was decanted, destain added and the blot rinsed several times with destain until bands appear. The destained blot was rinsed several times with dH<sub>2</sub>O.

### 3.2.5 Mass spectrometric analysis of proteins

After staining, the membranes were dried *in vacuo* overnight. The bands to be analysed were excised from the membrane and placed into 0.5 ml tubes. 3 µl of endoproteinase (usually sequencing grade trypsin) was added at a concentration of 40 µg/ml in 50 mM NH<sub>4</sub>HCO<sub>3</sub> containing 1% (w/v) n-octyl β-D-glucopyranose (Sigma). The tubes were incubated overnight at RT, after which 7 µl formic acid:ethanol (1:1 v/v) was added for 1 h at RT to elute the peptides. Then 0.5 µl of each sample was placed onto a mass spectrometer loading strip and air dried, and 0.5 µl of matrix solution containing insulin B as a mass marker was added to each sample and air dried before inserting the strip into the mass spectrometer (Finnigan MAT Lasermat). The samples were subjected to laser desorption mass spectrometric analysis to produce a mass spectrum characteristic of the protein analysed.

### 3.2.6 Immune precipitation

Glass beads were used to remove a confluent monolayer of cells from a roller bottle. The cells were transferred to a 50 ml Falcon tube and centrifuged at 2.5 K for 5 min at 4°C using a Sorval RT6000B centrifuge. The supernatant was removed and 1 ml 0.9% NaCl added per 1 g of cells, and left for 5 min at 4°C. Five ml of acetone (pre-chilled to -20°C) was added per 1 g of cells and left for 30 min at 4°C, mixing every 5 min. The sample was then centrifuged at 2.5 K for 10 min using a Sorval RT6000B centrifuge and the supernatant removed. The pellet was spread onto Whatman number 1 filter paper and allowed to air dry. The dry powder was transferred to an air-tight vial and stored at RT.

Antisera was pre-cleared by mixing 200 µl of the antisera with a small amount of the dried acetone powder (approximately 1/10 of the dried volume). The antisera and acetone powder was mixed on a rotary mixer for 90 min at 4°C. Following this, the antisera acetone powder mix was centrifuged at 12,000 rpm for 7 min using a MSE Mini Centaur.

The supernatant, which represented the pre-cleared antisera, was removed to a fresh vial. The pre-cleared antisera was stored at  $-20^{\circ}\text{C}$ .

Fifty  $\mu\text{l}$  of CNE was mixed with 150  $\mu\text{l}$  buffer A and the required pre-cleared antibody at  $4^{\circ}\text{C}$  for 5 h. Protein A insolubilized on Sepharose CL-4B was mixed 1:1 (v/v) with buffer E and washed twice. After mixing for 5 h, 75  $\mu\text{l}$  of the Protein A Sepharose was added to each sample and mixed at  $4^{\circ}\text{C}$  for 1 h. After 1 h the samples were centrifuged at 12,000 rpm for 1 min using a MSE Mini Centaur, the supernatant was removed and stored. The Protein A Sepharose beads were washed twice with buffer EB, once with buffer EN and four times with buffer E. After washing the beads were suspended in protein boiling mix and boiled for 5 min and analysed on SDS-PAGE. The gels were fixed, stained and destained and exposed if necessary.

### **3.3 *In vitro* phosphorylation reactions**

Sample preparation and phosphorylation reactions were performed as detailed by Coulter (1993).

#### **3.3.1 Preparation of nuclear and cytoplasmic extracts from infected cells**

Confluent monolayers of MeWo, RSC or BHK C13 cells in roller bottles were infected with HSV-1 at 5-10 pfu/cell and incubated at  $37^{\circ}\text{C}$  for 5 h. The cells were scraped into 10 ml complete PBS, pelleted by centrifugation at 2000 rpm for 10 min at  $4^{\circ}\text{C}$  using a Sorval RT6000B refrigerated centrifuge and resuspended in 10 ml Buffer A. The cells were then disrupted on ice using 20 strokes of a Dounce homogeniser and centrifuged at 3000 rpm for 10 min at  $4^{\circ}\text{C}$  using a Sorval RT6000B centrifuge. The supernatant, representing the crude cytoplasmic extract, was removed and frozen on dry ice to be stored at  $-70^{\circ}\text{C}$ . The nuclear pellet was resuspended in 3 ml Buffer A and subjected to ultrasonic disruption followed by centrifugation at 2000 rpm for 3 min at  $4^{\circ}\text{C}$  using a Sorval RT6000B centrifuge. The supernatant, representing the crude nuclear extract (CNE), was frozen on dry ice and stored at  $-70^{\circ}\text{C}$ .

#### **3.3.2 Treatment of virions for *in vitro* phosphorylation reactions**

Permeabilised virions were produced by mixing 30  $\mu\text{l}$  of virions with 1.2  $\mu\text{l}$  each of 0.25 M Tris-HCl pH 7.5, 0.025 M DTT and 1.25% (v/v) NP40. The mixture was incubated on

ice for 1 h and diluted with an equal volume of 10 mM Tris-HCl pH 7.5, 1 mM MgCl<sub>2</sub> and 1 mM DTT.

Stripped virions were produced by mixing a 90 µl sample of virions with 10 µl of 10% (v/v) NP40. This was incubated on ice for 15 min, followed by centrifugation at 12,000 rpm for 10 min using a MSE Mini Centaur. The supernatant, constituting the virion membranes were removed, and an equal volume of 1% (v/v) NP40 added to the pellet. The pellet was resuspended by sonication and centrifuged at 12,000 rpm for 10 min using an MSE Mini Centaur. The supernatant was discarded, an equal volume of complete PBS added and the pellet resuspended by sonication.

### 3.3.3 *In vitro* phosphorylation of infected cell extracts and virions

Five µl CNE or stripped or permeabilised virions were mixed with 10 µl NaCl (ranging from 0-3 M), 5 µl 4 x phosphorylation buffer and 1 µCi [ $\gamma$ -<sup>32</sup>P]ATP. The mixture was incubated at 37°C for 30 min. The products were analysed by SDS-PAGE. The gel stained, dried and exposed to X-ray film.

### 3.3.4 Assay for phosphate cycling

*In vitro* phosphorylation reactions were performed as described in section 3.3.3. After the 30 min incubation, half the sample was transferred to a fresh Eppendorf tube, protein boiling mix added and the sample placed on ice. To the other half, 1 µl of the relevant concentration of unlabelled ATP was added and incubated at 37°C for a further 30 min. The products were analysed by SDS-PAGE. The gel was stained, dried and exposed to X-ray film.

## 3.4 Computational analysis

Sequence alignments were produced using the PILEUP and PRETTY programs (University of Wisconsin, Genetics Computing Group).

3-D protein structures were obtained from the National Center for Biotechnology Information (NCBI) database and viewed using Cn3D version 3.0.

Secondary structure predictions were made using PsiPred, an on-line secondary structure prediction programme ([wwwrun@insulin.brunel.ac.uk](mailto:wwwrun@insulin.brunel.ac.uk)).

Peptide masses were obtained using Massmap software (Finnigan, MAT).

## 4 RESULTS

### 4.1 *In vitro* phosphorylation of nuclear extracts from infected cells

A previous study by Coulter *et al.* (1993) employed an *in vitro* assay to compare the phosphorylation profiles of *wt* HSV-1 and an HSV-1 UL13-*lacZ* mutant. The assay involved incubating membrane stripped virions or infected BHK cell CNEs for 30 min at 37°C in the presence of [ $\gamma$ -<sup>32</sup>P]ATP. Assays were performed at a variety of NaCl concentrations ranging from 0 to 1.5 M. Proteins were separated on a 9% polyacrylamide gel, and radiolabelled proteins were visualised by autoradiography. In *wt* CNE, two highly radiolabelled phosphoproteins were detected migrating with Mrs of 57 and 38 kDa. Radiolabelling of the 57 kDa protein was slightly reduced at low NaCl concentrations, whereas the 38 kDa protein showed peak radiolabelling at NaCl concentrations of 0.5 to 1 M. In UL13-*lacZ* CNE, the phosphorylated 57 kDa protein was absent and the 38 kDa protein was phosphorylated only at low NaCl concentrations. The data indicated that the 57 kDa protein, probably encoded by gene UL13, was involved in phosphorylation of a variety of CNE proteins, the 38 kDa protein prominent among them. Sequence analysis predicted that the UL13 protein is a PK (Fig. 1.13). Therefore, it was hypothesised that UL13 PK targeted the 38 kDa protein, shown to be encoded by the gene UL49, for phosphorylation. These experiments were carried out using a single mutant containing a large insertion in the UL13 gene, and without using a revertant virus to ensure that the phenotype was due to the UL13 mutation. In order to confirm and extend these observations, the assay was repeated using two additional independent UL13 mutants containing a small insertion or deletion in gene UL13.

MeWo cells were either mock infected (MI) or infected with *wt*, UL13I-16 bp, UL13D-4 bp or UL13-*lacZ* HSV-1 (see Table 1.12). Cells were infected at a moi of 10, and infection was allowed to proceed for 5 h at 37°C. Nuclear extracts were prepared and phosphorylated *in vitro* following the protocol defined by Coulter *et al.* (1993). An autoradiograph showing the radiolabelled phosphoproteins is shown in Fig. 4.1.1. Several phosphorylated proteins detected in *wt* CNE were absent from MI CNE, including strongly phosphorylated proteins migrating at 57 kDa and 38 kDa. The phosphorylation profiles of the UL13 mutants were similar to each other, but

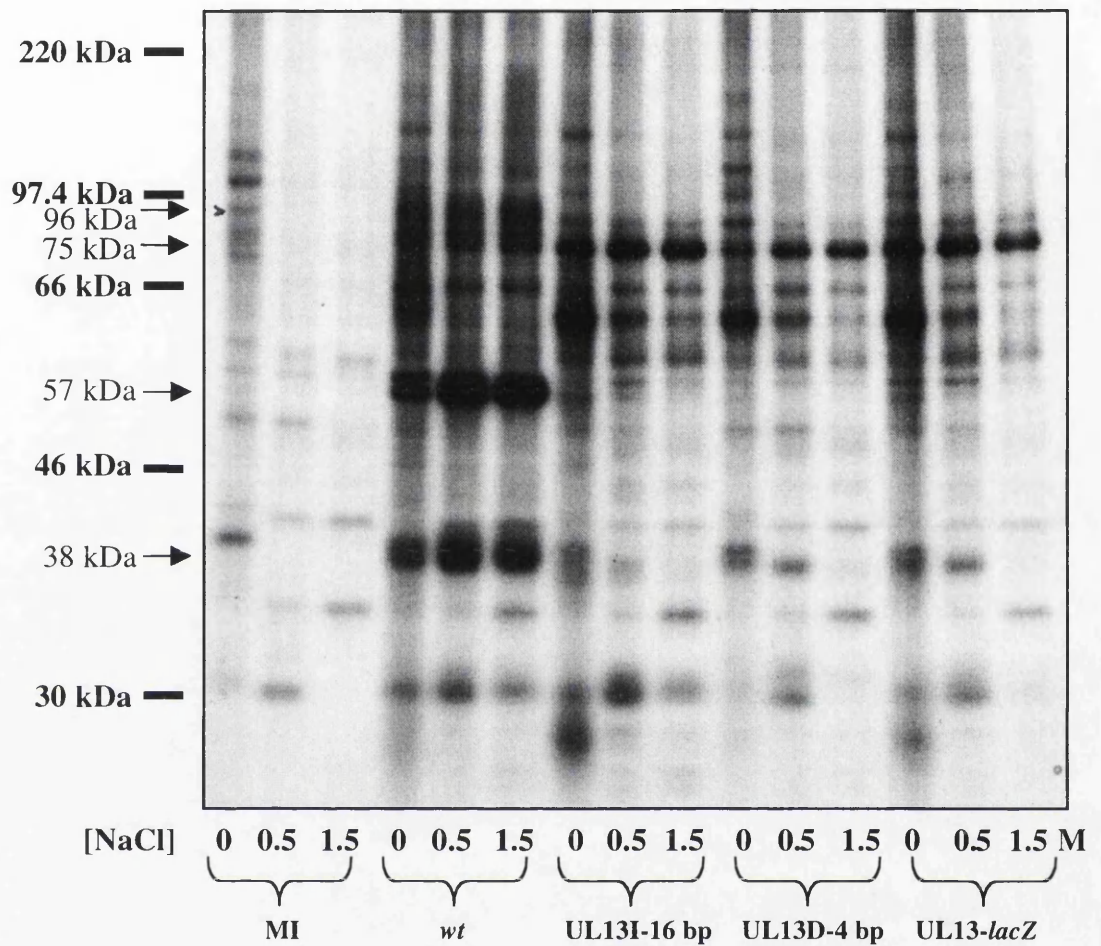


**Figure 4.1.1** Autoradiograph showing *in vitro* phosphorylation profiles of *wt* and UL13 mutant-infected cell CNE.

MeWo cells were mock-infected or infected with *wt* or UL13<sup>-</sup> mutants for 5 h at 37°C. CNEs were prepared and incubated in the presence of [ $\gamma$ -<sup>32</sup>P]ATP over a range of NaCl concentrations. The proteins were separated on a 9% polyacrylamide gel and visualised by exposure to X-ray film.

demonstrated a number of differences compared to *wt* CNE. Most strikingly, these included absence of the 57 kDa phosphoprotein, and substantially reduced phosphorylation of a number of proteins, most obviously the 38 kDa protein. In addition, the phosphorylation levels of some proteins were dependent on NaCl concentration. In *wt* CNE the 57 and 38 kDa proteins showed reduced phosphorylation at low NaCl concentrations. In UL13 mutant CNE the 38 kDa protein was most highly phosphorylated at 0 M NaCl.

Fig. 4.1.1 shows that deletion of the UL13 gene stimulates increased radiolabelling of a viral protein of approximately 75 kDa and decreased labelling of a 96 kDa phosphoprotein. As outlined in section 1.3.5.1, Purves & Roizman (1992) identified ICP22 in *wt* CNE as five phosphoprotein species ranging in Mr from 70 to 82 kDa. However, in UL13 mutant CNE the 70 kDa phosphoprotein appeared to be present in increased amounts while the higher Mr phosphoproteins were absent. In addition, Ogle *et al.* (1997) showed ICP0 to be a substrate for the UL13 PK. While the observations in this study correlate with the previous data, further work would be required to determine whether the 75 and 96 kDa phosphoprotein observed in Fig. 4.1.1 are ICP22 and ICP0.

These observations confirm those made by Coulter *et al.* (1993) and prove that the observed differences in phosphorylation profile are due to disruption of the UL13 gene. The presence of the 57 kDa and 38 kDa phosphoproteins in *wt* CNE but not MI CNE suggests that they are viral proteins. Since the 57 kDa phosphoprotein was totally absent from each mutant CNE, it is likely to represent the UL13 gene product. Indeed the predicted mass of the UL13 protein is 57,193 Da (McGeoch *et al.*, 1988). The prediction that the UL13 protein is a PK is consistent with reduced phosphorylation of several proteins in UL13 mutant CNEs, the most prominent being the 38 kDa protein. These proteins could act as direct or indirect targets for the putative UL13 PK. However, phosphorylation of the 38 kDa protein in mutant CNE, albeit greatly reduced, indicates the activity of additional PKs.

The *in vitro* phosphorylation assay shown in Fig. 4.1.1 followed the protocol defined by Coulter *et al.* (1993), in which CNE samples are incubated for 30 min at 37°C in the presence of [ $\gamma$ -<sup>32</sup>P]ATP. To ensure maximal phosphorylation was achieved *in vitro*,

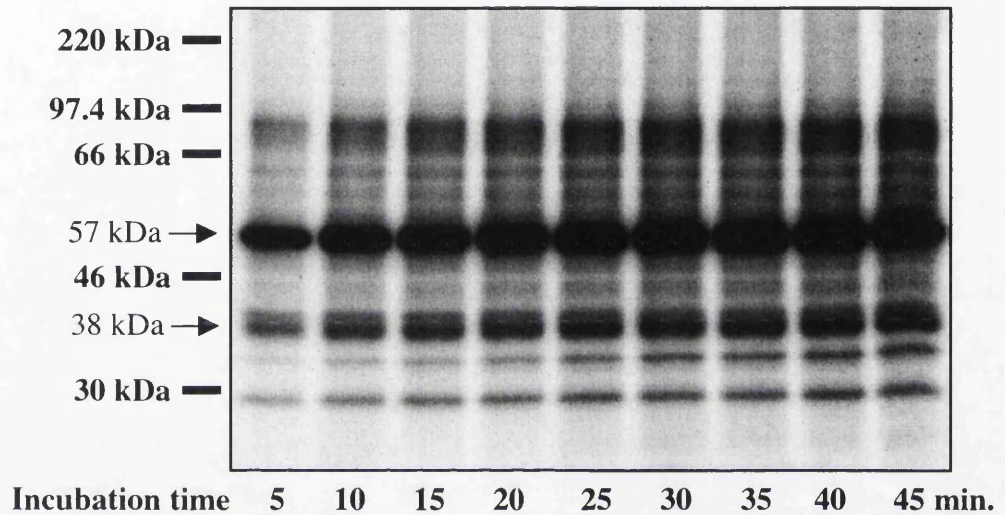


**Figure 4.1.2** Autoradiograph showing the effects of varying *in vitro* phosphorylation incubation times.

Aliquots of *wt* HSV-1 infected MeWo cell CNE were incubated at 37°C and 1.5 M NaCl in the presence of [ $\gamma$ - $^{32}$ P]ATP for the times indicated. Reactions were stopped by immediate addition of protein boiling mix (PBM) and boiling the samples. Proteins were separated on a 9% polyacrylamide gel and visualised by exposure to X-ray film.

phosphorylation assays were carried out for a range of times from 5 to 45 min. The resulting autoradiograph is shown in Fig. 4.1.2. The level of phosphorylation of all proteins, including the 57 and 38 kDa proteins, increased between 5 and 10 min, and was followed by a gradual increase up to 25 min. From 30 min onwards, radiolabelling did not increase. Because there is no obvious increase in the phosphorylation levels beyond 30 min incubation, this would appear to be the optimal incubation time. Despite increased radiolabelling, the phosphorylation profile remained unchanged at all time points, indicating that an incubation time of less than 30 min could be used if necessary.

The phosphorylation protocol defined by Coulter *et al.* (1993) required incubating infected cell CNE in a buffer comprising 10 mM MgCl<sub>2</sub>, 50 mM Tris-HCl pH 7.5 and 1 mM DTT, in addition to [ $\gamma$ -<sup>32</sup>P]ATP and a range of NaCl concentrations. A variety of phosphorylation buffers have been used in other studies. A study on the PRV UL13 PK by De Wind *et al.* (1992) showed that replacing MgCl<sub>2</sub> with MnCl<sub>2</sub> in the phosphorylation buffer stimulated PK activity. A separate study on HSV-2 UL13 found that PK activity increased with increasing pH, peaking when buffered by Tris-HCl pH 8.8-9.2 (Daikoku *et al.*, 1997). To examine the effects of buffer conditions on the HSV-1 UL13 PK, a series of *in vitro* phosphorylation reactions were performed on CNE samples using different buffer compositions and concentrations. Fig. 4.1.3 shows the phosphorylation profiles of aliquots of *wt* and UL13-*lacZ* CNE incubated in a buffer comprising either 10 mM MgCl<sub>2</sub> or MnCl<sub>2</sub>, either 50 mM Tris-HCl pH 7.5 or 9.2 and 1 mM DTT. The samples were incubated at 37°C for 30 min in the presence of [ $\gamma$ -<sup>32</sup>P]ATP.

The most highly radiolabelled phosphoprotein in *wt* CNE was the 57 kDa UL13 protein, which was absent from UL13-*lacZ* CNE. Phosphorylation of the UL13 protein was greater in *wt* CNE incubated at pH 7.5, and MnCl<sub>2</sub> stimulated phosphorylation in comparison with MgCl<sub>2</sub> at both pHs. These data are in agreement with De Wind *et al.* (1992), who showed that MnCl<sub>2</sub> stimulated phosphorylation of the PRV UL13 protein. However, they are at variance with Daikoku *et al.* (1997), who found that phosphorylation of the HSV-2 UL13 protein was greater at pH 9.2 than at pH 7.5. It should be noted, however, that HSV-2 UL13 also differs from HSV-1 UL13 in its NaCl sensitivity. HSV-2 UL13 is inhibited at NaCl concentrations above 0.5 M, compared to

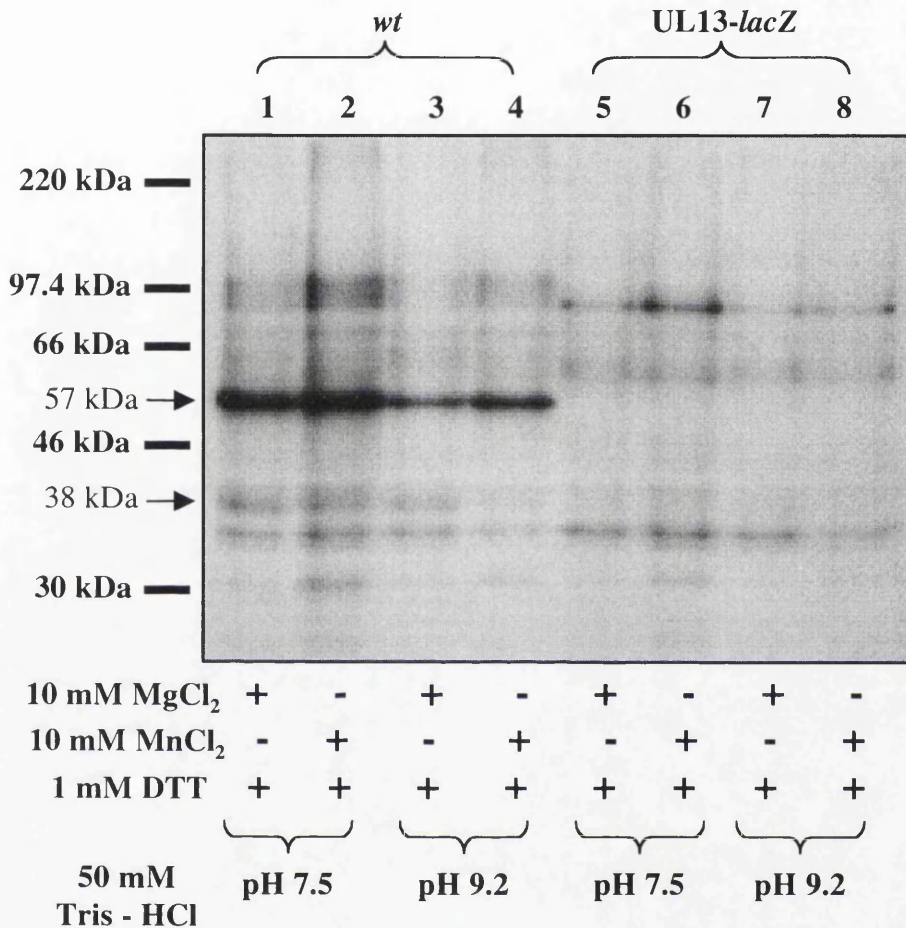


**Figure 4.1.3** Autoradiograph showing the *in vitro* phosphorylation profiles of *wt* and UL13-*lacZ* CNE under a variety of buffer conditions.

Aliquots of *wt* and UL13-*lacZ* infected MeWo cell CNE were incubated at 37°C in the presence of [ $\gamma$ -<sup>32</sup>P] ATP and the indicated phosphorylation reaction buffer. All assays were performed at 1.5 M NaCl. The proteins were separated on a 9% polyacrylamide gel and the radiolabelled proteins visualised by exposure to X-ray film.

the well documented stimulation of HSV-1 UL13 at higher NaCl concentrations (Cunningham *et al.*, 1992; Coulter *et al.*, 1993).

## 4.2 Multiple phosphorylation of the 57 kDa protein

The data so far confirm that a large number of proteins in *wt* CNE are phosphorylated when incubated *in vitro* with [ $\gamma$ - $^{32}$ P]ATP. The two most highly phosphorylated migrate with apparent Mrs of 57 and 38 kDa. The phosphorylated 57 kDa protein was absent from each of the three independent UL13 mutant CNEs, indicating that it was encoded by the UL13 gene. Disruption of the UL13 gene also resulted in reduced phosphorylation of a variety of proteins, including a 38 kDa protein encoded by the gene UL49 (Coulter *et al.*, 1993). The hypothesis that the UL13 protein possesses PK activity, phosphorylating a variety of proteins including the 38 kDa protein was investigated further by attempting to map phosphorylated amino acid residues within the 57 and 38 kDa proteins. Initially, however, it was important to determine basal phosphorylation levels of these proteins in CNE. Since CNE proteins can be radiolabelled *in vitro* using [ $\gamma$ - $^{32}$ P]ATP, if these proteins are phosphorylated prior to radiolabelling they must be able to cycle phosphate. An *in vitro* assay was devised to test for phosphate cycling.

Aliquots of *in vitro* radiolabelled *wt* and UL13-*lacZ* CNE (unchased) were incubated with excess unlabelled ATP (chased). The details and results of the assay are shown in Fig. 4.2.1. Two highly phosphorylated proteins migrating at 57 and 38 kDa were present in radiolabelled, unchased *wt* CNE. Both were absent from unchased UL13-*lacZ* CNE. In chased *wt* CNE, radiolabelling of both the 57 and 38 kDa phosphoproteins was reduced. In addition, a novel, highly phosphorylated protein migrating with a Mr of approximately 62 kDa was present. No phosphoproteins of 38, 57 or 62 kDa were present in chased UL13-*lacZ* CNE.

Analysis of the UL13D-4 bp and UL13I-16 bp mutants produced similar results. In Fig. 4.2.2 the two major radiolabelled phosphoproteins in the unchased *wt* CNE migrated as before with Mrs of 57 and 38 kDa. In all unchased UL13 mutant CNEs the 57 kDa phosphoprotein was completely absent and the 38 kDa protein demonstrated a marked reduction in phosphorylation. Chased *wt* CNE exhibited reduced phosphorylation of the 57 and 38 kDa proteins and appearance of the 62 kDa phosphoprotein. All of these radiolabelled phosphoproteins were absent from the chased UL13 mutant CNEs.

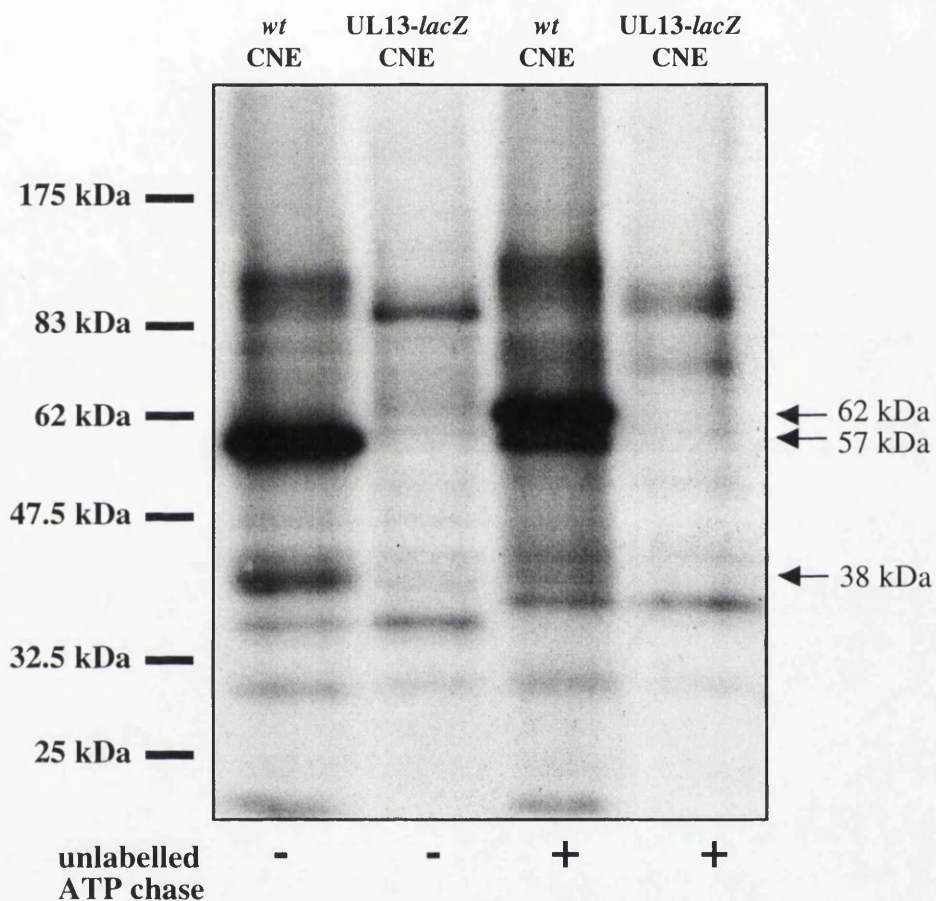


**Figure 4.2.1** Autoradiograph showing an *in vitro* assay for phosphate cycling.

Aliquots of *wt* or UL13-*lacZ* infected MeWo cell CNE were incubated at 37°C and 1.5 M NaCl in the presence of [ $\gamma$ - $^{32}$ P]ATP. After 30 min incubation, half of each sample was added to PBM and boiled. The remaining half was incubated for a further 30 min in the presence of 5 mM unlabelled ATP. Proteins were separated on a 9% polyacrylamide gel, and radiolabelled proteins visualised by exposing the dried gel to X-ray film.

**Figure 4.2.2 Autoradiographs showing an *in vitro* assay for phosphate cycling.**

Aliquots of MeWo cell CNE infected with either *wt* or UL13<sup>-</sup> mutants were incubated at 37°C and 1.5 M NaCl in the presence of [ $\gamma$ -<sup>32</sup>P]ATP. After 30 min incubation, half of each sample was added to PBM and boiled. The remaining half was incubated for a further 30 min in the presence of 5 mM unlabelled ATP. Protein were separated on a 9% polyacrylamide gel and radiolabelled proteins visualised by exposing the dried gel to X-ray film.

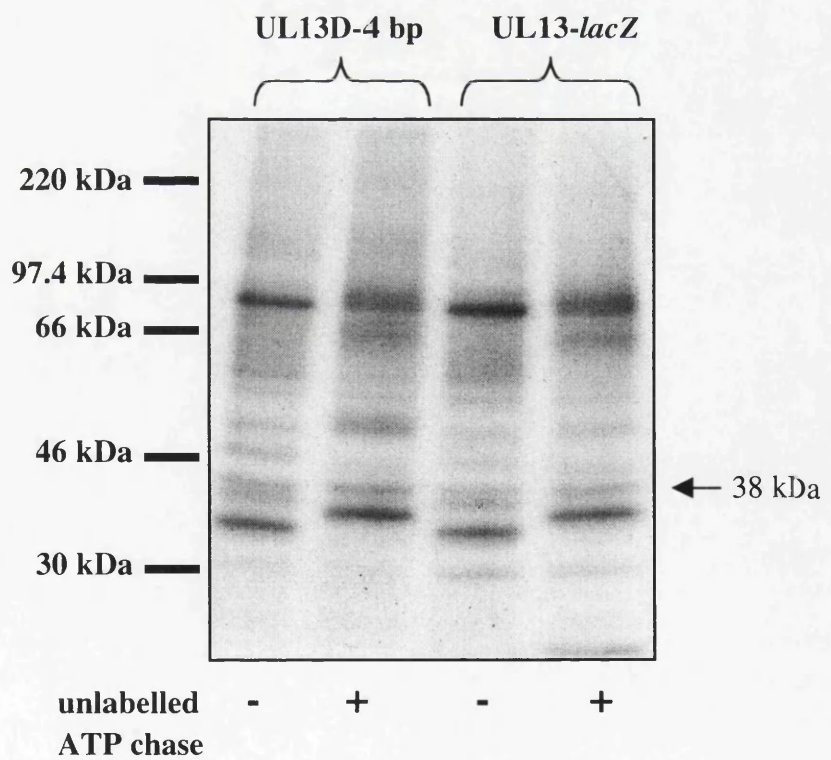
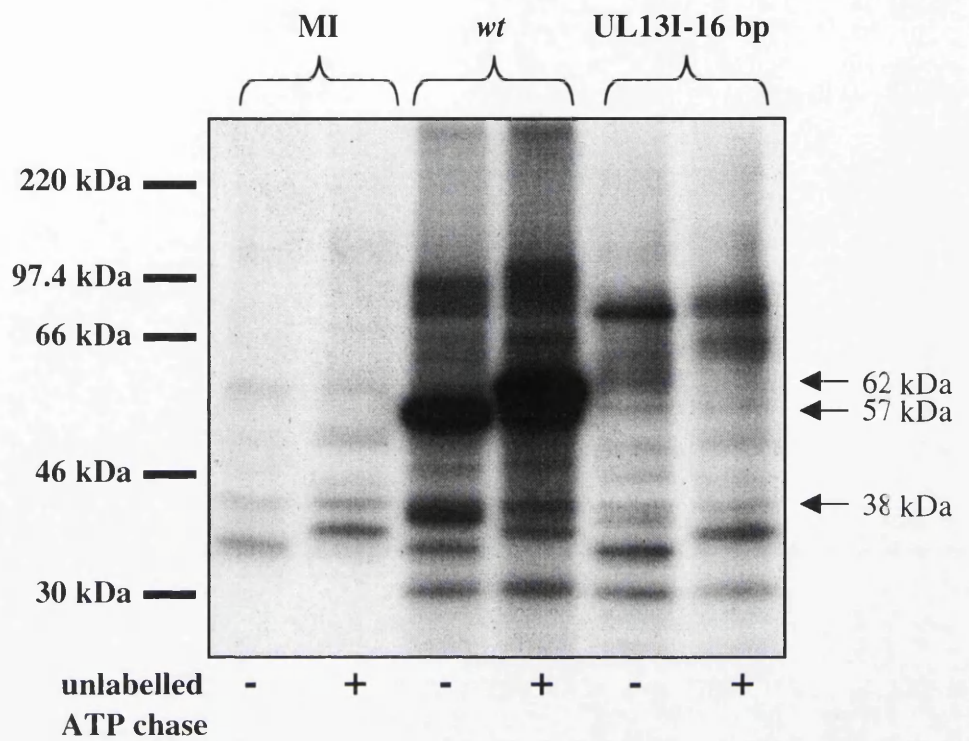
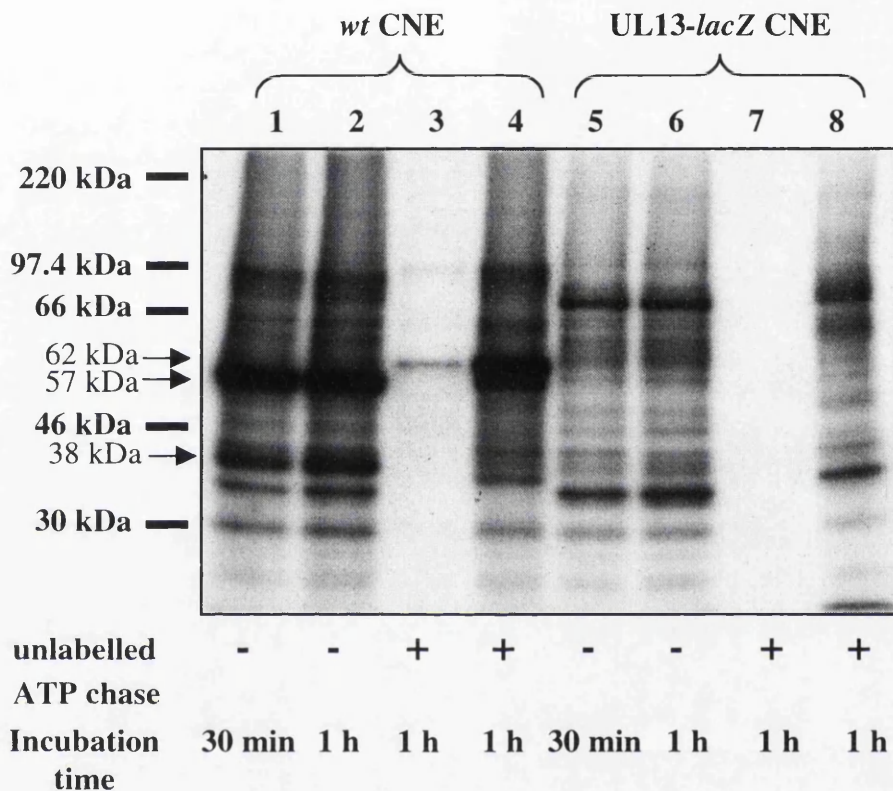


Figure 4.2.2

Chase assays involve incubating CNE with excess ATP for 30 min beyond the normal phosphorylation incubation time. Fig. 4.2.3 details a series of phosphorylation assays designed to determine whether the chased CNE phosphorylation profile resulted from excess ATP or increased incubation time. Comparing lanes 1 and 2 shows no change in the phosphorylation profile. In lane 3, radiolabelling was greatly reduced when unlabelled ATP was added at the start of the assay. Under these conditions, two faintly radiolabelled phosphoproteins were detected in *wt* CNE with Mrs of approximately 97 and 62 kDa. Both proteins were absent from UL13-*lacZ* CNE. In lane 4 the unlabelled ATP chase was added after radiolabelling for 30 min and phosphoproteins with Mrs of 57 and 62 kDa were clearly detected. No radiolabelled phosphoproteins with these Mrs were seen in UL13-*lacZ* CNE treated under the same conditions. These data prove that excess ATP and not extended incubation time stimulated phosphorylation of the 62 kDa protein. As expected, unlabelled ATP added at the start of the incubation resulted in a very low level of radiolabelling, with the 62 kDa phosphoprotein being one of the products.

To determine conclusively whether phosphorylation of the 62 kDa protein is stimulated by excess ATP independent of incubation time, a series of assays was performed as detailed in Fig. 4.2.4. Aliquots of *wt* CNE were phosphorylated *in vitro* with [ $\gamma$ - $^{32}$ P]ATP, followed by an unlabelled ATP chase ranging from 5 to 45 min. The radiolabelled 57 and 62 kDa phosphoproteins were detected in all samples, confirming that production of the 62 kDa phosphoprotein is stimulated in the presence of excess ATP regardless of incubation time. It is unclear why the 10 min and 35 min samples demonstrate reduced radiolabelling. On the basis of these data it was hypothesised that the 62 kDa protein is a hyperphosphorylated protein. Phosphorylation interferes with SDS binding causing the protein to migrate more slowly, as such a hyperphosphorylated protein would migrate with an artificially high Mr. The best candidate for the precursor of the 62 kDa protein was the highly radiolabelled 57 kDa protein. To test this hypothesis, immunoprecipitations were performed on aliquots of *in vitro* radiolabelled CNE samples using polyclonal antisera raised against amino acid residues 149 to 207 of the UL13 protein (Cunningham *et al.*, 1992).



**Figure 4.2.3** Autoradiograph showing an *in vitro* assay to determine the effect of varied incubation and chase times on phosphorylation profiles.

Aliquots of *wt* and *UL13-lacZ* infected MeWo cell CNE were incubated at 37°C and 1.5 M NaCl in the presence of [ $\gamma$ - $^{32}$ P]ATP. Samples 1 and 5 were incubated unchased for 30 min and samples 2 and 6 incubated unchased for 1 h. Samples 3 and 7 were simultaneously radiolabelled and chased for 1 h. Samples 4 and 8 were radiolabelled for 1 h, chased with 5 mM unlabelled ATP for the final 30 min. Proteins were separated on a 9% polyacrylamide gel and radiolabelled proteins visualised by exposing the dried gel to X-ray film.

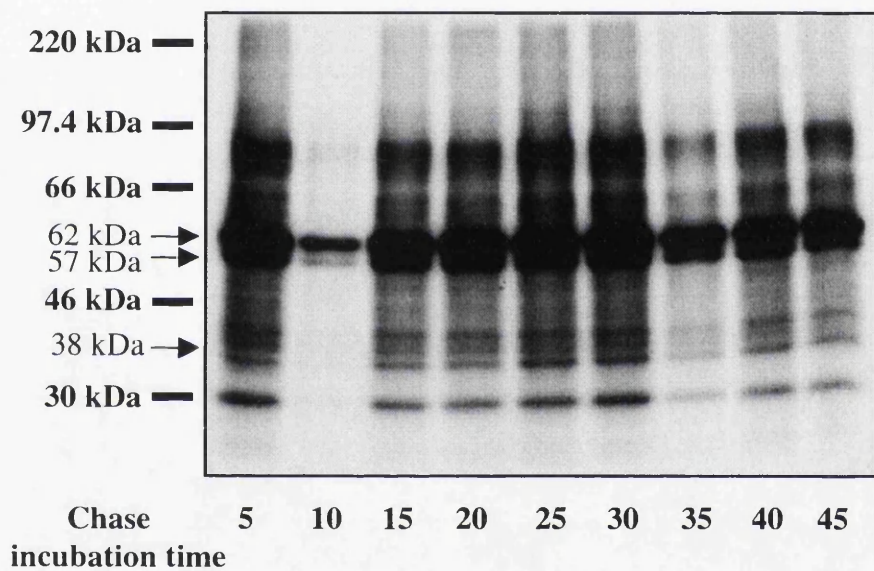


**Figure 4.2.4** Autoradiograph showing an *in vitro* assay to determine the effect of varied chase times on phosphorylation profiles.

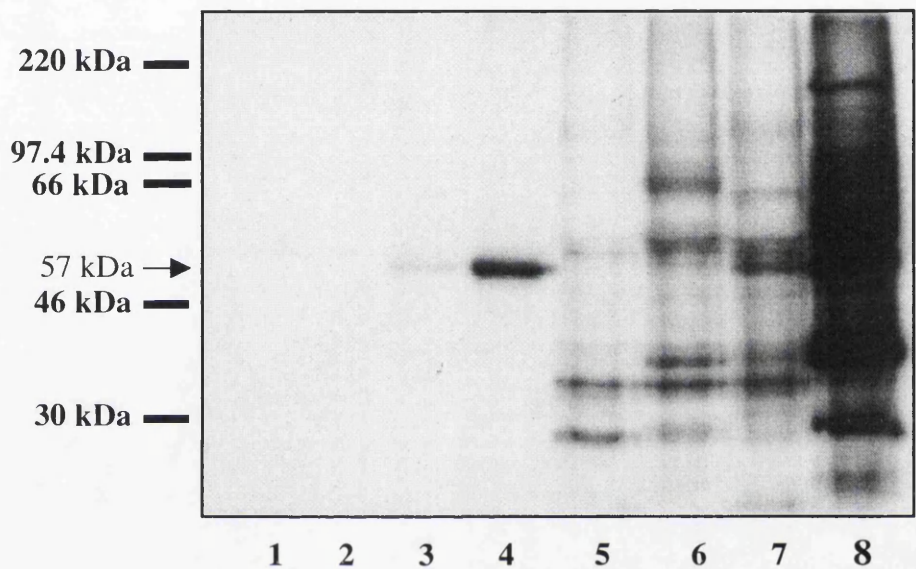
Aliquots of *wt* infected MeWo cell CNE were incubated at 37°C and 1.5 M NaCl in the presence of [ $\gamma$ - $^{32}$ P]ATP. After 30 min 5 mM unlabelled ATP was added and the samples were incubated at 37°C for the indicated time. Reactions were stopped by adding PBM and boiling. Proteins were separated on a 9% polyacrylamide gel, and radiolabelled proteins were visualised by exposing the dried gel to X-ray film.

Fig. 4.2.5 shows the immunoprecipitates derived from MI, UL13-*lacZ* and *wt* CNE. No radiolabelled phosphoproteins were immunoprecipitated from MI and UL13-*lacZ* CNE. A single radiolabelled protein with a Mr of approximately 57 kDa was precipitated from *wt* CNE. The yield of this protein was greater from CNE derived from cells infected for 20 h than for 5 h. This result confirms that the 57 kDa protein is the UL13 protein. To determine whether the 57 and 62 kDa proteins are related, the immunoprecipitation was repeated using unchased and chased *wt* CNE. The results are shown in Fig. 4.2.6.

The 57 kDa phosphoprotein was precipitated in small amounts from unchased 5 h *wt* CNE and in greater amounts from unchased 20 h *wt* CNE. The 57 and 62 kDa phosphoproteins were immunoprecipitated from chased samples, again more obviously in 20 h *wt* CNE. It is not possible to rule out that the 57 kDa and 62 kDa protein co-immunoprecipitate. However, these data, coupled with the fact that the 62 kDa protein must be a chased form of a previously highly labelled phosphoprotein, show that the 62 kDa phosphoprotein is a hyperphosphorylated form of the UL13-encoded 57 kDa phosphoprotein. Thus, the putative UL13 PK possesses multiple phosphorylation sites.

The majority of PKs utilise only ATP as a phosphate donor, but a few, including the putative UL13 PK, utilise both ATP and GTP. The nucleotide specificity of phosphorylation of the 62 kDa protein was tested by performing chase assays using unlabelled GTP, CTP or UTP. The results are shown in Fig. 4.2.7.

Aliquots of *wt* CNE were incubated at 37°C for 30 min in the presence of [ $\gamma$ -<sup>32</sup>P]ATP and chased with 5 mM (reaction concentration) unlabelled GTP, CTP or UTP. Chasing with GTP resulted in reduced phosphorylation of the 57 and 38 kDa proteins and production of the 62 kDa phosphoprotein. Neither CTP nor UTP stimulated reduced radiolabelling of the 57 or 38 kDa protein or production of the 62 kDa phosphoprotein. Therefore, phosphate cycling of the 38 kDa protein and production of the 62 kDa phosphoprotein specifically utilises GTP or ATP. These data further confirm that the 62 kDa protein is a hyperphosphorylated protein and show that the PK responsible is able to utilise both ATP and GTP.



**Figure 4.2.5** Autoradiograph showing immunoprecipitation of *in vitro* phosphorylated CNE by a UL13 antiserum.

MeWo cells were mock-infected (lanes 1 and 5) or infected with UL13-*lacZ* (lanes 2 and 6) or *wt* for 5 h (lanes 3 and 7) or 20 h (lanes 4 and 8). CNE were prepared and incubated at 37°C and 1.5 M NaCl in the presence of [ $\gamma$ - $^{32}$ P]ATP. The phosphorylated CNE samples were then incubated with polyclonal antiserum raised against amino acid residues 149 to 207 of the UL13 protein. The precipitated antibody-antigen complexes were separated on a 9% polyacrylamide gel and visualised by exposing the dried gel to X-ray film.

Lanes 1-4 represent immunoprecipitated samples and lanes 5-8 represent 20% of the supernatant.

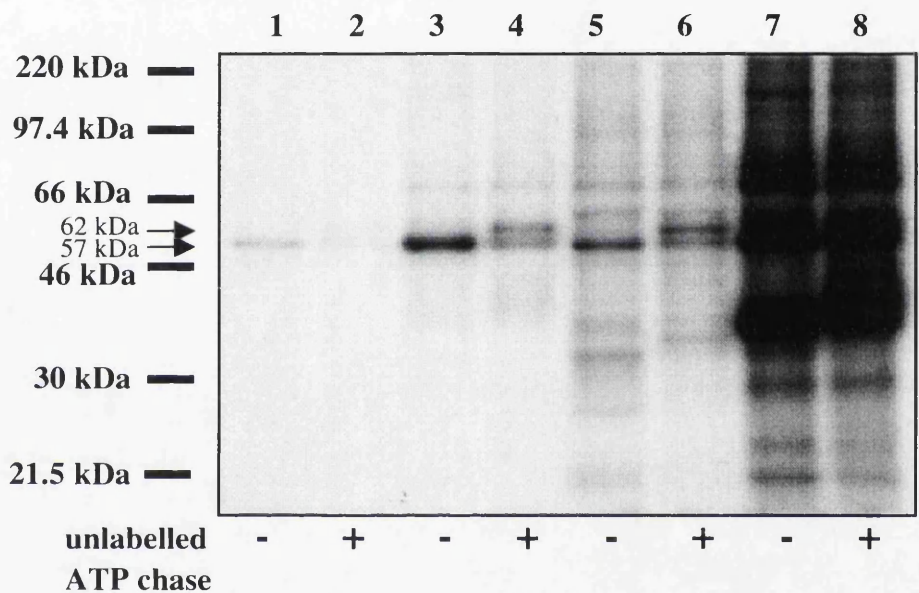


**Figure 4.2.6** Autoradiograph showing immunoprecipitation of *in vitro* phosphorylated unchased and chased *wt* CNE by a UL13 antiserum.

MeWo cells were infected with *wt* virus for 5 h (lanes 1, 2, 5 and 6) or 20 h (lanes 3, 4, 7 and 8). CNE were prepared and incubated at 37°C and 1.5 M NaCl in the presence of [ $\gamma$ - $^{32}$ P]ATP. After 30 min, 1  $\mu$ l unlabelled ATP was added to samples 2 and 4 to a reaction concentration of 5 mM and incubated for a further 30 min. The phosphorylated CNE samples were incubated with polyclonal antiserum raised against amino acid residues 149 to 207 of the UL13 protein. The precipitated antibody-antigen complexes were separated on a 9% polyacrylamide gel and visualised by exposing the dried gel to X-ray film.

Lanes 1-4 represent the immunoprecipitated samples and samples 5-8 represent 20% of the supernatant.

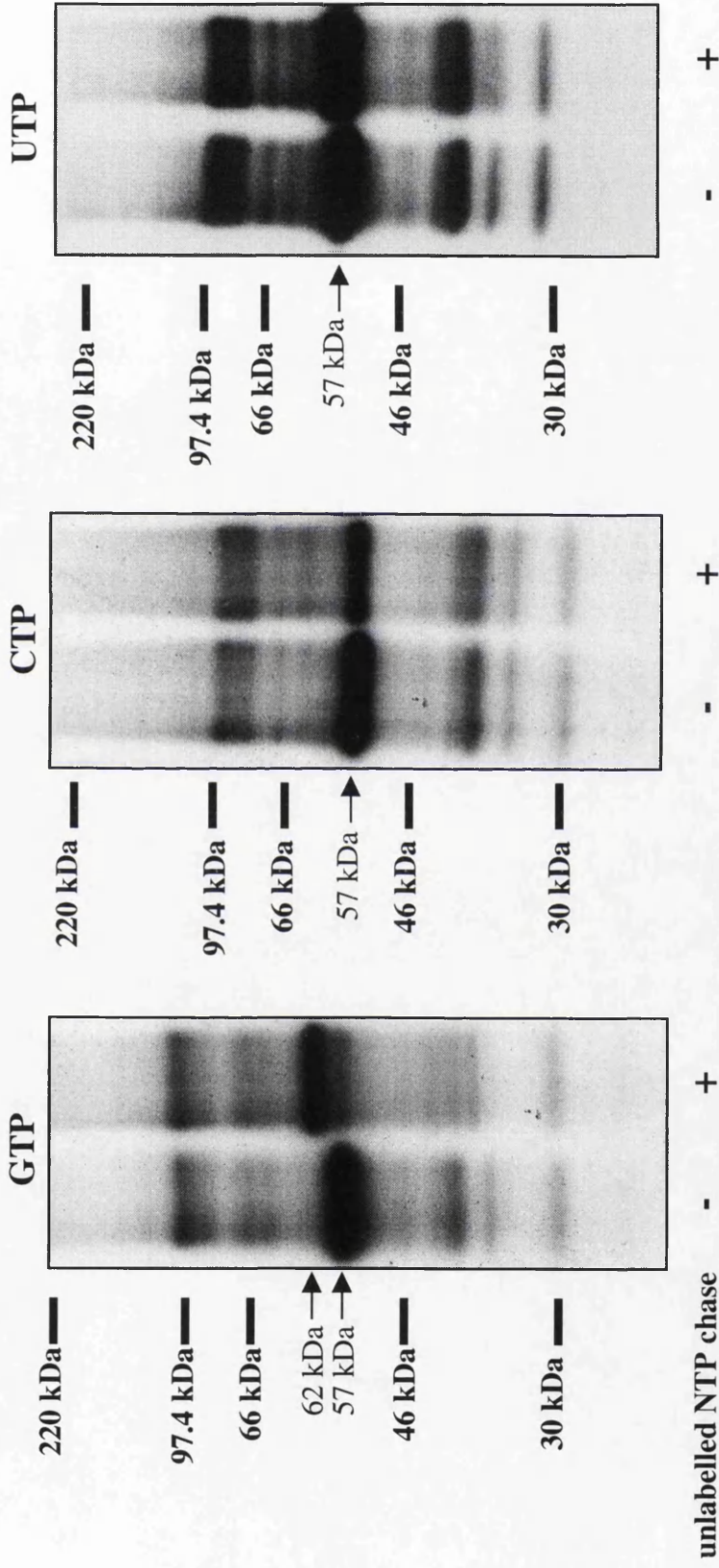


**Figure 4.2.7** Autoradiograph showing an *in vitro* assay for nucleoside specificity of phosphorylation.

Aliquots of *wt* infected MeWo cell CNE were incubated at 37°C and 1.5 M NaCl in the presence of [ $\gamma$ - $^{32}$ P]ATP. After 30 min incubation, half the sample was added to PBM and boiled. The remaining half was incubated for a further 30 min in the presence of 5 mM cold GTP, CTP or UTP. Proteins were separated on a 9% polyacrylamide gel and radiolabelled proteins were visualised by exposing the dried gel to X-ray film.

On the basis of the previous finding, chase assays were performed with various concentrations of unlabelled ATP or GTP to determine the relative efficiency of each as phosphate donor. The results are given in Figs. 4.2.8 and 4.2.9. Aliquots of *wt* CNE were incubated for 30 min at 37°C in the presence of [ $\gamma$ -<sup>32</sup>P]ATP, followed by an unlabelled ATP or GTP chase of the indicated concentration. Fig. 4.2.8 shows the effect of decreasing the ATP concentration. Chasing with 5 mM unlabelled ATP resulted in reduced labelling of the 57 and 38 kDa proteins and phosphorylation of the 62 kDa protein. This phosphorylation profile was maintained as the ATP concentration in the chase was reduced to 5  $\mu$ M. At 500 nM, labelling of the 57 and 38 kDa proteins was only slightly reduced compared to unchased *wt* CNE. Under these conditions, the 62 kDa phosphoprotein was absent, and instead a novel phosphoprotein of approximately 60 kDa was produced. The phosphorylation profile produced in the presence of 50 nM ATP is indistinguishable from that of an unchased sample, and remains unchanged at lower ATP concentrations. Fig. 4.2.9 shows the effect of unlabelled GTP chase concentration on the phosphorylation profile. Chasing with 500  $\mu$ M GTP stimulated only a partial reduction in the level of radiolabelling of the 38 and 57 kDa phosphoproteins. It stimulated phosphorylation of a 60 kDa protein, but not the 62 kDa protein. At 50  $\mu$ M GTP the phosphorylation profile was identical to unchased *wt* CNE and remained unchanged at lower GTP concentrations.

There appear to be three distinct phosphorylation profiles depending upon ATP or GTP concentration. At higher concentrations, an unlabelled ATP or GTP chase stimulated reduced radiolabelling of the 57 and 38 kDa phosphoproteins and phosphorylation of a 62 kDa protein. At low ATP or GTP chase concentrations the phosphorylation profiles were indistinguishable from those of unchased CNE. At intermediate chase concentrations, radiolabelling of the 57 and 38 kDa phosphoproteins was partially reduced. In addition, the 62 kDa phosphoprotein was not detected, but a novel 60 kDa phosphoprotein was detected instead. Production of the 60 kDa phosphoprotein was stimulated by a 500 nM ATP or 500  $\mu$ M GTP chase. The novel 60 kDa phosphoprotein probably represents an additional level of phosphorylation between the hypophosphorylated 57 kDa and hyperphosphorylated 62 kDa UL13 proteins.

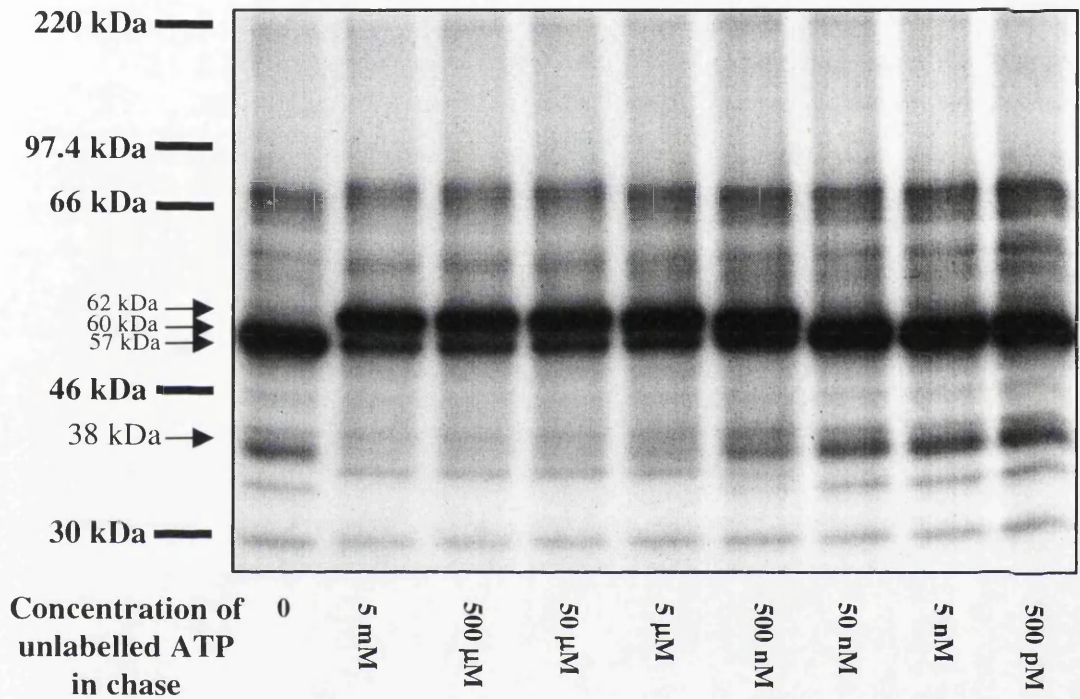
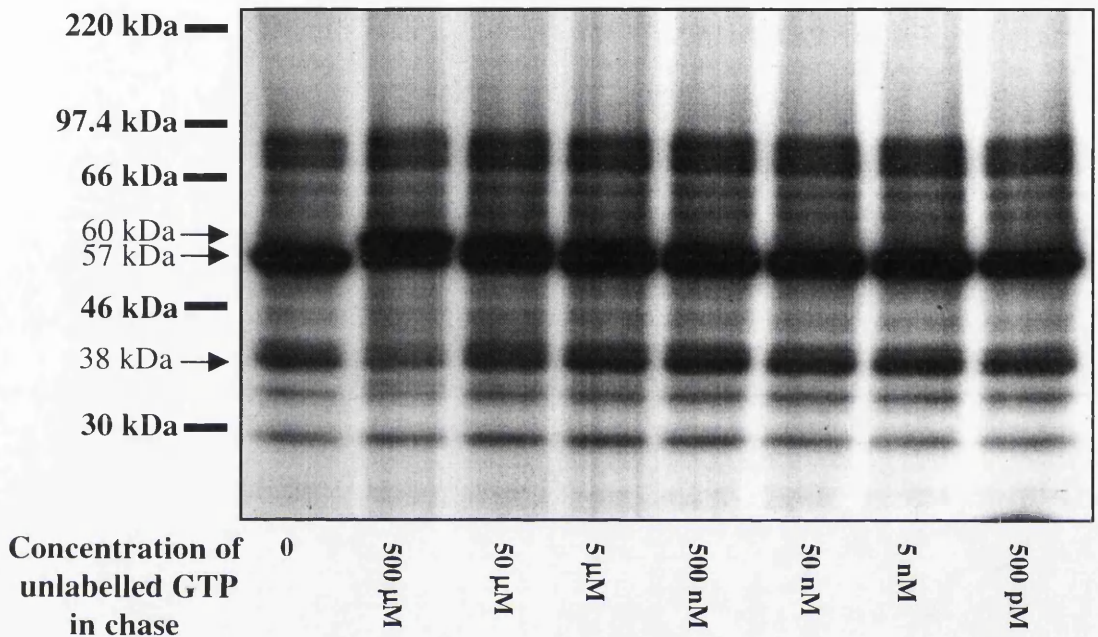


**Figure 4.2.8** Autoradiograph showing an *in vitro* assay for phosphate cycling with decreasing unlabelled ATP chase concentrations.

Aliquots of *wt* infected MeWo cell CNE were incubated at 37°C and 1.5 M NaCl in the presence of  $[\gamma\text{-}^{32}\text{P}]\text{ATP}$ . After 30 min incubation, 1 μl of unlabelled ATP was added to give the indicated reaction concentration and the samples were incubated for 30 min. The proteins were separated on a 9% polyacrylamide gel and visualised by exposing the dried gel to X-ray film.

1.



2.



**Figure 4.2.9** Autoradiograph showing an *in vitro* assay for phosphate cycling with decreasing unlabelled GTP chase concentrations.

Aliquots of *wt* infected MeWo cell cell CNE were incubated at 37°C and 1.5 M NaCl in the presence of  $[\gamma\text{-}^{32}\text{P}]\text{ATP}$ . After 30 min incubation, 1  $\mu\text{l}$  of unlabelled GTP was added to give the indicated reaction concentration and the samples were incubated for 30 min. The proteins were separated on a 9% polyacrylamide gel and visualised by exposing the gel to X-ray film.

Panel 2 shows a lower exposure of the 57 to 60 kDa region.

All the chase-stimulated phosphorylation profiles discussed to this point were visualised by separating the proteins on small (55 x 95 mm) polyacrylamide gels. Fig. 4.1.1 shows radiolabelled, unchased *wt* CNE separated on a large (120 x 175 mm) polyacrylamide gel. On this autoradiograph a phosphoprotein migrating slightly more slowly than the 57 kDa phosphoprotein can be clearly seen. The migration of this phosphoprotein in relation to the chase-stimulated 62 kDa phosphoprotein was unknown. To clarify the situation, radiolabelled, chased CNE samples were separated on a large polyacrylamide gel. The results are shown in Fig. 4.2.10.

A highly phosphorylated protein was detected in unchased *wt* CNE migrating with a Mr of 57 kDa. It is clearly visible at 0 M and 1.5 M NaCl, with increased phosphorylation at the higher NaCl concentration. A second phosphoprotein migrated at 59 kDa, and phosphorylation of this protein appears to be similar at both NaCl concentrations. As expected, radiolabelling of the 57 kDa phosphoprotein was greatly reduced in chased *wt* CNE. The 59 kDa protein also showed reduced radiolabelling in chased *wt* CNE. Chasing with unlabelled ATP stimulated phosphorylation of the 62 kDa protein at 0 M and 1.5 M NaCl, moreso at 1.5 M NaCl. These results show that a 59 kDa phosphoprotein is present in unchased and chased *wt* CNE, and it is only possible to differentiate the 57 and 59 kDa phosphoproteins when they are visualised on “large” gels, as they co-migrate on mini gels. It is unclear whether the 59 kDa phosphoprotein in unchased samples and the chase stimulated 60 kDa proteins are the same. However, the 60 kDa phosphoprotein is only detected in CNE incubated with a 500 nM ATP or 500  $\mu$ M GTP chase. The concentration of [ $\gamma$ - $^{32}$ P]ATP in unchased CNE was only 80 pM, far too low to stimulate phosphorylation of the 60 kDa phosphoprotein. However, further work, such as western blot analysis, would be required to confirm this.

Because phosphorylation of the 57 and 62 kDa proteins depends on NaCl concentration, ATP chase assays were performed over a range of NaCl concentrations. The results are shown in Fig. 4.2.11. As in previous experiments, two highly phosphorylated proteins migrating at 57 and 38 kDa were produced by unchased *wt* CNE. The 38 and 57 kDa phosphoproteins were marginally more highly phosphorylated at 1.0 M NaCl. The 57 kDa protein was absent from phosphorylated UL13-*lacZ* CNE under all conditions, and radiolabelling of the 38 kDa decreased dramatically as NaCl concentration increased.

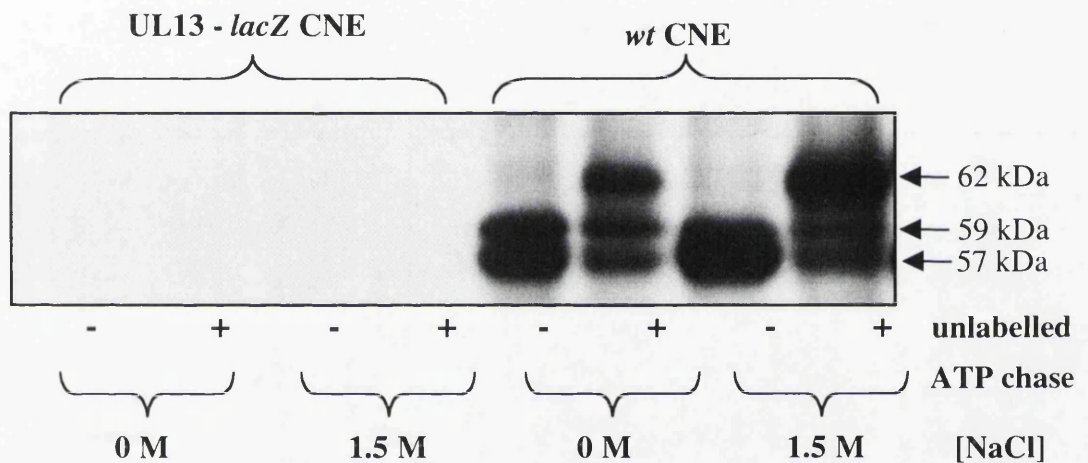


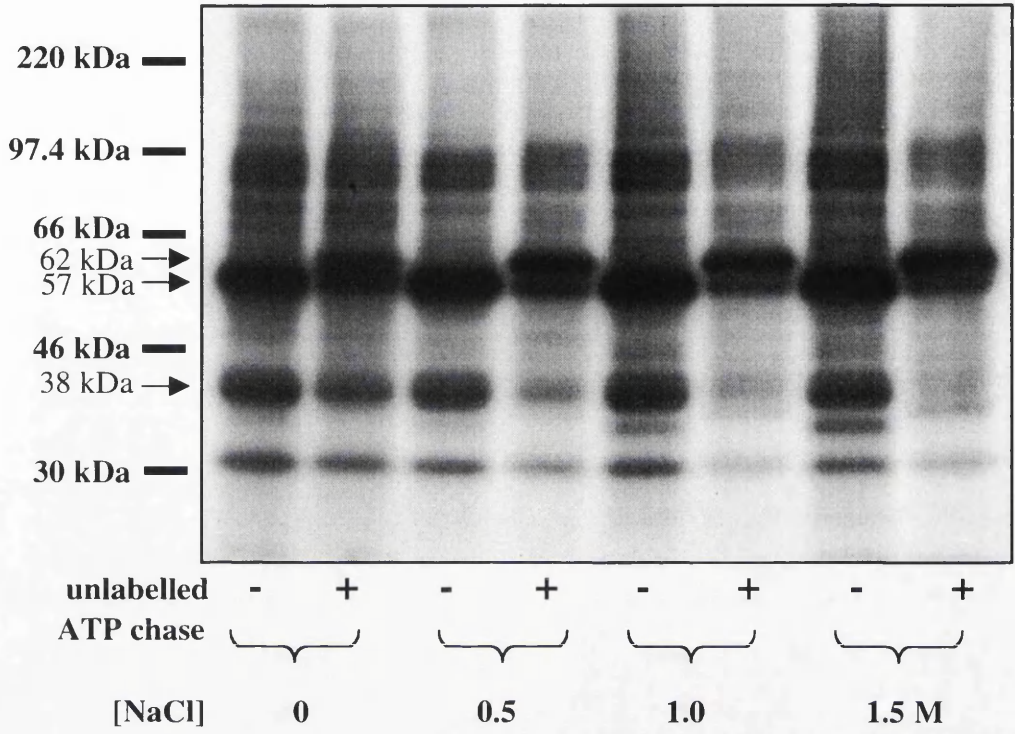
**Figure 4.2.10** Autoradiograph showing the relative migration of the 57, 59 and 62 kDa phosphoproteins.

Aliquots of *wt* and UL13-*lacZ* infected MeWo cell CNE were incubated at 37°C in the presence of 0 M or 1.5 M NaCl and [ $\gamma$ - $^{32}$ P]ATP. After 30 min incubation, half the sample was added to PBM and boiled. The remaining half was incubated for a further 30 min in the presence of 5 mM unlabelled ATP. Proteins were separated on a 9% polyacrylamide gel and visualised by exposing the dried gel to X-ray film.

**Figure 4.2.11 Autoradiograph showing an *in vitro* assay for phosphate cycling over a range of NaCl concentrations.**

Aliquots of *wt* and UL13-*lacZ* infected MeWo cell CNE were incubated at 37°C at the indicated NaCl concentration in the presence of [ $\gamma$ -<sup>32</sup>P]ATP. After 30 min incubation, 1  $\mu$ l of unlabelled ATP was added to a final concentration of 5 mM and the samples were incubated for 30 min. Proteins were separated on 55 x 95 mm 9% polyacrylamide gels and visualised by exposing the dried gels to X-ray film. Panel 1 represents *wt* CNE and panel 2 represents UL13-*lacZ* CNE

1.



2.

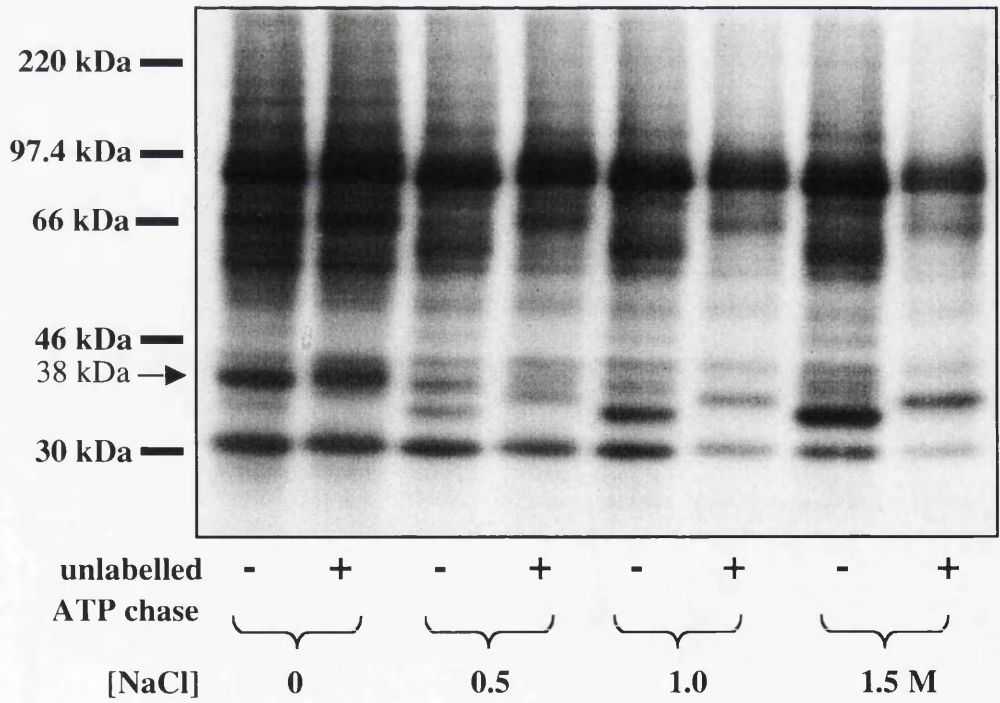


Figure 4.2.11

The effects produced by the unlabelled ATP chase depended upon NaCl concentration. In chased *wt* CNE, radiolabelling of the 38 and 57 kDa phosphoproteins decreased as NaCl concentration increased, whereas radiolabelling of the 62 kDa phosphoprotein increased between 0 and 0.5 M NaCl concentrations. In chased UL13-*lacZ* CNE the 57 and 62 kDa phosphoproteins were totally absent and the 38 kDa phosphoprotein was only detected at 0 M NaCl.

It can be concluded from the data presented in this chapter that the 57 kDa and the 62 kDa phosphoprotein represent two differently phosphorylated forms of the UL13 protein. Hyperphosphorylation of the UL13 protein was stimulated by increased ATP or GTP concentration, and was independent of incubation time. It is noteworthy that both ATP and GTP were utilised in hyperphosphorylating the UL13 protein. Utilisation of both ATP and GTP as phosphate donors is relatively uncommon; CKI, CKII and the UL13 PK (Cunningham *et al.*, 1992) are examples of PKs that can use either nucleotide.

The data presented here shows that the UL13 protein possesses multiple phosphorylation sites, but the exact number is difficult to determine. The 57 and 62 kDa species imply at least two sites of phosphorylation. The third 60 kDa species, only found at intermediate ATP or GTP concentrations, implies a third site. As outlined earlier, because the minimum chase concentration required to phosphorylate the 60 kDa protein is far above the  $[\gamma\text{-}^{32}\text{P}]\text{ATP}$  concentration, it is unlikely that the 60 kDa and the 59 kDa phosphoproteins are the same. Interestingly, although it is known that multiple PKs target the UL49 protein, presumably at different sites, there was no evidence that the UL49 protein was capable of being hyperphosphorylated under any of the conditions tested.

### 4.3 Post-translational modification of the UL49 protein

The data presented in Chapter 4.2 showed that the UL13 protein was hyperphosphorylated in CNE incubated with excess ATP or GTP. However, the UL49 protein was found to cycle phosphate, and there was no evidence that the UL49 protein was hyperphosphorylated beyond a basal level. Because buffer composition affects phosphorylation (Fig. 4.1.3), the phosphorylation potential of UL49 was examined under different conditions. Fig. 4.3.1 shows the effects of a variety of buffer conditions on migration of the UL49 protein. The assay was performed using membrane stripped virions. As the UL49 protein is a highly abundant protein it could be clearly visualised by Coomassie staining as well as by radiolabelling.

An abundant 38 kDa protein, identified previously as the UL49 gene product (Coulter *et al.*, 1993), was seen migrating as a sharply defined, heavily staining band in unphosphorylated *wt* virions. Phosphorylating *wt* virions at 0 M NaCl in 10 mM MgCl<sub>2</sub> and 10 mM Tris-HCl stimulated the 38 kDa protein to migrate as a slightly broader, more diffuse band. The 38 kDa protein migrated as an equally diffuse band when the Tris-HCl concentration was increased to 50 mM. At 50 mM MgCl<sub>2</sub> and 10 mM Tris-HCl, the 38 kDa protein migrated as a more diffuse band. Incubating *wt* virions in 50 mM Tris-HCl and 50 mM MgCl<sub>2</sub> resulted in a diffuse 38 kDa band coupled with the appearance of a novel band migrating slightly more slowly than the 38 kDa protein, with an Mr of approximately 40 kDa. In all *wt* virions phosphorylated at 1.5 M NaCl, the 38 kDa protein migrated as a sharp, heavily stained band regardless of buffer composition.

Altering the composition of the phosphorylation buffer clearly stimulated changes in the migration of the 38 kDa protein. Individually, the effect of increasing MgCl<sub>2</sub> concentration was greater than increasing Tris-HCl concentration, and increasing both stimulated the appearance of a novel protein, migrating with an Mr of approximately 40 kDa. This 40 kDa protein is very likely to be a species of the 38 kDa protein demonstrating aberrant migration due to phosphorylation. To determine if the appearance of the 40 kDa protein is dependent upon ATP, a series of *in vitro* phosphorylation assays was performed as detailed in Fig. 4.3.2.

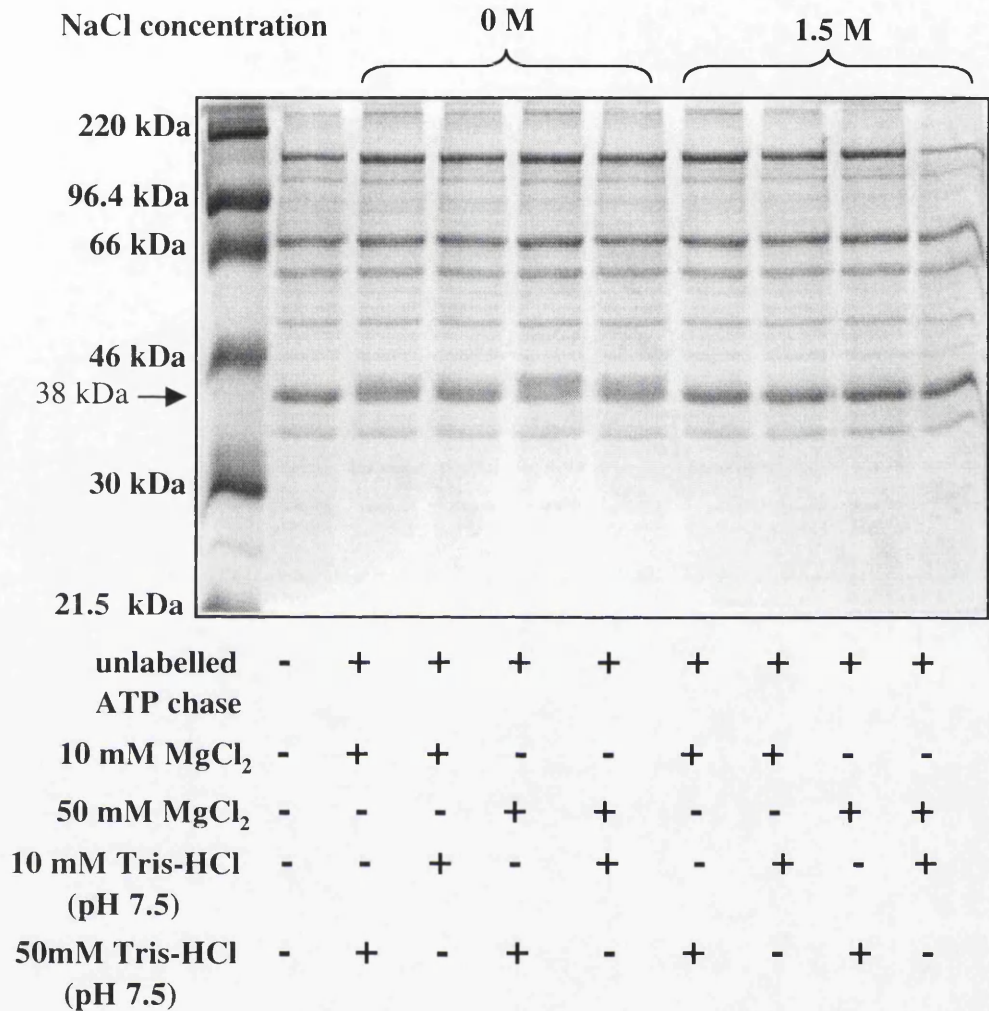


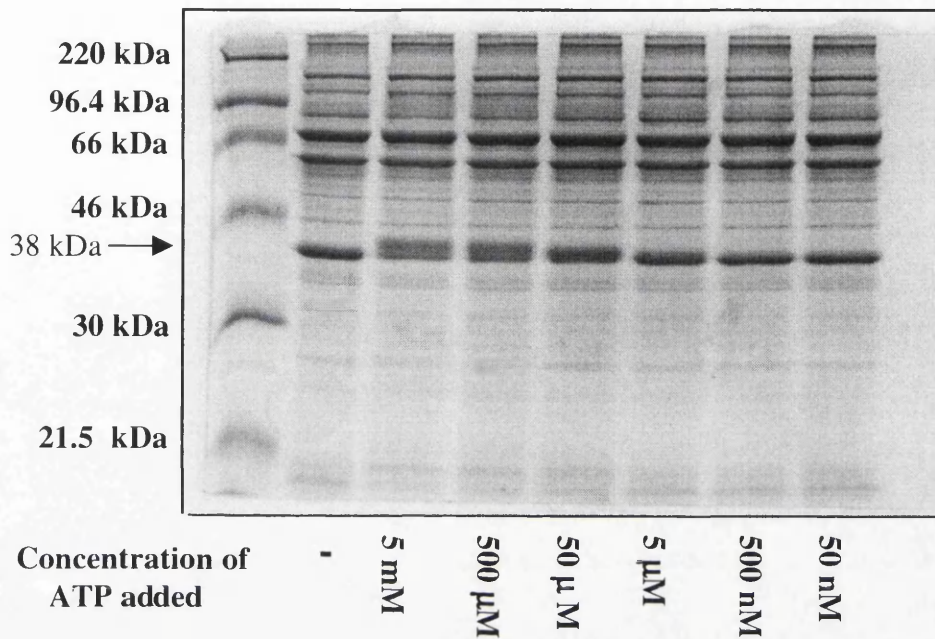
**Figure 4.3.1** Coomassie stained gel of *wt* virions phosphorylated *in vitro* at different buffer concentrations.

*Wt* virions were purified, treated with NP40 and incubated in the indicated phosphorylation buffer at either 0 M or 1.5 M NaCl in the presence of 5 mM ATP. The proteins were separated on a 10% polyacrylamide gel and visualised by staining with Coomassie Brilliant Blue.

**Figure 4.3.2 Coomassie stained gels of *wt* virions phosphorylated *in vitro* at a range of ATP concentrations.**

*Wt* virions were purified, treated with NP40 and incubated in phosphorylation buffer (50 mM MgCl<sub>2</sub>, 50 mM Tris-HCl pH 7.5, 1 mM DTT) at either 0 or 1.5 M NaCl in the presence of the indicated reaction concentration of ATP. The proteins were separated on a 10% polyacrylamide gel and visualised by staining with Coomassie Brilliant Blue. Panel 1 shows the virion proteins after phosphorylation at 0 M NaCl, panel 2 shows the virion proteins after phosphorylation at 1.5 M NaCl.

1.



2.

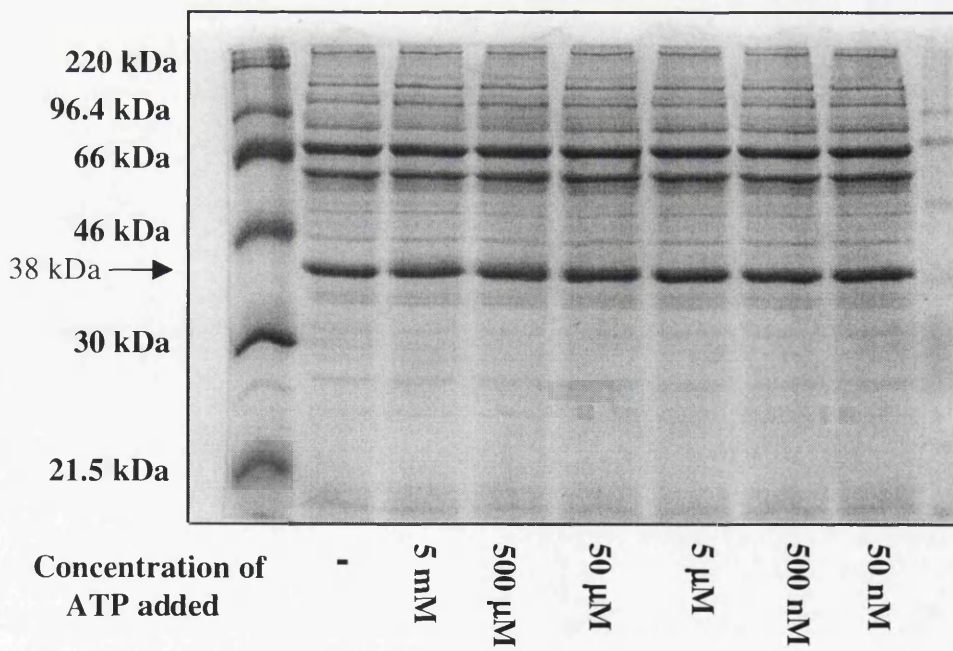


Figure 4.3.2

Phosphorylating *wt* virions in a buffer comprising 50 mM MgCl<sub>2</sub> and 50 mM Tris-HCl pH 7.5 at 0 M NaCl in the presence of 5 mM or 500 μM ATP stimulated the appearance of the 40 kDa protein. Incubating *wt* virions in the presence of 50 μM ATP caused the 38 kDa protein to migrate as a diffuse band. Migration of the 38 kDa protein in *wt* virions phosphorylated at ATP concentrations of 5 μM or less was indistinguishable from unphosphorylated samples. Migration of the 38 kDa protein was unaffected if phosphorylated at 1.5 M NaCl, regardless of the ATP concentration.

These data show that altered migration of the 38 kDa protein is dependent upon ATP concentration, thus indicating that the effect may be due to phosphorylation. In addition, Figs. 4.3.1 and 4.3.2 clearly show that NaCl concentration affected processing of the 38 kDa protein. To obtain a more detailed picture, a series of *in vitro* phosphorylation assays was performed over a range of NaCl concentrations. The results are shown in Fig. 4.3.3.

The 38 kDa protein migrated aberrantly when incubated at 0 or 0.1 M NaCl in the presence of 50 mM MgCl<sub>2</sub> and 10 or 50 mM Tris-HCl. In both buffers, NaCl concentrations of 0.5 M and above failed to stimulate a change in migration. Thus, it appears that altered migration of the 38 kDa protein is highly sensitive to NaCl concentration. If phosphorylation caused the aberrant migration, the PK targeting the 38 kDa protein was inhibited at NaCl concentrations above 0.1 M.

To ensure that the abundant 38 kDa protein under examination was the product of the HSV-1 UL49 gene, the assay was repeated using a mutant virus (vUL49del268-301) (Leslie, 1996). The mutant encodes a truncated UL49 protein which is missing the C-terminal 34 amino acids. The truncated version is under the control of the HCMV IE promoter which leads to overexpression of the truncated form. This is preferentially packaged into virions at the expense of the *wt* form (Leslie, 1996). The details and results are shown in Fig. 4.3.4.

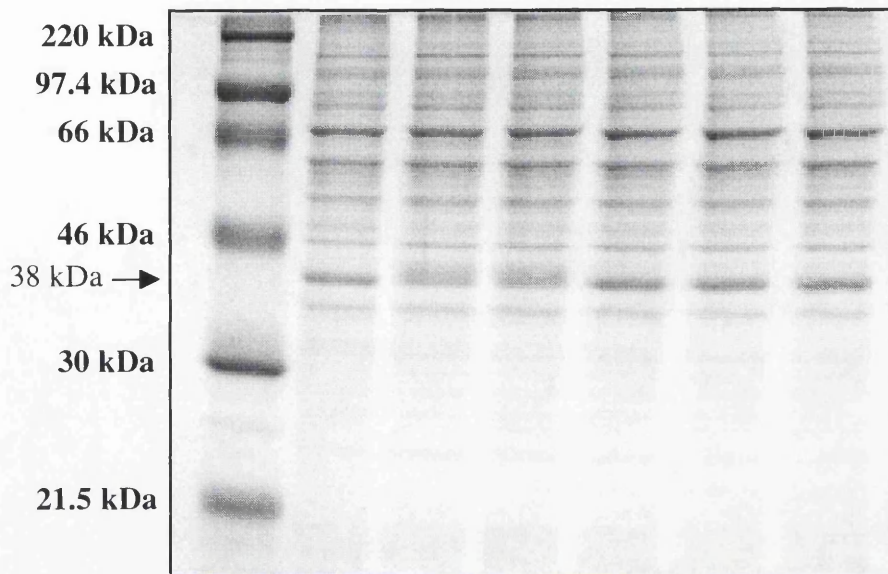
The strongly staining 38 kDa protein is clearly visible in unphosphorylated *wt* virions. As expected, the 38 kDa protein was completely absent from the unphosphorylated vUL49del268-301 profile, and a novel protein of approximately 36 kDa was detected. A novel 40 kDa protein was clearly detected in phosphorylated *wt* virions. The 40 kDa

**Figure 4.3.3 Coomassie stained gels of *wt* virions phosphorylated *in vitro* at different buffer and NaCl concentrations.**

*Wt* virions were purified, treated with NP40 and incubated in the indicated phosphorylation buffer and salt concentration in the presence of ATP. The proteins were separated on a 10% polyacrylamide gel and visualised by staining with Coomassie Brilliant Blue.

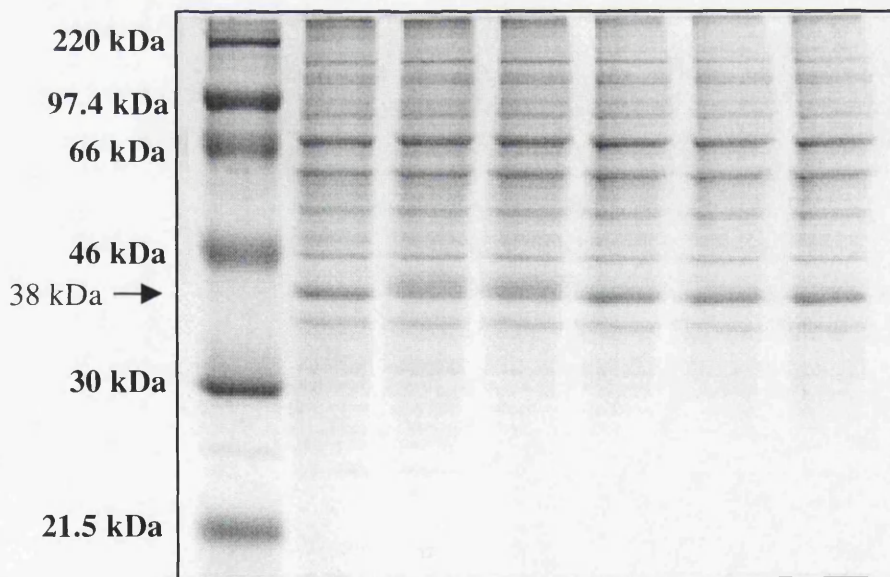
Panel 1 shows the virion proteins after phosphorylation at 50mM MgCl<sub>2</sub>, 50mM Tris-HCl pH 7.5 and 1mM DTT. Panel 2 shows the virion proteins after phosphorylation at 50mM MgCl<sub>2</sub>, 10mM Tris-HCl pH 7.5 and 1mM DTT. In all cases a 5 mM ATP reaction concentration was used.

1.



ATP added	-	+	+	+	+	+
[NaCl]	-	0	0.1	0.5	1.0	1.5

2.



ATP added	-	+	+	+	+	+
[NaCl]	-	0	0.1	0.5	1.0	1.5

Figure 4.3.3

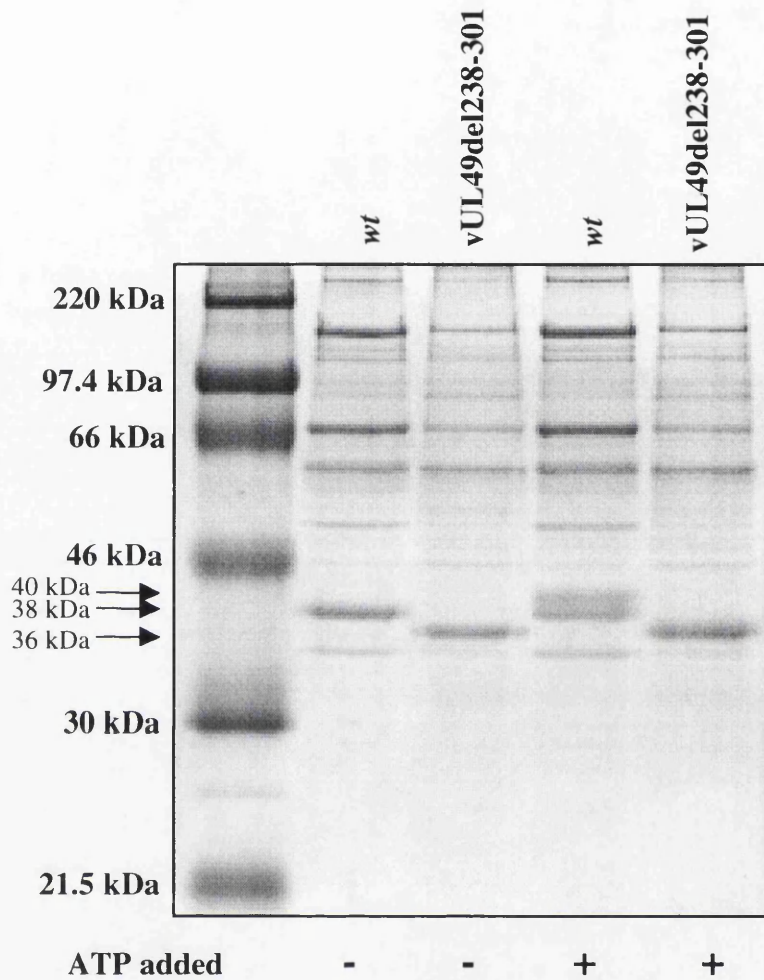


**Figure 4.3.4 Coomassie stained gel of showing the migration of the UL49 protein in *wt* and *vUL49ep* virions.**

*Wt* virions and *vUL49del268-301* were purified, treated with NP40 and incubated in phosphorylation buffer (50 mM Tris-HCl pH 7.5, 50 mM MgCl<sub>2</sub> and 1 mM DTT) at 0 M NaCl in the presence of a 5 mM ATP reaction concentration. The proteins were separated on a 10% polyacrylamide gel and visualised by staining with Coomassie Brilliant Blue.

protein, or any novel, slowly migrating proteins, are absent from the phosphorylated vUL49del268-301 virions, although the 36 kDa protein does appear to migrate as a slightly broader band.

Comparing the *wt* and vUL49del268-301 profiles, it is clear that the 38 kDa protein is encoded by gene UL49. Phosphorylated *wt* virions showed the expected protein profile, with a novel 40 kDa protein migrating slightly slower than the 38 kDa protein. Previous data (Figs. 4.3.1, 4.3.2 and 4.3.3) indicate that this protein may be a hyperphosphorylated form of the UL49 protein. Since a more slowly migrating form of the UL49 protein was not apparent in phosphorylated vUL49del268-301 virions, it is possible that the UL49 protein is phosphorylated in the C-terminal 34 amino acids. If hyperphosphorylation of the UL49 protein is indeed occurring it is unclear whether a cellular or viral PK is responsible, although a requirement for low NaCl concentrations implies that a cellular PK is more likely. To elucidate this, additional characterisation of the putative PK activity was necessary. Fig. 4.3.5 shows the effect of incubating *wt* virions in the presence of ATP, GTP, UTP or CTP.

Unexpectedly, all four NTPs stimulated the UL49 protein to migrate as a smeared band, ATP and CTP more noticeably than GTP or UTP. This result is unexpected because, although some PKs are known to utilise ATP or GTP as phosphate donor, utilisation of UTP and CTP is unusual.

Thus far, the data show that under certain conditions the 38 kDa protein, encoded by gene UL49, could be stimulated to migrate with a higher apparent Mr. Because this occurred under phosphorylating conditions and was ATP-dependent, it was attributed at first to hyperphosphorylation. However, aberrant migration of the UL49 protein was stimulated by all four NTPs, a feature not previously reported for a PK. An NTP-dependent candidate processing event other than phosphorylation, nucleotidylation, has been reported for the UL49 protein (Blaho *et al.*, 1994). However, phosphorylation cannot be ruled out, since reports have demonstrated PKs which utilise TTP as a phosphate donor (Nghiem *et al.*, 2000).

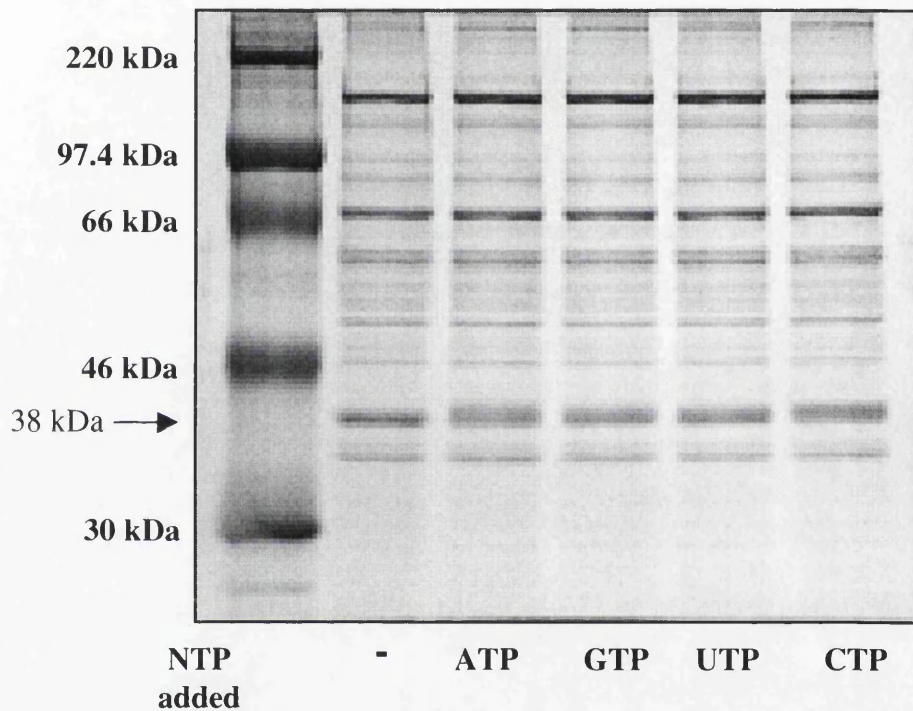


**Figure 4.3.5** Coomassie stained gel showing the effect of a variety of dNTPs on migration of the UL49 protein derived from *wt* virions.

*Wt* virions were purified, treated with NP40 and incubated in phosphorylation buffer (50 mM MgCl<sub>2</sub>, 50 mM Tris-HCl pH 7.5, 1 mM DTT) at 0 M NaCl in the presence of 5 mM ATP, GTP, UTP or CTP. The proteins were separated on a 10% polyacrylamide gel and visualised by staining with Coomassie Brilliant Blue.

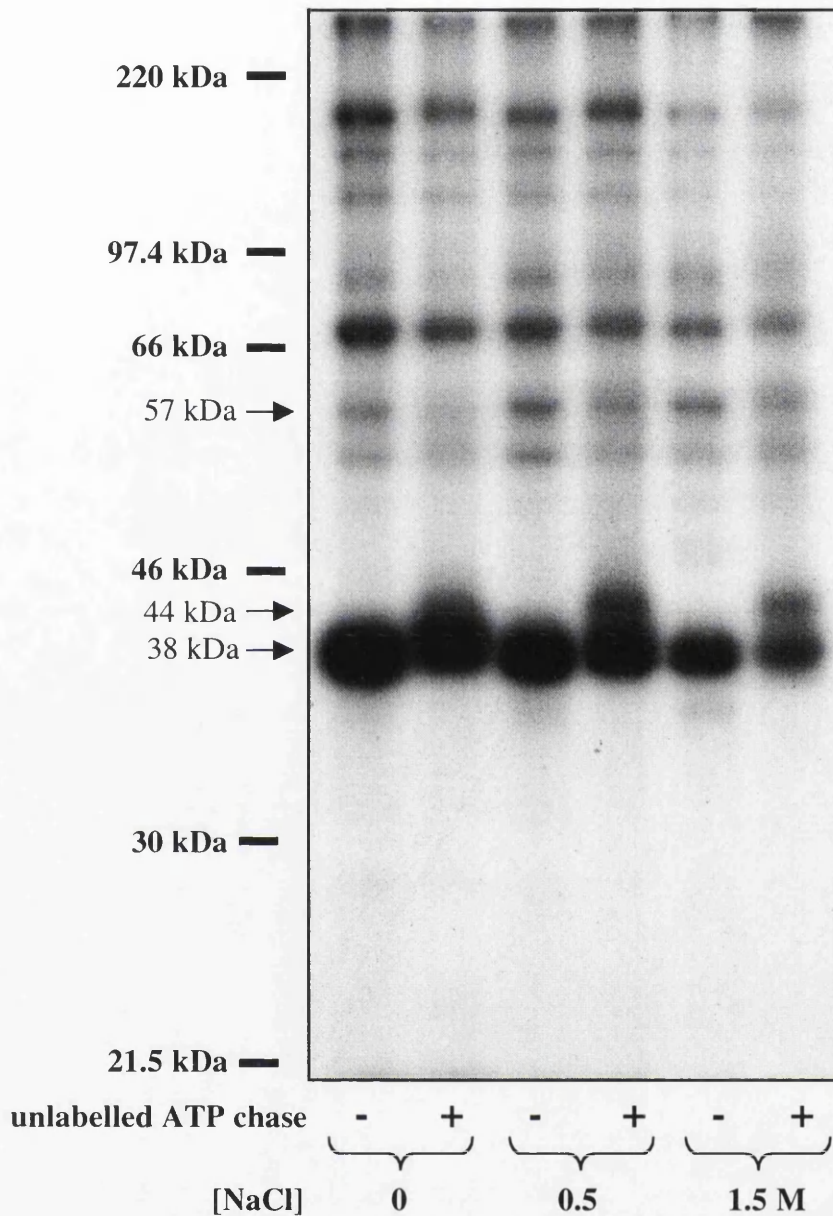


**Figure 4.3.6** Autoradiograph showing the *in vitro* phosphorylation profile of the UL49 protein upon incubation in 50 mM MgCl<sub>2</sub> and 50 mM Tris-HCl phosphorylation buffer.

Aliquots of detergent stripped *wt* virions were incubated at 37°C and the indicated NaCl concentration in the presence of [ $\gamma$ -<sup>32</sup>P]ATP. After 30 min incubation, half the sample was added to PBM and boiled. The remaining half was incubated for a further 30 min in the presence of 5 mM unlabelled ATP. Proteins were separated on a 9% polyacrylamide gel, and the radiolabelled proteins visualised by exposure to X-ray film.

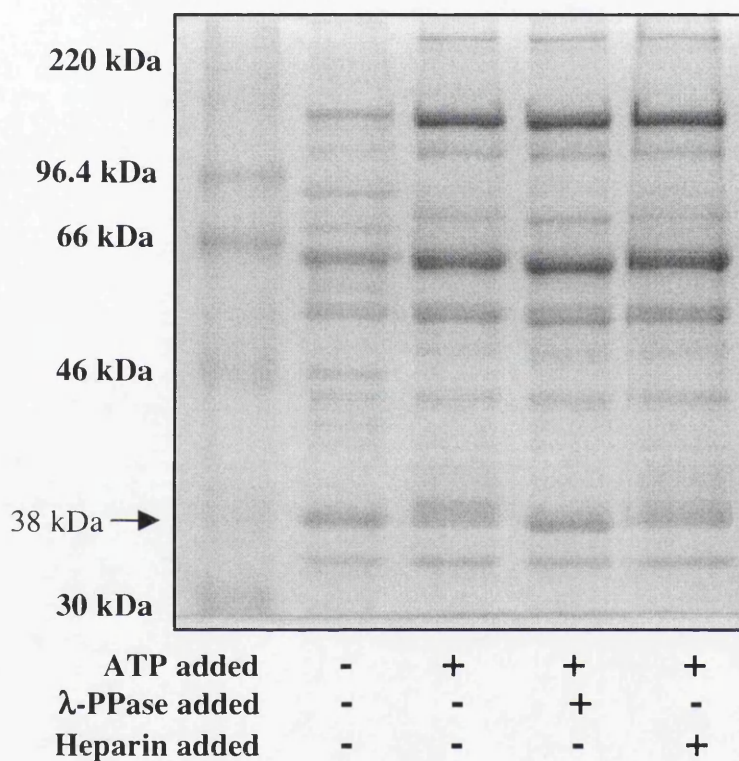


**Figure 4.3.7** Coomassie stained gel showing the effect of  $\lambda$ -protein phosphatase and heparin on migration of the UL49 protein.

Aliquots of detergent stripped *wt* virions were incubated at 37°C in 50 mM MgCl<sub>2</sub>, 50 mM Tris-HCl pH 7.5 and 5 mM ATP. In addition sample 4 was incubated with 50 µg/ml heparin. After 30 min incubation PBM was added to samples 1, 2 and 4, and 1 µl (400 units)  $\lambda$ -PPase was added to sample 2 and the sample incubated for 30 min at 30°C. Proteins were separated on a 10% polyacrylamide gel, and the proteins visualised by staining with Coomassie Brilliant Blue.

When *wt* virions were radiolabelled and chased with unlabelled ATP at 50 mM MgCl<sub>2</sub> and 50 mM Tris-HCl pH 7.5 radiolabelled proteins were detected as shown in Fig. 4.3.6. In both unchased and chased samples, phosphorylation of the 38 kDa protein diminished as NaCl concentration increased. In the chased samples, the 38 kDa protein migrated as a diffuse band at 0 M NaCl, as seen in Fig. 4.3.1. The migration of the 38 kDa protein was reduced at 0.5 and 1.5 M NaCl, and a novel band appeared with an approximate Mr of 44 kDa. Clearly, the aberrant migration of the UL49 protein is stimulated at high NaCl concentrations. To determine which post-translational event was responsible for the aberrant migration of the UL49 protein, membrane-stripped *wt* virions were incubated at 50 mM MgCl<sub>2</sub> and 50 mM Tris-HCl pH 7.5 and were then treated with λ-protein phosphatase (λ-PPase). An additional sample was incubated in 50 mM MgCl<sub>2</sub> and 50 mM Tris-HCl in the presence of 50 µg/ml heparin which inhibits CK II activity (Mitchell *et al.*, 1994). The results are shown in Fig. 4.3.7.

In Fig. 4.3.7 the UL49 protein clearly migrated aberrantly when incubated with ATP, a phenomenon attributed to either nucleotidylylation or phosphorylation. However, migration of the UL49 protein in the sample incubated with λ-PPase is almost indistinguishable from the unphosphorylated UL49 protein. In the sample incubated with ATP and heparin, the UL49 protein migrated as a band which was slightly less diffuse than in the absence of heparin.

These data clearly indicate that the UL49 protein is hyperphosphorylated when incubated with ATP in a buffer comprising 50 mM MgCl<sub>2</sub> and 50 mM Tris-HCl, and that hyperphosphorylation is the major cause of aberrant migration. However, nucleotidylylation cannot be entirely excluded. Mitchell *et al.* (1994) showed that CKII was capable of nucleotidylylating proteins. The buffer used by Mitchell *et al.* (1994) was similar to the phosphorylation buffer used in this study, and nucleotidylylation was observed to occur in the absence of NaCl, with the nucleotidylylating activity inhibited by heparin. Phosphorylation of the UL49 protein to this level has not been previously reported, but it is known to be nucleotidylylated. As such the aberrant migration stimulated under these conditions could be a result of both types of post-translational modification.

#### 4.4 Dependence of phosphorylation of the UL13 protein on cell type

The highly phosphorylated 57 kDa protein present in *wt* CNE is encoded by UL13, a gene which had previously been predicted to encode a PK (Section 1.3.3.1). The 38 kDa phosphoprotein, encoded by gene UL49, demonstrated a considerable reduction in phosphorylation in UL13 mutant CNE (Fig. 4.1.1). This protein was therefore considered a target for phosphorylation by the putative UL13 PK. Nevertheless, the 38 kDa protein is still phosphorylated in UL13 mutant CNE, indicating that it is targeted by a second PK, most probably of cellular origin.

Hyperphosphorylation of the UL13 protein occurred in *wt* CNE phosphorylated in the presence of 5  $\mu$ M ATP or 5 mM GTP (Figs. 4.2.7 and 4.2.8), but not in virions incubated under the same conditions (Fig. 4.4.3). It was hypothesised that hyperphosphorylation could be orchestrated by a second PK, possibly of cellular origin. Thus far all assays had been performed on CNE prepared from infected MeWo cells. If cellular PKs target the UL13 or UL49 proteins, it is possible that phosphorylation profiles may differ between cell lines. To test this hypothesis, a line of rabbit skin cells (RSCs) was infected with *wt* or UL13-*lacZ* virus and aliquots of CNE were phosphorylated *in vitro*.

Fig. 4.4.1 shows the phosphorylation profiles of *wt* and UL13-*lacZ* RSC CNE phosphorylated at a variety of NaCl concentrations, with each sample phosphorylated in duplicate. A highly radiolabelled 57 kDa phosphoprotein was clearly detected in *wt* CNE, demonstrating a small increase in phosphorylation as NaCl concentration increased. A 38 kDa phosphoprotein was poorly phosphorylated at 0 M NaCl, with phosphorylation increasing slightly at higher NaCl concentration. In UL13-*lacZ* CNE a phosphoprotein of approximately 57 kDa was detected. However, phosphorylation of this protein was greatly reduced compared to *wt* CNE. Radiolabelling of the 38 kDa phosphoprotein was also reduced in the UL13-*lacZ* CNE.

Clearly there are differences between the phosphorylation profiles of *wt* and UL13-*lacZ* CNE prepared from RSC and MeWo cells (Fig. 4.1.1). Phosphorylation of the 38 kDa protein was reduced in UL13-*lacZ* CNE from both cell lines. However, unlike MeWo CNE, UL13-*lacZ* RSC CNE contained a 57 kDa phosphoprotein, albeit with greatly

**Figure 4.4.1 Autoradiographs showing *in vitro* phosphorylation profiles of *wt* and UL13-infected RSC CNE.**

Rabbit skin cells (RSC) were infected with *wt* or UL13-*lacZ* mutant virus for 5 h at 37°C. CNEs were prepared and incubated in duplicate in the presence of [ $\gamma$ -<sup>32</sup>P]ATP over a range of NaCl concentrations. The proteins were separated on 9% polyacrylamide gels and visualised by exposure to X-ray film. Panel 1 shows *wt* CNE and panel 2 shows UL13-*lacZ* CNE.

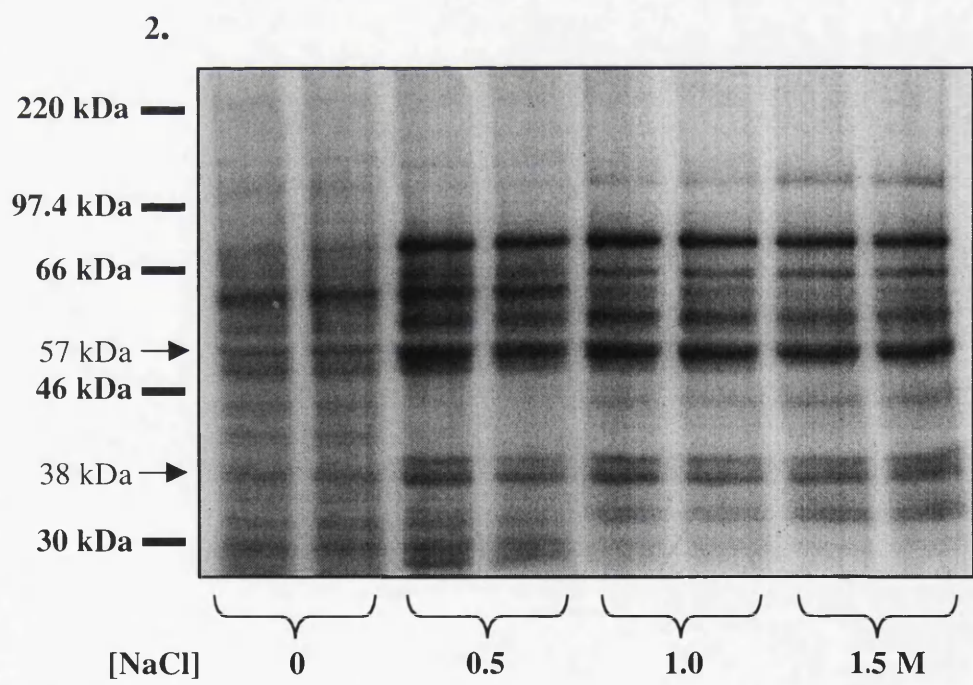
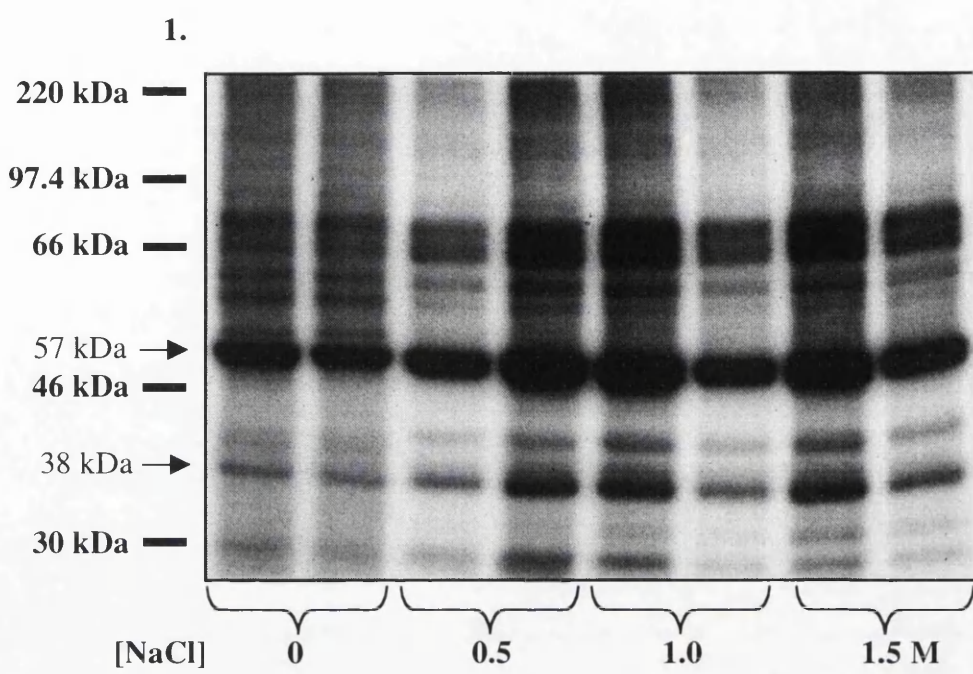


Figure 4.4.1

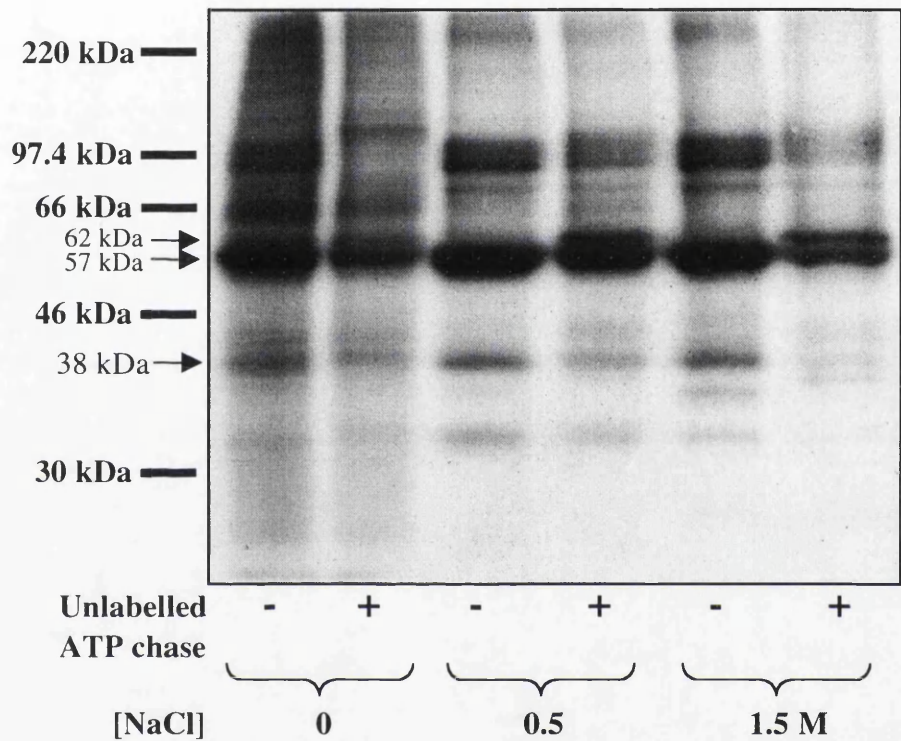
reduced radiolabelling compared to *wt* CNE. Mass spectrometric analysis showed that this protein is probably vimentin, an abundant cytoskeletal phosphoprotein (data not shown).

Figure 4.4.2 shows the results of chasing radiolabelled *wt* RSC CNE with unlabelled ATP at a variety of NaCl concentrations. In unchased *wt* CNE, the 57 and 38 kDa phosphoproteins were detected at all NaCl concentrations assayed, with the 57 kDa protein much more highly phosphorylated. However, in chased *wt* CNE the 57 and 38 kDa proteins exhibited reduced radiolabelling, with the greatest reduction at 1.5 M NaCl. The ATP chase also stimulated phosphorylation of the 62 kDa protein at all NaCl concentrations, most noticeably at 1.5 M NaCl concentrations. The 62 kDa phosphoprotein in RSC CNE was not as highly radiolabelled as in MeWo CNE (see Fig. 4.2.1).

These observations are summarised in Fig. 4.4.3, in which the unchased and chased phosphorylation profiles of infected MeWo CNE, RSC CNE and virions are compared. Both infected MeWo CNE and RSC CNE demonstrated a 62 kDa phosphoprotein in chased samples, but this phosphoprotein was much more highly radiolabelled in the former. In addition, radiolabelling increased with NaCl concentration in MeWo CNE, while it remained reasonably constant in chased RSC CNE. Neither the 57 nor 62 kDa phosphoproteins was visible in chased *wt* virions.

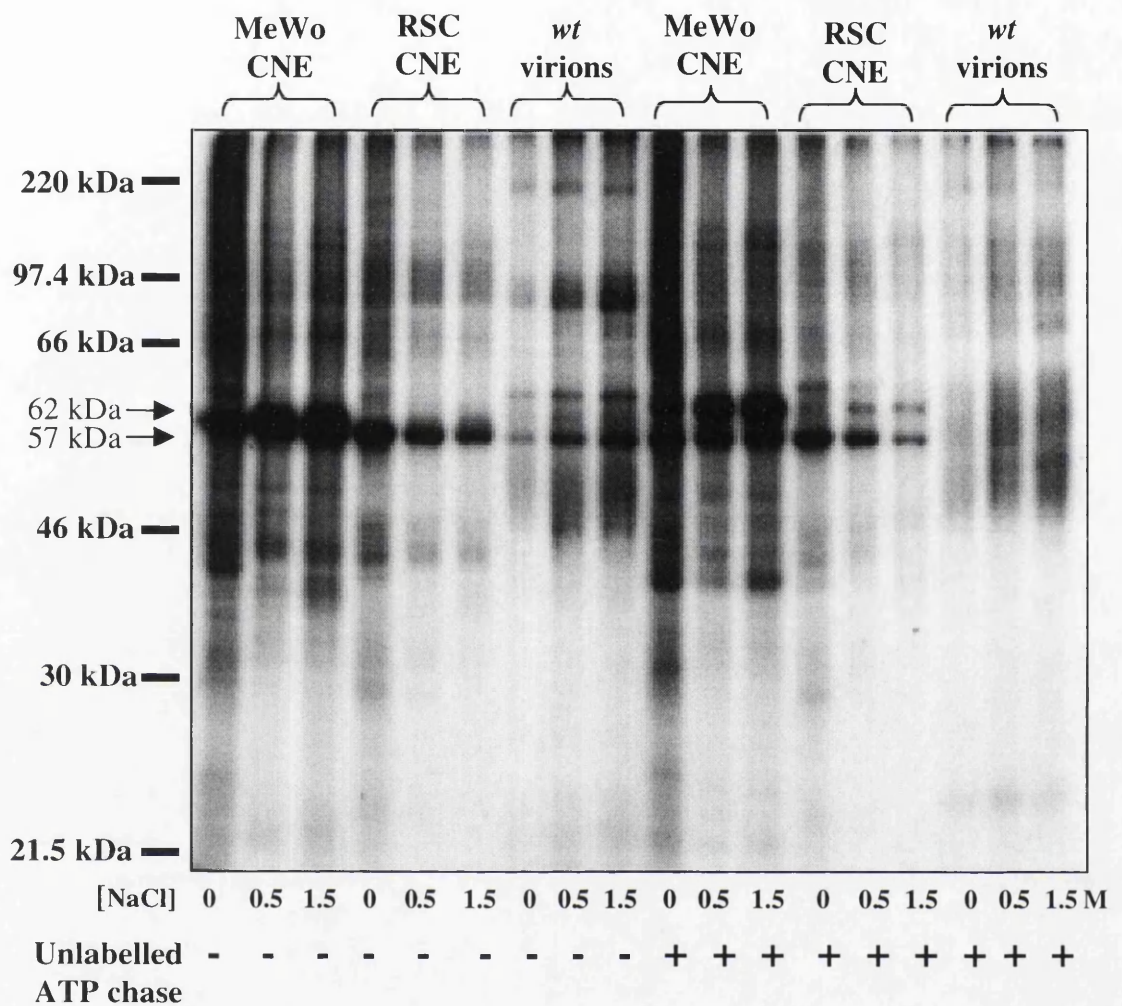
Production of the 57 and 62 kDa phosphoproteins differed in *wt*-infected MeWo and RSC CNEs under chased and unchased conditions. Assuming that the 62 kDa in RSC CNE represents the hyperphosphorylated UL13 protein, its production may have been less efficient in RSC CNE. To test this, a series of chase assays were performed using varying concentrations of unlabelled ATP chase. The results are shown in figure 4.4.4.

Fig. 4.4.4 demonstrates that a highly radiolabelled 57 kDa phosphoprotein was present at all ATP chase concentrations tested. A radiolabelled 62 kDa phosphoprotein is seen at ATP chase concentrations of 500  $\mu$ M and higher, while a third radiolabelled phosphoprotein, migrating between the 57 and 62 kDa phosphoproteins was visible when



**Figure 4.4.2** Autoradiograph showing the effect of an unlabelled ATP chase on radiolabelled *wt*-infected RSC CNE at a variety of NaCl concentrations.

Aliquots of *wt* infected RSC CNE were incubated at 37°C at the indicated NaCl concentration in the presence of [ $\gamma$ - $^{32}$ P] ATP. After 30 min incubation half of each sample was added to PBM and boiled. The remaining half was incubated for a further 30 min in the presence of 5 mM unlabelled ATP. Proteins were separated on a 9% polyacrylamide gel and visualised by exposure to X-ray film.



**Figure 4.4.3** Autoradiograph comparing the effects of an unlabelled ATP chase on radiolabelled *wt*-infected MeWo CNE, RSC CNE and *wt* virions.

Aliquots of *wt* infected MeWo and RSC infected CNE and detergent stripped *wt* virions were incubated at 37°C and 1.5 M NaCl in the presence of [ $\gamma$ - $^{32}$ P]ATP. After 30 min incubation, half of each sample was added to PBM and boiled. The remaining half was incubated for a further 30 min in the presence of 5 mM unlabelled ATP. Proteins were separated on a 9% polyacrylamide gel and visualised by exposure to X-ray film.

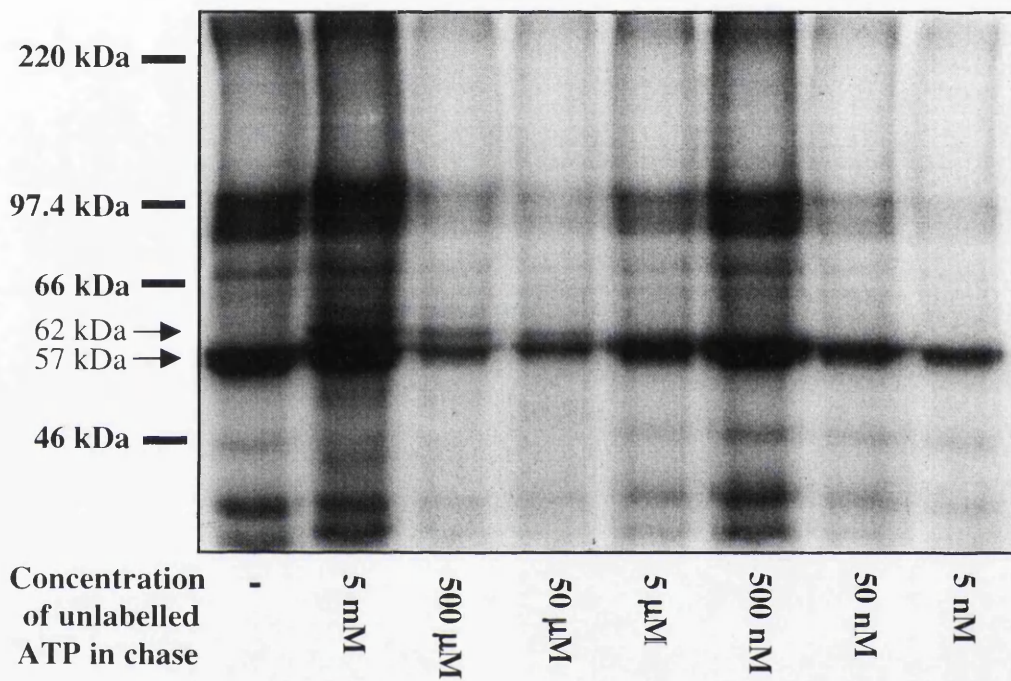


**Figure 4.4.4** Autoradiograph showing the effect of various unlabelled ATP chase concentrations on radiolabelled *wt*-infected RSC CNE.

Aliquots of *wt* infected RSC CNE were incubated at 37°C and 1.5 M NaCl in the presence of [ $\gamma$ - $^{32}$ P] ATP. After 30 min incubation 1  $\mu$ l of unlabelled ATP was added to give the indicated reaction concentration. Proteins were separated on a 9% polyacrylamide gel and visualised by exposure to X-ray film.

a 50  $\mu\text{M}$  chase was added. CNE samples incubated with ATP chase concentrations of 5  $\mu\text{M}$  and below are indistinguishable from unchased samples.

These data prove that phosphorylation of the 62 kDa protein in RSC CNE is dependent upon ATP concentration, similar to MeWo CNE. In MeWo CNE the 62 kDa protein was shown to be a hyperphosphorylated form of the UL13 protein, and this is likely also to be the case for the 62 kDa phosphoprotein in RSC CNE. The minimum ATP chase concentration required to stimulate hyperphosphorylation of the UL13 protein in MeWo CNE was 5  $\mu\text{M}$  and 500  $\mu\text{M}$  in RSC CNE. The 100-fold difference could reflect differences in cellular PKs. Cellular PKs are more sensitive to heparin inhibition than viral PKs, and, to test whether cellular PKs target the UL13 PK, a series of *in vitro* phosphorylation assays were performed on *wt* MeWo CNE in the presence of 100  $\mu\text{g/ml}$  heparin as detailed in Fig. 4.4.5.

As expected, both the 57 and 38 kDa phosphoproteins appeared in *wt* CNE, whereas the 57 kDa phosphoprotein is totally absent from UL13-*lacZ* CNE and radiolabelling of the 38 kDa phosphoprotein was greatly reduced. Heparin appeared only to inhibit protein phosphorylation at 0 M NaCl, with a slight reduction in phosphorylation of the 38 kDa protein in *wt* CNE and almost total abolition of phosphorylation of the 38 kDa protein in UL13-*lacZ* CNE. Phosphorylation of the 57 kDa protein appeared unaffected by heparin. These data show that the 38 kDa protein is targeted by a heparin-sensitive PK, most probably of cellular origin. Production of the 57 kDa phosphoprotein was unaffected by heparin, consistent with autophosphorylation.

The heparin inhibition assay was repeated using unchased and chased RSC CNE as detailed in Fig. 4.4.6. Chase assays were performed on *wt* CNE samples at 0 and 1.5 M NaCl in the presence of various concentrations of heparin. While there was a general reduction in labelling as heparin concentration increased, neither phosphorylation nor hyperphosphorylation of the UL13 protein appeared to be specifically affected.

While heparin inhibits many cellular PKs, there are a number of potent inhibitors to specific PKs. CKII has been implicated in the phosphorylation of several viral proteins, and has also been shown to phosphorylate proteins thought to be targeted by UL13. 5,6-

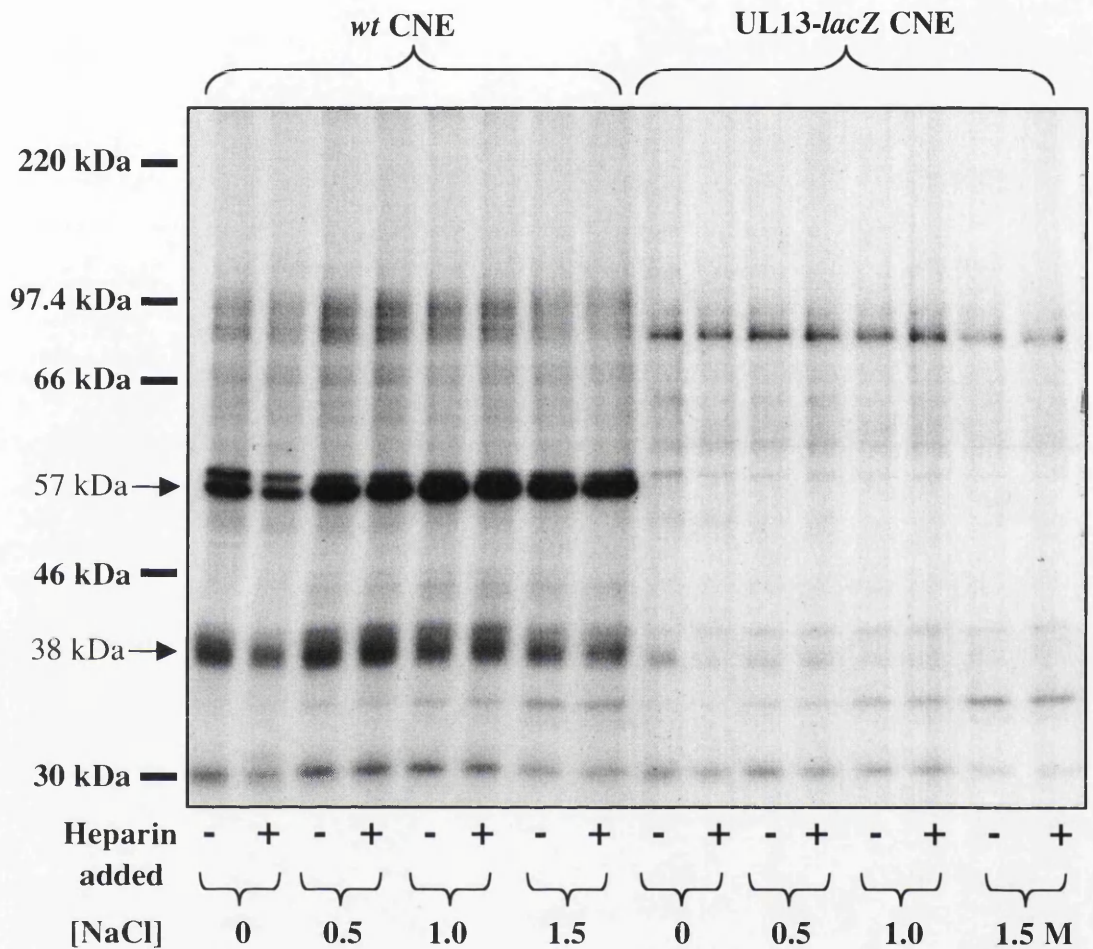


**Figure 4.4.5** Autoradiograph showing an *in vitro* assay for heparin sensitivity of phosphorylation of the UL13 and UL49 proteins.

Aliquots of *wt* or *UL13-lacZ* infected MeWo cell CNE were incubated at 37°C and the indicated NaCl concentration in the presence of [ $\gamma$ - $^{32}$ P]ATP. Where indicated 100  $\mu$ g/ml heparin (reaction concentration) was included in the reaction. Proteins were separated on a 9% polyacrylamide gel and visualised by exposure to X-ray film.

**Figure 4.4.6 Autoradiograph showing an *in vitro* assay for heparin sensitivity of the unlabelled ATP chase.**

Aliquots of *wt* infected RSC CNE were incubated at 37°C and the indicated NaCl concentration in the presence of [ $\gamma$ -<sup>32</sup>P]ATP. The indicated reaction concentration of heparin was included where incubated. After 30 min incubation, half of each sample was added to PBM and boiled. The remaining half was incubated for a further 30 min in the presence of 5 mM unlabelled ATP. Proteins were separated on a 9% polyacrylamide gel and visualised by exposure to X-ray film. Panel 1 shows samples incubated at 0 M NaCl, panel 2 shows samples incubated at 1.5 M NaCl.

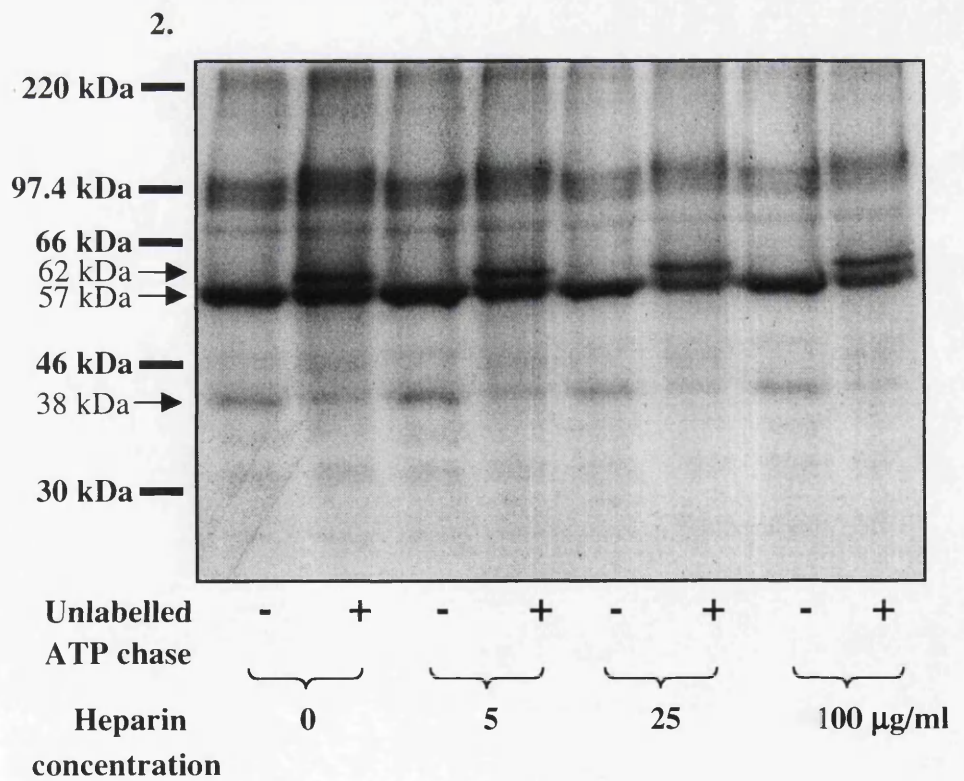
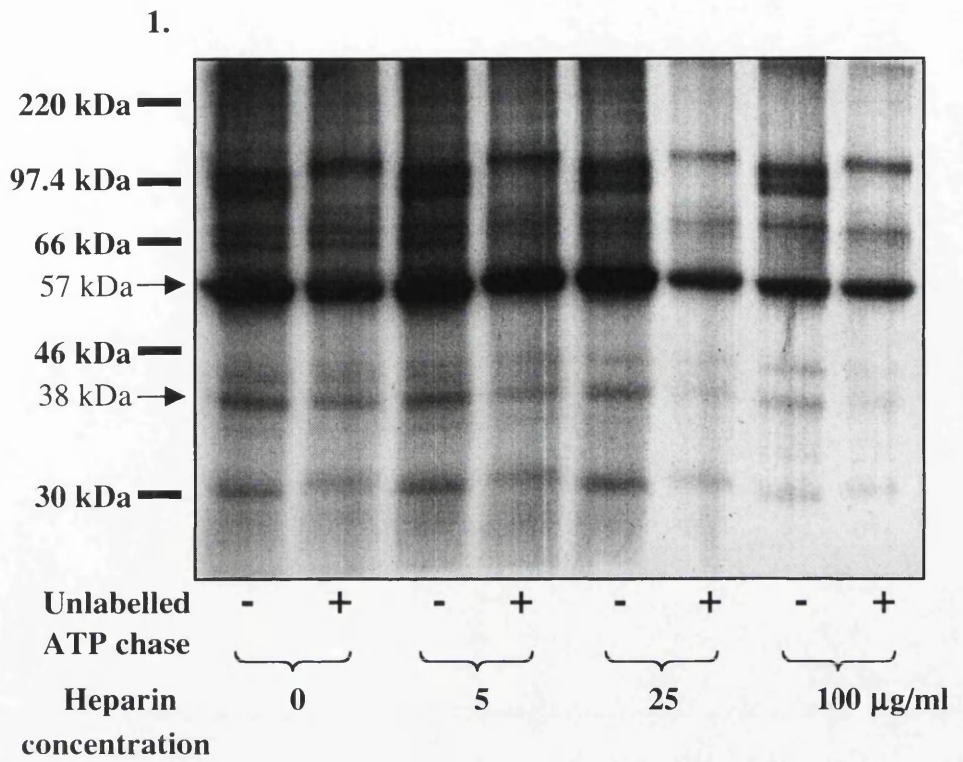
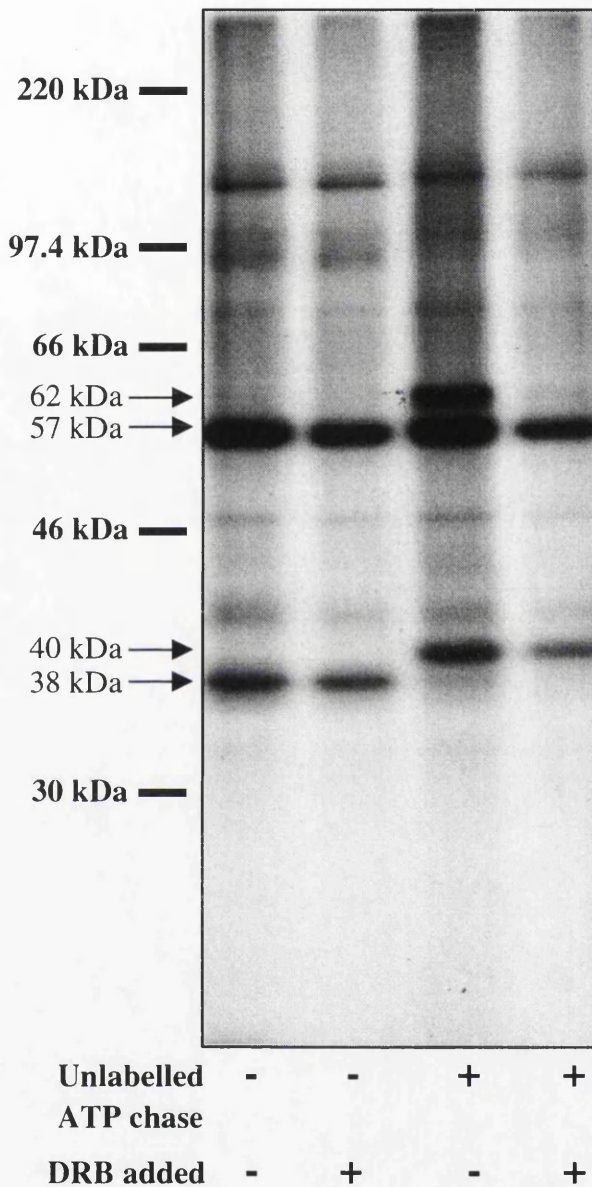


Figure 4.4.6



**Figure 4.4.7** Autoradiograph showing an *in vitro* assay to determine the effect of 5, 6-dichloro-1- $\beta$ -D-ribofuranosylbenzimidazole (DRB) on the phosphorylation profile of MeWo CNE.

Aliquots of *wt* infected MeWo cell CNE were incubated at 37°C and 0 M NaCl in the presence of [ $\gamma$ - $^{32}$ P]ATP. Where indicated 100 mM DRB (reaction concentration) was included. After a 30 min incubation, half of each sample was added to PBM and boiled. The remaining half was incubated for a further 30 min in the presence of 5 mM unlabelled ATP. Proteins were separated on a 9% polyacrylamide gel and visualised by exposure to X-ray film.

dichloro-1- $\beta$ -D-ribofuranosylbenzimidazole (DRB) is a known inhibitor of CKII activity (Zandomeni *et al.*, 1986; Zandomeni, 1989). Fig. 4.4.7. shows the effect of DRB on hyperphosphorylation of the UL13 protein in *wt* MeWo CNE at 0 M NaCl. Earlier data showed that incubation in 50 mM MgCl<sub>2</sub>, 50 mM Tris-HCl caused retardation of the UL49 protein on SDS-PAGE which was attributed to hyperphosphorylation. The experiment was performed under these conditions to examine the effect of DRB on migration of the UL13 and UL49 proteins.

DRB slightly inhibited phosphorylation of the 38 kDa protein in unchased *wt* CNE, and phosphorylation of the 57 kDa protein was largely unaffected. In the chased samples, DRB caused a slight reduction in phosphorylation of the 38 kDa protein, but completely inhibited production of the 62 kDa protein. These results indicate that at low NaCl concentrations the UL13 protein is phosphorylated by cellular CKII. Although it affected the level of phosphorylation slightly, DRB did not alter the migration of the UL49 protein. If the UL49 protein is phosphorylated by CKII there may be other cellular PKs also targeting the protein. This would agree with the identification of both CKII and PKC consensus motifs in the N-terminal portion of the UL49 protein (Elliott *et al.*, 1996).

## 4.5 Mapping sites of phosphorylation

The initial intention of this research project was to identify the sites of phosphorylation within the UL13 PK and its target protein UL49. A variety of techniques were employed, but a number of problems arose which will be discussed.

Previous data (Fig. 4.1.1) showed the UL13 and UL49 proteins were the most highly radiolabelled proteins in *in vitro* phosphorylated *wt* infected MeWo cell CNE. The phosphorylated peptides produced by proteolytic cleavage of either protein should be highly radiolabelled, and thus easily detected in a gross digest of phosphorylated MeWo CNE samples. Fig. 4.5.1 shows a gross proteolytic digest of phosphorylated *wt* and UL13-*lacZ* infected MeWo CNE. The CNE samples were phosphorylated at 1.5 M NaCl as detailed in section 4.1, and boiled for 5 minutes to denature the proteins prior to adding the endoproteinase. Three endoproteinases were used, Glu-C (*S. aureus* V8 protease), Lys-C and Arg-C (clostripain), which cleave at the carboxylic side of glutamic acid, lysine and arginine respectively.

Arg-C stimulated little change in the phosphorylation profiles of either *wt* or UL13-*lacZ* CNE, whereas incubating *wt* CNE with Glu-C produced two weakly radiolabelled peptides of 21.5 and 6.5 kDa. The 21.5 kDa phosphopeptide was also detected in Glu-C digested UL13-*lacZ* CNE, albeit with reduced radiolabelling, but the 6.5 kDa peptide was absent. Three highly radiolabelled peptides of approximately 24, 15 and 12.5 kDa were detected in Lys-C digested *wt* CNE, but only a weakly phosphorylated 24 kDa peptide was detected in Lys-C digested UL13-*lacZ* CNE.

This preliminary digest showed that Arg-C and Glu-C failed to digest the protein samples completely, in contrast to Lys-C. The 12.5 and 15 kDa Lys-C peptides were probably derived from either UL13 or UL49, and the 24 kDa Lys-C peptide could represent a UL49 peptide phosphorylated by a PK other than UL13. Despite repeated attempts, neither Glu-C nor Arg-C digested the input CNE efficiently. However, the experiment was repeated using Lys-C with a broader sample range. Fig. 4.5.2 shows the phosphopeptide profiles derived from Lys-C digestions of *wt* and UL13-*lacZ* CNE

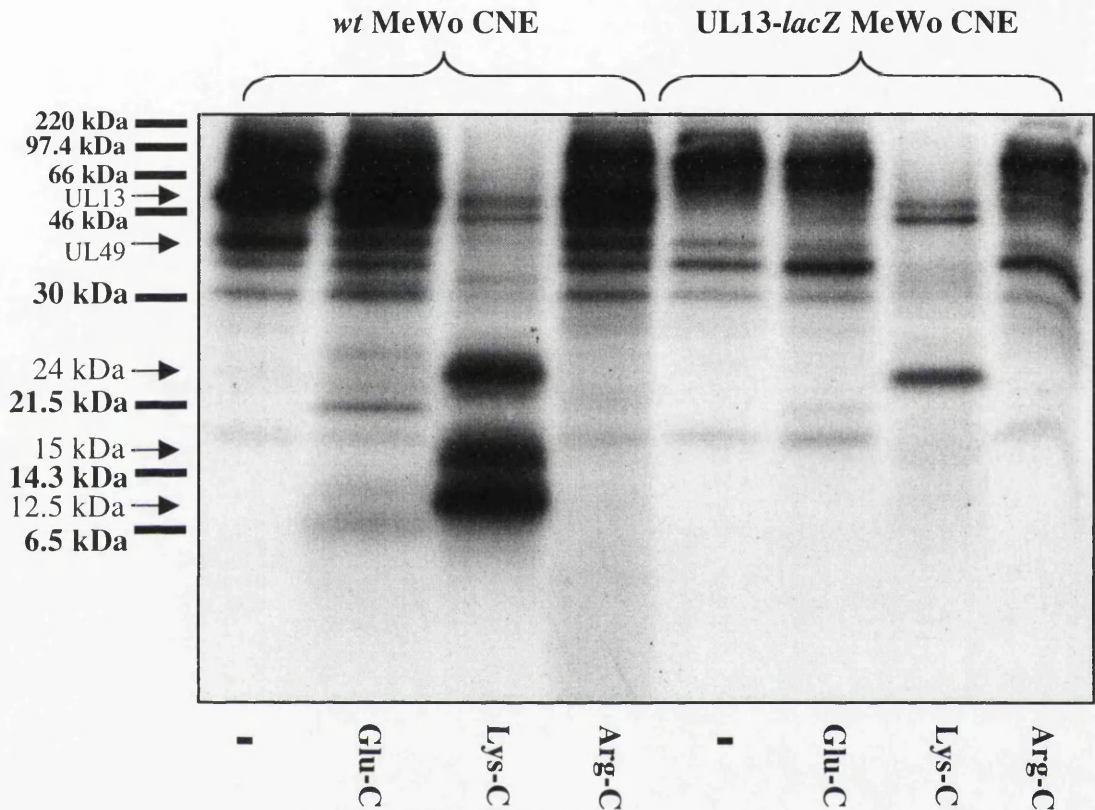


**Figure 4.5.1** Autoradiograph showing the phosphopeptide profiles of *in vitro* phosphorylated *wt* and *UL13-lacZ* CNE.

MeWo cells were infected with *wt* or *UL13-lacZ* mutant virus for 5 h at 37°C. Nuclear extracts were prepared and incubated with [ $\gamma$ - $^{32}$ P]ATP at 1.5 M NaCl. After 30 min incubation the samples were boiled for 5 min to denature the proteins and 1  $\mu$ l of the indicated protease (10  $\mu$ g/ml) was added to each sample and incubated for a further 30 min. The proteins were separated on an 18% polyacrylamide gel and visualised by exposure to X-ray film.

phosphorylated at two different NaCl concentrations with or without an unlabelled ATP chase.

A highly radiolabelled 12 kDa phosphopeptide was detected in all *wt* CNE samples, regardless of the NaCl concentration or use of an ATP chase. A 15 kDa phosphopeptide was detected only in unchased *wt* CNE phosphorylated at 1.5 M NaCl. A 18.5 kDa phosphopeptide was detected in chased *wt* CNE phosphorylated at both NaCl concentrations, and a 21 kDa phosphopeptide was detected only in chased *wt* CNE phosphorylated at 1.5M NaCl. All of these peptides were absent from UL13-*lacZ* CNE.

Interpretation of these results is difficult, not least because phosphorylated peptides migrate with an artificially high Mr. However, some of the phosphorylated peptides can be tentatively identified. The UL13 protein was shown to be hyperphosphorylated in the presence of excess ATP or GTP (see Fig. 4.2.1). It seems reasonable to suggest that the 18.5 kDa phosphopeptide, seen only in chased *wt* CNE, represents the hyperphosphorylated UL13 peptide. The 12 kDa phosphopeptide was highly phosphorylated at both NaCl concentrations, with a slight reduction in phosphorylation in chased *wt* CNE, suggesting that it is derived from the hypophosphorylated UL13 protein. Even if these peptides are correctly identified, it is not known whether the 18.5 kDa peptide is a hyperphosphorylated form of the 12 kDa peptide or a separate peptide from a different region of the UL13 protein. The 15 kDa phosphopeptide may be derived from the UL49 protein phosphorylated at 1.5 M NaCl since it is present in UL13-*lacZ* CNE. The 21 kDa phosphopeptide is unlikely to be derived from the UL49 protein, since the UL49 protein was not hyperphosphorylated under these buffer conditions, and thus may be an additional UL13 peptide.

#### 4.5.1 Phosphorylation of the UL49 protein

Gross digestion of labelled CNE provided a limited approach to identifying the phosphorylated peptides within UL13 and UL49. A more useful approach would require the isolation of each protein followed by individual digestion. To this end, an in-gel proteolytic digestion system was adopted. This involves isolating individual proteins by SDS-PAGE, excising each in a gel slice, and infusing the gel slice with the selected proteolytic enzyme in the relevant buffer. The gel slice was incubated overnight, and

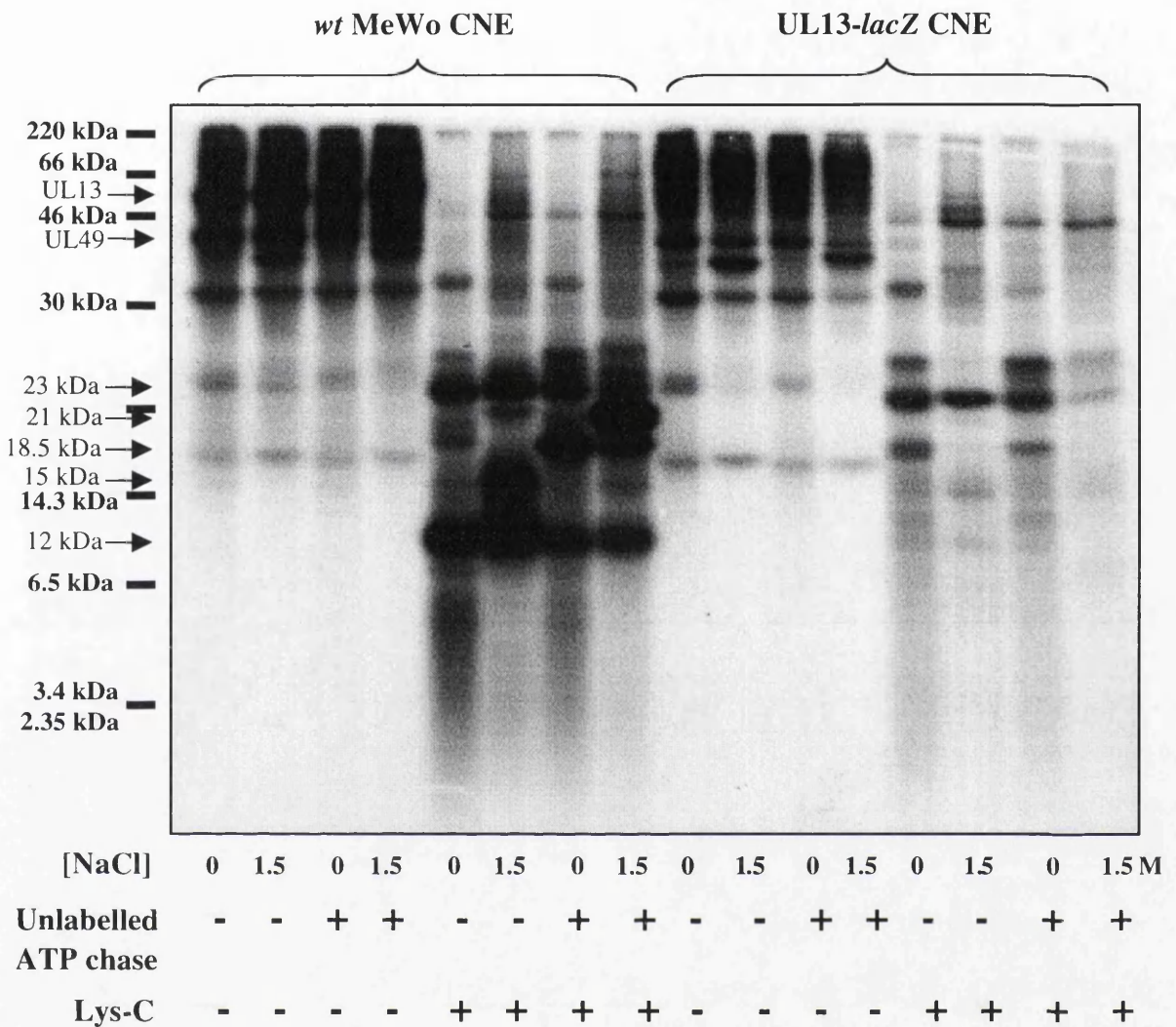


**Figure 4.5.2** Autoradiograph showing the phosphopeptide profiles of chased and unchased *wt* and *UL13-lacZ* CNE phosphorylated at a variety of NaCl concentrations.

MeWo cells were infected with *wt* or *UL13-lacZ* mutant virus for 5 h at 37°C. Nuclear extracts were prepared and incubated with [ $\gamma$ - $^{32}$ P]ATP at 0 M or 1.5 M NaCl. After 30 min half the sample was removed and the reaction stopped by boiling in PBM. The remaining half was incubated for a further 30 min in the presence of 5 mM unlabelled ATP. After the labelling and chase reactions, 1  $\mu$ l of Lys-C (10  $\mu$ g/ml) was added to each sample and incubated for a further 30 min. The proteins were separated on an 18% polyacrylamide gel and visualised by exposure to X-ray film.

peptides were eluted from the gel slice by sequential washes with 25 mM  $\text{NH}_4\text{HCO}_3$ , 5% formic acid and acetonitrile. The eluted peptides were dried *in vacuo*, resuspended in protein loading buffer and analysed by electrophoresis on 16.5% Tris-Tricine polyacrylamide gels. To maximise peptide resolution, the dye front was electrophoresed off the bottom of the gel. To examine the efficiency of this technique, UL49 protein isolated from *in vitro* phosphorylated *wt* virions was digested with various concentrations of Arg-C, Glu-C, Lys-C or trypsin, the latter cleaving after most Lys and Arg residues. The results are shown in Fig. 4.5.3.

Trypsin produced the same phosphopeptide profile when used at 12.5  $\mu\text{g/ml}$  or 1.25  $\mu\text{g/ml}$ , whereas 125  $\text{ng/ml}$  gave partial digests, and 12.5  $\text{ng/ml}$  did not yield detectable peptide fragments. Glu-C treatment appeared to produce only partially digested peptides, even at 12.5  $\mu\text{g/ml}$ . A highly radiolabelled peptide was detected when Arg-C was used at 125  $\text{ng/ml}$ , but higher or lower concentrations of the enzyme resulted in reduced yields. Lys-C produced a weakly labelled phosphopeptide profile at all dilutions except at 12.5  $\text{ng/ml}$ , where no peptides were detected.

This experiment identified trypsin as potentially the most useful enzyme for in-gel digestion, while Glu-C appeared to be the least effective. On the basis of these data, 12.5  $\mu\text{g/ml}$  trypsin was used to examine the phosphopeptide profile of the UL49 protein derived from *wt* virions phosphorylated over a range of NaCl concentrations. The results are shown in Fig. 4.5.4.

UL49 repeatedly yielded a single labelled tryptic band regardless of the NaCl concentration at which the protein was phosphorylated. The phosphopeptide migrated with an approximate  $M_r$  of 2 kDa, but it is difficult to determine its actual size because phosphorylated peptides migrate aberrantly on SDS-PAGE. As with native UL49 protein (Fig. 4.1.1) radiolabelling of the peptide peaked at 0.5 M NaCl, but was reduced at 1.5 M NaCl. This could indicate that phosphorylation of the UL49 protein is restricted to residues within the 2 kDa phosphopeptide. However, this is unlikely since the UL49 protein was still highly phosphorylated at 1.5 M NaCl, whereas the 1.5 M NaCl peptide was poorly phosphorylated. Although a single labelled band was detected, this could contain more than one peptide, and other phosphorylation sites may be located on

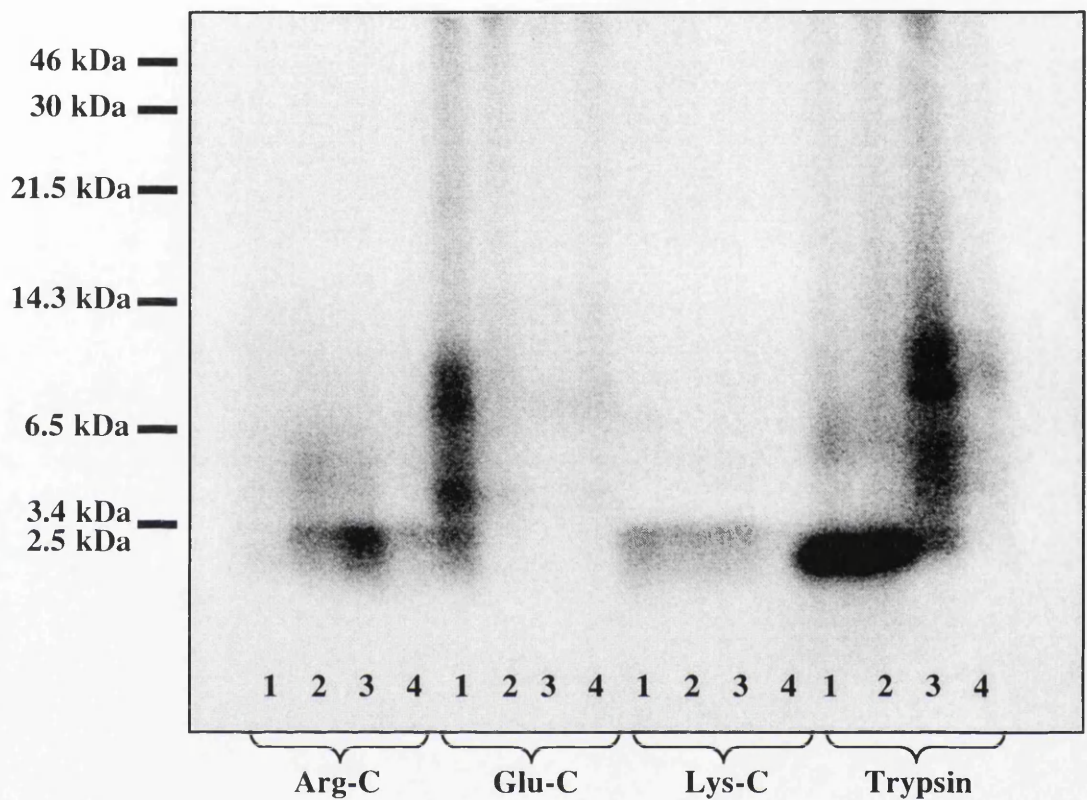


**Figure 4.5.3** Autoradiograph showing phosphopeptide profiles of the UL49 protein digested with various concentrations of selected proteolytic enzymes.

*Wt* virions were purified, treated with NP40 and incubated at 0 M NaCl in the presence of  $[\gamma\text{-}^{32}\text{P}]\text{ATP}$ . The proteins were separated on a 9% polyacrylamide gel and visualised by staining with Coomassie brilliant blue and exposure to X-ray film. UL49 was excised and digested in-gel using the following concentrations of each enzyme: 1, 12.5  $\mu\text{g/ml}$ ; 2, 1.25  $\mu\text{g/ml}$ ; 3, 125  $\text{ng/ml}$ ; 4, 12.5  $\text{ng/ml}$ . The peptides were separated on a 16.5% Tris-Tricine polyacrylamide gel and visualised by exposure to a phosphorimaging plate.

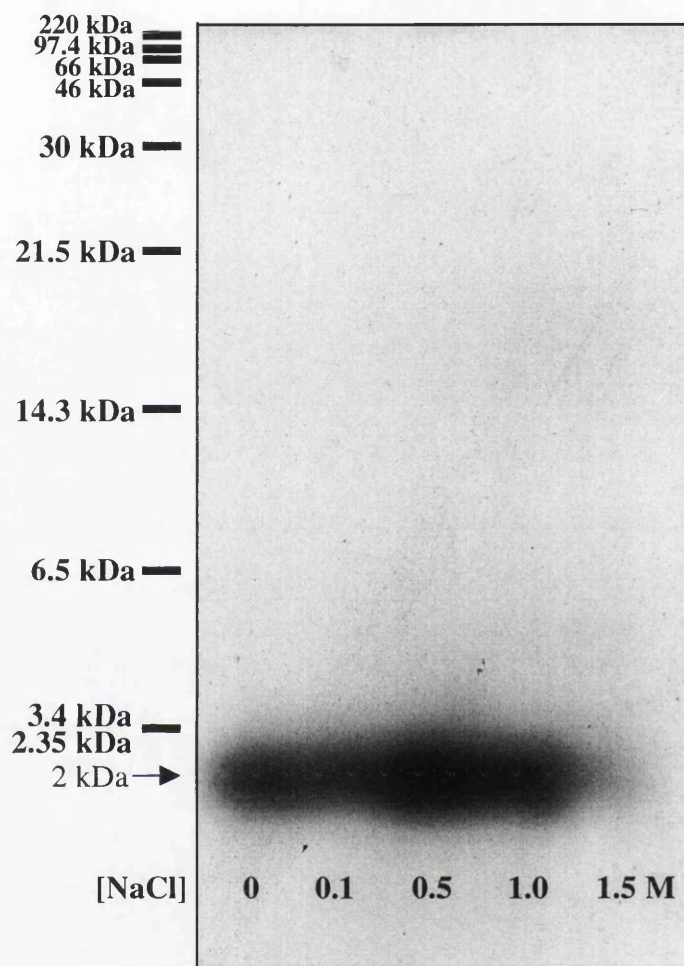


**Figure 4.5.4** Autoradiograph showing the tryptic phosphopeptide profile of the UL49 protein from *in vitro* phosphorylated *wt* virions.

*Wt* virions were purified, treated with NP40 and incubated at the indicated salt concentration in the presence of [ $\gamma$ - $^{32}\text{P}$ ]ATP. The protein were separated on a 9% polyacrylamide gel and visualised by staining with Coomassie brilliant blue and exposure to X-ray film. UL49 was excised and digested in-gel using 12.5  $\mu\text{g}/\text{ml}$  trypsin. The peptides were separated on a 16.5% Tris-Tricine polyacrylamide gel, which was electrophoresed until the dye front was off the bottom of the gel. Phosphopeptides were visualised by exposure to X-ray film.

peptides too small to be resolved using a gel-based method. A similar experiment was performed using UL49 protein isolated from phosphorylated *wt* HSV-1 infected RSC CNE rather than virions. The protein was digested with 12.5  $\mu\text{g/ml}$  trypsin, Arg-C and Lys-C, and the results are shown in Fig. 4.5.5.

Both Arg-C and Lys-C produced what appeared to be a series of partial digests, with the smallest Arg-C phosphopeptide demonstrating an  $M_r$  of approximately 2 kDa and the smallest Lys-C phosphopeptide approximately 3 kDa. The tryptic phosphopeptide migrated with an  $M_r$  of approximately 2 kDa. While the tryptic phosphopeptide from RSC CNE corresponded in size with the phosphopeptide derived from *wt* virions, the assay would need to be repeated using a variety of NaCl concentrations to confirm whether UL49 is phosphorylated on the same residues in virions and infected RSC CNE. Arg-C and Lys-C probably gave partial digests, as such the phosphorylation profiles are difficult to interpret. However, it is noteworthy that the smallest Arg-C peptide was the same size as the tryptic peptide. This would indicate that the peptide is flanked at its N- and C-termini by Arg residues. This is not unexpected, however, since the UL49 protein is richer in Arg residues than in Lys residues.

Liao *et al.* (1994) described an alternative approach for locating phosphorylation sites which used matrix-assisted laser desorption/ionisation time-of-flight mass spectrometry (MALDI-TOF-MS). The protocol involves degradation of the phosphoprotein into peptides by specific enzymatic or chemical reactions, followed by identification of the phosphopeptides by 80 (or multiple of 80)-Da mass shifts in certain peptides after phosphorylation or dephosphorylation.

Both *wt* HSV-1 virions and the HSV-1 mutant which produced a truncated form of the UL49 protein (vUL49del268-301) were analysed using this method. Purified *wt* HSV-1 and vUL49del268-301 virions were dephosphorylated or phosphorylated at 0 or 1.5 M NaCl. The proteins were separated by SDS-PAGE, blotted onto PVDF membrane and visualised by staining with sulforhodamine. The UL49 bands were excised (see Fig. 4.5.6) and subjected to proteolytic digestion using trypsin. The resulting peptides were identified using MALDI-TOF-MS. An example of the spectra obtained are shown in Figs. 4.5.7 to 4.5.13.

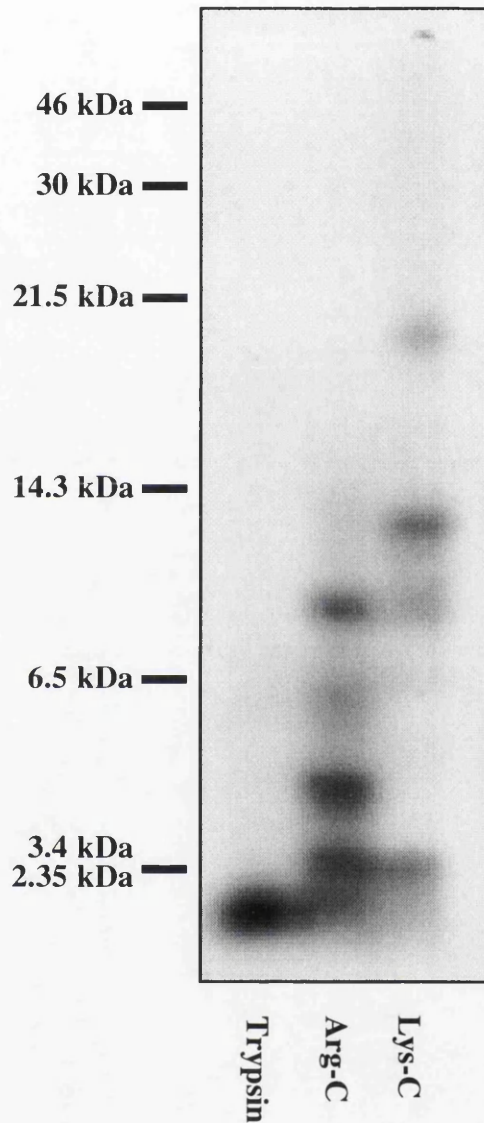


**Figure 4.5.5** Autoradiograph showing the phosphopeptide profiles of the UL49 protein from *in vitro* phosphorylated *wt* RSC CNE.

*Wt* RSC cell CNE were prepared and incubated with [ $\gamma$ - $^{32}\text{P}$ ]ATP at 1.5 M NaCl. Radiolabelled UL49 protein was isolated on a 9% polyacrylamide gel and excised. In-gel proteolytic digestion was performed using 12.5  $\mu\text{g}/\text{ml}$  trypsin, Arg-C or Lys-C and the peptides separated on 16.5% Tris-Tricine SDS-PAGE, the phosphorylated fragments were visualised by exposure to X-ray film

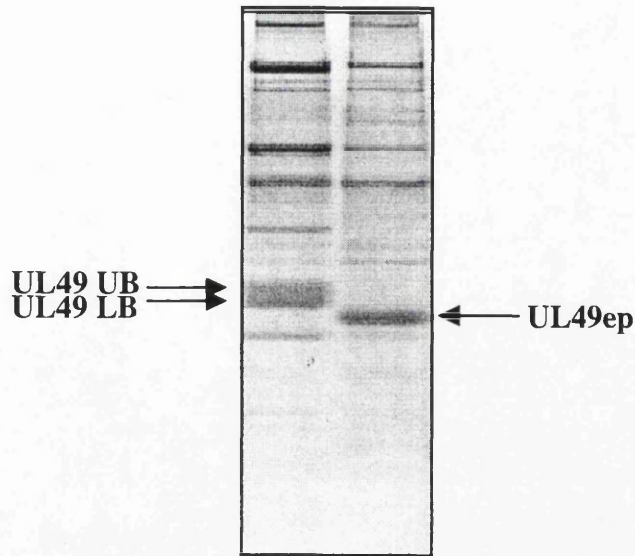


**Figure 4.5.6 Coomassie stained gel showing the phosphorylation induced alteration in migration of the UL49 protein**

Membrane stripped virions were phosphorylated *in vitro* in either 0 M or 1.5 M NaCl in the presence of 5 mM ATP. The proteins were separated on a 10% polyacrylamide gel, excised, digested using trypsin and subjected to mass spectrometric analysis. The marked proteins were analysed. UL49 UB refers to the slowly migrating "upper band," UL49 LB refers to the faster migrating "lower band." The mutant UL49 protein lacking the C-terminal 28 amino acids is shown as UL49ep.

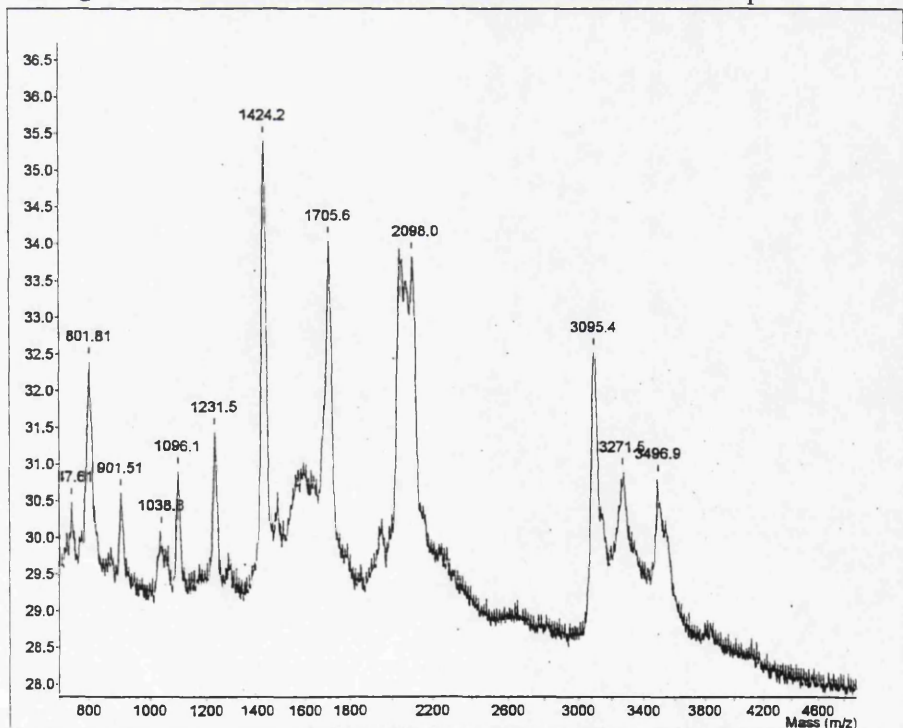


**Figure 4.5.7 Mass spectrometric analysis of the UL49 protein from phosphatase treated *wt* virions**

A mass spectrum generated from analysis of dephosphorylated UL49 protein. All the masses represent the protonated forms. The 3496.9 peak is the insulin B chain marker used to calibrate the spectrum.

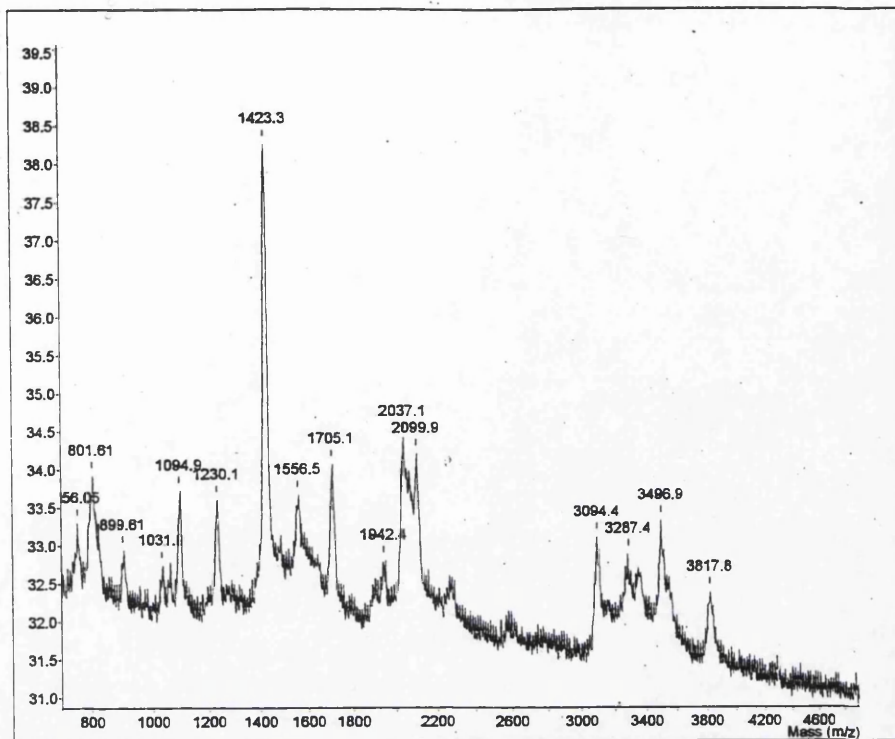


**Figure 4.5.8 Mass spectrometric analysis of the UL49 protein from *wt* virions phosphorylated at 0 M NaCl**

A mass spectrum generated from analysis of UL49 LB (see Fig. 4.5.6). All the masses represent the protonated forms. The 3496.9 peak is the insulin B chain marker used to calibrate the spectrum.

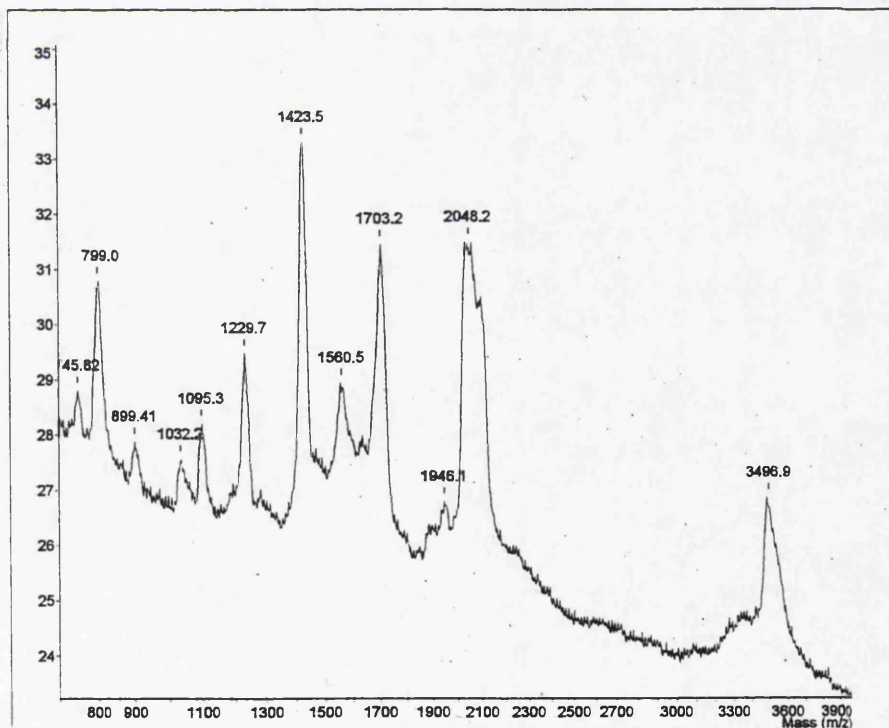


**Figure 4.5.9 Mass spectrometric analysis of the UL49 protein from *wt* virions phosphorylated at 0 M NaCl**

A mass spectrum generated from analysis of UL49 UB (see Fig. 4.5.6). All the masses represent the protonated forms. The 3496.9 peak is the insulin B chain marker used to calibrate the spectrum.

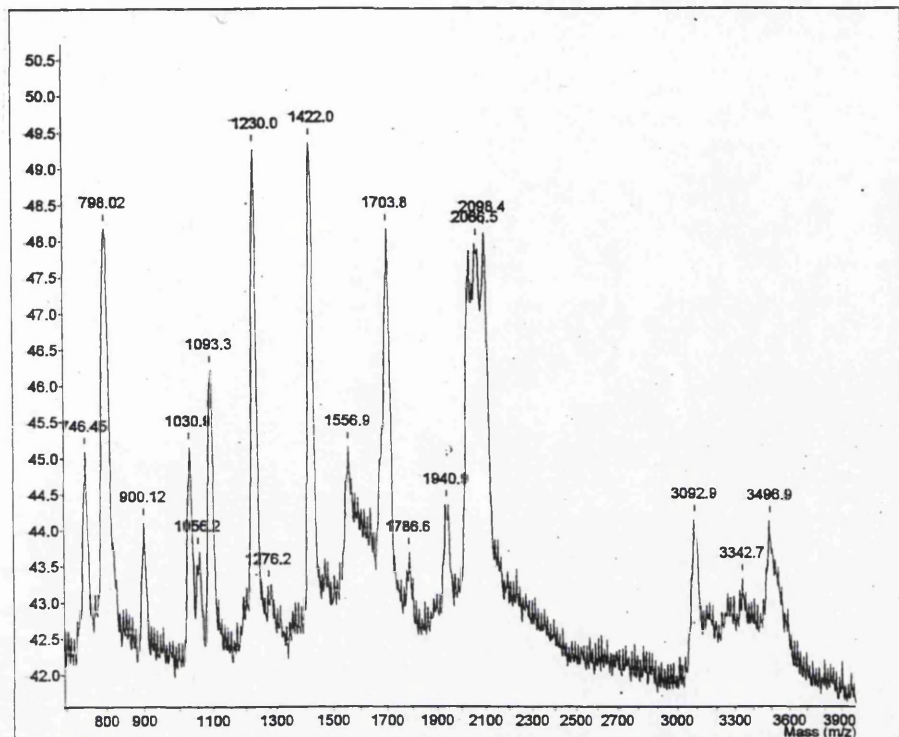


**Figure 4.5.10** Mass spectrometric analysis of the UL49 protein from *wt* virions phosphorylated at 1.5 M NaCl

A mass spectrum generated from analysis of UL49 protein. All the masses represent the protonated forms. The 3496.9 peak is the insulin B chain marker used to calibrate the spectrum.

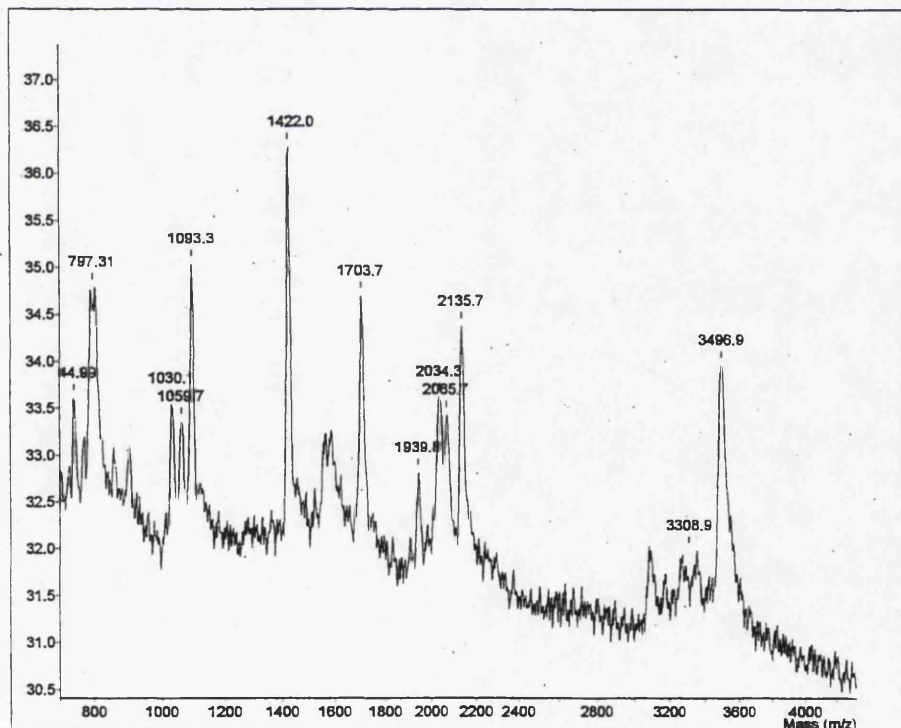


**Figure 4.5.11** Mass spectrometric analysis of the UL49ep protein from phosphatase treated vUL49ep virions

A mass spectrum generated from analysis of dephosphorylated UL49ep. All the masses represent the protonated forms. The 3496.9 peak is the insulin B chain marker used to calibrate the spectrum.

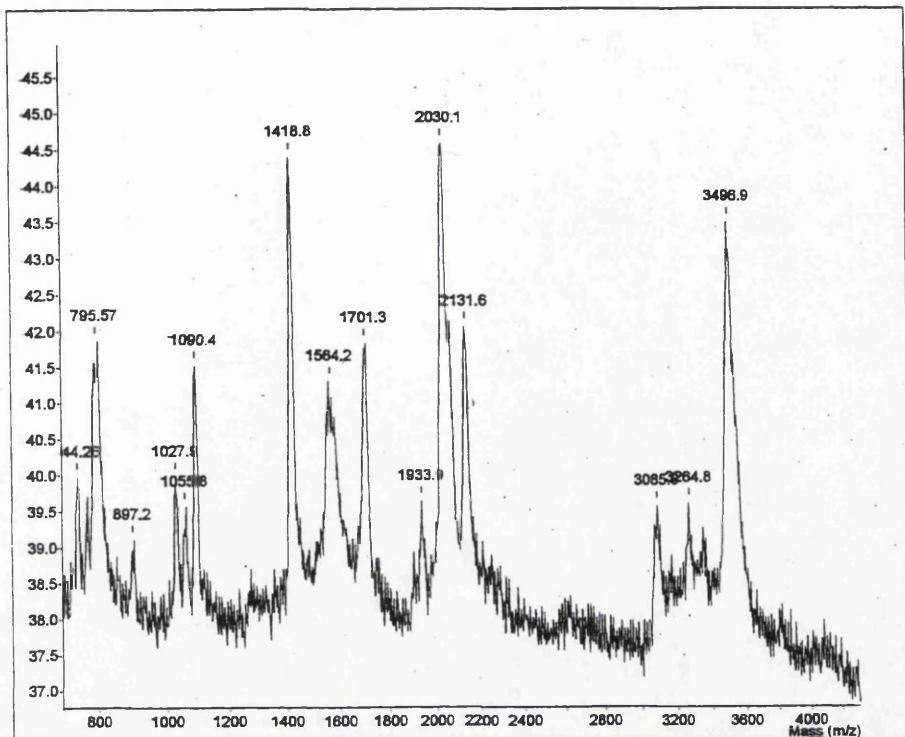


**Figure 4.5.12** Mass spectrometric analysis of the UL49ep protein from vUL49ep virions phosphorylated at 0 M NaCl

A mass spectrum generated from analysis of UL49ep protein (see Fig. 4.5.6). All the masses represent the protonated forms. The 3496.9 peak is the insulin B chain marker used to calibrate the spectrum.

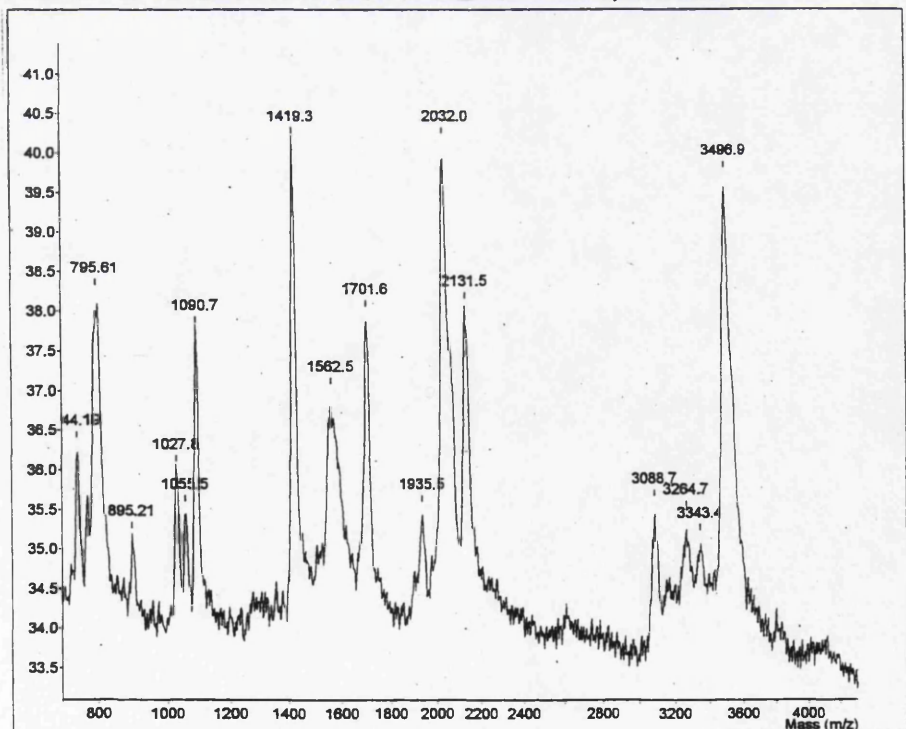


**Figure 4.5.13** Mass spectrometric analysis of the UL49ep protein from vUL49ep virions phosphorylated at 1.5 M NaCl

A mass spectrum generated from analysis of UL49ep protein. All the masses represent the protonated forms. The 3496.9 peak is the insulin B chain marker used to calibrate the spectrum.

Only one peptide reproducibly demonstrated an 80-Da mass shift. The 1786.6 Da peptide, possibly corresponding to a phosphorylated form of the 1705.6 Da peptide, was detected in *wt* UL49 phosphorylated at 1.5 M (Fig. 4.5.10) but was absent from all other samples. Although this peptide corresponds roughly in size with the radiolabelled phosphopeptide detected in Figs. 4.5.4 and 4.5.5, the 1786.6 Da peptide was detected in the UL49 protein phosphorylated at 1.5 M NaCl, while Fig. 4.5.4 shows radiolabelling of the phosphopeptide is reduced at 1.5 M NaCl.

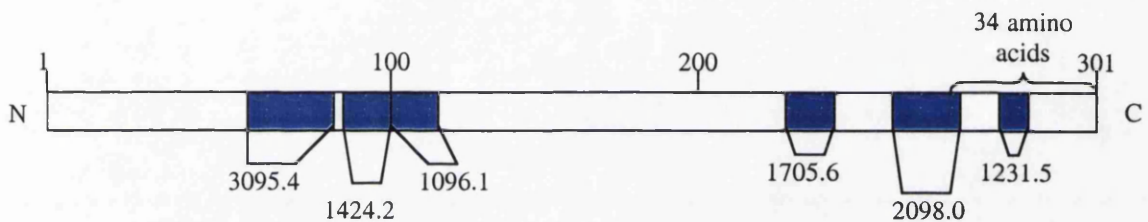


**Figure 4.5.14** A schematic representation of the 301 residue UL49 protein showing the position of the peptides detected in mass spectra generated from dephosphorylated UL49.

The N- and C-termini are marked, as are the C-terminal 34 amino acids. The peptides detected are shown in blue, and their unphosphorylated masses marked.

The mutant vUL49del268-301 produced a truncated form of the UL49 protein lacking the C-terminal 34 amino acids. Indeed, the 1231.5 Da peptide (residues 277-287), situated within the C-terminal 34 amino acids (see Fig. 4.5.14), was absent from Figs. 4.5.11 to 4.5.13. The 1705.6 Da peptide (228-242) is not situated in the C-terminal 34 amino acids (see Fig. 4.5.14), and was detected in all UL49del268-301 samples. However, no phosphorylated 1705.6 Da peptide was detected in the UL49del268-301 protein at any of the NaCl concentrations tested (Figs. 4.5.11 to 4.5.13).

Interpretation of these data is complicated, not least because only a subset of peptides are ionised in the mass spectrometer. However, when *wt* virions or *wt*-infected RSC CNE were phosphorylated *in vitro* at NaCl concentrations between 0 and 1.0 M, the UL49 protein was phosphorylated on a tryptic peptide with a Mr of approximately 2 kDa. When the UL49 protein was phosphorylated at 1.5 M NaCl, phosphorylation of the 2 kDa peptide was reduced and a phosphorylated 1705.6 Da tryptic peptide was detected. This

interpretation agrees with the established hypothesis that two PKs target the UL49 protein, one cellular and the other viral (Coulter *et al.*, 1993). It is likely that the UL13 PK phosphorylates residues within the 1705.6 Da UL49 peptide at 1.5 M NaCl.

#### 4.5.2 Phosphorylation of the UL13 protein

Previous data (Figs. 4.5.1 and 4.5.2) indicated that hypophosphorylated UL13 protein was phosphorylated on a 12 kDa Lys-C peptide, and hyperphosphorylated UL13 was phosphorylated on both the 12 kDa and an 18.5 kDa peptide. However, these data were derived from gross digests of phosphorylated CNE. To confirm these observations, UL13 phosphopeptides were examined using in-gel digestion. Fig. 4.5.15 shows the phosphopeptide profiles obtained from digesting phosphorylated UL13 protein from *wt*-infected RSC CNE with Arg-C and Glu-C.

Digesting the UL13 phosphoprotein with Glu-C produced a single major phosphopeptide with an approximate Mr of 11 kDa. Two additional peptides were faintly visible at 14.5 and 22 kDa, and may represent partial digestion products. The Arg-C digest yielded no detectable phosphopeptides, and it is not known whether this was due to failure to digest or to the peptides being too small to be detected on the gel. The digestion protocol was repeated on UL13 from *wt*-infected RSC CNE using Glu-C and Lys-C, individually and in combination. The results are shown in Fig. 4.5.16.

Digesting the UL13 protein with Glu-C give an 11 kDa peptide, which corresponds in size to the Glu-C phosphopeptide in Fig. 4.5.15. Digestion with Lys-C produced four strongly phosphorylated peptides with Mrs of approximately 15, 12, 11 and 4.8 kDa. The phosphopeptide profile of the Lys-C/Glu-C double digest resembles that of Lys-C, with the addition of an 8.6 kDa peptide. The two most highly radiolabelled peptides detected after digesting hyperphosphorylated UL13 with Lys-C/Glu-C migrated with approximate Mrs of 15 and 18.5 kDa.

The phosphopeptide profiles shown in Fig. 4.5.16 were derived from *wt* HSV-1 infected RSC CNE. The Lys-C digests were repeated using *wt* virions and *wt* HSV-1 infected MeWo cells, phosphorylated at 0 or 1.5 M NaCl (Fig. 4.5.17). Lys-C treatment of UL13 from phosphorylated *wt* virions yielded a single phosphopeptide of 12 kDa, regardless of

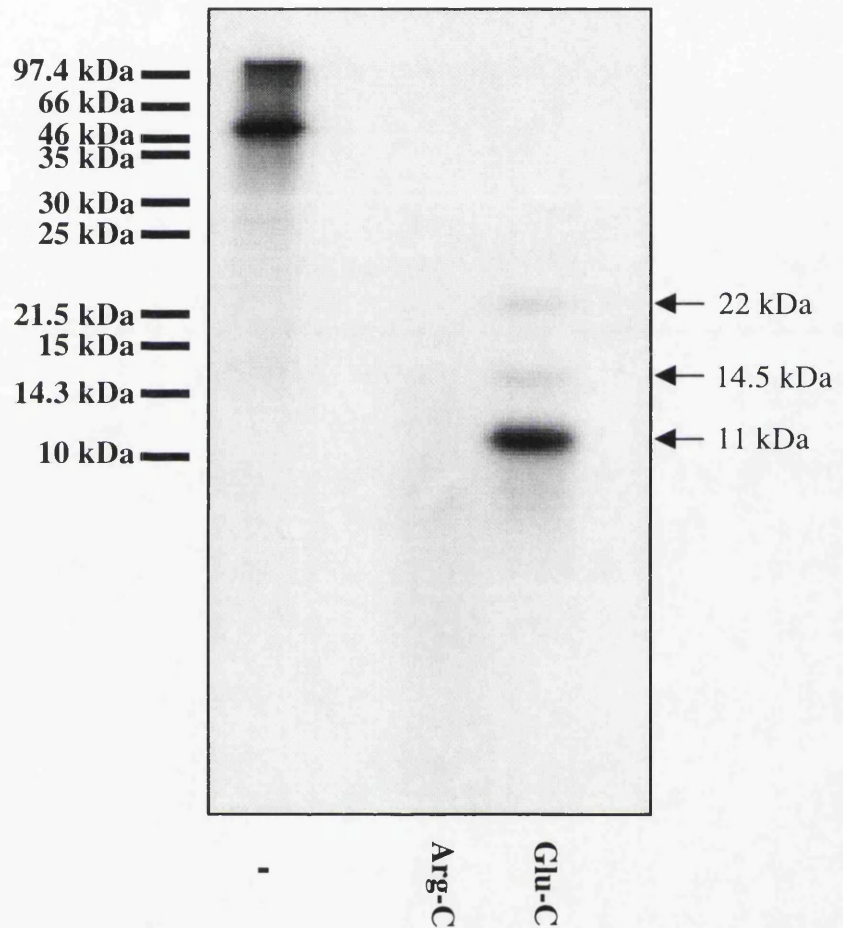


**Figure 4.5.15** Autoradiograph showing the phosphopeptide profile of the UL13 protein from *in vitro* phosphorylated *wt* RSC CNE. *Wt* RSC CNE were phosphorylated *in vitro* at 1.5 M NaCl. Radiolabelled UL13 protein was isolated on a 9% polyacrylamide gel and excised. In-gel proteolytic digestion was performed using 12.5  $\mu\text{g/ml}$  Arg-C or Glu-C and the fragments separated on a 18% polyacrylamide gel. Phosphopeptides were visualised by exposure of the wet gel to X-ray film.

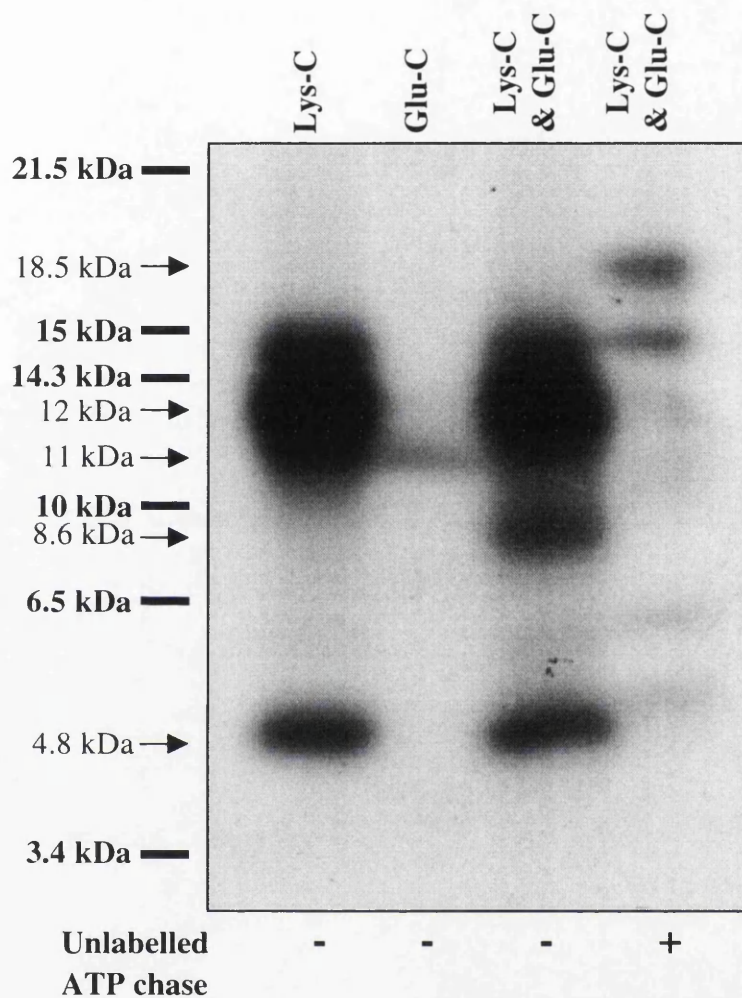


**Figure 4.5.16** Autoradiograph showing the phosphopeptide profiles of the UL13 protein from *in vitro* phosphorylated *wt* RSC CNE.

*Wt* RSC cell CNE was phosphorylated *in vitro* at 1.5 M NaCl with or without an unlabelled ATP chase. Radiolabelled UL13 protein was isolated on a 9% polyacrylamide gel and excised. In-gel proteolytic digestion was performed using 12.5  $\mu\text{g/ml}$  Lys-C, Glu-C or a combination of both and the fragments were separated on a 16.5% Tris-Tricine polyacrylamide gel. Phosphopeptides were visualised by exposure of the wet gel to X-ray film.

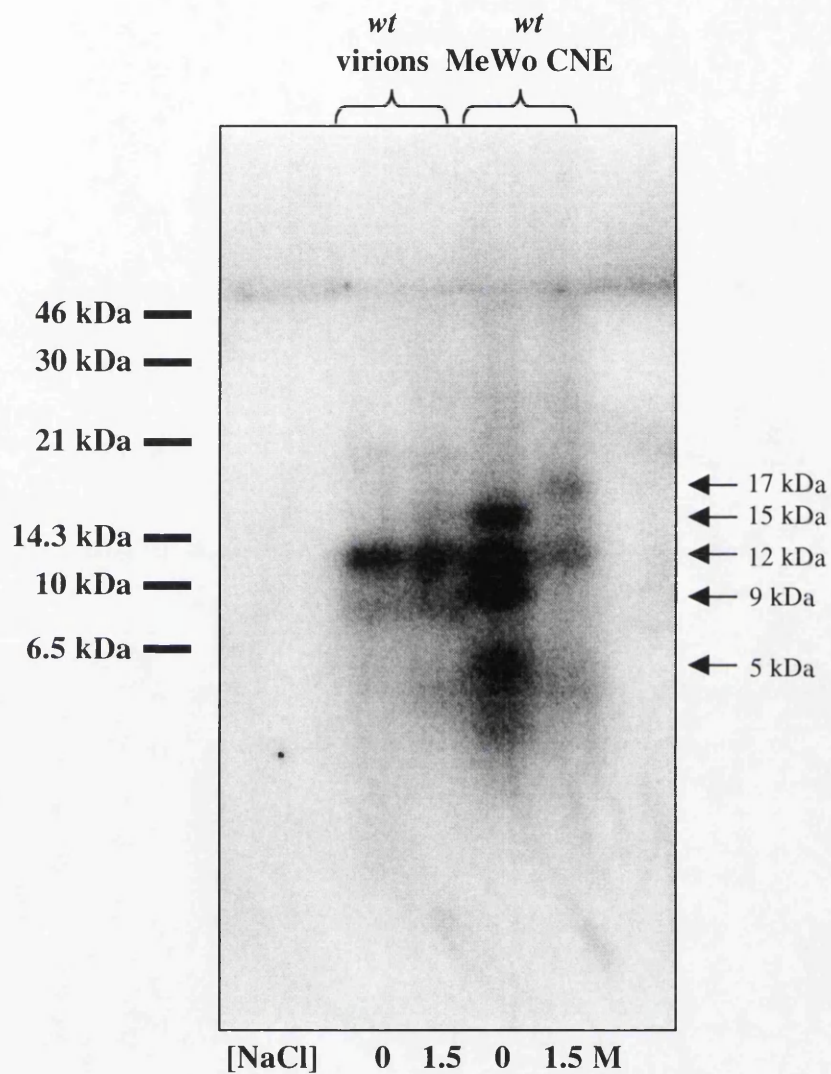


**Figure 4.5.17** Autoradiograph showing the phosphopeptide profile of the UL13 protein from *in vitro* phosphorylated *wt* virions and *wt* MeWo CNE.

*Wt* virion and infected MeWo cell CNE were phosphorylated *in vitro* at either 0 or 1.5 M NaCl. Radiolabelled UL13 protein was isolated on a 9% polyacrylamide gel and excised. In-gel proteolytic digestion was performed using 12.5 µg/ml Lys-C and the fragments separated on a 16.5% Tris-Tricine polyacrylamide gel, the phosphorylated fragments were visualised by exposure to X-ray film.

NaCl concentration. However, in MeWo CNE phosphorylated at 0 M NaCl, Lys-C treatment of the UL13 protein yielded four phosphopeptides with Mrs of approximately 15, 12, 9 and 5 kDa. When the experiment was performed on UL13 phosphorylated at 1.5 M NaCl, the peptide recovery was reduced, and the strongest radiolabelled phosphopeptides migrated with Mrs of 17 and 12 kDa.

Because of the low abundance of the UL13 protein in CNE and virions and because it co-migrated with an abundant cellular protein, vimentin, it was not possible to generate useful mass spectrometric data. An attempt to identify UL13 Lys-C phosphopeptides using mass spectrometry and N-terminal amino acid sequencing succeeding only in identifying vimentin (data not shown).

Clearly, the 12 kDa Lys-C phosphopeptide, detected in Figs. 4.5.1, 4.5.16 and 4.5.17 is derived from the UL13 protein. The 12 kDa Lys-C peptide was the only phosphopeptide detected in both cell lines and virions. This could mean that the 12 kDa Lys-C peptide contains the residue or residues which form the autophosphorylation domain of the UL13 PK. A 5 kDa Lys-C phosphopeptide was detected in Figs. 4.5.16 and 4.5.17, but not in the gross digests (Figs. 4.5.1 and 4.5.2). In fact, the 5 kDa phosphopeptide was only detected when Tris-Tricine gels were used (Fig. 4.5.16 and 4.5.17), reflecting their improved resolution compared to Tris-Glycine gels (Fig. 4.5.1) It was concluded that the 18.5 kDa phosphopeptide probably represents the hyperphosphorylated UL13 protein (Fig. 4.5.2). This was confirmed in Fig. 4.5.15, where a 18.5 kDa phosphopeptide was detected in chased *wt* RSC CNE but not in unchased samples. Because phosphorylation interferes with SDS binding, causing phosphorylated peptides to migrate with aberrantly high Mrs peptide identification is difficult. However, it is possible tentatively to identify the phosphorylated peptides, and an assessment of peptide identification is given in the Discussion.

## 5 DISCUSSION

### 5.1 UL13

#### 5.1.1 UL13 sequence analysis

When Smith & Smith (1989) and Chee *et al.* (1989) aligned known PKs with UL13 and its homologues, they identified a number of conserved PK subdomain motifs. However, neither identified all the PK motifs defined by Hanks *et al.* (1988). The availability of UL13 sequence data from additional herpesviruses allows an updated alignment to be analysed. Fig. 5.1 shows an alignment of several the sequenced alphaherpesviruses, with the PK subdomain motifs marked according to Hanks *et al.* (1988).

Motifs I, II, III, VI, IX and XI are well conserved, with all the expected invariant residues present. Motif VII retains the invariant Asp but not the Gly, usually considered invariant. Motif VIII also diverges from the established pattern, with three of the sequences lacking the invariant Glu. Only ILTV displays the prototypical APE sequence, and a further three have PPE motifs. Motifs IV, V and X are less well defined (see Table 1.1), and are thus harder to identify. The highly conserved Leu/Ala fits the defined consensus sequence of motif X. Motif IV shown in Fig. 5.1 was identified by Chee *et al.* (1989), but because there are no conserved residues within these motifs there are a variety of residues which could equally represent motifs IV and V.

As expected, updated alignments of 8 betaherpesvirus and 8 gammaherpesvirus UL13 homologues (data not shown) show lower conservation of motifs compared to the alphaherpesviruses. Importantly, the highly conserved APE motif is barely identifiable in the betaherpesvirus alignment and very poorly conserved in the gammaherpesviruses, with the invariant Glu missing from all. Although the difficulties in identifying PKs using sequence motifs has been highlighted in section 1.3.3.1, there is sufficient conservation of PK motifs to support the earlier conclusion by Chee *et al.* (1989) and Smith & Smith (1989) that UL13 and its homologues encode active PKs. However, because there are significant variations in the conservation and position of functionally important amino acids residues, the herpesviral PKs represent a significant departure from known PKs.

**Figure 5.1. A multiple sequence alignment of 10 alphaherpesvirus UL13 homologues.**

Numerals indicate the positions of the sequence motifs indicative of the 11 PK subdomains (Hanks *et al.*, 1988). A consensus sequence (con) showing fully conserved residues is shown for the catalytic domain.

HSV1 MDESRRQR PASHVAANLS PQGAR  
HSV2 MDESGRQR PASHVAADIS PQGAH  
EHV1 MARSRRSSVDEMDVGGSATSEYENC GGPSF SPLNLSR PKKSTRGRSLRSQA WGGKQLH PERST PLARNDCG PPSKRRRHEVGRSNKGLGASLDRTDE  
EHV4 MARSRRSSVDEMDVGGSTTSEYENC GGPSF SPLNMSCAKSTKRRSLRSRIWGGKSSDSEHT PLLTRNSCGPTGNTRRKH . AGI SNHKRGASLNHENG  
MDV1 MDTESKNKKTNGGENS  
MDV2 MDL DLKARKPGRGREN D  
VZV MDAD  
BHV1  
PRV  
ILTV

HSV1 QRSFKDWLASYVHNSPHGASGRPSG SPLQDAAVSRSSHGSRHRSGLRERLRAGLSRWRMSRSSHRRAS PETPGTAAKLNRPPLRRSQAALTAPPSSPSHI  
HSV2 RRSFKAWLASYI HSLRRASGRPSG SPRDGA VSGAR PGRSSRSFRERLRAGLSRWRVSRSSRRSSPEAPGPAAKLRPPLRRSETAMTSPSPSPSHI  
EHV1 DTS . . . . QCPRI RASAIRCGASTRKIVRITGECDAQQGDSR PGRSEMAGWHSPPKRRRTPSRHGNSDNERSHLPRLSSHGVVVRVGGRLPTQT PLQKTI I  
EHV4 DKS FQSGHNCPRI RASAVRCGAATR KIVRI TEEGASRQDNI WPGQSMAGWHSPPKRRRTPSRHGNSDNERSHL GQSPQSQSVVVRVGGRLPTQT PLRKTII  
MDV1 NCSHSTRTPDKSIEERFYNWERRSRTNRFGTTVNSRSYMYFQGTHTSRRHTYGNIHRRRFS DNIRCLRQLCMKRKT PAKKRS DKLVS RPSLPEHV  
MDV2 ECPHWKLSDISDQEDFSGPKYSSTDD . . . . . LQGT FAPARRDS CRKDHQHI SVNIRRC LKQFYRRRKHISRKTS DILLSRPSLPDHI  
VZV DTPENLQISPTAGPLRSHHNTDGHEPNATAADQQERESTNPTHGCVNH PWANPSTAT CMES PERSQQTSLFL LKHLGTRDPIHQERVDVFPQFNKPPWV  
BHV1 MQARRQRRARLGLPLLSGRDGRPTAPDPDRAGSSAP LRRRARGRRP PRGGCGAAALASGRIRAT PRADP PREPPAARSRAHIL  
PRV MAAGGGGGVSRRAALAHRTSAPGGAIAAAGGDGDGDEASRLLGRAQP  
ILTV MATRKRKSSDATAITTTCTKSRQRELAKNSTD SQSNFSRRRMP SRPPIRILSNDDGIDLEHIAFPVSEDLTKESR

I II III IV? V?  
HSV1 LTLTRIRKLCSPVFAINPALHYTTLEIPGARSFGSGGYGDVQLIREHKLAVKTIKEKEWFAVELIATLLVGEVLRAGRTHNIRGFIAPLGFSLQQRQI  
HSV2 LSLARIHKLCIPVFAVNPALRYTTLEIPGARSFGSGGYGEVQLIREHKLAVKTIKEKEWFAVELIATLLVGEVLRAGRTHNIRGFIAPLGFSLQQRQI  
EHV1 LQPKLVKRVEMPTFTVNPMPHYRRVALGEIPKFGGAGSYGEVQIFKQTLAIKTASSRSCFEHELAVSLTLLVGEVLRAGRTHNIRGFIAPLGFSLQQRQI  
EHV4 LQPKLVKRVEMPTFTVNPMPHYRRVALGEIPKFGGAGSYGEVQIFKQTLAIKTASSRSCFEHELAVSLTLLVGEVLRAGRTHNIRGFIAPLGFSLQQRQI  
MDV1 FTLARIKNVTTFI FNVTESELHYSHIDLKEMPIYAGSGSYGVVQI FKKTDIAVKKV . . . . . ECFKTELLM LIAGEC ACRARSTLALNSVLSLAFSIPSKEL  
MDV2 FTLSRIKNITSLIFDISPGLHYSTIDLQETPIYAGSGSYGEVQIFKQTLAIKTASSRSCFEHELAVSLTLLVGEVLRAGRTHNIRGFIAPLGFSLQQRQI  
VZV FRISKLSRLIVPIFTLNEQLCFSKLQIRDRPRFAGRTYGRVHIY PPSKIAVKTMDSR . VFNRELI NAILASEGSI RAGERLIGSIVCLLGFSLQKQL  
BHV1 RLAAVERPGCFVVDASLRIRSAEELAGPAQLRGAGGYGVVHEAAGVAVKT FASAADFEHELAVSLTLLVGEVLRAGRTHNIRGFIAPLGFSLQQRQI  
PRV REAPYLI PRPDGDLAVPDDLQYATLDLTDGDPVAVGAGSYGSVLVY . . . . . GSVAVKTL . . . . . RAGFGHEAVMTLAAE . . . . . EARSAGVGRVIRMLGSLAPLRLQ  
ILTV QLAIYIMPKNKICLVNPKMSYRWFNLEGSTVINGGYGSVQYAPKHMVAVKI FESDGHFRWELAMSLI LLSNAARRPELSDIAKHF LQIYAFSKIERAF  
con G-G-YG-V-----A-K-----F--E-----S-----

VI VII  
HSV1 VFPAYDMDLGKYGQLASLRATTNSVSTALHQCFTELARAVVFLNNTCGISHLDIKCANILVMLRSDA . VSLRRAVLADFSLVTLNSNSTIARGQFCLQE  
HSV2 VFPAYDMDLGKYGQLASLRATTNSVSTALHHCFTDLARAVVFLNTRCGISHLDIKCANILVMLRSDA . VSLRPAVLADFSLVTLNSNSTISRGQFCLQE  
EHV1 VFPAYDADLNAYGYRLSRGPPSVLVTESIERAFI GLGRALVYLN TSCGLTHLDVKGNGI FVN . . . . . HSHFVSDCVIGDLSLMTLNTNSMAMRAEF EIDT  
EHV4 VFPAYDADLNAYGYRLSRGPPSVLVTESIERAFI GLGRALVYLN TSCGLTHLDVKGNGI FVN . . . . . HSHFVSDCVIGDLSLMTLNTNSMAMRAEF EIDT  
MDV1 VFPAYHMDMSYHYRLARI . DKT VQHWAIEKTFMDL GKAVVFLN VSCGLTHLDIKCGNI FVNVTGPNPI LVDVAVIGDLSLALNTNSTILKSRFDVNI  
MDV2 VFPAYDMDMSYCHRLRKM . DKTARHWRAIEKAFMGLGRVAVVFLN VSCGLTHLDIKCGNI FVNVTGPNPI IVEAVIGDLSLALNTNSTITKARFDITV  
VZV LFPAYDMDMDEYIVRLSRRLTIPDHI DRKIAHVFLDLAQALTFNLN TSCGLTHLDVKGNGI FVNVTGPNPI IVEAVIGDLSLALNTNSTITKARFDITV  
BHV1 ALPAYDADLVAYA . EAAGRAVLS PAALAIERAFVGLGRAV VFLNASCGLAHLDIKCGNI FVNT . . . . . AGALITRAVLGDFSLMTLTAQSALADAE FLVST  
PRV MFPAYEMDMDAYRRSLTAR . . . . . PGHVVALGRVTELGRALVFLNGR . GLSHLDVKGNGI FVRTCGN . . . . . MVVTA VIGDLSLALNTNSTISRGQFCLQE  
ILTV VMEPLSHDLKTYAKRYKDNF . . . . . TMETLNTLTFSEFKGLAKALAFNLIDCGLVHMVDKSNILVKC . . . . . DANGKLSRLVLDLDFSLTGRPTNSILNQSM . MVC  
con -----D--Y-----F--L--A---LN---G--H-D-K--N-----V--D-SL-----S-----

VIII IX  
HSV1 PDLKSPRM . . . . . FGMPALT TANFHTLVGHGYNQPPPELVKYLNNNERAEFTNHRLKHDVGLAVDLYALGQTLLELLVSVYVAPSLGVPVTRFPG  
HSV2 PDLES PRG . . . . . FGMPAALT TANFHTLVGHGYNQPPPELVKYLNNNERAEFNNRPLKHDVGLAVDLYALGQTLLELLVSVYVAPSLGVPVTRVPG  
EHV1 GE . EEIKT . . . . . LRLPRSASQMT FSVI GHGLNPISVIADFINNSGLAKSTGPIKHDVGLTIDLYALGQALLELLLVGICISPLCSVPILRTAT  
EHV4 GE . EEIKT . . . . . LRLPKSASQMT FSVVGHGHNPQLSVIADFINNSGLAKSTGPIKHDVGLAVDLYALGQALLELLLVGICISPLCSVPILRTAT  
MDV1 SS . DKIQS . . . . . LKVCGRNIKPVFDLVLGHGQTQPCELMIKALNGVGFERRSTPLTSDEGVSIDMYALGQSLMEVILAAGMNFTHRFGISNPL  
MDV2 SS . DRVYS . . . . . VKVSRANIREVFDLVLGHGQTQPCELVVKALNGTGLERGSQSSDEGVAIDMYALGQSLMEVILAAGMNFTRDFATPGNVP  
VZV PS . HPEHV . . . . . LRVPRDASQMSFRLLVLSHGNTQPPPEL LDYINGTGLTKYTGTL PQRVGLAIDLVALGQALLEVILLGRLPQGLPISVHRTPH  
BHV1 DDGNSD GASDAVAGGRLLRLLPDDARMPDPEIVMGHCATR PSEM LDFLNRHGLRGRPELPADLGLAIDLVALGHALLELVLTGARETPEVQCARRQA  
PRV . . . . . ARRKALKITSLARSPTGVLLGHARDRPRVLMDFIN . . . . . GRPPPPGLPYEVGLAIDLVALGHVLLDVAL . . . . . GLRQRQALTR . . . . .  
ILTV PSRGVVEGLKIIDSTTVKNHIPS . . . . . SFIIYNGHCRAPEVIINYCN . . . . . GKRYRDQPMDALETGLD LDFSLGQVQVEILFEGILCRSREFSFKPKPN  
con -----D--Y-----F--L--A---LN---G--H-D-K--N-----V--D-SL-----S-----

X  
HSV1 YQYFNNQLSPDFALALAYRCVLPALFVNSAETNTHGLAYDVPEGIRRHRLNPKIRRAFTDRCINY . QHTHKAILSSVALPPELPLLVLSRSLCHTNP  
HSV2 YQYFNNQLSPDFAVALLAYRCVLPALFVNSAETNTHGLAYDVPEGIRRHRLNPKIRRAFTDRCINY . QRTHKAVLSSVSLPPELPLLVLSRSLCHTNP  
EHV1 YYYYSNRLSVDYALD LLAYRCVLPALFPTTPTTYIGI PWDQVEGVFES IAGAHHREAFAHRLRY . RLTHRRLFASIRIPSAFTGVLELVSLCHANE  
EHV4 YYYYSNRLSVDYALD LLAYRCVLPALFPTTPTTYIGI PWDQVEGVFES IAGAHHREAFAHRLRY . RLTHRRLFASIRIPSAFTGVLELVSLCHANE  
MDV1 HFYYHRLMRADYLDLID LAYRCVLPALFPTTPTTYIGI PWDQVEGVFES IAGAHHREAFAHRLRY . RLTHRRLFASIRIPSAFTGVLELVSLCHANE  
MDV2 HFYYHRLMRADYLDLID LAYRCVLPALFPTTPTTYIGI PWDQVEGVFES IAGAHHREAFAHRLRY . RLTHRRLFASIRIPSAFTGVLELVSLCHANE  
VZV YHYGHKLSPLDALD LLAYRCVLPALFPTTPTTYIGI PWDQVEGVFES IAGAHHREAFAHRLRY . RLTHRRLFASIRIPSAFTGVLELVSLCHANE  
BHV1 LHMSARVTCGLVIGI LAHRCALLPLVFPATPRTAACGVWDEPAAVRAAIGNVAIRAAFDRTTEAH . RARYTERVREALAAPVRRRALELAALFCHPNP  
PRV . . . . . EYAVEVLAARRCVLFAALLPPGSGPSAEALAGDILEE . . . . . ELAAGFREGVASS . RPNQ . . . . . PRTVAPLELVARFCGDG  
ILTV . . . . . TIHEKLSHDYMMRVLAYRIVLSDNLSRGCDSLFTGTPLSGTVESVNASL FRELDRILFQSHVEMYERIDLREKLLNVIIPETRGLCTLGLLCHDWA  
con -----LA-R--L-----F-----D--LG-----C-----

XI  
HSV1 CARHALS  
HSV2 AARHSL  
EHV1 KARLSIPLLWTPRP  
EHV4 KARLSIPLLWTPHP  
MDV1 VARTADL LWN  
MDV2 EARAATRL LNK  
VZV EIRSDHPLLWHDRDWIGST  
BHV1 RARRAALV LWS  
PRV GARFAELAA  
ILTV DLRRSAVTFF  
con --R----

In addition to PK motif identification, these alignments also highlight the heterogeneity in sequence length of the N-terminal domain of UL13 and its homologues. A convincing alignment cannot be produced for the alphaherpesviruses (Fig. 5.1), and lengths range from 86-233 amino acid residues. There is a Pro-x-x-x-x-Cys motif conserved in beta- and gammaherpesviruses, 20 and 10 residues before motif I, but not in alphaherpesviruses, and lengths vary from 185-400 amino acid residues in the betaherpesviruses and from 80-90 amino acid residues in the gammaherpesviruses. The extended N-terminal domain acts as a regulatory subunit in some PKs, but it is not known whether it plays such a role in the herpesvirus UL13 PKs.

While identification of conserved PK motifs is a strong indicator that a protein is a PK, their structural arrangement must be appropriate. Fig. 5.2 shows the catalytic domains of cAPK, HSV-1 US3 and HSV-1 UL13 aligned according to their conserved PK motifs, with the known secondary structure of cAPK indicated along with the predicted secondary structure of the two HSV-1 proteins. The secondary structures of US3 and UL13 were predicted using PsiPred.

As described in Chapter 1, PKs consist of two lobes. The dominant feature of the small lobe (motifs I to IV) is an antiparallel  $\beta$ -sheet comprising five strands ( $\beta$ 1-5). In contrast, the large lobe is dominated by  $\alpha$ -helices with a small  $\beta$ -sheet near the cleft. Fig. 5.2 shows that in all three PKs the N-terminal region is dominated by  $\beta$ -strands, whereas the C-terminal region consists almost entirely of  $\alpha$ -helices. However, closer analysis reveals areas of apparently poor structural correlation. In Fig. 5.2 the small lobe of US3 contains four  $\beta$ -strands, whereas UL13 only contains three. In cAPK, the glycine-rich motif (motif I) is situated between  $\beta$ -sheets 1 and 2 ( $\beta$ 1 and 2) and motif II is situated within  $\beta$ 3. Fig. 5.2 shows that both UL13 and US3 have the same structural arrangement. In cAPK, motif III is situated within  $\alpha$ -helix C ( $\alpha$ C). In UL13 and US3 motif III is positioned within a predicted  $\alpha$ -helix, but  $\alpha$ B is missing from both herpesviral PKs. Also, both herpesviral PKs lack  $\beta$ 5, bringing motifs IV and V closer together. Motif V is positioned within the region linking the two lobes. In cAPK motif V is positioned just before  $\alpha$ D, whereas in both herpesviral PKs motif V is positioned at the start of  $\beta$ 5.

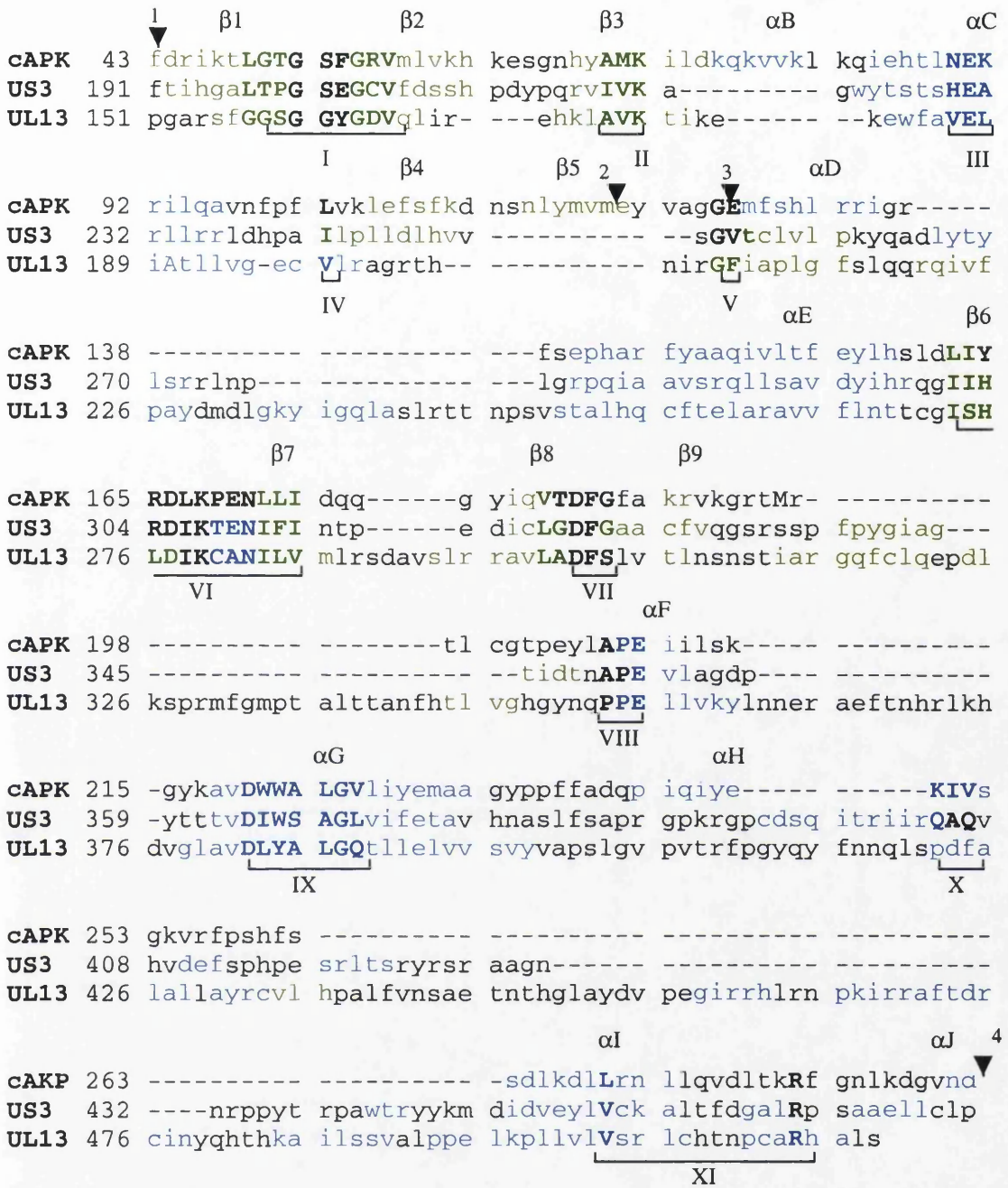


Figure 5.2 Amino acid sequence alignment of the catalytic cores of cAPK and the HSV-1 PKs encoded by US3 and UL13.

Residues shown in green represent  $\beta$ -stands, residues in blue represent  $\alpha$ -helices and residues shown in bold are residues indicative of PK subdomains. Arrows 1 and 2 represent the boundaries of the small lobe, between arrows 2 and 3 represents the linker region and the area between arrows 3 and 4 constitutes the large lobe.

The large lobe of all three PKs begins with a long  $\alpha$ -helix followed by motif VI. Both motif VI and VII are situated between two short  $\beta$ -strands. The conservation and position of motif VI between the two  $\beta$ -strands ( $\beta 6$  and 7) is significant, with the conserved residues between  $\beta 6$  and  $\beta 7$  forming a loop which, in cAPK, contacts the

autophosphorylation site. There is a slightly larger gap between motifs VI and VII in UL13, and in all three cases the APE motif (motif VIII) lies at the start of a short  $\alpha$ -helix, and motif IX is situated within a long  $\alpha$ -helix ( $\alpha$ G). Despite the extended region between motifs X and XI, the remaining motifs are reasonably well conserved, and are situated within predicted  $\alpha$ -helices.

There appears to be strong structural similarity between cAPK and the herpesviral PKs across the region of the small lobe containing the first two motifs, followed by a region of poor similarity. Generally there is greater similarity between cAPK and the herpesviral PKs in the large lobe, with the large lobe of all three PKs composed mainly of  $\alpha$ -helices. Conservation of the structural elements around the catalytic loop ( $\beta$ 6 and 7) is a good indicator of PK activity. While this analysis highlights the structural similarities and differences between cAPK and the herpesviral PKs, supporting the view that both are active PKs, the precise structure and exact nature of the amino acid interactions within both UL13 and US3 would require the solution of their crystal structures.

### 5.1.2 Phosphorylation of the UL13 protein

The first aim of this research was to confirm and extend the work of Coulter *et al.* (1993), who showed that disrupting HSV-1 gene UL13 resulted in reduced *in vitro* phosphorylation of certain proteins, most obviously the 38 kDa UL49 protein. Because Coulter *et al.* (1993) used a single UL13-*lacZ* mutant and did not test a revertant, it was necessary to analyse additional UL13 mutants in order to ensure that the observed effects were due solely to disruption of the UL13 gene. Two additional mutants were used (Table 1.12, Fig. 5.3) one with a small deletion and one with a small insertion in different regions of the UL13 gene.

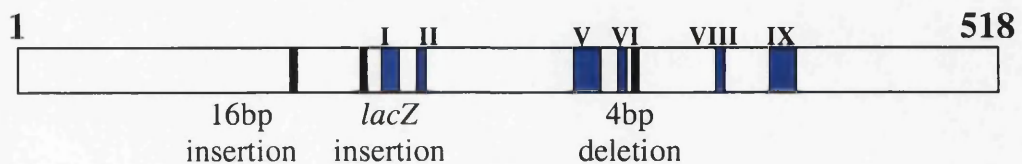


**Fig. 5.3 Schematic representation of the positions of the lesions within the three UL13 mutants employed in this study.**

The mutated sites are shown as thick, vertical black lines. The positions of six of the eleven PK subdomains are shown as blue boxes.

Fig. 4.1.1 showed that these two mutants produced phosphorylation profiles indistinguishable from the UL13-*lacZ* mutant which carried a sizeable insertion in the UL13 gene. Importantly, reduced phosphorylation of the 38 kDa UL49 protein was detected in the phosphorylation profiles of all three mutants.

Some PKs are known to phosphorylate themselves as a form of auto-regulation. Consequently, autophosphorylation is a common feature used in PK identification. The data presented in this thesis confirm that the putative UL13 PK is highly phosphorylated *in vitro* in infected CNE samples (Fig. 4.1.1) and in virions (Fig. 4.4.3). Phosphorylation of the HSV-1 UL13 PK was shown to be stimulated by  $Mn^{2+}$  in comparison with  $Mg^{2+}$ , thus agreeing with the study performed on PRV UL13 by De Wind *et al.* (1992). However, HSV-1 UL13 PK activity was reduced at pH 9.2, a pH which promoted optimal activity of the HSV-2 UL13 PK (Daikoku *et al.* 1997). Phosphorylation of the HSV-1 UL13 PK was sensitive to NaCl concentration, with phosphorylation of the UL13 PK in MeWo cells and virions increasing as NaCl concentration increased (Fig. 4.4.3). This observation is in agreement with Cunningham *et al.* (1992) and Coulter *et al.* (1993). However, Daikoku *et al.* (1997) found that activity of the purified HSV-2 UL13 PK suffered a 70% reduction in activity at 0.5 M NaCl.

Since the amino acid sequence of the HSV-1 and HSV-2 UL13 proteins are 86% identical (Fig. 5.1) it is unclear why the two PKs appear to demonstrate such different characteristics. However, it is interesting to note the HSV-2 UL13 PK activity purified by Daikoku *et al.* (1997) demonstrated many characteristics similar to CKI (Table 1.15). Attempts to purify the HSV-1 UL13 PK have resulted in loss of activity, and it is possible that Daikoku *et al.* (1997) purified an inactive UL13 PK, and that the observed PK activity was due to trace amounts of a contaminating cellular PK, perhaps CKI. However, the PK activity detected by Daikoku *et al.* (1997) was highly resistant to heparin, as would be expected for the HSV-2 PK. Thus, the disparity in NaCl sensitivity and optimum pH between the HSV-1 and HSV-2 UL13 PKs remains unresolved.

### 5.1.3 Hyperphosphorylation of the UL13 protein

The UL13 protein was shown to be hyperphosphorylated in CNE samples incubated with excess ATP or GTP (Fig. 4.2.1). Hyperphosphorylation of the UL13 protein

demonstrated cell type dependence, and did not occur in virions (Fig. 4.4.3). Hyperphosphorylation of the UL13 PK was not inhibited by heparin (Fig. 4.4.6), but was inhibited by DRB, a potent CKII inhibitor (Fig. 4.4.7).

While hyperphosphorylation is a relatively common phenomenon, it has not before been observed to occur with the HSV-1 UL13 protein, and might be of physiological significance. For example, the hypo- and hyperphosphorylated forms of RNA polymerase II are associated with distinct aspects of transcription. CKII has been reported to phosphorylate viral proteins such as the papillomavirus E7 protein (Barbosa *et al.*, 1990), the adenovirus E1A protein (Carroll *et al.*, 1988) and simian virus 40 large T antigen (Grasser *et al.*, 1988). It is also relatively common for PKs to function in cascade systems, with their activity upregulated by additional PKs. However, it must be borne in mind that hyperphosphorylation of the UL13 PK was achieved in an *in vitro* assay. PKs are very active enzymes, often phosphorylating proteins *in vitro* with recognisable target sequences but which are not necessarily of physiological significance.

There are a number of residues throughout the PK catalytic domain which when mutated inactivate PK activity. For example charge-to-Ala mutations at Lys<sup>72</sup>, Glu<sup>91</sup>, Asp<sup>166</sup> and Lys<sup>168</sup> within cAPK abolish activity (Taylor *et al.*, 1993). Mutation of the invariant Lys in HHV-8 (Lys<sup>108</sup>) (Park *et al.*, 2000) and in HCMV (Lys<sup>355</sup>) (He *et al.*, 1997) dramatically reduced the PK activity of the proteins. Mutating the invariant Lys (Lys<sup>180</sup>) in the HSV-1 UL13 PK would help determine whether hyperphosphorylation of the UL13 PK was an extreme form of autophosphorylation or a result of a second PK targeting the UL13 PK.

#### 5.1.4 Mapping sites of phosphorylation in the UL13 PK

At the start of this project, it was not known where or on how many residues the UL13 PK was phosphorylated. However, detection of three different phosphorylated forms of the UL13 PK with Mrs of approximately 57, 60 and 62 kDa suggests that the protein is phosphorylated at a minimum of three sites. Attempts were made to locate the sites by phosphopeptide mapping.

The UL13 protein derived from virions and MeWo and RSC CNEs was shown to be phosphorylated on a 12 kDa Lys-C peptide. Indeed, the 12 kDa Lys-C phosphopeptide

was the only phosphopeptide detected in UL13 from phosphorylated virions. In addition, an 11 kDa phosphopeptide was detected in UL13 protein from RSC CNE digested with Glu-C. One interpretation of this is that the 12 kDa Lys-C phosphopeptide contains the autophosphorylation domain of the UL13 PK. The major autophosphorylation domain is usually situated between PK motifs VII and IX, near motif VIII. The predicted Lys-C and Glu-C peptides containing motif VIII are shown, along with their predicted Mws, in Fig. 5.3.

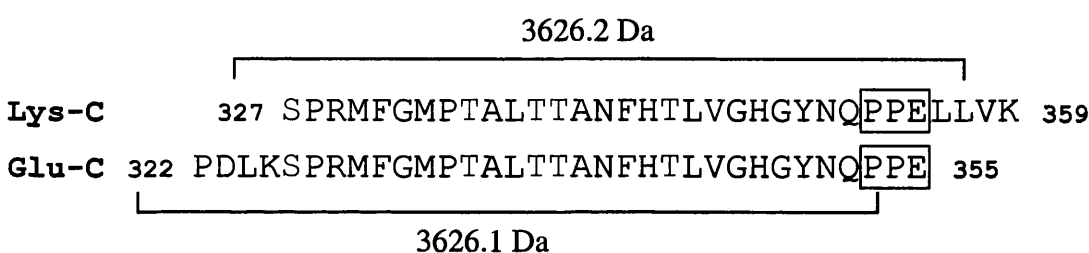


**Figure 5.4 Amino acid sequences of the predicted Lys-C and Glu-C peptides containing UL13 PK motif VIII.**

The Ser (S) and Thr (T) residues are shown in blue and PK motif VIII is boxed. Non-phosphorylated peptide masses are indicated.

Because phosphorylated proteins and peptides can migrate with aberrantly high Mrs, it is possible that these two peptides are the 12 kDa Lys-C and 11 kDa Glu-C peptides detected in Figs. 4.5.16 and 4.5.15. However, there are problems with this interpretation. The Mws of the two peptides differ by only 0.1 Da, but the Lys-C phosphopeptide migrated with an Mr 1 kDa greater than the Glu-C peptide. Since the Lys-C peptide contains no additional sites for phosphorylation, this difference cannot be attributed to phosphorylation. Also, whereas only one peptide was detected from Glu-C digests of CNE, a 5 kDa peptide was derived from the Lys-C digest in addition to the 12 kDa peptide (Figs. 4.5.15 and 4.5.16). It is possible that the phosphorylated residue within the 5 kDa Lys-C peptide was situated within a Glu-C peptide too small to be visualised by SDS-PAGE. This is unlikely because the smallest predicted Glu-C peptide containing a Ser or Thr residue is 1166.4 Da. The data presented here do therefore not readily support phosphorylation of the UL13 PK within the accepted autophosphorylation domain. However, phosphorylation of residues within the Ser rich N-terminal 100 residues are predicted to produce the phosphopeptide patterns shown in Figs. 4.5.15 to 4.5.17. Fig. 5.4 shows the predicted Lys-C and Glu-C peptides derived from this region.

As shown in Fig. 5.4, digesting the N-terminal 100 residues with Lys-C is predicted to yield two peptides of 3151.5 and 7829.6 Da, whereas Glu-C treatment would yield fragments of 393.4, 7326.0 and 2653.0 Da. The 7829.6 Da Lys-C peptide and 7326.0 Da Glu-C peptide overlap by 43 residues, 10 of which are Ser residues. The predicted Lys-C peptide is approximately 0.5 kDa larger than the Glu-C peptide, which corresponds well with the 1 kDa difference in  $M_r$  between the Lys-C phosphopeptide and Glu-C phosphopeptide in Fig. 4.5.16. Also, if the 7326.0 Da Glu-C peptide is phosphorylated on any of its three N-terminal Ser residues, these would appear on the 3151.5 Da Lys-C peptide, which would correspond well with the 5 kDa Lys-C phosphopeptide seen in Figs. 4.5.16 and 4.5.17. It is unlikely that the 7829.6 Da Lys-C is phosphorylated on the C-terminal five Ser residues, as this would result in a second, smaller Glu-C phosphopeptide in addition to the 11 kDa phosphopeptide detected in Fig. 4.5.15.

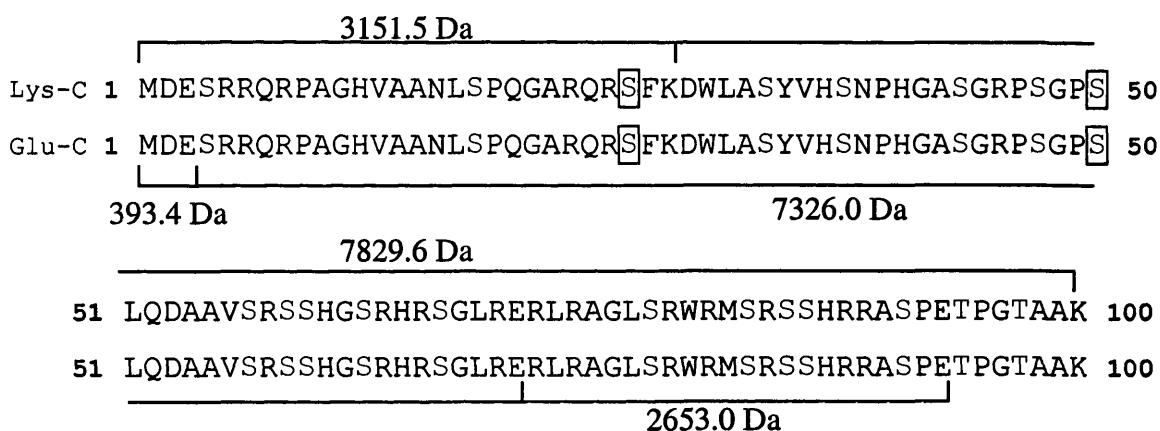


**Figure 5.5. Sequences of the Lys-C and Glu-C peptides derived from the N-terminal 100 amino acid residues of the UL13 PK.**

Ser (S) and Thr (T) residues are shown in blue, the boxed residues lying within CKII consensus sequences. Non-phosphorylated peptide masses are indicated in Da.

Of the two possibilities, that phosphorylation occurs in the autophosphorylation domain or in the Ser-rich N-terminal domain, the latter is better supported by the data. This region is not within the conserved catalytic core of the PK, and the alignments in Fig. 5.1 highlights the lack of conservation and heterogeneity in length of the N-terminal domain of UL13 and its homologues. However, it should be noted that mutational analysis of BGLF4, the UL13 counterpart in EBV, identified the N-terminal 26 residues as essential

for autophosphorylation (Chen *et al.*, 2000). The N-terminal 26 residues of UL13 all lie within the 3151.6 Da Lys-C fragment, supporting the hypothesis that the HSV-1 UL13 PK is phosphorylated on residues at its N-terminal region. Further mapping experiments are needed to elucidate the situation further.

No success at mapping phosphorylated residues within HSV-1 UL13 or its homologues has been reported. Using phosphoamino acid analysis, the PRV UL13 (De Wind *et al.*, 1992), HCMV UL97 (He *et al.*, 1997) and HHV-8 ORF36 PKs (Park *et al.*, 2000) were shown to be phosphorylated on Ser and Thr residues. In the PRV UL13 PK there is a greater preference for phosphorylation on Ser residues and the HHV-8 ORF36 PK autophosphorylated solely on Ser residues. The 7829.6 Da N-terminal Lys-C peptide shown in Fig. 5.4 is very Ser-rich. Indeed, the best supported interpretation of the data presented here implies that the HSV-1 UL13 PK is phosphorylated solely on Ser residues. During the course of this work, phosphoamino acid analysis of radiolabelled HSV-1 UL13 PK was attempted, but the results were inconclusive. This would be an important avenue for future investigation. Identification of the phosphorylated residues could be achieved by protein sequencing. However, this approach is unlikely to yield results easily because the UL13 protein is a very minor component of the virion, and is present in low levels in infected cells. Identification of phosphorylated residues would require phosphopeptide mapping at a very detailed level, supported by mutation of the potential target residues.

## 5.2 Targets for phosphorylation

### 5.2.1 Phosphorylation of the UL49 protein

Using three independent UL13 mutants, it was confirmed that phosphorylation of a 38 kDa viral protein was dependent upon a functional UL13 protein. Coulter *et al.* (1993) used HSV-1/HSV-2 intertypic recombinants to identify the 38 kDa protein as the UL49 gene product. Data in this thesis obtained using a UL49 truncation mutant (UL49del268-301) and mass spectrometry confirmed this identification. Importantly, the UL49 protein was still phosphorylated in UL13 mutant CNE samples, albeit to a greatly reduced level. This indicated that a second PK targets the UL49 protein. On the basis of NaCl sensitivity, Coulter *et al.* (1993) suggested that the second PK was of cellular origin. The work presented here confirmed that the PK targeting the UL49 protein in UL13 mutant

CNE was inhibited at high NaCl concentrations (Fig. 4.1.1.) and that it was sensitive to heparin (Fig. 4.4.5) but not DRB, a potent CKII inhibitor (Fig. 4.4.7). Elliott *et al.* (1996) identified a number of CKII and PKC sites in the N-terminal 120 residues of the UL49 protein, which they suggested are targeted for phosphorylation. On the basis of the data presented here, it seems likely that the heparin-sensitive but DRB-insensitive PKC phosphorylates the UL49 protein in addition to the UL13 PK.

### 5.2.2 Hyperphosphorylation of the UL49 protein

Initially, the UL49 protein was not detectably hyperphosphorylated when incubated in the presence of excess ATP or GTP (Fig. 4.2.1). This seemed unusual, especially since it was apparent that multiple PKs may target the UL49 protein. However, under different buffer conditions, the UL49 protein demonstrated an altered mobility indicative of hyperphosphorylation (Fig. 4.4.1). This novel mobility shift was abolished by phosphatase treatment (Fig. 4.4.7), showing that it was due to phosphorylation. However, there was an additional post-translational modification which was stimulated by incubation with each of the four dNTPs (Fig. 4.4.5). The UL49 protein is known to be both nucleotidylated and mono-(ADP)-ribosylated (Blaho *et al.*, 1994), however the identity of the second post-translational modification remains elusive. Neither hyperphosphorylation nor the second post-translational modification were detected when a mutant producing UL49 protein lacking the C-terminal 34 amino acids (UL49del268-301) was analysed.

Using the vUL49del268-301 mutant to map phosphorylated residues in the UL49 protein, Elliott *et al.* (1996) found no indication of phosphorylation within the C-terminal 34 residues. Indeed, the truncated form of the UL49 protein was radiolabelled when phosphorylated *in vitro* (data not shown). However, the data indicates that hyperphosphorylation, undetected by Elliott *et al.* (1996) requires the C-terminal 34 residues.

### 5.2.3 Phosphorylation mapping of the UL49 protein

Tryptic digests of the UL49 protein, phosphorylated at NaCl concentrations between 0 and 1.0 M, produced a radiolabelled tryptic phosphopeptide of approximately 2 kDa (Fig. 4.5.4). When the UL49 protein was phosphorylated at 1.5 M NaCl, a tryptic peptide of

1703.91 Da was found to be phosphorylated. This phosphorylated peptide was not detected in UL49 phosphorylated at 0 M NaCl. These data confirm that the UL49 protein is phosphorylated at multiple sites, probably by multiple PKs. It seems likely that one of the PKs is a NaCl- and heparin-sensitive cellular PK (Figs. 4.1.1 and 4.4.5) and that the second is the HSV-1 UL13 PK. It is likely that the herpesviral PK targets the 1703.91 Da peptide. The 1703.91 Da peptide constitutes residues 228 to 242 of the UL49 protein and the sequence is shown in Fig. 5.5. It was not determined which of the three Thr residues was phosphorylated.

228 TDEDLNELLGITTIR 242

**Fig. 5.6 The sequence of the 1703.91 Da tryptic peptide representing residues 228 to 242 of the UL49 protein.**

Potentially phosphorylated residues are shown in blue.

Elliott *et al.* (1996) identified a number of residues in the N-terminal 120 residues of the UL49 protein which they believed were targeted by CKII or PKC. Four Ser residues were identified on a 13 kDa Lys-C peptide which was located in the established CKII consensus motif. The predicted peptides resulting from complete tryptic digestion would place one of these Ser residues on a 2.7 kDa peptide and the other three on a 3.1 kDa peptide. Unfortunately neither corresponds in size to the 2 kDa tryptic phosphopeptide derived from the UL49 protein (Figs. 4.5.4 and 4.5.5). Further work by Elliott *et al.* (1999) identified a cluster of three N-terminal serines present at residues 71, 72 and 73 (Ser<sup>71, 72, 73</sup>) as a substrate for CKII. In addition, Elliott *et al.* (1999) identified two C-terminal Ser residues (Ser<sup>292, 294</sup>) which acted as a substrate for another, as yet unidentified, cellular kinase. These C-terminal residues identified by Elliott *et al.* (1999) do not lie within the 1703.91 Da fragment identified in this study. Elliott *et al.* (1996) stated that they believed VP22 was modified solely on Ser residues located in the N-terminal 120 residues of the protein. Within 3 years they had identified two further phosphorylated residues in the C-terminus, it is possible that further phosphorylated residues remain undetected by them.

### 5.2.3 Critical appraisal of identified UL13 PK targets

A number of proteins have been identified as targets for phosphorylation by the HSV-1 UL13 PK (Table 1.16). However, critically appraising the validity of these target proteins is difficult, not least because all the target proteins were identified using *in vitro* assays which poorly reproduce the *in vivo* situation.

All the studies outlined in Section 1.5 used UL13 mutants to identify targets for the UL13 PK. However, only ICP22 (US1), ICP0 (RL1), EF-1 $\delta$ , gE (US8) and gI (US7) were proposed to be directly phosphorylated by the UL13 PK, as demonstrated by incubating immune complexes of putative target proteins with immune-precipitated UL13 under phosphorylating conditions. The major flaw in this technique, as outlined in section 1.3.1, is that the likelihood of co-precipitating contaminating PKs, such as CKI and CKII, cannot be excluded. Prod'hon *et al.* (1996) used *in vitro* transcribed and translated UL13 protein and ICP22 to show that the UL13 PK can directly phosphorylate ICP22. However, even though the UL13 PK is capable of phosphorylating proteins in the assays used, it is far from clear whether phosphorylation of these proteins is physiologically relevant and whether they are actually targeted *in vivo*.

One means of determining whether a protein is a true target for phosphorylation by the UL13 PK is to show that phosphorylation is required for an aspect of target protein function. The observation that the phenotypes of UL13 and US1 mutants are similar indicates that UL13 phosphorylation may be important for an aspect of ICP22 function. Hyperphosphorylation of RNA polymerase II and EF-1 $\delta$  has been shown to be of physiological importance, and the UL13 PK has been implicated in hyperphosphorylation of both proteins. While a hyperphosphorylated form of *vhs* is preferentially packaged into virions this has not been related to host-shutoff function. Phosphorylation of the UL49 protein has been implicated in tegument dissociation, but only *in vitro*, and although gE, gI and ICP0 are known to be phosphorylated in HSV-1 no functional importance of this modification has been identified.

The claim that ICP22 is a true target of the UL13 PK is perhaps the strongest of those available, but it is not yet proved. Conservation of the UL13 protein across the herpesvirus subfamilies implies that the true target is a conserved herpesviral protein or a

cellular protein. However, the HSV-1 US1 gene encoding ICP22 has counterparts only in the alphaherpesviruses, and the VZV UL13 homologue, ORF47, has been shown not to phosphorylate the VZV ICP22 homologue, ORF63 (Heineman *et al.*, 1995). Indeed, the only protein identified as a potential target for VZV ORF47 is the ORF32 protein, which lacks counterparts in other herpesviruses (Reddy *et al.*, 1998). Despite the large number of studies concerning the UL13 PK and its targets no one has produced compelling evidence that argues for one target over the rest. The function of the UL13 PK seems no closer to being elucidated, and it will take much more research to determine the true targets from the artifactual evidence.

### 5.3 Future work

Many of the experiments required to produce a more complete picture have been outlined in the results sections. More accurate mapping of the UL49 protein would be possible following the protocols outlined in this thesis followed by protein sequencing studies. The UL13 protein, however, would require a different approach. Because the UL13 protein is produced in minor amounts it is not feasible to map phosphorylated residues by isolation of the protein from purified virus or infected cell CNE followed by mass spectrometric analysis or protein sequencing. While further mapping experiments would identify the phosphopeptide with greater accuracy, mutational analysis would be required to identify the individual phosphorylated residues. Any interpretation would have to accommodate multiple residues targeted by more than one PK.

By its nature, research on PKs tends to be slow and fraught with potential pitfalls. It is perhaps not surprising that herpesviral PKs are no exception. Little work has been performed on the herpesviral PKs beyond characterisation of their enzymatic activities. Purification of the active HSV-1 UL13 PK would represent an important step and would allow structural information to be obtained for a divergent member of the PK superfamily. In addition, purification of the HSV-1 UL13 PK would allow new approaches to be adopted in the search for significant target proteins.

- 
- Ackerman, M., Braun, D.K., Pereira, L. and Roizman, B.** (1984). Characterisation of herpes simplex virus 1  $\alpha$  proteins 0, 4 and 27 with monoclonal antibodies. *J. Virol.* **52**, 108-118.
- Adams, J.A., McGlone, M.L., Gibson, R. and Taylor, S.S.** (1995). Phosphorylation modulates catalytic function and regulation in the cAMP-dependent protein kinase. *Biochemistry* **34**, 2447-2454.
- Aimes, R.T., Hemmer, W. and Taylor, S.S.** (2000). Serine-53 at the tip of the glycine-rich loop of cAMP-dependent protein kinase: Role in catalysis, P-site specificity, and interaction with inhibitors. *Biochemistry* **39**, 8325-8332.
- Albrecht, J.C., Nicholas, J., Biller, D., Cameron, K.R., Biesinger, B., Newman, C., Wittmann, S., Craxton, M.A., Coleman, H., Fleckenstein, B. and Honess, R.W.** (1992). Primary structure of the herpesvirus saimiri genome. *J. Virol.* **66**, 5047-5058.
- Ali, M.A.** (1995). The 140-kDa RR1 protein from both HSV-1 and HSV-2 contains an intrinsic protein kinase activity capable of autophosphorylation but it is transphosphorylation defective. *Virology* **207**, 409-416.
- Ali, M.A., Prakash, S.S. and Jariwalla, R.** (1992). Localisation of the antigenic sites and intrinsic protein kinase domain within a 300 amino acid segment of the ribonucleotide reductase large subunit from herpes simplex virus type 2. *Virology* **187**, 360-367.
- Baer, R., Bankier, A.T., Biggin, M.D., Deininger, P.L., Farrell, P.J., Gibson, T.J., Hatfull, G.S., Satchwell, S.C., Séguin, C., Tufnell, P.S. and Barrell, B.G.** (1984). DNA sequence and expression of the B95-8 Epstein-Barr virus genome. *Nature* **310**, 207-211.
- Barbosa, M.S., Edmonds, C., Fisher, C., Schiller, J.T., Lowy, D.R. and Vousden, K.H.** (1990). The region of the HPV E7 oncoprotein homologous to Adenovirus E1A
-

---

and SV40 large T-antigen contains separate domains for RB binding and casein kinase-II phosphorylation. *EMBO J.* **9**, 153-160

**Batterson, W. and Roizman, B.** (1983). Characterisation of the herpes simplex virion associated factor responsible for the induction of alpha genes. *J. Virol.* **46**, 371-377.

**Bean, M.A., Bloom, B.R., Heberman, R.B., Old, L.J., Oettgen, A.F., Klein, G. and Terry, W.D.** (1975). Cell-mediated cytotoxicity for bladder carcinoma: Evaluation of a workshop. *Cancer Res.* **33**, 2902-2913.

**Blaho, J.A., Mitchell, C. and Roizman, B.** (1993). Guanylylation and adenylylation of the  $\alpha$  regulatory proteins of herpes simplex virus require a viral  $\beta$  or  $\gamma$  function. *J. Virol.* **67**, 3891-3900.

**Blaho, J.A., Mitchell, C. and Roizman, B.** (1994). An amino-acid-sequence shared by the herpes-simplex virus 1  $\alpha$  regulatory proteins 0, 4, 22 and 27 predicts the nucleotidylylation of the UL21, UL31, UL47 and UL49 gene-products. *J. Biol. Chem.* **269**, 17401-17410.

**Blue, W.T. and Stobbs, D.G.** (1981). Isolation of a protein kinase by herpes simplex virus type 1. *J. Virol.* **38**, 383-388.

**Boehmer, P. and Lehman, I.** (1997). Herpes simplex virus DNA replication. *Ann. Rev. Biochem.* **66**, 347-384.

**Booy, F.P., Newcomb, W.W., Trus, B.L., Brown, J.C., Baker, T.S. and Steven, A.C.** (1991). Liquid-crystalline, phage-like packing of encapsidated DNA in herpes simplex virus. *Cell* **64**, 1007-1015.

**Booy, F.P., Trus, B.L., Davison, A.J. and Steven, A.C.** (1996). The capsid architecture of channel catfish virus, an evolutionary distant herpesvirus, is largely conserved in the absence of discernible sequence homology with herpes simplex virus. *Virology* **215**, 134-141.

---

**Bossmeyer, D.** (1993). Loss of kinase activity. *Nature* **363**, 590.

**Bossmeyer, D., Engh, R.A., Kinzel, V., Ponstingl, H. and Huber, R.** (1993). Phosphotransferase and substrate binding mechanism of the cAMP-dependent protein kinase catalytic subunit from the porcine heart as deduced from the 2.0 Å structure of the complex with Mn<sup>2+</sup> adenylyl imidodiphosphate and the inhibitor peptide PKI(5-24). *EMBO. J.* **12**, 849-859.

**Britt, W.** (1996). Human cytomegalovirus overview: the virus and its pathogenicity. *Baillieres Clinical Infectious Diseases* **3**, 307-325.

**Bronstein, J.M., Farber, D.B. and Wasterlain, C.G.** (1986). Autophosphorylation of calmodulin kinase II: functional aspects. *FEBS Letters* **196**, 135-138

**Brown, S.M., Ritchie, D.A. and Subak-Sharpe, J.H.** (1973). Genetic studies with herpes simplex virus type 1. The isolation of temperature-sensitive mutants, their arrangement into complementation groups and recombination analysis leading to a linkage map. *J. Gen. Virol.* **18**, 329-346.

**Brunovskis, P. and Velicer, L.F.** (1995). The Marek's-disease virus (MDV) unique short region: alphaherpesvirus-homologous, fowlpox virus-homologous, and MDV-specific genes. *Virology* **206**, 324-338.

**Buechler, J.A. and Taylor, S.S.** (1989). Dicyclohexycarbodiimide cross-links two conserved residues, Asp-184 and Lys-72, at the active site of the catalytic subunit of cAMP-dependent protein kinase. *Biochemistry* **28**, 2065-2070

**Cai, W., Gu, B. and Person, S.** (1988). Role of glycoprotein B of herpes simplex virus type 1 in viral entry and cell fusion. *J. Virol.* **62**, 2596-2604.

---

**Campbell, M., Palfreyman, J. and Preston, C.** (1984). Identification of herpes simplex virus DNA which encode a trans-acting polypeptide responsible for stimulation of immediate early transcription. *J. Mol. Biol.* **180**, 1-19.

**Canagarajah, B.J., Khokhlatchev, A., Cobb, M.H. and Goldsmith, E.J.** (1997). Activation mechanism of the MAP kinase ERK2 by dual phosphorylation. *Cell* **90**, 859-869.

**Cannon, J.S., Hamzeh, F., Moore, S., Nicholas, J. and Ambinder, R.F.** (1999). Human herpesvirus 8-encoded thymidine kinase and phosphotransferase homologues confer sensitivity to ganciclovir. *J. Virol.* **73**, 4786-4793.

**Carroll, D., Santoro, N. and Marshak, D.R.** (1988). Regulating cell-growth – casein kinase-II-dependent phosphorylation of nuclear oncoproteins. *Cold Spring Harb. Symp. Quant. Biol.* **53**, 91-95.

**Carter, K.L. and Roizman, B.** (1996). The promoter and transcriptional unit of a novel herpes simplex virus 1  $\alpha$  gene are contained in, and encode a protein in frame with, the open reading frame of the  $\alpha 22$  Gene. *J. Virol.* **70**, 172-178.

**Challberg, M.** (1991). Herpes simplex virus DNA replication. *Seminars in Virology* **2**, 247-256.

**Chee, M.S., Lawrence, G.L. and Barrell, B.G.** (1989). Alpha-, Beta- and Gammaherpesviruses encode a putative phosphotransferase. *J. Gen. Virol.* **70**, 1151-1160.

**Chen, M-R., Chang, S-J., Huang, H. and Chen, J-Y.** (2000). A protein kinase activity associated with Epstein-Barr virus BGLF4 phosphorylates the viral early antigen EA-D *in vitro*. *J. Virol.* **74**, 3093-3104.

---

- 
- Chen, W.S., Lazar, C.S., Poenie, M., Tsien, R.Y., Gill, G.N. and Roenfeld, M.G.** (1987). Requirement for intrinsic protein tyrosine kinase in the immediate and late actions of the EGF receptor. *Nature* **328**, 820-823.
- Chung, T.D., Wymer, J.P., Smith, C.C., Kulka, M. and Aurelian, L.** (1989). Protein kinase activity associated with the large subunit of herpes simplex virus type 2 ribonucleotide reductase (ICP10). *J. Virol.* **63**, 3389-3398.
- Clements, J.B., Watson, R.J. and Wilkie, N.M.** (1977). Temporal regulation of herpes simplex virus type 1 transcription: location of transcripts on the viral genome. *Cell* **12**, 275-285.
- Cleveland, D.W., Fischer, S.G., Kirschner, M.W. and Laemmli, U.K.** (1977). Peptide mapping by limited proteolysis in sodium dodecyl sulfate and analysis by gel electrophoresis. *J. Biol. Chem.* **252**, 1102-1106.
- Comps, M. and Cochenec, N.** (1993). A herpes-like virus from the European oyster *Ostrae edulis* L. *J. Invertebrate Pathology* **62**, 201-203.
- Conner, J.** (1999). The unique N terminus of herpes simplex virus type 1 ribonucleotide reductase large subunit is phosphorylated by casein kinase 2, which may have a homologue in *Escherichia coli*. *J. Gen. Virol.* **80**, 1471-1476.
- Conner, J., Marsden, H. and Clements, J.B.** (1994). Ribonucleotide reductase of herpesviruses. *Rev. Med. Virol.* **4**, 25-34.
- Cook, M. and Stevens, J.** (1973). Pathogenesis of herpes simplex neuritis and ganglionitis in mice. Evidence of axonal transport of infection. *Infection and Immunity* **7**, 272-276.
- Cooper, J., Conner, J. and Clements, J.B.** (1995). Characterisation of the novel protein kinase activity present in the R1 subunit of herpes simplex virus ribonucleotide reductase. *J. Virol.* **69**, 4979-4985.
-

**Costanzo, L., Campadelli-Fiume, G., Foa-Tomasi, L. and Cassai, E.** (1977). Evidence that herpes simplex virus DNA is transcribed by cellular RNA polymerase B. *J. Virol.* **21**, 996-1001.

**Coulter, L.J.** (1993). Studies on the US3 and UL13 protein kinase genes of herpes simplex virus type 1. Ph.D thesis, University of Glasgow.

**Coulter, L.J., Moss, H.W.M., Lang, J. and McGeoch, D.J.** (1993). A mutant of herpes simplex virus type 1 in which the UL13 protein kinase gene is disrupted. *J. Gen. Virol.* **74**, 387-395

**Cunningham, C. and Davison, A.J.** (1993). A cosmid-based system for constructing mutants of herpes simplex virus type 1. *Virology* **197**, 116-124.

**Cunningham, C., Davison, A.J., Dolan, A., Frame, M.C., McGeoch, D.J., Meredith, D.M., Moss, H.W.M. and Orr, A.** (1992). The UL13 virion protein of herpes simplex virus type 1 is phosphorylated by a novel virus-induced protein kinase. *J. Gen. Virol.* **73**, 303-311.

**Daikoku, T., Kurachi, R., Tsurumi, T. and Nishiyama, Y.** (1994). Identification of a target protein of US3 protein kinase of herpes simplex virus type 2. *J. Gen. Virol.* **75**, 2065-2068.

**Daikoku, T., Shibata, S., Goshima, F., Oshima, S., Tsurumi, T., Yamada, H., Yamashita, Y. and Nishiyama, Y.** (1997). Purification and characterisation of the protein kinase encoded by the UL13 gene of herpes simplex virus type 2. *Virology* **235**, 82-93.

**Daikoku, T., Yamashita, Y., Tsurumi, T., Maeno, K. and Nishiyama, Y.** (1993). Purification and biochemical characterisation of the protein kinase encoded by US3 gene of herpes simplex virus type 2. *Virology* **197**, 685-694.

---

**Daikoku, T., Yamashita, Y., Tsurumi, T. and Nishiyama, Y.** (1995). The US3 protein kinase of herpes simplex virus type 2 is associated with phosphorylation of the UL12 alkaline nuclease *in vitro*. *Arch. Virol.* **140**, 1637-1644.

**Dargan, D.J.** (1986). The structure and assembly of herpesviruses. In: Electron microscopy of proteins, vol. 5. Virus structure, pp. 359-437. Edited by J.R. Harris and R.W. Horne. Academic Press Inc., London.

**Davison, A.J.** (1983). DNA sequence of the U<sub>s</sub> component of the varicella-zoster virus genome. *EMBO J.* **2**, 2203-2209.

**Davison, A.J. and Davison, M.D.** (1995). Identification of structural proteins of channel catfish virus by mass spectrometry. *Virology* **206**, 1035-1043.

**Davison, A.J. and Scott, J.E.** (1986). The complete DNA sequence of varicella-zoster virus. *J. Gen. Virol.* **67**, 1754-1816.

**Davison, A.J. and Wilkie, N.** (1983). Location and orientation of homologous sequences in the genomes of five herpesviruses. *J. Gen. Virol.* **64**, 1927-1942.

**De Wind, N., Domen, J. and Berns, A.** (1992). Herpesviruses encode an unusual protein-serine/threonine kinase which is nonessential for growth in cultured cells. *J. Virol.* **66**, 5200-5209.

**Deatly, A., Spivack, J., Lavi, E. and Fraser, N.** (1987). Reactivation from an immediate early region of the type 1 herpes simplex virus genome is present in the trigeminal ganglia of latently infected mice. *Proc. Natl. Acad. Sci. USA* **84**, 3204-3208.

**Desai, P., Schaffer, P. and Minson, A.** (1988). Excretion of non-infectious virus particles lacking glycoprotein H by a temperature sensitive mutant of herpes simplex type 1: evidence that gH is essential for virion infectivity. *J. Gen. Virol.* **69**, 1147-1156.

---

**Eckhart, W., Hutchinson, M.A. and Hunter, T.** (1979). An activity phosphorylating tyrosine in polyoma T antigen immunoprecipitates. *Cell* **18**, 925-933.

**Edson, C.M.** (1993). Phosphorylation of neurotropic alphaherpesvirus envelope glycoproteins: herpes simplex virus type 2 gE2 and pseudorabies virus gI. *Virology* **195**, 268-270.

**Edson, C.M., Hosler, B.A. and Waters, D. J.** (1987). Varicella-zoster virus gpI and herpes simplex virus gE: phosphorylation and Fc binding. *Virology* **161**, 599-602.

**Elgadi, M.M. and Smiley, J.R.** (1999). Picornavirus internal ribosome entry site elements target RNA cleavage events induced by the herpes simplex virus virion host shutoff protein. *J. Virol.* **73**, 9222-9231.

**Elliott, G, and Meredith, D.M.** (1992). The herpes simplex virus type 1 tegument protein VP22 is encoded by gene UL49. *J. Gen. Virol.* **73**, 723-726.

**Elliott, G., O'Reilly, D. and O'Hare, P.** (1996). Phosphorylation of the herpes simplex virus type 1 tegument protein VP22. *Virology* **226**, 140-145.

**Elliott, G., O'Reilly, D. and O'Hare, P.** (1999). Identification of phosphorylation sites within the herpes simplex virus tegument protein VP22. *J. Virol.* **73**, 6203-6206.

**Everett, R.** (1984). Transactivation of transcription by herpesvirus products. Requirement for two HSV-1 immediate early polypeptides for maximum activity. *EMBO* **3**, 3135-3141.

**Fenwick, M.L. and Everett, R.D.** (1990). Inactivation of the shutoff gene (UL41) of herpes simplex virus types 1 and 2. *J. Gen. Virol.* **71**, 2961-2967.

**Fischer, E.H., Charbonneau, H. and Tonks, N.K.** (1991). Protein tyrosine phosphatases: a diverse family of intracellular and transmembrane enzymes. *Science* **253**, 401-406.

---

**Flint, A.J., Paladini, R.D. and Koshland, D.E. Jr.** (1990). Autophosphorylation of protein kinase C at three separated regions of its primary sequence. *Science* **249**, 408-411.

**Frame, M.C., McGeoch, D.J., Rixon, F.J., Orr, A.C. and Marsden, H.S.** (1986). The 10k virion phosphoprotein encoded by gene US9 from herpes simplex virus type 1. *Virology* **150**, 321-332.

**Frame, M.C., Purves, F.C., McGeoch, D.J., Marsden, H.S. and Leader, D.P.** (1987). Identification of the herpes simplex virus protein kinase as the product of the viral gene US3. *J. Gen. Virol.* **68**, 2699-2704.

**Gibbs, C.S., Knighton, D.R., Sowadski, J.M., Taylor, S.S. and Zoller, M.J.** (1992). Systematic mutational analysis of cAMP-dependent protein kinase identifies unregulated catalytic subunits and defines regions important for the recognition of the regulatory subunit. *J. Biol. Chem.* **267**, 4806-4814.

**Grant, B.D., Hemmer, W., Tsigelny, I., Adams, J.A. and Taylor, S.S.** (1998). Kinetic analysis of mutations in the glycine-rich loop of cAMP-dependent protein kinase. *Biochemistry* **37**, 7708-7715

**Grasser, F.A., Scheidtmann, K.H., Tuazon, P.T., Traugh, J.A. and Walter, G.** (1988). *In vitro* phosphorylation of SV40 large T-antigen. *Virology* **165**, 13-22.

**Grose, C.** (1990). Glycoprotein encoded by varicella-zoster virus: biosynthesis, phosphorylation and intracellular trafficking. *Ann. Rev. Microbiol.* **44**, 59-80.

**Grose, C., Jackson, W. and Traugh, J.A.** (1989). Phosphorylation of varicella-zoster virus glycoprotein gpI by mammalian casein kinase II and casein kinase I. *J. Virol.* **63**, 3912-3918.

---

**Haarr, L. and Skulstad, S.** (1994). The herpes simplex virus type 1 particle: structure and molecular functions. *APMIS* **102**, 321-346.

**Hallenbeck, P.C. and Walsh, D.A.** (1983). Autophosphorylation of phosphorylase kinase. *J. Biol. Chem.* **258**, 13493-13501.

**Hanks, S.K. and Quinn, A.M.** (1991). Protein kinase catalytic domain sequence database: identification of conserved features of primary structure and classification of family members. In: *Methods in Enzymology vol. 200, Protein Phosphorylation, Part A* pp. 38-62. Edited by T. Hunter and B.M. Sefton. Academic Press Inc.

**Hanks, S.K., Quinn, A.M. and Hunter, T.** (1988). The protein kinase family: conserved features and deduced phylogeny of the catalytic domains. *Science* **241**, 42-52.

**Hardie, G. and Hanks, S.** (1995). The PK Fact Book. Protein-serine threonine kinases. Academic Press Inc., London

**Harris-Hamilton, E. and Bachenheimer, S.** (1985). Accumulation of herpes simplex virus type 1 RNAs of different kinetic classes in the cytoplasm of infected cells. *J. Virol.* **53**, 144-151.

**Hathaway, G.M and Traugh, J.A.** (1982). Casein kinases – multipotential protein-kinases. *Curr. Top. Cell. Reg.* **21**, 101-127

**Hayward, G.** (1993). Immediate early gene regulation in herpes simplex virus. *Seminars in Virology* **4**, 15-23.

**Hayward, G.S., Kacob, R.L., Wadsworth, S.C. and Roizman, B.** (1975). Anatomy of herpes simplex virus DNA: Evidence for four populations that differ in the relative orientations of their long and short components. *Proc. Natl. Acad. Sci. USA* **72**, 4243-4247.

---

---

**He, Z., He, Y-S., Kim, Y., Chu, L., Ohmstede, C., Biron, K.K. and Coen, D.M.** (1997). The human cytomegalovirus UL97 protein is a protein kinase that autophosphorylates on serines and threonines. *J. Virol.* **71**, 405-411.

**Herberg, F.W., Doyle, M.L., Cox, S. and Taylor, S.S.** (1999). Dissection of the nucleotide and metal-phosphate binding sites in cAMP-dependent protein kinase. *Biochemistry* **38**, 6352-6360.

**Hill, J., Sedarati, F., Javier, R., Wagner, E. and Stevens, J.** (1990). Herpes simplex virus latent phase transcription facilities *in vivo* reactivation. *Virology* **174**, 17-25.

**Ho, D. and Mocarski, E.** (1989). Herpes simplex virus latent RNA (LAT) is not required for latent infection in the mouse. *Proc. Natl. Acad. Sci. USA* **86**, 7596-7600.

**Honess, R. and Roizman, B.** (1974). Regulation of herpesvirus macromolecular synthesis. Cascade regulation of the synthesis of three groups of viral proteins. *J. Virol.* **14**, 8-19.

**Hubbard, S.R. Wei, L., Ellis, L. and Hendrickson, W.A.** (1994). Crystal structure of the tyrosine kinase domain of the human insulin receptor. *Nature* **372**, 746-754.

**Huggins, J.P. and Pelton, J.T.** (1991). Predictions of the cyclic GMP-dependent protein kinase structure from its primary sequence. *Biochem. Soc. Trans* **19**, 1625.

**Hutchinson, L., Browne, H., Wargent, V., Davis-Poynter, N., Primorac, S., Goldsmith, K., Minson, A. and Johnson, D.** (1992). A novel herpes simplex virus protein, gL, forms a complex with glycoprotein H (gH) and affects normal folding and surface expression of gH. *J. Virol.* **66**, 2240-2250.

**Hutter, M.C. and Helms, V.** (1999). Influence of key residues on the reaction mechanism of the cAMP-dependent protein kinase. *Protein Science* **8**, 2728-2733.

---

**Ingemarson, R. and Lankinen, H.** (1987). The herpes simplex virus type 1 ribonucleotide reductase is a tight complex of the type  $\alpha 2\beta 2$  composed of 40K and 140K proteins, of which the latter shows multiple forms due to proteolysis. *Virology* **156**, 417-422.

**Jacob, R.J. and Roizman, B.** (1977). Anatomy of herpes simplex virus DNA. VIII. Properties of the replicating DNA. *J. Virol.* **23**, 294-411.

**Jakobi, R. and Traugh, J. A.** (1992). Characterisation of the phosphotransferase domain of casein kinase II by site-directed mutagenesis and expression in *Escherichia coli*. *J. Biol. Chem.* **267**, 23894-23902.

**Jakobi, R. and Traugh, J.A.** (1995). Site-directed mutagenesis and structure/function studies of casein kinase II correlate stimulation of activity by the  $\beta$  subunit with changes in conformation and ATP/GTP utilisation. *Eur. J. Biochem.* **230**, 1111-1117.

**Javier, R., Stevens, J., Dissette, V. and Wagner, E.** (1988). A herpes simplex virus transcript abundant in latently infected neurons is dispensable for establishment of the latent state. *Virology* **166**, 254-257.

**Jerome, K.R., Fox, R., Chen, Z., Sears, A.E., Lee, H-Y. and Corey, L.** (1999). Herpes simplex virus inhibits apoptosis through the action of two genes, US5 and US3. *J. Virol.* **73**, 8950-8957.

**Johnson, L.N., Noble, M.E.M. and Owen D.J.** (1996). Active and inactive protein kinases: structural basis for regulation. *Cell* **85**, 149-158.

**Jugovic, P., Hill, A.M., Tomazin, R., Ploegh, H. and Johnson, D.C.** (1998). Inhibition of major histocompatibility complex class I antigen presentation in pig and primate cells by herpes simplex virus type 1 and 2 ICP47. *J. Virol.* **72**, 5076-5084.

**Kamps, M.P. and Sefton, B.M.** (1986). Neither arginine nor histidine can carry out the functions of lysine-295 in the ATP-binding site of P60SRC. *Mol. Cell. Biol.* **6**, 751-757.

---

**Katan, M., Stevely, W.S. and Leader, D.P.** (1985). Partial purification and characterisation of a new protein kinase from cells infected with pseudorabies virus. *Eur. J. Biochem.* **152**, 57-65.

**Kawaguchi, Y., Bruni, R. and Roizman, B.** (1997). Interaction of herpes simplex virus 1  $\alpha$  regulatory protein ICP0 with elongation factor 1 $\delta$ : ICP0 affects translational machinery. *J. Virol.* **71**, 1019-1024.

**Kawaguchi, Y., Matsumura, T., Roizman, B. and Hirai, K.** (1999). Cellular elongation factor 1 $\delta$  is modified in cells infected with representative alpha-, beta-, or gammaherpesviruses. *J. Virol.* **73**, 4456-4460.

**Kawaguchi, Y., Van Sant, C. and Roizman, B.** (1998). Eukaryotic elongation factor 1 $\delta$  is hyperphosphorylated by the protein kinase encoded by the UL13 gene of herpes simplex virus 1. *J. Virol.* **72**, 1731-1736.

**Kemp, B.E., Graves, D.J., Benjamini, E. and Krebs, E.G.** (1977). Role of multiple basic residues in determining the substrate specificity of cyclic AMP-dependent protein kinase. *J. Biol. Chem.* **252**, 4888-4894.

**Kennedy, I.M., Stevely, W.S. and Leader, D.P.** (1981). Phosphorylation of ribosomal proteins in hamster fibroblasts infected with pseudorabies virus or herpes simplex virus. *J. Virol.* **39**, 359-366.

**Knighton, D.R., Cadena, D.L., Zheng, J., Ten Eyck, L.F., Taylor, S.S., Sowadski, J.M. and Gill, G.N.** (1993). Structural features that specify tyrosine kinase activity deduced from homology modelling of the epidermal growth factor receptor. *Proc. Natl. Acad. Sci. USA* **90**, 5001-5005.

**Knighton, D.R., Zheng, J., Ten Eyck, L.F., Ashford, V.A., Xuong, N-H., Taylor, S.S. and Sowadski, J.M.** (1991a). Crystal structure of the catalytic subunit of cyclic adenosine monophosphate-dependent protein kinase. *Science* **253**, 407-413.

---

**Knighton, D.R., Zheng, J., Ten Eyck, L.F., Xuong, N-H., Taylor, S.S. and Sowadski, J.M.** (1991b). Structure of a peptide inhibitor bound to the catalytic subunit of cyclic adenosine monophosphate-dependent protein kinase. *Science* **253**, 414-420.

**Kongsuwan, K., Prideaux, C.T. and Johnson, M.A.** (1995). Nucleotide-sequence analysis of an infectious laryngotracheitis virus gene corresponding to the US3 of HSV-1 and a unique gene encoding a 67-kDa protein. *Arch. Virol.* **140**, 27-39.

**Krebs, E.G. and Fischer, E.H.** (1956). The phosphorylase *b* to *a* converting enzyme of rabbit skeletal muscle. *Biochim. Biophys. Acta.* **20**, 150-157.

**Krebs, E.G., Graves, D.J. and Fischer, E.H.** (1959). Factors affecting the activity of muscle phosphorylase *b* kinase. *J. Biol. Chem.* **234**, 2867-2873.

**Kristensson, K., Lycke, E., Roytta, M., Svennerholm, B. and Vahlne, A.** (1986). Neuritic transport of herpes simplex in rat sensory neurons *in vitro*. Effects of substances interacting with microtubular function and axonal flow (nocodazole, taxol and erythro-9-3-(2-hydroxyonyl)-adenine). *J. Gen. Virol.* **67**, 2023-2028.

**Kwong, A., Kruper, J. and Frenkel, N.** (1988). Herpes simplex virus virion host shut off function. *J. Virol.* **62**, 912-921.

**Langelier, Y., Champoux, L., Hamel, M., Guilbault, C., Lamarche, C., Gaudreau, P. and Mawwie, B.** (1998). The R1 subunit of herpes simplex virus ribonucleotide reductase is a good substrate for host cell protein kinases but is not itself a protein kinase. *J. Biol. Chem.* **273**, 1435-1443.

**Lawrence, G.L., Chee, M., Craxton, M.A., Gompels, U.A., Honess, R.W. and Barrell, B.G.** (1990). Human herpesvirus 6 is closely related to human cytomegalovirus. *J. Virol.* **64**, 287-299.

---

**Leader, D.P., Donella-Deana, F., Marchiori, F., Purves, F.C. and Pinna, L.A.** (1991). Further definition of the substrate specificity of the alphaherpesvirus protein kinase and comparison with protein kinases A and C. *Biochem. Biophys. Acta* **1091**, 426-431.

**Leader, D.P. and Katan, M.** (1988). Viral aspects of protein phosphorylation. *J. Gen. Virol.* **69**, 1441-1464.

**Lemaster, S. and Roizman, B.** (1980). Herpes simplex virus phosphoproteins II. Characterisation of the virion protein kinase and of the polypeptides phosphorylated in the virion. *J. Virol.* **35**, 798-811.

**Leopardi, R. and Roizman, B.** (1996). Functional interaction and co-localisation of the herpes simplex virus 1 major regulatory protein ICP4 with EAP, a nucleolar-ribosomal protein. *Proc. Natl. Acad. Sci. USA* **93**, 4572-4576.

**Leopardi, R., Van Sant, C. and Roizman, B.** (1997a). The herpes simplex virus 1 protein kinase US3 is required for protection from apoptosis induced by the virus. *Proc. Natl. Acad. Sci. USA* **94**, 7891-7896.

**Leopardi, R., Ward, P.L., Ogle, W.O. and Roizman, B.** (1997b). Association of herpes simplex virus regulatory protein ICP22 with transcriptional complexes containing EAP, ICP4, RNA polymerase II, and viral DNA requires posttranslational modification by the UL13 protein kinase. *J. Virol.* **71**, 1133-1139.

**Leslie, J.** (1996). An investigation into factors that influence the incorporation of proteins into the HSV-1 tegument. PhD thesis, University of Glasgow.

**Leslie, J., Rixon, J. and McLauchlan, J.** (1996). Overexpression of the herpes simplex virus type 1 tegument protein VP22 increases its incorporation into virus particles. *Virology* **220**, 60-68.

**Levine, A.** (1992). *Viruses*. Scientific American Library. NY.

---

**Levy, J.** (1997). Three new human herpesviruses (HHV-6, 7 and 8). *Lancet* **349**, 558-563.

**Li, J-S., Zhou, B-S., Dutschman, G.E., Grill, S.P., Tan, R-S. and Cheng, Y-C.** (1987). Association of Epstein-Barr virus early antigen diffuse component and virus-specified DNA polymerase activity. *J. Virol.* **61**, 2947-2949.

**Liao, P-C., Leykam, J., Andrews, P.C., Gage, D.A. and Allison, J.** (1994). An approach to locate phosphorylation sites in a phosphoprotein: mass mapping by combining specific enzymatic degradation with matrix-assisted laser desorption/ionisation mass spectrometry. *Anal. Biochem.* **219**, 9-20.

**Ligas, M. and Johnson, D.** (1988). A herpes simplex virus mutant in which glycoprotein D sequences are replaced by  $\beta$ -galactosidase sequences binds to but is unable to penetrate into cells. *J. Virol.* **62**, 1486-1494.

**Lin, P., Fung, W.J. and Gilfillan, A.M.** (1992). Phosphatidylcholine-specific phospholipase D-derived 1,2-diacylglycerol does not initiate protein kinase C activation in the RBL 2H3 mast-cell line. *J. Biochem.* **287**, 325-331.

**Littler, E., Stuart, A.D. and Chee, M.S.** (1992). Human cytomegalovirus UL97 open reading frame encodes a protein that phosphorylates the antiviral nucleoside analogue ganciclovir. *Nature* **358**, 160-162.

**Litwin, V., Jackson, W. and Grose, C.** (1992). Receptor properties of two varicella-zoster virus glycoproteins, gpI and gpIV, homologous to herpes simplex virus gE and gI. *J. Virol.* **66**, 3643-3651.

**Long, M.C., Leong, V., Schaffer, P.A., Spencer, C.A. and Rice, S.A.** (1999). ICP22 and the UL13 protein kinase are both required for herpes simplex virus-induced modification of the large subunit of RNA polymerase II. *J. Virol.* **73**, 5593-5604.

---

**McGeoch, D.J.** (1989). The genomes of the human herpesviruses: contents, relationships and evolution. *Ann. Rev. Microbiol.* **43**, 235-265.

**McGeoch, D.J. and Cook, S.** (1994). Molecular phylogeny of the alphaherpesvirinae subfamily and a proposed evolutionary timescale. *J. Mol. Biol.* **238**, 9-22.

**McGeoch, D.J., Dalrymple, M.A., Davison, A.J., Dolan, A., Frame, M.C., McNab, D., Perry, L.J., Scott, J.E. and Taylor, P.** (1988). The complete DNA sequence of the long unique region in the genome of herpes simplex virus type 1. *J. Gen. Virol.* **69**, 1531-1574.

**McGeoch, D.J. and Davison, A.J.** (1986). Alphaherpesviruses possess a gene homologous to the protein kinase gene family of eukaryotes and retroviruses. *Nucleic Acid Research* **14**, 1765-1777.

**McGeoch, D.J., Dolan, A., Donald, S. and Rixon, F.J.** (1985). Sequence determination and genetic content of the short unique region in the genome of herpes simplex virus type 1. *J. Mol. Biol.* **181**, 1-13.

**McGeoch, D.J., Dolan, A. and Frame, M.C.** (1986). DNA sequence of the region in the genome of herpes simplex virus type 1 containing the exonuclease gene and neighbouring genes. *Nucleic Acid Research* **14**, 3435-3448.

**McGeoch, D.J., Moss, H.W., McNab, D. and Frame, M.C.** (1987). DNA sequence and genetic content of the HindIII 1 region in the short unique component of the herpes simplex virus type 2 genome: identification of the gene encoding glycoprotein G, and evolutionary comparisons. *J. Gen. Virol.* **68**, 19-38.

**MacPherson, I. And Stoker, M.** (1962). Polyoma transformation of hamster cell clones – an investigation of genetic factors affecting all competence. *Virology* **16**, 147-151.

**Marsden, H.S., Campbell, M.E.M., Haarr, L., Frame, M.C., Parris, D.S., Murphy, M., Hope, R.G., Muller, M.T. and Preston, C.M.** (1987). The 65,000-M<sub>r</sub> DNA-binding

---

---

and virion *trans*-inducing proteins of herpes simplex virus type 1. *J. Virol.* **61**, 2428-2437.

**Marsden, H.S., Stow, N.D., Preston, V.G., Timbury, M.C. and Wilkie, N.M.** (1978). Physical mapping of herpes simplex virus-induced polypeptides. *J. Virol.* **28**, 624-642.

**Mellerick, D.M. and Fraser, N.W.** (1987). Physical state of the latent herpes simplex virus genome in mouse model system. Evidence suggesting an episomal state. *Virology* **158**, 265-275.

**Miller, G.** (1990). Epstein Barr virus: biology, pathogenesis and medical aspects. In: *Virology, 2<sup>nd</sup> edition*, pp1843-1887. Edited by B. Fields, D.M. Knipe, R.M. Chanode, M.S. Hirsch, J.L. Melnick, T.P. Monath and B. Roizman, Raven press, NY.

**Millhouse, S. and Wigdahl, B.** (2000). Molecular circuitry regulating herpes simplex virus type 1 latency in neurons. *J. Neurovirol.* **6**, 6-24.

**Minella, O., Cormier, P., Morales, J., Poulhe, R., Belle, R. and Mulner-Lorillon, O.** (1994). cdc2 kinase sets a memory phosphorylation signal on elongation factor EF-1 $\delta$  during meiotic cell division, which perdures in early development. *Cell. Mol. Biol.* **40**, 521-525.

**Miriagou, V., Stevenato, L., Manservigi, R. and Mavromara, P.** (2000). The C-terminal cytoplasmic tail of herpes simplex virus type 1 gE protein is phosphorylated *in vivo* and *in vitro* by cellular enzymes in the absence of other viral proteins. *J. Gen. Virol.* **81**, 1027-1031.

**Mitchell, C., Blaho, J.A. and Roizman, B.** (1994). Casein kinase II specifically nucleotidylates *in vitro* the amino acid sequence of the protein encoded by the  $\alpha$ 22 gene of herpes simplex virus 1. *Proc. Natl. Acad. Sci. USA* **91**, 11864-11868.

**Mitchison, T.** (1988). Microtubule dynamic and kinetochome function in mitosis. *Ann. Rev. Cell Biol.* **4**, 527-549.

---

**Montalvo, E.A. and Grose, C.** (1986). Varicella zoster virus glycoprotein gpI is selectively phosphorylated by a virus-induced protein kinase. *Proc. Natl. Acad. Sci. USA* **83**, 8967-8971.

**Montgomery, R., Warner, M., Lum, B. and Spear, P.** (1996). Herpes simplex virus 1 entry into cells mediated by a novel member of the TNF/NGF receptor family. *Cell* **87**, 427-436.

**Morrison, E.E., Wang, Y-F. and Meredith, D.M.** (1998). Phosphorylation of structural components promotes dissociation of the herpes simplex virus type 1 tegument. *J. Virol.* **72**, 7108-7144.

**Mossman, K.L., Sherburne, R., Lavery, C., Duncan, J. and Smiley, J.R.** (2000). Evidence that herpes simplex virus VP16 is required for viral egress downstream of the initial envelopment event. *J. Virol.* **74**, 6287-6299.

**Motley S.T. and Lory, S.** (1999). Functional characterisation of a serine/threonine protein kinase of *Pseudomonas aeruginosa*. *Infection and Immunity* **67**, 5386-5394.

**Mulner-Lorillon, O., Minella, O., Cormier, P., Capony, J-P., Cavadore, J.-C., Morales, J., Poulhe, R. and Belle, R.** (1994). Elongation factor EF-1 $\delta$ , a new target for maturation-promoting factor in *Xenopus* oocytes. *J. Biol. Chem.* **269**, 20201-20207.

**Neubauer, G. and Mann, M.** (1999). Mapping of phosphorylation sites of gel-isolated proteins by nanoelectrospray tandem mass spectrometry: potentials and limitations. *Anal. Chem.* **71**, 235-242.

**Ng, T.I., Keenan, L., Kinchington, P.R. and Grose, C.** (1994). Phosphorylation of varicella-zoster virus open reading frame (ORF) 62 regulatory product by viral ORF 47-associated protein kinase. *J. Virol.* **68**, 1350-1359.

---

**Ng, T.I., Ogle, W.O. and Roizman, B.** (1998). UL13 protein kinase of herpes simplex virus 1 complexes with glycoprotein E and mediates the phosphorylation of the viral Fc receptor: glycoproteins E and I. *Virology* **241**, 37-48.

**Ng, T.I., Talarico, C., Burnette, T.C., Biron, K. and Roizman, B.** (1996). Partial substitution of the functions of the herpes simplex virus 1 UL13 gene by the human cytomegalovirus UL97 gene. *Virology* **225**, 347-358.

**Nghiêm, H-O., Bettendorff, L. and Changeux, J-P.** (2000). Specific phosphorylation of Torpedo 43K rapsyn by endogenous kinase(s) with thiamine triphosphate as the phosphate donor. *FASEB J.* **14**, 543-554.

**Nikas, I., McLauchlan, J., Davison, A.J., Taylor, W.R. and Clements, J.B.** (1986). Structural features of ribonucleotide reductase. *Prot. Struct. Funct. Genet.* **1**, 376-384.

**Nishiyama, Y., Yamada, Y., Kurachi, R. and Daikoku, T.** (1992). Construction of a US3 *lacZ* insertion mutant of herpes simplex virus type 2 and characterisation of its phenotype *in vitro* and *in vivo*. *Virology* **190**, 256-268.

**Ogle, W.O., Ng, T.I., Carter, K.L. and Roizman B.** (1997). The UL13 protein kinase and the infected cell type are determinants of posttranslational modification of ICP0. *Virology* **235**, 406-413.

**Olson, J.K., Bishop, G.A. and Grose, C.** (1997). Varicella-zoster Fc receptor gE glycoprotein: serine/threonine and tyrosine phosphorylation of monomeric and dimeric forms. *J. Virol.* **71**, 110-119.

**Overton, H., McMillan, D., Hope, L. and Wong-Kai-In, P.** (1994). Production of host shutoff-defective mutants of herpes simplex virus type 1 by inactivation of the UL13 gene. *Virology* **202**, 97-106.

---

**Overton, H.A., McMillan, D.J., Klavinskis, L.S., Hope, L., Ritchie, A.J. and Wong-Kai-In, P.** (1992). Herpes simplex virus type 1 gene UL13 encodes a phosphoprotein that is a component of the virion. *Virology* **190**, 184-192.

**Palen, E.R., Venema, R.C., Chang, Y.-W.E. and Traugh, J.A.** (1994). GDP as a regulator of phosphorylation of elongation factor 1 by casein kinase II. *Biochemistry* **33**, 8515-8520.

**Parekh, D.B., Ziegler, W. and Parker, P.J.** (2000). Multiple pathways control protein kinase C phosphorylation. *EMBO J.* **19**, 496-503.

**Park, J., Lee, D., Seo, T., Chung, J. and Choe, J.** (2000). Kaposi's sarcoma-associated herpesvirus (human herpesvirus-8) open reading frame 36 protein is a serine protein kinase. *J. Gen. Virol.* **81**, 1067-1071.

**Payne, J.M., Laybourn, P.J. and Dahmus, M.E.** (1989). The transition of RNA polymerase II from initiation to elongation is associated with phosphorylation of the carboxyl-terminal domain of subunit IIa. *J. Biol. Chem.* **264**, 19621-19629.

**Penfold, M., Armati, P. and Cunningham, A.** (1994). Axonal transport of herpes simplex virions to epidermal cells: evidence for a specialised mode of virus transport and assembly. *Proc. Natl. Acad. Sci. USA* **91**, 6529-6533.

**Pereira, L., Wolff, M.H., Fenwick, M. and Roizman, B.** (1977). Regulation of herpesvirus macromolecular synthesis. V. Properties of the  $\alpha$  polypeptides made in HSV-1 and HSV-2 infected cells. *Virology* **77**, 733-749.

**Preston, C.** (1979). Abnormal properties of an immediate early polypeptide in cells infected with the herpes simplex virus type 1 mutant tsK. *J. Virol.* **32**, 357-369.

**Preston, C.** (2000). Repression of viral transcription during herpes simplex virus latency. *J. Gen. Virol.* **81**, 1-19.

---

**Prod'hon, C., Machuca, I., Berthomme, H., Epstein, A. and Jacquemont, B.** (1996). Characterization of regulatory functions of the HSV-1 immediate-early protein ICP22. *Virology* **226**, 393-402.

**Purves, F.C., Katan, M., Stevely, W.S. and Leader, D.P.** (1986). Characteristics of the induction of a new protein kinase in cells infected with herpesviruses. *J. Gen. Virol.* **67**, 1049-1057.

**Purves, F.C., Longnecker, R.M., Leader, D.P. and Roizman, B.** (1987). Herpes simplex virus 1 protein kinase is encoded by open reading frame US3 which is not essential for virus growth in cell culture. *J. Virol.* **61**, 2896-2901.

**Purves, F.C., Ogle, W.O. and Roizman, B.** (1993). Processing of the herpes simplex virus regulatory protein  $\alpha$ 22 mediated by the UL13 protein kinase determines the accumulation of a subset of  $\alpha$  and  $\gamma$  mRNAs and proteins in infected cells. *Proc. Natl. Acad. Sci. USA* **90**, 6701-6705.

**Purves, F.C. and Roizman, B.** (1992). The UL13 gene of herpes simplex virus 1 encodes the functions for posttranslational processing associated with phosphorylation of the regulatory protein  $\alpha$ 22. *Proc. Natl. Acad. Sci. USA* **89**, 7310-7314.

**Purves, F.C., Spector, D. and Roizman, B.** (1991). The herpes simplex virus 1 protein kinase encoded by the US3 gene mediates posttranslational modification of the phosphoprotein encoded by the UL34 gene. *J. Virol.* **65**, 5757-5764.

**Purves, F.C., Spector, D. and Roizman, B.** (1992). UL34, the target of the herpes simplex virus US3 protein kinase, is a membrane protein which in its unphosphorylated state associates with novel phosphoproteins. *J. Virol.* **66**, 4295-4303.

**Quinlan, M., Chen, L. and Knipe, D.** (1984). The intranuclear location of a herpes simplex virus DNA-binding protein is determined by the status of viral DNA replication. *Cell* **36**, 857-868.

---

**Read, G.S., Karr, B.M. and Knight, K.** (1993). Isolation of a herpes simplex virus type 1 mutant with a deletion in the virion host shutoff gene and identification of multiple forms of the *vhs* (UL41) polypeptide. *J. Virol.* **67**, 7149-7160.

**Reichard, P.** (1993). From RNA to DNA, why so many ribonucleotide reductases? *Science* **260**, 1773-1777.

**Rice, S.A., Long, M.C., Lam, V., Schaffer, P.A. and Spencer, C.A.** (1995). Herpes simplex virus immediate-early protein ICP22 is required for viral modification of host RNA polymerase II and the establishment of the normal viral transcription cycle. *J. Virol.* **69**, 5550-5559.

**Rice, S.A., Long, M.C. Lam, V. and Spencer, C.A.** (1994). RNA polymerase II is aberrantly phosphorylated and localised to viral replication compartments following herpes simplex virus infection. *J. Virol.* **68**, 988-1001.

**Richter, J.D., Wasserman, W.J. and Smith, L.D.** (1982). The mechanism for increased protein synthesis during *Xenopus* oocyte maturation. *Dev. Biol.* **89**, 159-167.

**Rixon, F.J.** (1993). Structure and assembly of herpesviruses. *Seminars in Virology* **4**, 135-144.

**Rixon, F.J. and McGeoch, D.J.** (1984). A 3' co-terminal family of messenger-RNAs from the herpes-simplex virus type-1 short region - 2 overlapping reading frames encode unrelated polypeptides one of which has a highly reiterated amino-acid-sequence. *Nucleic Acid Research* **12**, 2473-2487.

**Roizman, B.** (1979). The structure and isomerisation of herpes simplex virus genomes. *Cell* **16**, 481-494.

**Roizman, B.** (1996). The function of herpes simplex virus genes: a primer for genetic engineering of novel vectors. *Proc. Natl. Acad. Sci. USA* **93**, 11307-11312.

---

---

**Roizman, B., Carmicheal, L., Deinhardt, F., Nahmais, A., Plowright, W., Rapp, F., Seldrick, P., Takahashi, M. and Wolf, K.** (1981). Herpesviridae: definition, provisional nomenclature and taxonomy. *Intervirology* **16**, 201-217.

**Roizman, B. and Sears, A.E.** (1990). Herpes simplex viruses and their replication. In: *Virology*, pp. 1795-1841. Edited by B. Fields and D. Knipe. Raven press, NY.

**Roizman, B. and Sears, A.E.** (1993). Herpes simplex viruses and their replication. In: *The human herpesviruses*, pp. 11-68. Edited by Roizman *et al.* Raven press, NY.

**Roizman, B. and Sears, A.E.** (1996). Herpes simplex viruses and their replication. In *Fields Virology*, pp. 2231-2295. Edited by B. Fields *et al.* Raven publishers, Philadelphia.

**Romano, P.R., Garcia-Barrio, M.T., Zhang, X., Wang, Q., Taylor, D.R., Zhang, F., Herring, C., Mathews, M.B., Qin, J. and Hinnebusch, A.G.** (1998). Autophosphorylation in the activation loop is required for full kinase activity *in vivo* of human and yeast eukaryotic initiation factor 2alpha kinases PKR and GCN2. *Mol. Cell. Biol.* **18**, 2282-2297.

**Rothman, K., Schnölzer, M., Radziwill, G., Hildt, E., Moelling, K. and Schaller, H.** (1998). Host cell-virus cross talk: phosphorylation of a hepatitis B virus envelope protein mediates intracellular signalling. *J. Virol.* **72**, 10138-10147.

**Rubenstein, A.S., Gravell, M. and Darlington, R.** (1972). Protein kinase in enveloped herpes simplex virions. *Virology* **50**, 287-290.

**Russo, J.J., Bohenzky, R.A., Chein, M-C., Chen, J., Yan, M., Maddalena, D., Parry, J.P., Peruzzi, D., Edelman, I.S., Chang, Y. and Moore, P.S.** (1996). Nucleotide sequence of the Kaposi sarcoma-associated herpesvirus (HHV-8). *Proc. Natl. Acad. Sci. USA* **93**, 14862-14867.

---

**Saris, C.J.M., Domen, J. and Berns, A.** (1991). The *pim-1* oncogene encodes two related protein-serine/threonine kinases by alternative initiation at AUG and CUG. *EMBO. J.* **10**, 655-664.

**Sawtell, N., Poon, D., Tansky, C. and Thompson, R.** (1998). The latent herpes simplex virus type 1 genome copy number in individual neurons is virus specific and correlates with reactivation. *J. Virol.* **72**, 5343-5350.

**Schagger, H. and Von Jagow, G.** (1987). Tricine-sodium dodecyl sulfate-polyacrylamide gel electrophoresis for the separation of proteins in the range from 1 to 100 kDa. *Anal. Biochem.* **166**, 368-379.

**Schrag, J.D., Prasad, B.V.V., Rixon, F.J. and Chiu, W.** (1989). Three-dimensional structure of the HSV-1 nucleocapsid. *Cell* **56**, 651-660.

**Schulz, G.E.** (1992). Induced-fit movements in adenylate kinases. *Faraday Discuss.* **93**, 85-93.

**Sears, A.E., Halliburton, I.W., Meignier, B., Silver, S. and Roizman, B.** (1985). Herpes simplex virus 1 mutant deleted in the  $\alpha 22$  gene: growth and gene expression in permissive and restrictive cells and establishment of latency in mice. *J. Virol.* **55**, 338-346.

**Sheldrick, P. and Berthelot, N.** (1974). Inverted repetitions in the chromosome of herpes simplex virus. *Cold Spring Harbour Symposia on Quantitative Biology*, 39, part 2.

**Singh, J.** (1994). Comparison of conservation within and between the Ser/Thr and Tyr protein kinase family: proposed model for the catalytic domain of the epidermal growth factor receptor. *Protein Engineering* **7**, 849-858.

---

**Smith, R.F. and Smith, T.F.** (1989). Identification of a new protein-kinase related gene in three herpesviruses, herpes simplex virus, varicella-zoster virus, and Epstein-Barr virus. *J. Virol.* **63**, 450-455.

**Sodeik, B., Ebersold, M. and Helenius, A.** (1997). Microtubule mediated transport of incoming herpes simplex virus capsids to the nucleus. *J. Cell Biol.* **136**, 1007-1021.

**Spear, P.** (1993). Entry of alphaherpesviruses into cells. *Seminars in Virology* **9**, 143-159.

**Spivack, J. and Fraser, N.** (1988). Expression of herpes simplex type 1 (HSV-1) latency associated transcripts and transcripts affected by deletion in mutant HFEM: evidence for a new class of genes. *J. Virol.* **62**, 3281-3287.

**Stannard, L.M., Fuller, A.O. and Spear, P.G.** (1987). Herpes simplex virus glycoproteins associated with different morphological entities projecting from the virion envelope. *J. Gen. Virol.* **68**, 715-725.

**Stein, J.C., Sarkar, D. and Rubin, C.S.** (1983). Tryptic peptide mapping studies on the regulatory subunits of type II protein kinases from cerebral cortex and heart. Evidence for overall structural divergence and differences in the autophosphorylation and cAMP-binding domains. *J. Neurochemistry* **42**, 547-553.

**Steinburg, R.A., Cauthron, R.D., Symcox, M.M. and Shuntoh, H.** (1993). Autoactivation of catalytic (C alpha) subunit of cyclic AMP-dependent protein kinase by phosphorylation of threonine 197. *Mol. Cell. Biol.* **13**, 2332-2341.

**Stevly, W.S., Katan, M. Stirling, V., Smith, G. and Leader, D.P.** (1985). Protein kinase activities associated with the virions of pseudorabies and herpes simplex virus. *J. Gen. Virol.* **66**, 661-673.

---

**Stevens, J., Haarr, L., Porter, D., Cook, M. and Wagner, E. (1988).** Prominence of the herpes simplex virus latency associated transcripts in trigeminal ganglia of seropositive humans. *J. Inf. Disease* **158**, 17-22.

**Stevens, J. Wagner, E., Devi-Rao, G.B., Cook, M. and Feldman, L. (1987).** RNA complementary to a herpesvirus alpha gene mRNA is prominent in latently infected neurons. *Science* **235**, 1056-1059.

**Stevenson, D., Colman, K.L. and Davison, A.J. (1994).** Characterisation of the putative protein kinases specified by varicella-zoster virus genes 47 and 66. *J. Gen. Virol.* **75**, 317-326.

**Subak-Sharpe, J. and Dargan, D. (1998).** HSV molecular biology: general aspects of herpes simplex virus molecular biology. *Virus Genes* **16**, 239-251.

**Sullivan, V., Talarico, C.L., Stanat, S.C., Davis, M., Coen, D.M. and Biron, K.K. (1992).** Protein kinase homologue controls phosphorylation of ganciclovir in human cytomegalovirus-infected cells. *Nature* **358**, 162-164.

**Swanstrom, R. and Wagner, E. (1974).** Regulation of synthesis of herpes simplex type 1 virus mRNA during productive infection. *Virology* **60**, 522-533.

**Szilagyi, J.F. and Cunningham, C. (1991).** Identification and characterisation of a novel non-infectious herpes simplex virus-related particle. *J. Gen. Virol.* **72**, 661-668.

**Taylor, S.S., Knighton, D.R., Zheng, J., Sowadski, J.M., Gibbs, C.S. and Zoller, M.J. (1993).** A template for the protein kinase family. *TIBS.* **18**, 84-89.

**Taylor, S. and Radzio-Andzelm, E. (1994).** Three protein kinase structures define a common motif. *Structure*, **2**, 345-355.

---

**Taylor, S.S., Radzio-Andzelm, E. and Hunter, T.** (1995). How do protein kinases discriminate between serine/threonine and tyrosine? Structural insights from the insulin receptor protein-tyrosine kinase. *FASEB. J.* **9**, 1255-1266.

**Telford, E.A.R., Watson, M.S., McBride, K. and Davison, A.J.** (1992). The DNA sequence of equine herpes virus-1. *Virology* **189**, 304-316.

**Trousdale, M., Steiner, I., Spivack, J., Deshman, S., Brown, S., MacLean, A., Subak-Sharpe, J. and Fraser, N.** (1991). *In vivo* and *in vitro* reactivation impairment of herpes simplex virus type 1 latency associated variant in a rabbit eye model. *J. Virol.* **65**, 6989-6993.

**Venema, R.C., Peters, H.I. and Traugh, J.A.** (1991a). Phosphorylation of valyl-tRNA synthetase and elongation factor 1 in response to phorbol esters in association with stimulation of both activities. *J. Biol. Chem.* **266**, 11993-11998.

**Venema, R.C., Peters, H.I. and Traugh, J.A.** (1991b). Phosphorylation of elongation factor 1 (EF-1) and valyl-tRNA synthetase by protein kinase C and stimulation of EF-1 activity. *J. Biol. Chem.* **266**, 12574-12580.

**Wagner, E. and Roizman, B.** (1969). Ribonucleic acid synthesis in cells infected with herpes simplex. *J. Virol.* **4**, 36-46.

**Wagner, M.J. and Summers, W.C.** (1978). Structure of the joint region and the termini of the DNA of herpes simplex virus type 1. *J. Virol.* **27**, 374-387.

**Wierenga, R.K. and Hol, W.G.J.** (1983). Predicted nucleotide binding properties of P21 protein and its cancer-associated variant. *Nature* **302**, 842-844.

**Walsh, D.A., Perkins, J.P. and Krebs, E.G.** (1968). An adenosine 3',5'-monophosphate-dependent protein kinase from rabbit skeletal muscle. *J. Biol. Chem.* **243**, 3763-3774.

---

**Wasserman, R.C., Richter, J.D. and Smith, L.D.** (1982). Protein synthesis during maturation promoting factor- and progesterone-induced maturation in *Xenopus* oocytes. *Dev. Biol.* **89**, 152-158.

**Weinmaster, G. and Pawson, T.** (1986). Protein-kinase activity of FSV (Fujinami sarcoma-virus) P130GAG-FPS shows a strict specificity for tyrosine residues. *J. Biol. Chem.* **261**, 328-333.

**Whitley, R. and Schlitt, M.** (1991). Encephalitis caused by herpesviruses, including B virus. In: *Infections of the central nervous system*, pp. 41-69. Edited by W. Scheld, R. Whitley and D. Durack. Raven Press, NY.

**Wilcox, K.W., Kohn, A., Skylanskay, E. and Roizman, B.** (1980). Herpes simplex virus phosphoproteins. I. Phosphate cycles on and off some viral polypeptides and can alter their affinity for DNA. *J. Virol.* **33**, 167-182.

**Wildy, P., Russell, W. and Horne, R.** (1960). The morphology of herpesvirus. *Virology* **12**, 201-222.

**Wu, J.G., Ohta, N., Zhao, J.L. and Newton, A.** (1999). A novel bacterial tyrosine kinase essential for cell division and differentiation. *Proc. Natl. Acad. Sci. USA* **96**, 13068-13073.

**Yao, Z., Jackson, W. and Grose, C.** (1993). Identification of the phosphorylation sequence in the cytoplasmic tail of the varicella-zoster virus Fc receptor glycoprotein gpI. *J. Virol.* **67**, 4464-4473.

**Yoon, M.Y. and Cook, P.F.** (1987). Chemical mechanism of the adenosine cyclic 3', 5'-monophosphate dependent protein-kinase from pH studies. *Biochemistry* **26**, 4118-4125.

**Zandomeni, R.O.** (1989). Kinetics of inhibition by 5,6-dichloro-1- $\beta$ -D-ribofuranosylbenzimidazole on calf thymus casein kinase II. *J. Biochem.* **262**, 469-473.

---

**Zandomeni, R., Zandomeni, M.C., Shugar, D. and Weinmann, R.** (1986). Casein kinase type II is involved in the inhibition by 5,6-dichloro-1- $\beta$ -D-ribofuranosylbenzimidazole of specific RNA polymerase II transcription. *J. Biol. Chem.* **261**, 3414-3419.

**Zelnik, V., Darteil, R. and Audonnet, J.C.** (1993). The complete sequence and gene organisation of the short unique region of herpesvirus of turkeys. *J. Gen. Virol.* **74**, 2151-2162.

**Zhang, G., Stevens, R. and Leader, D.P.** (1990). The protein kinase encoded in the short unique region of pseudorabies virus: description of the gene and identification of the product in virions and in infected cells. *J. Gen. Virol.* **71**, 1757-1765.

**Zheng, J., Knighton, D.R., Ten Eyck, L.F., Karlsson, R., Xuong, N., Taylor, S.S. and Sowadski, J.M.** (1993). Crystal structure of the catalytic subunit of the cAMP-dependent protein kinase complexed with MgATP and peptide inhibitor. *Biochemistry* **32**, 2154-2161.

**Zhou, Z., Chen, D., Jakana, J., Rixon, F. and Chiu, W.** (1999). Visualisation of tegument/capsid interactions and DNA in intact herpes simplex virus type 1 virions. *J. Virol.* **73**, 3210-3218.

**Zhou, Z.H., Prasad, B.V.V., Jakana, J., Rixon, F.J. and Chiu, W.** (1994). Protein subunit structures in the herpes simplex virus A-capsid determined from 400 kV spot-scan electron cryomicroscopy. *J. Mol. Biol.* **242**, 456-469.

**Zolnierowicz, S. and Bollen, M.** (2000). EMBO conference report: protein phosphorylation and protein phosphatases, De Panne, Belgium, September 19-24, 1999. *EMBO. J.* **19**, 483-488.

